MEDIUM VOLTAGE PETROCHEMICAL DRIVES: SOFT START AND ADJUSTABLE SPEED SYSTEMS

by

Frieder Endrejat

B. Eng (UP), M. Eng (UP cum laude), Pr. Eng (ECSA), SMIEEE, SMSAIEE

Thesis Presented for the Degree of

DOCTOR OF PHILOSOPHY

in the Department of Electrical Engineering

UNIVERSITY OF CAPE TOWN

November 2010

D E C L A R A T I O N

I Frieder Endrejat hereby:

(a) grant the University of Cape Town free license to reproduce the thesis in whole or in part, for the purpose of research;

(b) declare that:

(i) the thesis is my own unaided work, both in conception and execution, and that apart from the normal guidance of my supervisor, I have received no assistance apart from that stated below.

Portions of this work have been published in peer-reviewed journals and at peer-reviewed international conferences (Appendix A). I was the primary researcher in all instances where work described in this thesis was published under joint authorship. Where collaboration with other people has taken place, or material generated by other researchers is included, the parties and/or materials are indicated in the acknowledgement section or are explicitly stated with references as appropriate;

(ii) neither the substance or any part of the thesis has been submitted in the past, or is being, or is to be submitted for a degree in the University or any other University;

Frieder Endrejat Date

A B S T R A C T

MEDIUM VOLTAGE PETROCHEMICAL DRIVES:
SOFT START AND ADJUSTABLE SPEED SYSTEMS

by

Frieder Endrejat

November 2010

Medium voltage synchronous machines are used for large petrochemical compressor motor drives (>13 MW) at high application voltages (e.g. ≥11 kV). Limited research exists on the application of Voltage Source Inverters (VSIs) for these petrochemical loads.

An application concept is described where the converter is used to start several motors and to drive one at adjustable speed. Associated benefits in terms of availability, hazardous areas and switching surge overvoltages are outlined. A technology feasibility study illustrates that new VSI Cascaded H Bridge (CHB) technology and the application concept is economically feasible. The study considers efficiency, hazardous areas, energy savings and additional benefits compared to the traditional Load Commutated Inverter (LCI) technology. It is however essential to ensure that plant availability is not compromised by unacceptable overvoltages and ride-through problems.

A drive system model is developed to simulate potential unacceptable resonance overvoltage conditions. Generalized analytical equations are developed to study a wide variety of cable lengths, ratings and applications. Experimental tests prove the occurrence of the unacceptable overvoltages even with modern multilevel technology. The model and equations are used to determine strategies to eliminate overvoltages proven by successful site implementation. Optimisation of the carrier frequency is one of the effective strategies

for VSI systems whereas additional filtering may be required for LCI systems. A generalized design approach is developed to determine when and what additional measures are required.

A ride-through simulation model for both inverter and line operation is validated with experimental tests. A simplified generalized analytical model is developed to study several ride-through conditions affecting inverter started synchronous machines. This model shows the importance of minimising inrush currents following fault conditions by limiting bus transfer angles and thereby ensuring compliance with power quality requirements in addition to system torque constraints. Machine (inverter started) and converter protection and design principles are researched for enhanced ride-through and fault tolerant operation. Disturbance recordings of a case study are analysed to justify ASD hardware design improvements including insulated cell connections and protection co-ordination improvements.

Ultimately the research illustrates how and where new VSI technology can economically be applied with a significantly lower risk level.

A C K N O W L E D G E M E N T S

I would like to thank:

- My supervisor, Prof. Pragasen Pillay (University of Cape Town / Concordia University) for his overall insightful guidance;

- Jozef Piorkowski (Chief Engineer, Sasol Technology Electrical Engineering) for reviewing this thesis and his valuable comments; for entrusting me with advanced & interesting medium voltage drive projects; for numerous fruitful discussions on drives, synchronous machines and transfer systems and thereby gaining from his vast experience and expert knowledge;

- Tony Machado (Consultant and retired Manager of Sasol Technology Electrical Engineering) for initial encouragement regarding PhD studies;

- Theuns Erasmus (Manager of Sasol Technology Electrical Engineering) and Barend Rademeyer (Sasol Technology Electrical Engineering Secunda Site Team Leader) for funding the research;

- Acknowledgment is given to: The late Rapha Pretorius (Rapha Pretorius Associates) for overvoltage verification tests with resistive divider circuitry; Boeta van Tonder (Sasol Synfuels) for test support; Andre Maritz (Sasol Synfuels) for providing funding for the tests; Dr. Mukul Rastogi (Siemens R & D) for performing additional verification simulations and technical evaluation of a higher carrier frequency (temperature conformance, rating and processing capability); Bruce van Blerk (Sasol Technology) for PLC support during testing, long associated commissioning hours and participating in energy saving investigations; Meyer Naude (Mittal Steel) for providing the capacitive divider circuitry;

- Peter Burmeister (ABB MV Drives Switzerland), for participating in the Petroleum and Chemical Industry Committee (PCIC) Europe 2009 paper publication and providing the associated Load Commutated Inverter (LCI) data and simulations (regarding overvoltages) for comparison with VSI systems;

- Dr. Robert Hanna (RPM Engineering Canada) for review of the proposed VSI-CHB availability, protection and hardware improvements and associated participation in the IEEE Petroleum and Chemical Industry 2009 Publication;

- The valuable contribution of the following people is acknowledged during the VSI-CHB SSASD design and/or commissioning stages - Siemens Energy & Automation (USA): Giovanni Vignolo, John Shultz, Dr. Mukul Rastogi, Albert Roc; Sasol: Boeta van Tonder, Bruce van Blerk, Jan Booysen, Andre Maritz, Bill Graham (consultant);

- Sourav Paul (Sasol Technology Electrical Engineering) for his significant contribution and dedication to the 16th Oxygen Train substation construction and commissioning in the period when I was finalising this thesis;

- Dr. Azeem Khan and the UCT Electrical Engineering Department & Advanced Machines and Energy Systems Group (AMES) as a forum for insightful discussions on drives/machines research & feedback and their funding of the IEEE International Electrical Machines and Drives (IEMDC) 2009 conference attendance;

- My late father Erich Endrejat for inspiration to perform the research;

- Carika (my wife) and my parents for their invaluable love, interest and encouragement.

Dedicated to my wife and soon to be born daughter.

Deo gratias

TABLE OF CONTENTS

LIST OF FIGURES

LIST OF TABLES

LIST OF ABBREVIATIONS

AC	Alternating current
ASD	Adjustable speed drive
ASDS	Adjustable speed drive system
AWA	Aluminium wire armour
CHB	Cascaded H-bridge
CG	Cable group
CSI	Current source inverter
CT	Current transformer
DC	Direct current
DOL	Direct on line
EMF	Electro motive force
FFT	Fast Fourier transform
HRG	High resistance grounding
IEEE	Institute for Electrical and Electronics Engineers
IEC	International electrotechnical commission
IDMT	Inverse definite minimum time
IGBT	Insulated gate bipolar transistor
IGCT	Insulated gate commutated thyristor
IM	Induction motor
IOC	Instantaneous over current
IP	Ingress protection
MFPR	Multi function protection relay
MG	Motor generator
MV	Medium voltage
p	Pole

PLC	Programmable logic controller
PIT	Process immunity time
PT	Potential transformer
PWM	Pulse-width modulation
LCI	Load commutated inverter
LV	Low voltage
PCIC	Petroleum and chemical industry committee
RCB	Run circuit breaker
RS	Reduced speed
SM	Synchronous machine
SS	Selection system
SCB	Start circuit breaker
SCR	Silicon-controlled rectifier
SFC	Static frequency converter
SWA	Steel wire armour
THD	Total harmonic distortion
TP	Test point
VSI	Voltage source inverter

LIST OF SYMBOLS

Symbol	Description	Unit[1]
ω	Speed	rad/s
η	Efficiency	p.u.
ψ	Flux linkage	p.u.
δ_s	Angle between the source supply voltage and the motor internal EMF just before the transfer breaker closing (i.e. the transfer angle)	rad
C_{CG}	Cable group capacitance	F
C_M	Machine capacitance phase to earth	F
C_{uc}	Capacitance per unit length	F/m
C_{TC}	Total cable capacitance between reactor and motor	F
Ev	Vectorial Volts / Hz	V/Hz
E	Electromotive force	V
f	Frequency	Hz
f_c	Carrier frequency	Hz
$f_{sw,inv}$	Effective inverter frequency	Hz
f_m	Modulating/fundamental frequency	Hz
f_o	Resonant frequency	Hz
$f_{m\pi}$	Maximum frequency that can be represented by a single π / transmission line model	Hz
H	Voltage transfer function	-
I	Current	A

[1] Units are converted in most cases to per unit (p.u.) form (as defined in P. C. Krause, O. Wasynczuk, S. D. Sudhoff, *Analysis of Electric Machinery*, IEEE Press, 1995, machine base as per IEEE std. 115) to simplify analysis.

I_{mm}	Maximum motor withstand current (for bracing of windings)	A
I_t	Maximum transformer withstand (for bracing of windings)	A
J	Inertia	kgm^2
K	Number of cells per phase	-
K_E	Exciter constant K_E	p.u.
l_{max}	Maximum length without rotor position detection	m
L	Inductance	H
L_{CG}	Cable group inductance	H
L_M	Equivalent machine reactance for resonance studies	H
$L_{REACTOR}$	Reactor inductance	H
L_{uc}	Inductance per unit length	h/m
m	Number of levels in voltage waveform	-
m_a	Modulation index	-
P	Power	W
r_s	Stator resistance	p.u.
S_{Emax}	Saturation function	p.u.
V	Voltage	V
V_A	ASD input bus voltage	V
V_B	Voltage of remote bus	V
V_C	Voltage of ASD output bus	V
V_f	Motor terminal voltage directly after transfer closure	V
V_M	Motor voltage	V
V_{IN}	Input voltage to load model	V
V_a	Air-gap voltage	V
V_{rm}	Rated motor voltage	V
V_t	Rated transformer voltage	V
X	Reactance	Ω
T_d'	d-axis transient short circuit time constant (saturated test)	s
T_d''	d-axis sub-transient short circuit time constant	s

	(saturated/unsaturated test)	
T_q''	q-axis sub-transient short circuit time constant	s
T_E	Exciter time constant	s
Uins	Rated stator insulation voltage	V
X_d	d-axis synchronous reactance (saturated test)	Ω
X_d'	d-axis transient reactance (saturated test)	Ω
X_d''	d-axis sub-transient reactance (saturated test)	Ω
Xl	leakage reactance	Ω
X_m''	Effective sub-transient motor reactance	Ω
X_q	q-axis synchronous reactance	Ω
X_q''	q-axis sub-transient reactance (saturated)	Ω
X_s	Source reactance	Ω
X_t	Transformer reactance	Ω
Z	Impedance	Ω
δ	Angle	rad

SUBSCRIPTS

d	d axis
l	Leakage inductance
f	Field winding
k	Damper winding or equivalent
M	Machine
q	q axis
s	Stator
S	Source
m	Magnetising inductance

SUPERSCRIPTS

o	Pre-fault or closing condition
f	Fault or post closing condition
r	Rotor reference frame
‘	Rotor variable referenced to stator winding

1 INTRODUCTION

High power drives with high output voltages are evaluated in this thesis for application in the petrochemical industry. Detailed analysis of the feasibility of high power drive systems for the petrochemical industry is clearly described. A design approach to eliminate unacceptable output overvoltages is provided. The system design requirements have been researched to enhance ride-through performance. In this chapter, the background to the research is provided, a review of large medium voltage drive systems is given, a literature review is compiled and an overview of the thesis is presented.

1.1 BACKGROUND

The number of large Adjustable Speed Drives (ASDs) used in industry has rapidly increased from 1985 to 2005, mainly due to process control and energy saving benefits as illustrated in Fig. 1.1 [1.1]. The Medium Voltage (MV)[2] ASD market has thereafter continued to grow and is expected to grow further in the future as shown in Fig. 1.2 based on information in [1.3] and [1.4]. MV and Low Voltage (LV) ASDs are utilized in the power ranges between 300 kVA and 2 MVA and only MV ASDs are used in the high power ranges between 2 MVA and 60 MVA (and in limited cases above 60 MVA) [1.5].

Worldwide there is a strong demand to achieve energy savings with MV ASDs due to rising energy costs [1.3], [1.5]. Energy savings are especially important in South Africa due to rapid escalation of electricity costs [1.6]. Smaller MV ASDs (<7.2 kV & < 10 MVA) and Low Voltage (LV) ASDs have extensively been applied for energy savings. MV ASDs for high power application and energy saving have not been widely applied

[2] "Medium Voltage" is used in the thesis as per IEEE Std. 141 [1.2], i.e. representing the voltage levels 2.4 kV-34.5 kV.

mainly due to concerns of process availability since the associated motors normally feed essential loads. Extensive research and development on large MV ASDs have been conducted in the last four decades to develop alternative technologies to compete with the traditional Load Commutated Inverter (LCI) technology (discussed in next section).

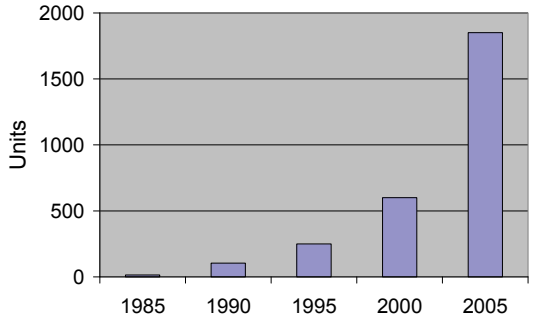

Fig. 1.1 Estimated number of large (>375 kW) ASDs (for pumps, fans and compressors) produced globally [1.1]

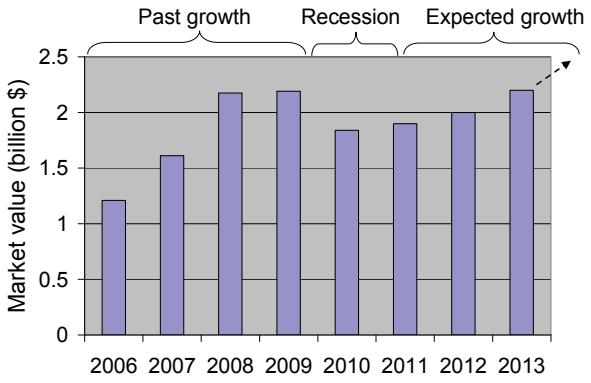

Fig. 1.2 Global market value of MV ASDs [1.3], [1.4]

MV Synchronous Machines (SMs) are normally used for high power petrochemical compressor motor drives (>15 MW) at high application voltages (e.g. ≥11 kV) [1.7]. Very limited research, literature and application examples currently exist on the related application of newer ASD technology for these petrochemical loads. This thesis focuses on closing this gap by outlining the benefits and by addressing critical issues to achieve a successful ASD application.

1.2 LITERATURE REVIEW

A literature survey was conducted to investigate the evolution of high power start and drive systems and to identify selected areas requiring further research.

1.2.1 Conventional High Power Start and Drive Systems

Direct-on-line (DOL) starting is most often used in petrochemical plants but is normally not practical for high power motors due to limitations associated with the starting current which may result in unacceptable busbar voltage drops, thermal and dynamic stresses as outlined in [1.8] and [1.9]. Other electrical system components, e.g., driven equipment, switchgear, incoming transformers, are also negatively affected [1.10]. A decrease in the starting current is often the only viable solution for starting large motors associated with the size range studied in this thesis.

Conventional technologies used to achieve lower starting current include the insertion of reactance, captive transformer starting, Korndorfer reduced voltage autotransformer, autotransformer with capacitor assistance, and reduced voltage power electronic starters [1.8], [1.11], [1.12]. The starters are also often specified when the driven equipment requires a lower starting torque.

Large motors (e.g. >15 MW), however, can often not be started effectively by any of the previously mentioned methods. These motors are associated with severe voltage drops during DOL starting [1.13], [1.14]. A less stressful and a more controllable soft start system is required, e.g., adjustable voltage and frequency starting methods. Traditionally, motor generator (MG) sets were used [1.13]-[1.15]. However, static frequency converters (SFCs) have become far more frequently used due to the elimination of rotating parts and maintenance-intensive mechanical equipment (e.g., the fluid coupling and the associated auxiliaries). Soft start technology is often defined as a technology that provides adjustable voltage to the motor via power electronic devices [e.g. silicon-controlled rectifiers (SCRs)]. SFC adjustable speed drive (ASD) technology is used for optimal soft starting [1.8] and known for the ease of starting motors on weak networks [1.1]. The load commutated inverter (LCI) technology [1.15]-[1.23] has been used almost exclusively for large motor applications (soft start and ASD applications).

It has been stated that the LCI technology is the obvious choice for large adjustable speed systems, although the power ratings of the alternative technologies are increasing [1.18]. The LCI technology has been proven as a mature and a reliable solution for many applications, but it has several disadvantages [1.15]-[1.23]:

a.) Significant motor output torque ripple;
b.) Significant line and motor side current and voltage harmonics;
c.) Power factor not close to unity over the entire load and speed range;
d.) Without modification only suitable for synchronous motors (often the motors must be designed specifically for LCI operation) [1.28];
e.) Limited input and output cable length ;
f.) Output voltages at 11kV and above are not offered/not economical (without a step-up transformer) for power ratings up to approximately 25 MW [1.5].

These disadvantages could be overcome only by very comprehensive and rather complicated system engineering. Normally, an application-specific special design of motors is required. Furthermore, additional harmonic reduction and power factor compensation techniques are often required. These are associated with costly additional equipment, which requires space and affects the efficiency and the reliability of the system [1.19], [1.20].

1.2.2 Medium Voltage Adjustable Speed Drive Technologies

Medium voltage ASD technologies are overviewed in [1.5], [1.23]-[1.29] and can be classified in accordance with Fig. 1.3. The cycloconverter technology is suitable for high power but preferred for low speed applications [1.28] and therefore not extensively used in the petrochemical industry (limited low speed applications in the high power range). Several newer medium voltage technologies have been developed to compete in power ranges previously only suitable for the widely applied LCI systems. These include several Voltage Source Inverter (VSI) and Current Source Inverter (CSI) Pulse Width Modulation (PWM) technologies that are readily suitable for standard motors.

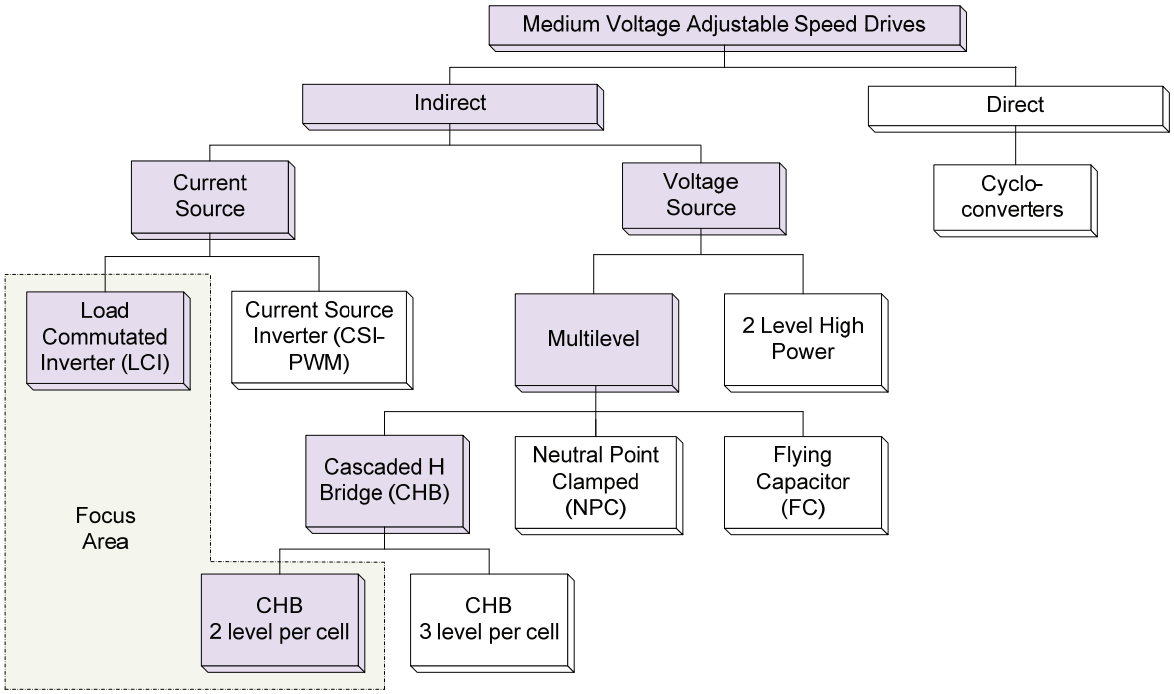

Fig. 1.3 Medium voltage adjustable speed drive classification

Each of these technologies has certain advantages and disadvantages and not all of them address all the disadvantages of the LCI alternative. Many additional variations of the technologies including the multi level VSI technology have been investigated and control and modulation strategies were improved to minimise the harmonic content of voltage output waveforms [1.27], [1.29]. This minimised the requirement for any additional front-end or load side modifications or additions [1.29], [1.30]. Nevertheless multilevel VSI technologies are becoming available to address all the disadvantages as outlined above, including high output voltages (≥11 kV) without a step-up transformer.

There has been a strong demand to build inverters at higher voltage levels (11-16 kV) [1.27]. This has significant benefits for very large applications due to the lower rated current, easier system construction and reduced cost of system components – e.g. interconnection cabling. An extreme example is the use of a very high power, high voltage source converter (with series connected IGBTs) based on High Voltage Direct Current (HVDC) technology. This was used for offshore applications with a long DC link cable with a high output voltage instead of LCI technology [1.31]. In an inland petrochemical plant facility a long distance HVDC link is not required and alternative integrated drive technologies (with the rectifier and inverter section in one package) with more sinusoidal

waveforms can be explored. Most commercially available related CSI PWM and VSI based drives have until 2004 only been available for application voltages up to 7.2 kV [1.24]. A topology that presently (2010) offers a solution for larger power and voltage rating is the VSI cascaded H bridge (CHB) with 2 levels per cell and with advantages described in [1.24]-[1.27], [1.33] and [1.34]. This VSI technology, which has mostly been applied with induction motors, has become a viable alternative to traditional LCI synchronous motor based systems [1.7]. Synchronous motors are however more suitable for larger applications above approximately 15 MW (as stated previously). In 2004, IGBTs with higher voltage rating were first used with this VSI topology to obtain an increased output voltage of up to 13.8 kV while minimizing the overall component counts [1.35]. The power density is also significantly improved. This next generation of the topology facilitates higher power ratings suitable for higher power synchronous motor applications. Film capacitors instead of electrolytic capacitors have been introduced in the DC link of the higher voltage IGBT based inverters with an expected associated improvement in drive reliability [1.36]. Voltage and power ratings of various topologies (on the market in 2010) are provided in [1.5] and summarised in Fig. 1.4. The focus area of this thesis is also shown.

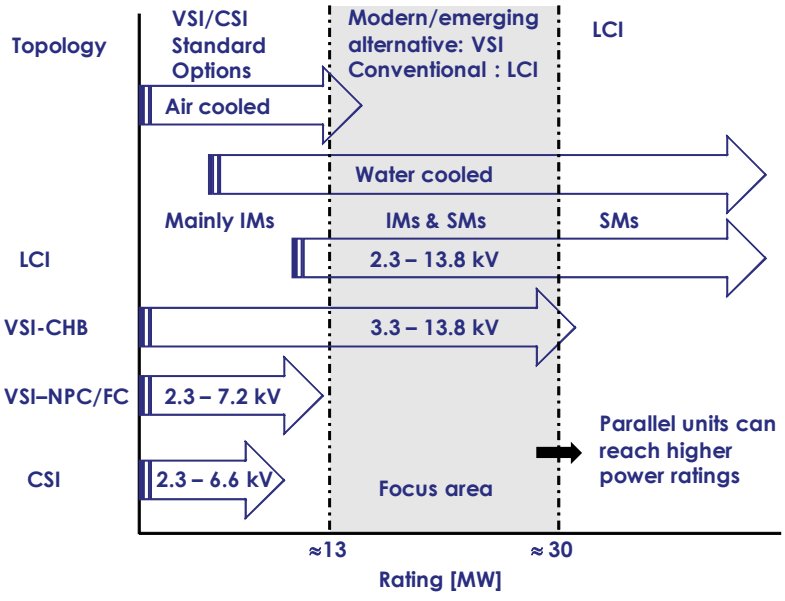

Fig. 1.4 Power and output voltage ranges for various MV ASDs (no parallel combinations shown)

The VSI-CHB can theoretically also be used with 6 cells rated 1400A to obtain a drive rating of 31 MVA at 13.8 kV [1.37]. Four of these ASD units may theoretically be used in parallel similar to a concept shown in [1.38] (for 7.2 kV units of the same topology but with lower voltage IGBT cells) to obtain a rated output of approximately 120 MVA which may compete in maximum output power ratings of LCI systems (the largest LCI system built to date is 101 MW [1.39]).

Reliability and availability concepts for medium voltage drives are described in [1.40] - [1.42]. The need for redundancy in cells has been illustrated in [1.41], [1.42] to improve reliability and availability. The cell bypass principle addresses this need where a faulty cell is bypassed without an interruption with the capability to still achieve the rated voltage [1.36], [1.37], [1.43]. The evaluation in [1.41] is performed for VSI-CHBs with LV IGBTs (e.g. for 690 V rated cells). VSI-CHBs with higher voltage IGBTs (e.g. for 1375 V rated cells) have been introduced thereafter into the market with expected reliability figures at least as good as the lower voltage cells. Furthermore higher voltage and power ratings can be achieved with the same amount of cells. It is shown in [1.41] that the VSI-CHB topology with 5 cells per phase including a redundant cell per phase can compete with LCI and VSI NPC reliability figures. In the case of a cell failure, replacement of the faulty cell is however recommended before a scheduled shutdown to ensure high reliability figures [1.41]. VSI-CHBs for very large power drives require parallel VSI-CHB systems (as mentioned above for the 120 MVA system) and in this case redundant cells might need replacement too often to maintain adequate reliability [1.41]. LCIs are therefore still recommended for very high power applications from a reliability point of view. This thesis focuses on non-parallel VSI-CHB systems and the power range shown in Fig. 1.4.

A significant advantage of the VSI alternative is that higher output voltages can be obtained (i.e. minimizing the output current). Newer electric motor technology [1.44] has allowed fabrication of higher voltage motors and the SFC topology provides a platform for potential future development of even higher output voltages (well in excess of 13. 8 kV) that can be matched ideally with the motor for very large applications.

Some of the new or alternative technologies can be used for existing motor applications (no special motor design required) [1.45]. Specific advantages associated with some

multilevel technologies (e.g., VSI-CHB) are the minimization of du/dt output wave change rates, common mode voltages, and electromagnetic interference (in addition to the near sinusoidal voltages) [1.47]. Therefore the probability of bearing failures is reduced [1.47]. Multilevel inverters of the VSI-CHB topology are superior to most other VSI topologies regarding the minimisation of shaft voltages [1.45]. Multilevel inverters (especially VSI-CHBs) are also associated with near sinusoidal current waveforms [1.24] making them suitable for existing motors especially in hazardous areas. Conventional six step inverters / drive systems [1.48], forming part of the 2 level high power category in Fig. 1.3, may have been a suitable consideration for potential high power synchronous machine applications with high reliability characteristics similar to those of LCI systems. Six step drive systems, however, are not associated with near sinusoidal current waveforms (unlike VSI-CHBs) and have significant current harmonics [1.48]. A special evaluation is required for standard/existing motors, when fed from sources with significant current harmonics, especially if they are located in hazardous areas, to ensure that operation below the ignition temperature of the gas is achieved [1.18], [1.53]. In LCI systems this additional heating due to harmonics is significant and extra caution with the motor design is necessary that normally results in a motor specially designed for the LCI application [2.39]. Similarly, six step inverter current waveforms have significant distortion and may require similar measures. These motors may also require derating from a thermal perspective due to additional losses associated with harmonic currents [1.48]. This may not be possible for existing motors since large MV motors are often required to operate close to their capability (unlike LV motors which are commonly overrated). A six step drive system may also require a step-up transformer to reach > 11 kV voltages (there is no readily available six step system for the power range, on the market in 2010, to reach 11kV directly). The step-up transformer requires a significant number of undesired high current rated cables between the ASD and step-up transformer (which is another undesired single point of failure). Six step drive systems have therefore not been selected to form part of the research in this thesis.

In summary, the power electronics research community and industry have reacted to the high power demand in two different ways [1.25]: developing semiconductor technology to reach higher nominal voltages and currents while maintaining traditional converter topologies (mainly two-level voltage including the six step topology and current source

converters); and by developing new multilevel converter topologies, with traditional semiconductor technology. The first approach has the benefit of well-known circuit structures and control methods. High power applications, however, has additional quality requirements to be fulfilled, which may require power filters. The second approach uses the well-known semiconductors, but the more complex circuit structures introduced several challenges for implementation and control.

The focus of this thesis is on the second approach with VSI-CHBs where associated challenges are addressed and new opportunities are explored.

1.2.3 Multiple Motor Soft Starting with the Capability to Operate One Motor at Adjustable Speed Using a Single SFC

Energy saving projects for existing motor drives may often be difficult to justify due to the capital investment required. Furthermore the reliability of some MV drive systems are not always high enough dictating expensive redundancy options, making the project even less feasible. Energy saving principles, energy saving studies and energy saving projects associated with medium voltage drives are documented in [1.10], [1.53], [1.50] with a focus on single motor applications. Quantification of the losses of typical applications associated with flow valves and other dissipative flow control methods is given in [1.10]. Energy savings (based on the affinity law principle [1.10]) can be achieved in some cases where multiple motors are driving compressors or pumps. The concept of a combination soft starter and adjustable speed drive (SSASD) has been proposed in [1.51] mainly for efficient flow or pressure control where multiple motors are used for a specific application (e.g., pipeline or compressor/pump applications). The concept is also suitable for certain energy saving applications. Instead of driving all the motors at rated speed with dissipative process control methods (e.g., inlet valves), it is proposed that one motor be driven at an adjustable speed according to the load demand of the varying process. The other loads can then be driven at their optimal efficiency (it may be necessary to switch off one or more motors in accordance to the demand of the process).

A single SFC used as a multiple motor soft-starter ASD (SSASD) may address the aforementioned needs. When a motor needs to be started, the SSASD is ramped up and

synchronized with the fixed frequency supply. The SSASD is then isolated from the fixed frequency supply after which any of the other motors can be soft started. Thereafter the SSASD is synchronized again with the fixed frequency supply and ramps down the adjustable speed motor according to the process demand. The necessary process control is implemented during ramp-up and ramp-down conditions to meet the required process flow and pressures and to minimize process upsets. A graphical illustration of the conventional approach versus the proposed alternative approach is shown in Fig. 1.5.

In summary, instead of applying two different units for different loads (i.e., the adjustable-speed load and loads requiring soft starting), only one unit is used alternatively by both types of loads.

The benefit of this concept is recognized in [1.51] but the motivation was mainly based on economic flow/pressure control where multiple motors are used for a specific application (e.g. pipeline/compressor station applications).

The failure of a dedicated ASD may cause significant production losses. This risk may be reduced by including further redundancy in the ASD, but added capital cost and a subsequent failure can still result in expensive production losses. The shutdown periods of some petrochemical plants can typically be every four to six years [1.14]. Some of the new SFC technologies have not been applied long enough in the industry to prove that this availability requirement will be met.

One major advantage is that the concept of a SSASD system may address this reliability and availability requirements when at least N-1 redundancy (operation continues after the failure of a one component/subsystem) is built into the important system components with the highest risk of failure that may result in production loss. As soon as a component in the SSASD system fails, the SSASD can still be ramped up and synchronized with the fixed frequency supply. The SSASD is then removed where-after the faulty component may be repaired/replaced without any production loss.

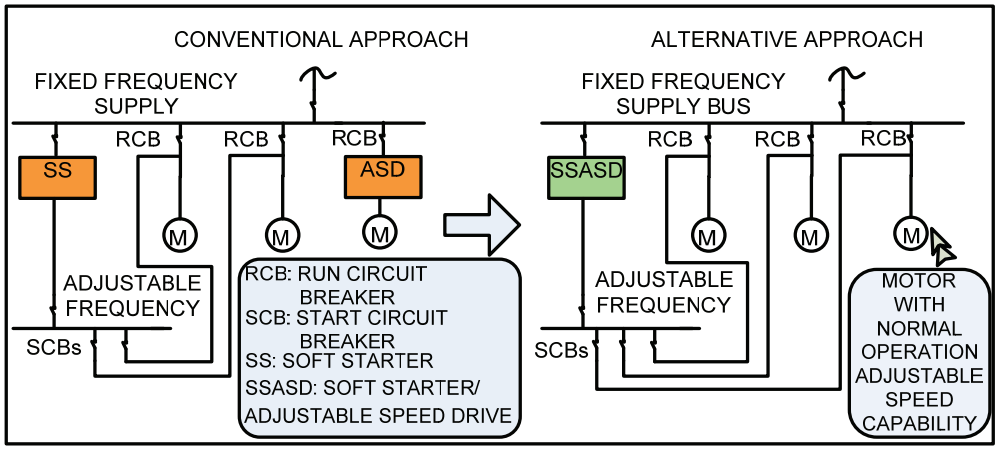

Fig. 1.5. Single SFC applied as a SSASD

The concept of an SSASD that was originally documented in [1.51] is further investigated in the thesis to address the availability requirements when at least N -1 redundancy is built into the important system components (with the highest risk of failure that may result in production loss). As soon as a component in the SSASD system fails, it will be investigated whether the SSASD can still be ramped up and the motor load synchronized with the fixed frequency supply, with subsequent replacement of the faulty component without production loss. The associated research was not previously documented. This addresses also the recommendation [1.41] discussed earlier to replace a faulty cell prior to a scheduled shutdown to ensure high reliability figures. Further operating principles in a petrochemical environment are described in [1.14]. Application possibilities of the SSASD scheme for both existing and new projects in the petrochemical industry are proposed in [1.14] with case studies in Chapter 2.

It is important to emphasize that the intention of the SSASD scheme is not that all synchronous motors are synchronized to the line but that one machine will normally operate at adjustable speed. There is therefore still significant merit to have a high output voltage of the ASD (i.e. equivalent to the bus voltage, e.g. 11 kV). This eliminates the step-up transformer as an additional single point of failure and eliminates transformer losses. Furthermore cable connections at the output of the converter are then simplified (lower current due to the higher voltage, which is especially important for high power applications since current ratings are already high).

1.2.4 Large Drive Problems

Problems associated with large DOL (high starting currents) and/or motors driven by conventional ASD technology (non – sinusoidal waveforms) in the petrochemical industry are widely reported in literature. The SSASD concept in conjunction with the CHB topology may address selected problems:

A. Difficulty/uncertainty in achieving hazardous area compatibility/certification

Most petrochemical motors must be suitable for application in zone 2 (in terms of IEC 60079-15 [1.52]) hazardous areas. DOL-started MV motors may cause sparking during starting, which may ignite the potentially explosive atmosphere. A purging system or a prestart ventilation system may be required to avoid the presence of the gas during motor starting [1.9].

The application of an SSASD to soft start the applicable motors can minimize the risk of sparking, and the startup current can be limited not to exceed the rated current. This may remove the requirement of a purging / prestart system in some cases (subject to a risk evaluation in terms of [1.52]). More relaxed certification requirements may be applicable for certain MV technologies because of more sinusoidal output waveforms. Important aspects that must still be evaluated are given in [1.37], [1.53], [1.54] and [1.55] with special attention to ignition energy and thermal considerations.

B. Motor Rotor Design and Protection Challenges

DOL-started large motors may have longer startup times than the rated locked rotor withstand time [1.8]. A speed monitoring system may then be required in conjunction with the motor protection relay to protect the rotor from overheating [1.8]. An alternative is to design the rotor for a locked rotor withstand time that is longer than the startup time. An SSASD eliminates these requirements.

C. Motor Stator Winding Insulation Damage and Protection

DOL-started motors are occasionally switched (interrupted) during starting (e.g., locked rotor condition, emergency stop, or process trip). It may result in overvoltages because of multiple re-ignitions and virtual current chopping, which may be significant depending on the system's reactances and capacitances [1.56], [1.57]. Frequent overvoltages can result in motor stator insulation damage. The situation is more significant during starting because of the poor power factor. An SSASD system (high power factor and power electronic soft switching) eliminates these overvoltages during starting and switching; therefore, the life of the motor insulation may be prolonged. Motors with a high voltage (e.g., 10 kV versus 6 kV), high power (e.g. 3 MW versus 200 kW), and fairly long cable distance (e.g., 800 m) may present a dangerous combination for generating overvoltages [1.58]. This combination is also typical for an ideal SSASD application, which increases its feasibility. It is shown in [1.58] that larger motors (typically above 1 MW) do not experience significant overvoltages following interruptions in the running mode. Surge arrestors or suppressors are, therefore, not required with an SSASD system.

1.2.5 Research Needs

This section outlines high power soft start and ASD application research needs and challenges which are not extensively addressed in the literature or standards. (The IEC 61800-4 standard [1.23] provides detailed requirements for the ASD and IEEE standard 1566 [1.59] focuses more performance related requirements [1.60]).

A. Integration of Soft Start Systems, Long Cable Lengths and Overvoltages

Motors are often associated with long cable distances for onshore (e.g [1.61]) and offshore/subsea applications (e.g. [1.62], [1.63]). Large petrochemical plants normally have one or more existing soft start systems which may only be used to soft start the motors in the close vicinity of the existing soft starter due to maximum cable length limitations of the technology used. The soft starters may not have full redundancy built in or may not have expensive spare parts readily available (e.g. transformers or reactors).

These soft starters are often also located far away from each other and can therefore normally not serve as back-up to each other. Although SFCs can be reliable, [1.40], [1.64] a failure of a major component (with a long lead time) can not be ruled out. Major production losses can occur in such an instance. A new SSASD will normally be specified with the adequate redundancy due to the continuous operation requirement, whereas a soft starter often does not have this requirement due to its infrequent use. An SSASD may therefore be used as back-up for an existing soft starter without the requirement of back-up from the existing soft starter (due to the built in redundancy). This integration may significantly improve the availability of a soft start installation to all the applicable large motors in a petrochemical plant.

Nevertheless, it is still desirable to investigate the capabilities of mature technologies to be used over long cable distances as back-up starting devices. A need therefore exists to research the capabilities of both VSI and LCI technologies with long cable lengths for back-up systems and motors located far away from the SFC.

Higher voltage IGBTs are now used for VSI-CHBs to minimize overall component counts as discussed earlier but are associated with fewer and/or larger voltage steps when compared to the application of traditional low voltage IGBTs. It is however important to investigate the possibility of potential overvoltages associated with the larger/fewer voltage steps.

Motor insulation requirements associated with medium voltage (MV) Adjustable Speed Drives (ASDs) are well documented in literature and the recently published IEC 60034-18-42 standard [1.65] - [1.67]. The standards and literature focus, however, on the expected waveforms at the motor terminals considering cable effects, MV PWM waveforms and the reflective wave phenomenon. It has been stated that the switching surges associated with VSI-ML-H systems are not likely to contribute to motor insulation problems due to the relatively small steps in voltage [1.68]. This was however based on low voltage IGBT cells. Further research has still been performed to reduce the effects of reflective wave phenomenon specifically for CHB technologies by optimised modulation strategies [1.69]. Resonance overvoltages (not specifically addressed in IEC 60034-18-42) have been reported in literature for certain applications associated with significant voltage

steps/surges. References [1.61] and [1.62] show that unacceptable motor terminal resonance overvoltages can occur with a lower voltage two level inverter with a step-up transformer feeding a MV motor with a long cable distance. A filter [1.61] or alternative modulation strategy [1.62] were required to rectify this problem. Circuit breaker switching transients can excite resonance overvoltages at captive transformer fed motors [1.70]. In CSI PWM systems resonance can occur due to the inverter output capacitance and motor impedance, excited by drive harmonics [1.24]. Typical solutions include correct sizing of capacitors and/or selective harmonic elimination [1.24].

The standards also do not cover other topologies i.e. current source inverter / LCI topologies (and the standard is not customised for soft start requirements). Manufacturers of LCI systems normally specify that an output cable length of only a few hundred meters is allowed (e.g. 200 m) [1.71], however application requirements can call for far longer cable lengths. Lower power VSI (not CHB) and CSI resonance conditions with long cables and induction motors are documented in [1.61], [1.62]. Solutions to overcome output resonance problems with high power LCI systems with synchronous motors are however not documented in the literature. The thesis focuses on the VSI-CHB and LCI technologies with synchronous motors. A comparison of requirements associated with the two technologies is needed.

Specific research attention should therefore be given to potential reflective wave and especially resonance induced overvoltage interactions between the drive and motor which can be potentially dangerous or damaging to the drive system.

B. Synchronisation

The feasibility of the SSASD concept is heavily dependant on the correct functioning of the synchronization system. Synchronization principles and methods for up and down transfers of motors to and from a single bus are described in [1.51]. Previously internal ASD synchronous transfer schemes only allowed transfers to the same bus from where the ASD is fed [1.37]. Internal sensors to synchronize the drive output with the drive input are usually used. Synchronization may also be required to a different bus (with a different phase angle and voltage) at nearby location [1.37] or at a remote location (e.g when SFCs

serve as back up to each other). One option is to use a transfer scheme (with external synchronization commands to the SFC), typically used with LCI systems [1.15]. It is possible with some drive topologies and control schemes to phase the current back prior to the paralleling time and therefore a synchronization reactor is not required to limit the current during the transfer [1.51]. A synchronisation reactor may be used for very smooth transfers [1.37] (the current is not phased back). Further development is however required for systems using the synchronisation reactor and internal ASD transfer scheme to cater for multiple busses.

C. Efficiency

Efficiency of different medium voltage ASD technologies is compared in [1.72]-[1.74]. In all these references so far the focus is on applications with motors rated 7.2 kV and below. Large drives which may benefit from adjustable speed energy savings are often rated at ≥ 11 kV as stated previously. There is therefore a need to perform efficiency comparisons, energy saving evaluations and project feasibility evaluations for large 11 kV adjustable speed motor systems.

D. Ride-through

Machines associated with SFC soft starting or in a SSSASD scheme must also be capable to operate directly one line. Significant currents may occur due to synchronous machine transfer switching currents. An example is a fast bus transfer [1.75] which is often encountered in the petrochemical industry to enhance the ride-through capability of machines during bus transfers following upstream fault conditions. The associated transfer currents are traditionally not considered in the system design with DOL started motors. This is because the DOL currents are normally considered to be more significant than the transfer currents. Drives must be able to ride through the voltage dips produced externally. This applies to the direct-on-line mode of operation and to ASD mode of operation.

Dynamic voltage restoration or additional energy storage elements were suggested to achieve ASD ride-through for the power rating and topology addressed in this thesis (VSI-CHB) [1.76]. Power system stabilizers are sometimes suggested for on-line SM ride-

through [1.77]. There is a need to investigate whether these additional measures are essential for large compressor drives used in the petrochemical industry.

ASD internal protection should be designed to ensure that the system can ride through faults associated with fault tolerant schemes. General protection principles, issues and schemes associated with medium voltage drives are outlined in [1.78]. Specific attention is however not given to the VSI-CHB fault tolerant schemes and internal ASD protection co-ordination to ensure ride-through which requires further research.

1.3 OBJECTIVES

1.3.1 Main Objective

The main objective of this thesis is to extent the body of knowledge towards the successful application of large MV ASD systems in petrochemical industry.

1.3.2 Key Research Questions to be Addressed

Key questions to be addressed to meet the main objective are:

- What are the advantages of applying large MV VSI-CHB technology in the petrochemical industry?
- Is MV VSI-CHB technology superior to traditional LCI technology and when should it be used?
- Is MV VSI-CHB technology economically feasible for application at high output voltages and for large machines?
- What schemes can be implemented to address availability requirements of driven equipment? Is the proposed SSASD scheme feasible?
- Are the output waveforms suitable for reliable machine operation, especially with long cable lengths?
- What strategies can be implemented to achieve acceptable output waveform quality?

- Can machines ride through ASD faults/disturbances and external disturbances without disrupting the process?
- How can the ride-through performance be improved?

1.3.3 Specific Objectives

- The specific objectives are individually addressed in each chapter and are therefore provided in the **summary** section of this chapter (section 1.7).

1.4 METHODOLOGY

The research applicable to this thesis is mainly based on analytical, numerical and experimental methods. The following methodology is followed to obtain the research results:

- Research into the application of conventional and modern large drive systems is conducted by means of a literature survey and site case studies on large petrochemical plants. Identification of improvement areas and possible additional benefits which can be achieved with the new technology are investigated. This forms part of the motivation of application of the new technology.
- The economic feasibility of the MV VSI CHB technology and SSASD scheme is researched by considering efficiency, energy savings and additional benefits. The economic business case is based on practical case studies.
- A conceptual proposal of an actual SSASD system incorporating VSI-CHB technology is developed, the subsequent design is reviewed, factory acceptance testing, site acceptance testing and commissioning are supervised to ensure that the proposal objectives are met.
- A model is developed for the VSI-CHB technology in conjunction with the output circuitry, cabling and the machine. The model is used to simulate the voltage waveform at the machine terminals to investigate possible harmful overvoltage conditions. A simulation package for the numerical solution of the differential

equations of the model is used. Generalized analytical equations are developed that can be used in a convenient manner to study a wide variety of conditions and applications. Site experimental tests is conducted to prove the presence of potentially harmful overvoltages simulated by the model. The model and equations are used to determine strategies to eliminate overvoltage conditions. Site tests are performed to prove the successful elimination of harmful overvoltages predicted by the model. Several case studies are included based on parameters of large machines on a petrochemical site.

- A model is developed to simulate ride-through performance of synchronous machines for both ASD and line operation. A simulation package for the numerical solution of the differential equations of the model is used. The model is validated with ride-through experimental tests on site (run down recordings). A simplified generalized analytical model is developed to evaluate several ride-through conditions affecting ASD started synchronous machines. The results of the analytical model are verified with the simulation model. Several case studies are included based on parameters of large machines on a petrochemical site.
- Machine (ASD started) and ASD protection and protection co-ordination principles are researched to determine whether fault tolerant operation can be improved to enhance ride-through. Disturbance recordings of a case study on site are analysed to justify ASD protection improvement recommendations.

1.5 ORIGINAL CONTRIBUTION

Numerous publications exist on multilevel medium voltage adjustable speed drives discussing their topology, internal control, harmonic output content etc. Research into the actual practical application of multilevel drives with a high output voltage for synchronous motors is however very limited.

The original contribution of this thesis does therefore not focus on developing new power electronic devices, topologies or internal modulation strategies. The contribution is based on the methodology described in the previous section resulting in the identification of

application opportunities and applying latest available technology in an optimised manner while ensuring that the availability of the plant is not compromised.

It is shown that these application opportunities are economically feasible by means of case studies focussing on efficiency, energy savings and further identified benefits of the SSASD concept.

Most MV drive manufacturers previously did not have the technology to provide an ≥ 11kV high power SSASD system for synchronous and induction motors (for new and existing motors) which may be located a significant distance away from the drive. Unique and advanced application research is applied to achieve new identified benefits of the SSASD concept. The system is further proven by an actual first of its kind application of an 11kV 15.5 MW SSASD system.

Previously the MV CHB drive suppliers, capable of supporting the SSASD concept, did not allow transfers to multiple busses and therefore back-up to remote starters and starting motors on a different bus were not possible. A solution is proposed to overcome the limitation and is applied to an actual system with more than one bus (11kV 15.5 MW SSASD system).

It is also shown where conventional technologies are still more feasible, supported by application research and implemented case studies. Novel research is performed to investigate the integration of individual soft start systems to improve plant availability. A critical factor of the integration of these systems is the successful accommodation of long cable lengths. Long cable lengths may also be associated with standalone ASDs in certain large petrochemical plants.

The developed model and equations show that harmful overvoltages can occur associated with long cable lengths even with modern multilevel MV CHB technology. This was proven with experimental testing on site. A solution is described to eliminate the problem supported by tests on site. Solutions for a wide variety of motor sizes and cable distances are proposed with comprehensive case studies.

ASD design and protection limitations affecting the system ride-through abilities associated with internal fault tolerance are identified. Alternatives are proposed to enhance the ASD ride-through ability and improve availability of the drive system. Fast bus transfer ride-through challenges associated with ASD started machines are identified and solutions are proposed.

Several actual case studies are presented which include the first installed VSI-CHB at ≥ 11 kV and also the first installed 4 pole synchronous motor rated ≥ 55 MW. Problem areas identified by research objectives are illustrated and associated solutions have been provided.

The results of the research may significantly improve the feasibility of large drive system and associated energy saving projects. Ultimately significant energy savings may be associated with large drive systems in petrochemical plants that were previously not economically nor technically feasible to achieve. In addition the reliability and availability of large drive systems may be improved significantly.

Original Contribution Summary

The multiple motor SSASD concept is applied in a unique manner with near sinusoidal high output voltages (>11 kV) with the capability to synchronize and de-synchronize synchronous motors safely to multiple utility sources. New opportunities and benefits associated with the SSASD concept are identified. It is shown that harmful overvoltages can occur even with modern multilevel technology. Successful strategies are proposed to eliminate the overvoltage problem. Ride-through problems are identified for both ASD and on-line operation and successful solutions have been proposed and implemented to achieve ride through with first of its kind case studies. Ultimately the research illustrates how new technology can be applied economically with significantly lower risk levels.

1.6 SCOPE AND LIMITATIONS

The research is limited to onshore petrochemical ASD started and driven high power synchronous machine applications with machine power ratings above approximately 13

MW and with voltages ≥ 11 kV. The focus is on SFCs power ranges shown in Fig. 1.4 While many of the outcomes of the research are also applicable to high speed applications and other industries, the focus on this research is not on specialized high speed applications.

1.7 OVERALL SUMMARY, STRUCTURE AND SPECIFIC OBJECTIVES

The work contained in the thesis is now summarised in chapter format. Each chapter contains its own results, discussion, references and conclusion for clarifying purposes, and to ensure good continuity throughout the thesis. The summaries of the chapters below can be considered as *specific objectives* of the research addressing key questions.

Chapter 1 provides the background, literature study and motivation for the research conducted in this thesis.

Chapter 2 investigates the feasibility of the VSI-CHB technology. There is a need to determine whether the technology is economically feasible, efficient and whether the benefits can be achieved. Case studies are presented to prove the feasibility of VSI-CHB and SSASD schemes. These studies also serve as technical background to further case studies.

Chapter 3 provides research results regarding the possibility of load side overvoltages associated with VSI-CHB systems (specific attention is given to resonance overvoltages). The general model for simulating resonance is provided. The parameters needed for analysis are defined. The model is proven with test results.

Chapter 4 describes the development of a generalized design approach for VSI-CHB and LCI systems with long cable lengths and illustrates the application with various case studies. The requirements for VSI-CHB and LCI systems with long cable lengths are determined and compared. A comprehensive case study is presented involving both technologies with several large synchronous motors and cable lengths up to 3 km.

Chapter 5 investigates ride-through for both on-line and ASD operation. A general machine model is presented to model these conditions dynamically. The overall ride-through modelling and a simplified general strategy which addresses constraints on the re-closing angle are presented.

Chapter 6 illustrates the application of the models to investigate on-line and ASD ride-through ability. Protection co-ordination and ASD design are reviewed to enhance availability and ride-through. Case studies are presented throughout.

Chapter 7 summarises the conclusions of the research, provides recommendations and suggests further research possibilities.

1.8 REFERENCES

[1.1] B. Lockley, B.Wood, and R. Paes, "IEEE Std. 1566—The need for a large adjustable speed drive standard," in *Proc. IEEE Petroleum and Chemical Industry Committee (PCIC)*, Philadelphia, PA, 2006, pp. 15–23.

[1.2] *IEEE Recommended Practice for Electric Power Distribution for Industrial Plants*, IEEE Standard 141, 1994.

[1.3] IMS Research (2008, August, 8), *Medium voltage motor drives market grows rapidly as energy prices soar* [Online]. Available: http://www.imsreserach.com

[1.4] IMS Research (2010, March), *The world market for medium voltage motor drives (Research Report)* [Online]. Available: http://www.imsreserach.com

[1.5] M. Hiller, R. Sommer, M. Beuermann, "Medium voltage drives: An overview of the common converter topologies and power semiconductor devices," *IEEE Ind. Appl. Mag.*, vol. 16, no. 2, pp. 22-30, Mar./Apr. 2010.

[1.6] National Energy Regulator of South Africa (2010, February), *Media statement - NERSA's decision on Eskom's required revenue application - multi-year price determination 2010/11 to 2012/13* [Online]. Available: http://www.nersa.org.za

[1.7] J.C. Rama, A. Giesecke, "High-speed electric drives: technology and opportunity," *IEEE Ind. Appl. Mag.*, vol. 3, no. 5, pp. 48-55, Sep./Aug. 1997.

[1.8] J. Nevelsteen and H. Aragon, ''Starting of large motors—Methods and economics,'' *IEEE Trans. Ind. Appl.,* vol. 25, no. 6, pp. 1012–1018, Nov./Dec. 1989.

[1.9] J. Bredthauer and N. Struck, ''Starting of large medium voltage motors: Design, protection and safety aspects,'' *IEEE Trans. Ind. Appl.,* vol. 31, no. 5, pp. 1167–1176, Sept./Oct. 1995.

[1.10] H. N. Hickok, ''Adjustable speed—A tool for saving energy losses in pumps, fans, blowers and compressors,'' *IEEE Trans. Ind. Appl*., vol. IA-21, no. 1, pp. 124–136, Jan./Feb. 1985.

[1.11] B. J. Chalmers, Electric Motor Handbook. London, U.K.: Butterworths, 1988.

[1.12] C. Hsu, H. Chuang, C Chen, "Power quality assessment of large motor starting and loading for the integrated steel-making cogeneration facility", *IEEE Trans. Ind. Appl., vol. 43, no. 2, pp.395-402, Mar/Apr. 2007.*

[1.13] F. Endrejat, P. Pillay, "Soft start/adjustable speed systems for multiple MW rated motors," in *Proc. IEEE Petroleum and Chemical Industry Committee (PCIC)*, Philadelphia, PA, 2006, pp. 349-358.

[1.14] F. Endrejat, P. Pillay, "The soft starters - adjustable speed systems for multiple MW Rated Motors," *IEEE Ind. Appl. Mag,* vol.14*,* no.6, pp. 27-37*,* Nov./Dec. 2008.

[1.15] F. Endrejat and J. Piorkowski, ''Multiple large motor solid state soft start, control and communication system,'' in *Symp. on Power Electronics Electrical Drives Automation and Motion (SPEEDAM)*, Capri, 2004, pp. 561-566.

[1.16] T. F. Kaiser, R. H. Osman, R. O. Dickau, "Analysis guide for variable frequency drive operated centrifugal pumps," in *Proc. of the Twenty-Fourth International Pump Users Symposium*, pp. 81-106, 2008.

[1.17] N. Granö, "Electrical drive systems, drive systems with synchronous motors (LCI)," in *ABB Industrial Manual,* Lund, Sweden, Wallin & Dalholm Tryckeri, 1998, ch. 4, pp. 365-375.

[1.18] R. Emery and J. Eugene, ‘‘Harmonic losses in LCI-fed synchronous motors,’’ *IEEE Trans. Ind. Applicat.,* vol. 38, no.4, pp. 948–954, Jul./Aug. 2002.

[1.19] R. A. Roberton and A. H. Børnes, ‘‘Adjustable-frequency drive system for North Sea gas pipeline,’’ *IEEE Trans. Ind. Appl*., vol. 34, no. 1 pp. 187–189, Jan./Feb. 1998.

[1.20] G. Duchon, W. Shultz, C. Unger, L. Voss, B. Lockley, and J. Leuw, ‘‘Experience with the connection of large variable speed compressor drives to HV utility distribution systems,’’ *IEEE Trans. Power Syst.,* vol. 15, no.1, pp. 455– 459, Feb. 2000.

[1.21] R. Guyomard, D. Dessogne, B. Martinot, E. Thibaut, “20 years of experience in VSDs for high power compressors of steam crackers,” in *Proc. Petroleum and Chemical Industry (PCIC) Europe*, 2007 © IEEE. doi: 10.1109/ PCICEUROPE.2007.4354011

[1.22] H. Walter, A. Moehle, M. Bade, “Asynchronous solid rotors as high-speed drives in the megawatt range,” in *Proc. IEEE Petroleum and Chemical Industry (PCIC)*, 2007, © IEEE. doi: 10.1109/PCICON.2007.4365799

[1.23] *Adjustable Speed Electrical Power Drive Systems, Part 4: General Requirements—Rating Specifications for ac Power Drive Systems Above 1,000 V ac and Not Exceeding 35 kV*, IEC Standard 61800-4, 2002.

[1.24] B. Wu, *High Power Converters and AC Drives*. Piscataway, NJ: IEEE Press, 2006.

[1.25] J. Rodriguez, L.G. Franquelo, S. Kouro, J.I. Leon, R.C. Portillo, M.A.A Prats, M.A. Perez, “Multilevel Converters: An Enabling Technology for High-Power Applications,” *Proc. IEEE,* vol. 97, no. 11, pp. 1786-1817, Nov. 2009.

[1.26] J. Rodrıguez, S. Bernett, B. Wu, J. Pontt, S. Kouro, “Multilevel voltage source converter topologies for industrial medium voltage drives,” IEEE *Trans. on Ind. Electron.*, vol. 54, no. 6, pp. 2930-2945, Dec. 2007.

[1.27] J. Rodríguez, J. Lai, and F. Z. Peng, “Multilevel inverters: A survey of topologies, controls, and applications,” *IEEE Trans. Ind. Electron.*, vol. 49, no.4, pp. 724–738, Aug. 2002.

[1.28] B. Wu, J. Pontt, J. Rodriguez, S. Bernet, S. Kouro, "Current-Source Converter and Cycloconverter Topologies for Industrial Medium-Voltage Drives," *IEEE Trans. Ind. Electron.*, vol. 55, no. 4, pp. 2786-2797, Jul. 2008.

[1.29] L. Li, D. Czarkowski, Y. Liu, P. Pillay, "Multilevel selective harmonic elimination pwm technique in series-connected voltage inverters," *IEEE Trans. on Ind. Applicat.*, Vol. 36, no.1, pp. 160-170, Jan./Feb. 2000.

[1.30] M. Veenstra and A. Rufer, ''Control of a hybrid asymmetric multilevel inverter for competitive medium-voltage industrial drives,'' *IEEE Trans. Ind. Appl.,* vol. 41, no. 2, pp. 655–664, Mar./Apr. 2005.

[1.31] J. O. Lamell, T. Trumbo, T. F. Nestli, "Offshore platform powered with new electrical motor drive system," in Proc. *IEEE Petroleum and Chemical Industry Committee (PCIC)*, 2005, Denver, CO, pp. 259-266.

[1.32] D. Eaton, J. Rama, P. Hammond, "Neutral Shift - five years of continuous operation with adjustable frequency drives," *IEEE Ind. Appl. Mag.*, vol. 9, no. 6, pp. 40-49, Nov/Dec 2003.

[1.33] P. Hammond, "A New Approach to Enhance Power Quality for Medium Voltage AC Drives," *IEEE Trans. on Industry Appl.*, vol. 33, no. 1, pp. 202-208, Jan./Feb. 1997.

[1.34] J. Rodríguez, L. Morán, J. Pontt, J. L. Hernández, L. Silva, C. Silva, P. Lezana, "High-voltage multilevel converter with regeneration capability," *IEEE Trans. on Ind. Electron.*, vol. 49, no. 4, pp. 839-846, Aug. 2002.

[1.35] F. Endrejat, R. Hanna, J. Shultz, "Ensuring Availability of a Large Adjustable Speed Drive for Process Gas Compressor Application Rated 11 kV, 15.5 MW (20778 hp)," in *Proc. IEEE Petroleum and Chemical Industry Committee (PCIC),* Anaheim, CA, 2009, pp. *133-139.*

[1.36] D. Eaton, J. Rama, and A. Macak, "Zero downtime—Five years of operation w/ new adjustable speed electric drive on critical non-spared compressors," in *Proc. IEEE Petroleum and Chemical Industry Committee (PCIC)*, Philadelphia, PA, 2006, pp. 225-230.

[1.37] F. Endrejat, B. van Blerk, and G. Vignolo, ''Experience with new large adjustable speed drive technology for multiple synchronous motors,'' in *Proc. Petroleum and*

Chemical Industry Committee (PCIC) Europe, 2008, Weimar, Germany, pp. 196–205.

[1.38] P. Bordignon, L. Vucetich, "Large medium voltage drives for industrial and marine applications: state of the art," in *Symp. on Power Electronics Electrical Drives Automation and Motion (SPEEDAM), Capri,* 2004, pp. 397-402

[1.39] J.T. Inge, G. H. Sydnor, R. Lubasch, H. Kobi, R. Bhatia, H. Krattiger. **"**Commissioning and operational experience for the 135000 HP adjustable speed drive at NASA national transonic facility," in *Int. Conf. on Electric Machines and Drives (IEMD)*, 1999 pp. 694 – 697

[1.40] P. Wikström, A. Terens, H. Kobi, "Reliability, Availability and Maintainability of High-Power Variable-Speed Drive Systems," *IEEE Trans. Ind. Appl*., Vol. 36 No.1, pp. 231-241 Jan/Feb 2000

[1.41] R. D. Klug, A. Mertens, "Reliability of megawatt drive concepts," in *IEEE International Conference on Technology (ICIT 2003),* Maribor, Slovenia, pp. 636-641

[1.42] R. D. Klug, M. Griggs, "Reliability and availability of megawatt drive concepts," in *International Conf. on Power System Technology (POWERCON),* Singapore, 2004, pp. 665-671

[1.43] J. Rodríguez*,* P. W. Hammond*,* J. Pontt*,* R Musalem, P Lezana, M. J. Escobar, "Operation of a Medium-Voltage Drive Under Faulty Conditions," *IEEE Trans. on Ind. Electron.,* vol. 52, no. 4, pp. 1080-1085, Aug. 2005.

[1.44] T. Trumbo, O. Forsell, J. O. Lamell, G.L. Porsby, C. Sundström, "42 kV Compressor Motor for Air Separation Plant in Sweden," in *Proc. IEEE Petroleum and Chemical Industry Committee(PCIC)*, 2002, New Orleans, LA, pp. 261-269

[1.45] O. Drubel, "Converter Dependent Design of Induction Machines in the Power range below 10MW", in *Proc. IEEE Int. Electrical Machines and Drives Conf. (IEMDC)*, 2007, Antalya, Turkey, pp. 1465-1470

[1.46] D. A. Rendusara, E. Cengelci, P. N. Enjeti*,* V. R. Stefanovic, J. W. Gray*, "*Analysis of Common Mode Voltage—"Neutral Shift" in Medium Voltage PWM Adjustable Speed Drive (MV-ASD) Systems", *IEEE Trans. Power Electron.*, vol. 15, no. 6, pp. 1124-1133, Nov. 2000

[1.47] L. M. Tolbert, F. Z. Peng, and T. G. Habetler, ‘‘Multilevel converters for large electric drives,’’ *IEEE Trans. Ind. Appl.,* vol. 35, no.1, pp. 36–44, Jan./Feb. 1999.

[1.48] J.M.D. Murphy, F.G. Turnbull, *Power Electronic Control of AC Motors*, Pergamon Press, 1988

[1.49] R.A. Gutzwiller, R.J. Gerhart, H.N. Hickok, “A 10,000 HP AC adjustable-frequency compressor drive the economics of its application,” *IEEE Trans. on Ind. Appl.*, Vol IA-20, no. 1, pp. 80-91, Jan./Feb. 1984.

[1.50] B.P Schmitt, R. Sommer, “Retrofit of fixed speed induction motors with medium voltage drive converters using NPC three-level inverter high-voltage IGBT based topology,” in Proc. *IEEE Symp. on Industrial Electronics*, vol. 2, 2001, pp. 746-751

[1.51] G. Saggewiss, R. Kotwitz, and D. J.McIntosh, “AFD synchronizing applications: Identifying potential methods and benefits,” in *Proc. IEEE Petroleum and Chemical Industry Committee (PCIC)*, 2001, Toronto, Canada, pp. 83–89.

[1.52] *Electrical apparatus for explosive gas atmospheres-Part 15: Construction, test and marking of type “n” electrical apparatus* ,IEC Standard 60079-15 (4rd edition), 2010

[1.53] R. H. Paes, B. Lockley, T. Driscoll, M. J. Melfi, V. Rowe, and S. C. Rizzo, ‘‘Application considerations for class-1 div-2 inverter-fed motors,’’ *IEEE Trans. Ind. Appl.,* vol. 42, pp. 164–170, Jan./Feb. 2006.

[1.54] W. E. McBride, R. Ellis, and C. Wylie, ‘‘Testing for application of motors on ASDs in class I, division 2 locations,’’ in in *Proc. IEEE Petroleum and Chemical Industry Committee (PCIC)*, Philadelphia, PA, 2006, pp. 279–288.

[1.55] F. Endrejat, “Power drive systems used in potentially explosive atmospheres – factors to consider,” presented at the *South African Flame Proof Association Symp.*, July 2007

[1.56] A. Luxa and A. Priess, ‘‘Switching of motors during start-up,’’ *Siemens Power Eng. Autom.*, vol. 7, no. 3, pp. 29 33, 1985.

[1.57] J. P. Eichenberg, H. Hennenfent, and L. Liljestrand, ‘‘Multiple restrikes phenomenon when using vacuum circuit breakers to start refiner motors,’’ in *Proc. IEEE Pulp and Paper Industry Conf.*, 1998, pp. 266–273.

[1.58] A. M. Chaly, A. T. Chalaya, V. N. Poluyanuv, and I. N. Poluyanova, ‘‘The peculiarities of interruption of the medium voltage motors by VCB with CuCr contacts,’’ in *Proc. IEEE 18th Int. Symp. Discharges and Electrical Insulation in Vacuum*, Eindhoven, 1998, pp. 439–442.

[1.59] *Standard for Performance of Adjustable Speed AC Drives Rated 375 KW and Larger,* IEEE Standard 1566, 2006.

[1.60] B. Lockley, R. Paes, J. Flores, “A Comparison between the IEEE 1566 standard for large adjustable speed drives and comparable IEC Standards,” in *Proc. Petroleum and Chemical Industry Committee (PCIC) Europe,* 2007, © IEEE. doi: 10.1109/PCICEUROPE.2007.4354012

[1.61] J. Rodríguez, J. Pontt, C. Silva, R. Musalem, P. Newman, R. Vargas, and S. Fuentes, “Resonances and overvoltages in a medium-voltage fan motor drive with long cables in an underground mine,” *IEEE Trans. Ind. Appl.*, vol. 42, no. 3, pp. 856–863, May/Jun. 2006.

[1.62] R. O. Raad, T. Henriksen, H. Raphael, and A. Hadler-Jacobsen, “Converter-fed subsea motor drives,” *IEEE Trans. Ind. Appl.*, vol. 32, no. 5, pp. 1069–1079, Sep./Oct. 1996.

[1.63] G. Scheuer, B. Monsen, K. Rongve, T. Moen, E. Vitanen, “Subsea compact gas compression with high speed VSDs and very long step-out cables,” in *Proc. Petroleum and Chemical Industry Committee (PCIC) Europe,* Barcelona, Spain, 2009, pp.163-173.

[1.64] R. A. Hannah, S. Pabhu, “Medium Voltage Adjustable Speed Drives – Users’ and Manufacturers’ Experiences,” *IEEE Trans. Ind. Appl.,* vol. 33, no.6, pp. 1407-1415 Nov/Dec 1997

[1.65] W. Chen, G. Gao, and C. A. Mouton, “Stator insulation system evaluation and improvement for medium voltage adjustable speed drive applications,” in *Proc. IEEE Petroleum and Chemical Industry Committee (PCIC)*, 2008, Cincinnati, OH, pp. 1–7.

[1.66] M. K.W. Stranges, G. C. Stone, and D. L. Bogh, "Progress on IEC 60034-18-42 for qualification of stator insulation for medium-voltage inverter duty applications", in *Proc. IEEE Petroleum and Chemical Industry Committee (PCIC)*, 2007, Calgary, pp. 1–7.

[1.67] S. U. Haq, "A study on insulation problems in drive fed medium voltage induction motors," Ph.D thesis, Dept. Elec. Comp. Eng., University of Waterloo, Ontario, Canada, 2007

[1.68] J. A. Oliver and G. C. Stone, "Implications for the application of adjustable speed drive electronics to motor stator winding insulation," *IEEE Electr. Insul. Mag.*, vol. 11, no. 4, pp. 26–32, Jul./Aug. 1995.

[1.69] V. Naumanen, "Multilevel converter modulation: implementation and analysis," D.Sc. thesis, Dept. Elect. Eng., Lappeenranta University of Technology, Finland, 2010.

[1.70] M. Berth, L. Küng, and E. F. D. E. Limbeck, "Switching overvoltages in motor circuits," *IEEE Trans. Ind. Appl.*, vol. 37, no. 6, pp. 1582–1589, Nov./Dec. 2001

[1.71] F. Endrejat, P. Burmeister, P. Pillay "Large adjustable speed and soft-started drives with long cable lengths", in *Proc. Petroleum and Chemical Industry Committee (PCIC) Europe,* Barcelona, Spain, 2009, pp.153-162.

[1.72] S. Yongsug, J. Steinke, P. Steimer. "Efficiency comparison of voltage source and current source drive systems for medium voltage applications", *IEEE Trans. Ind. Electron.*, vol. 54, no. 5, pp. 2521–2531, Oct. 2007.

[1.73] S. S. Fazel, "Investigation and comparison of multi-level converters for medium voltage applications," Dr. Ing. dissertation, Technische Universität Berlin, Berlin, Germany, 2007.

[1.74] E. P. Wiechmann, P. Aqueveque, R. Burgos, J. Rodríguez, "On the efficiency of voltage source and current source inverters for high-power drives", *IEEE Trans. on Ind. Electron.*, vol. 55, no. 4, pp. 1771-1782, April 2008.

[1.75] D. L. Hornak, D.W. Zipse, "Automated bus transfer control for critical industrial processes," *IEEE Trans. on Ind. Appl.*, vol. 27, no. 5, pp. 862-871, Sept./Oct. 1991.

[1.76] A. von Jouanne, P. N. Enjeti and B. Banerjee, "Assessment of Ride-Through Alternatives for Adjustable Speed Drives," *IEEE Trans. on Ind. Appl.*, vol. 35, no. 4, pp. 908-916, Jul./Aug. 1999.

[1.77] O. T. Tan and R. Thottappillil, "Static VAR Compensators for Critical Synchronous Motor Loads During Voltage Dips," *IEEE Trans. on Power Syst.*, vol. 9, no. 3, pp. 1517-1523, Aug. 1994.

[1.78] J. Gardell, P. Kumar (2008), "Adjustable Speed Drive Motor Protection Applications and Issues", Rotating Machinery Protection Subcommittee of the IEEE Power System Relaying Committee Working Group J1 report [Online]. Available: http://www.pes-psrc.org

2 TECHNOLOGY FEASIBILITY

This chapter investigates the feasibility of the VSI-CHB technology compared to the traditional LCI technology. The feasibility evaluation considers adjustable speed drive system efficiency, possible efficiency improvement areas, and energy savings. A VSI SSASD case study is presented to prove the technical feasibility, to describe the implementation of the first system on site and to provide a comparison with the LCI alternative. The case study also provides the technical system description as background to further case studies in remaining chapters focussing on system overvoltages and ride-through ability of the drive system. A wider system plant overview is also presented as background to further soft start/SSASD integration case studies.

2.1 INTRODUCTION

The previous chapter provides the benefits of applying the SSASD concept in conjunction with new VSI-CHB technology. There is however a need to determine whether the technology is feasible and whether the technical and economic benefits can be achieved.

Important aspects for evaluation in the feasibility study include the efficiency and possible energy savings. Efficiency of different medium voltage technologies is compared in [2.1] [2.3]. Energy saving principles, energy saving studies and energy saving projects associated with medium voltage drives are documented in [2.4]-[2.6]. In all these references the focus is on applications with motors rated 7.2 kV and below. Large existing fixed speed drives which may benefit from adjustable speed energy savings are often rated at ≥ 11 kV. There are also significant benefits if new project large adjustable speed motors are selected at a nominal rating of ≥ 11kV (as outlined in the previous chapter). Furthermore it is important to include the motor and auxiliaries in efficiency comparisons as well as entire power drive system in energy saving studies. There is therefore a need for

energy saving evaluations and project feasibility evaluations for large 11 kV adjustable speed motor systems.

The impact of efficiency improvement opportunities is investigated. The importance of a holistic evaluation of efficiency, energy savings, ASD benefits, the SSASD concept and system availability is illustrated by means of feasibility case studies.

One case study includes the design, installation, commissioning and initial operation experience of the first commissioned high output voltage MV VSI CHB drive for multiple standard insulation synchronous motors at a major petrochemical plant. Comparison is made to LCI systems to determine whether the proposed system is a viable alternative.

2.2 HIGH POWER AND HIGH OUTPUT VOLTAGE TECHNOLOGIES

The two main technologies (introduced in the previous chapter) which are presently available for high power (>13 MW) and high output voltage applications (> 11 kV) are compared in this chapter. The traditional LCI technology is described in [2.7], [2.8] and the modern VSI CHB technology is further described in this chapter. A typical LCI single line diagram to achieve 11 kV nominal output voltage is shown in Fig. 2.1.

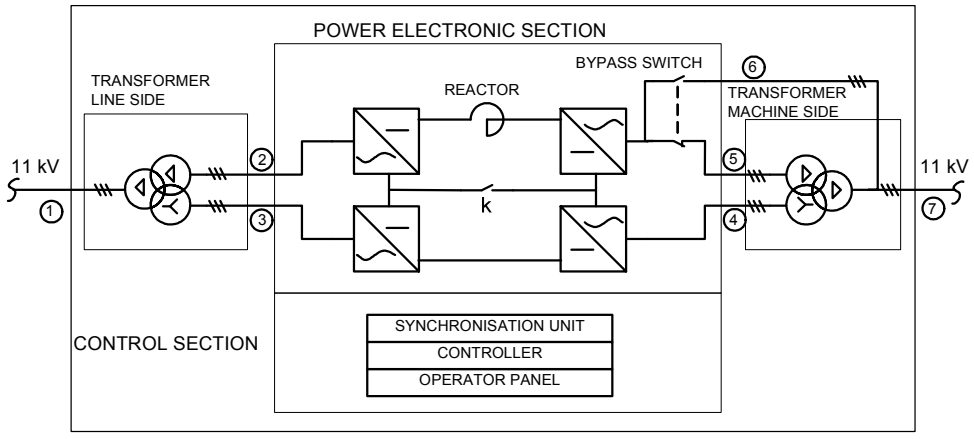

Fig. 2.1. LCI single line diagram to obtain 11 kV (phase to phase) output voltage [2.9]

A description of the diagram is given in [2.9]. The 11 kV output voltage without a step-up transformer is only offered, depending on the manufacturer, at a power rating typically above 25 MW [2.10] or 36 MW [2.11] (smaller ratings at this output voltage are normally not economical).

A VSI CHB single line diagram is shown in Fig. 2.2 [2.12].

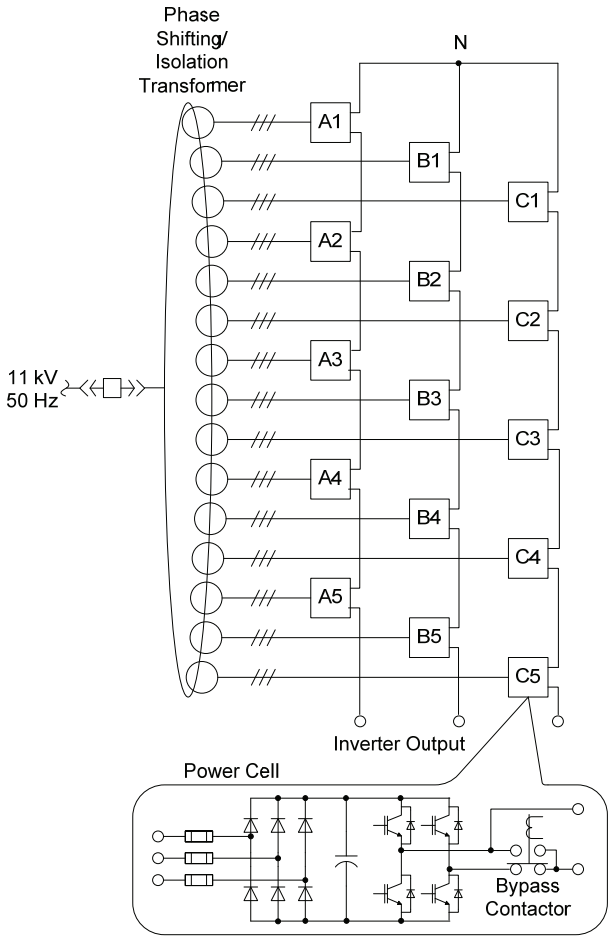

Fig. 2.2 Simplified VSI-CHB topology to obtain 11 kV (phase to phase) output voltage [2.12]

The N-1 or better redundancy in power electronic components is normally required for energy saving projects since they are often associated with critical processes. The other alternative technologies (excluding LCI) proposed to industry with claimed output voltages ≥ 11 kV do not have the facility of N-1 redundancy e.g. NPC technology in [2.13]. In these cases complete redundant converter sets (2N) with additional switchgear/reactors or

transformers are offered which normally is not economic for energy saving projects and therefore the focus of the evaluation will be on the LCI and VSI CHB bridge technologies. Further details of the VSI-CHB technology are provided in section 2.5.2.

2.3 EFFICIENCY AND POWER FACTOR

The focus of this section is not to calculate/simulate or test efficiency in great detail but rather to provide high level background information.

2.3.1 ASD Efficiency

Typical efficiency-load curves are very flat for most converters in the 40-100% load range [2.1]. Furthermore operation in the petrochemical industry typically varies between 80%-100% load. Approximate ASD efficiencies are provided in [2.1], [2.2], [2.3], [2.43] for various topologies including the VSI-CHB topology which shows that VSI-CHB efficiency compare well with other ASD topologies.

2.3.2 Motor Efficiency and Power Factor

A. Conventional Motor Technologies

Motor efficiency and power factor example curves are shown in Fig. 2.3 and Fig. 2.4 based on motor data sheet information (M: Induction Motor, SM: Synchronous Motor). M1-M4 represents 14.5 MW motors from different manufacturers. Factory test data of selected motors (M1B, SM 23 MW, SM 55 MW, SM 17 MW) are within IEC tolerances compared to the data sheet values (design data of other motors are used). It is important to note that the motor efficiency varies more between manufacturers and motor types than ASD efficiency in the previous section.

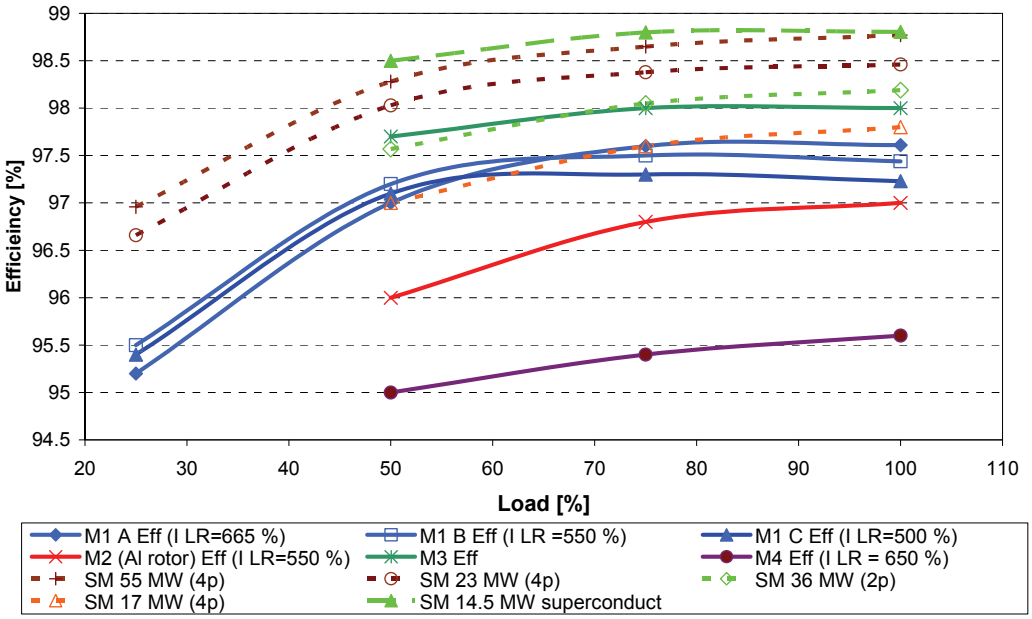

Fig. 2.3 Motor efficiency comparison

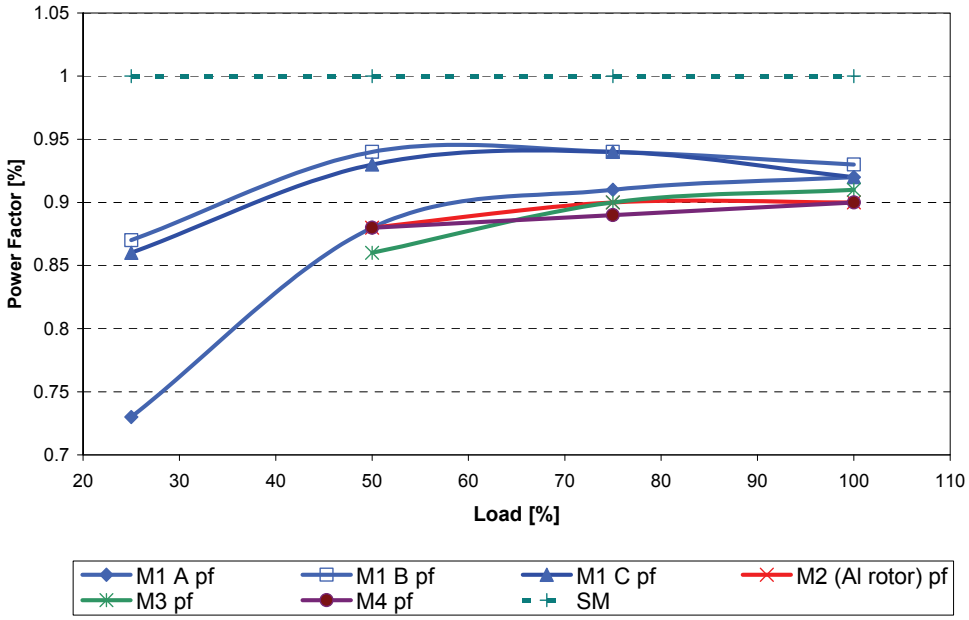

Fig. 2.4 Motor power factor comparison

Motor selection based on efficiency evaluation for new projects are therefore very important. Efficiency increases generally with motor size and synchronous motors generally have higher efficiencies but more importantly the SM can be designed for unity power factor or even leading power factor (when line operation is also desired opening the possibility of system power factor correction/improvement) which is not possible for induction motors. In the case of a purely ASD fed motor the overall input

displacement/fundamental power factor will be determined by the ASD characteristics which is typically > 0.97 p.u (over a wide load range) for VSI-CHB systems [2.8] and approximately 0.85 p.u. for LCI systems at rated load (power factor reduces with a decrease in load/speed). A higher power factor motor is mainly beneficial for VSI systems since the rated current of the ASD can then be reduced and therefore also possibly the capital cost of the ASD.

B. Alternative Motor Technologies

In [2.16] a 4.47 MW (6000 hp) superconducting synchronous motor is compared with an induction motor of similar power rating. The superconducting synchronous motor has at least 50% lower losses than the induction motor. The same assumed loss reduction applied to motor M1 A, for the purposes of illustration, results in the estimated efficiency curve shown in Fig. 2.3 resulting in the highest efficiencies of all motors. It has also been shown that permanent magnet motors with magnetic bearings can be considered for high speed MW range motors (with higher operating efficiency benefits than conventional machines) [2.17]. Conventional synchronous motors for very high power applications do however have very high efficiencies.

2.3.3 Adjustable Speed Drive System (ASDS) Efficiency

A. Losses and Loss Reduction

A comparison of losses that occurs throughout the ASDS is given in Table 2.I. The table shows that the largest potential in loss reduction exists by selecting a more efficient motor (in the case of new projects). Secondly, elimination of the step-up transformer (if applicable) has a significant loss reduction effect. LCIs at a high power rating (where a step-up transformer is not required) may therefore be a more efficient option since the additional harmonic losses associated with LCI operation is low in comparison. Magnetic harmonic losses with the VSI H bridge technology with an output reactor can be neglected due to near sinusoidal waves. A motor can be designed with a lower leakage reactance [2.18] since the higher starting current is not applicable with ASD operation with a typical loss benefit shown in the table. Optimal flux control has some benefit in reducing losses at lower loads but is not as significant as with LV ASD systems since the losses are smaller

in p.u. for the larger medium voltage machines and normally operation does not occur at low speeds and low loads. With optimal flux control ([2.19], [2.20]) the motor efficiency is not significantly reduced with lower speeds and loads (e.g. at 50% load). The table indicates possible loss reduction assuming there is no reduction in efficiency at 50 % load with optimal flux (as an optimistic approach). The loss minimisation that can be achieved is however still small compared to the losses that can be minimized by selecting a more efficient motor. The output reactor losses are small compared to overall losses. Cable loss reduction associated with elimination of reactive cable current due to unity power factor is minimal (with synchronous motors at unity power factor compared to induction motors – rated load and cable resistance values in Appendix C Table C.2.I).

Table 2.I

TYPICAL ASDS LOSSES AND POTENTIAL LOSS REDUCTION

Description - losses for a 14.5 MW load			**Loss (kW)**
Main System Components			
ASD losses (Efficiency 97.1% from [2.12])			420.5
Additional ASD auxiliary losses including cooling pumps, fans, blowers, control supply (from manufacturer)			37.1
Total ASD losses resulting in an efficiency of	96.94	%	457.6
Motor losses (Efficiency M1B 97.44 % from Fig. 2.3)			371.2
Potential Loss Reduction			
Maximum motor type loss reduction (between worst case and best case 14.5 MW motor from the efficiency graph at rated load)			491.99
Motor loss reduction between least and most efficient normal induction motors at rated load (M3 vs M4)			371.45
Loss comparison with motor lower leakage reactance at rated load (between motor M1A and M1C)			58.06
Optimal flux control at 50% load			46.71
Cable loss improvement with pf=1			2.06
Transformer losses (with transformer efficiency of 99%)			180.00
Reactor losses (with reactor efficiency of 99.8%)			31.00
Harmonic losses with LCI supply – estimated based on the principles in [2.21] and from the parameters of SM 17 MW			11.60

B. ASDS Efficiency

Overall efficiency can be estimated from:

$$\eta_{ASDS} = \eta_{ASD} \cdot \eta_{motor} \quad [\text{p.u.}] \tag{2-2}$$

Using the ASD efficiency in Table 2.I and the SM 17 MW efficiency, an overall efficiency of η_{ASDS}=94.81 % is obtained at rated load. A potential maximum efficiency η_{ASDS} =95.78% is estimated by using the maximum motor efficiency. The efficiency figures will be used later in the chapter in the energy savings case study.

2.4 TECHNOLOGY FEASIBILITY CASE STUDIES

Chapter 1 introduces the benefits of the SSASD technology and the application of the VSI-CHB technology instead of LCI technology. Case studies at a major petrochemical plant with serval large machines are used in this chapter to determine the feasibility of the VSI-CHB and the SSASD scheme. The case study machines and drive systems are also used to research the benefits and concerns associated with the technologies in further chapters. This chapter therefore also provides the necessary background to the case studies.

2.5 SSASD FOR A NEW PETROCHEMICAL PLANT (NPP)

2.5.1 Introduction

Very limited actual site application and operational experience exists for the high output voltage drives with synchronous motors. It is critical to ensure that process availability is not compromised due to new technology. Process losses associated with failures (due to ASDs) can easily negate ASD benefits. The fault tolerant operation of the ASD can be complimented, with a synchronisation, de-synchronisation and process control scheme to improve process availability (to synchronise the adjustable speed driven motor before certain drive trip conditions arise) and also to facilitate soft starting of other motors as described in chapter 1. New opportunities and benefits were identified when the multiple

motor Soft Start and Adjustable Speed Drive (SSASD) concept is applied with near sinusoidal high output voltages with the capability to synchronize and de-synchronize Synchronous Motors (SMs) safely to multiple utility sources [2.22]. Benefits include significantly reduced capital cost of equipment, improved waveforms, energy savings, improved process controllability, reduced system stresses, reduced hazardous area requirements, improved power factor control and improved condition monitoring, whereof some are explored in further detail in this chapter.This chapter describes the design, installation, commissioning and initial operation experience of the first commissioned high output voltage MV VSI CHB drive for multiple standard insulation synchronous motors.

2.5.2 System Description and Design

A. Project Overview

Adjustable speed operation for a process gas compressor 1 (C1) is required for initial process start-up, energy savings and optimized normal process operation. The process also requires Compressor 2 (C2) and Compressor 3 (C3) motors that need to be soft started. The partial plant single line diagram is shown in Fig. 2.5. The motivation for the SSASD system was based on the reduced switchgear fault level and busbar voltage drops which would not have been possible with the DOL start-up of the large motors. The only alternative to the SSASD concept would have been a dedicated starter of the adjustable frequency type and a dedicated ASD associated with significant additional capital cost and disadvantages as outlined in chapter 1. Furthermore the project requires a high availability which required redundancy in most drive system components especially since many of the components have not yet been proven in the field. The SSASD concept was selected to improve availability further as described in Chapter 1.

B. System Components

1) Adjustable Speed Drive: The topology is shown in Fig. 2.2 with 1375V / 800A cells. Five cells per phase were selected to obtain the rated bus voltage even when one cell has

failed to allow successful synchronization of the ASD and subsequent off-line cell replacement without any production loss. The cell bypass principles are outlined in [2.23].

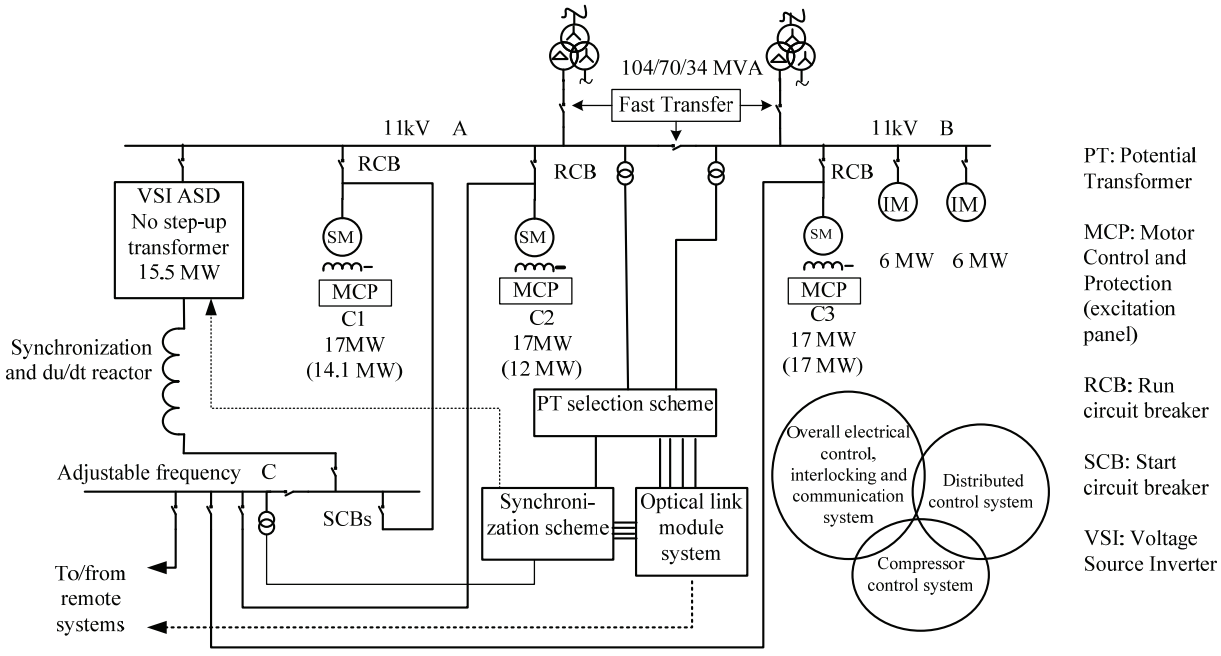

Fig. 2.5 Single line diagram of SSASD system (figures in brackets represent maximum load)

2) Motor Excitation Control and Protection: The AC excitation system for each motor is designed with comprehensive redundancy including dual three phase, phase angle fired controller modules (with thyristors and explained in further detail in Chapter 6), dual PLC processors and dual I/Os. A block diagram is given in Fig. 2.6. Excitation control modes for line operation include power factor, fixed excitation and VAR control. The normal operation for the line operated motors is in leading power factor control mode (maximum 0.9 leading at rated power) to compensate for lagging power of induction motors and to keep the overall plant power factor close to unity. The ASD, control and excitation panels are shown in Fig. 2.7.

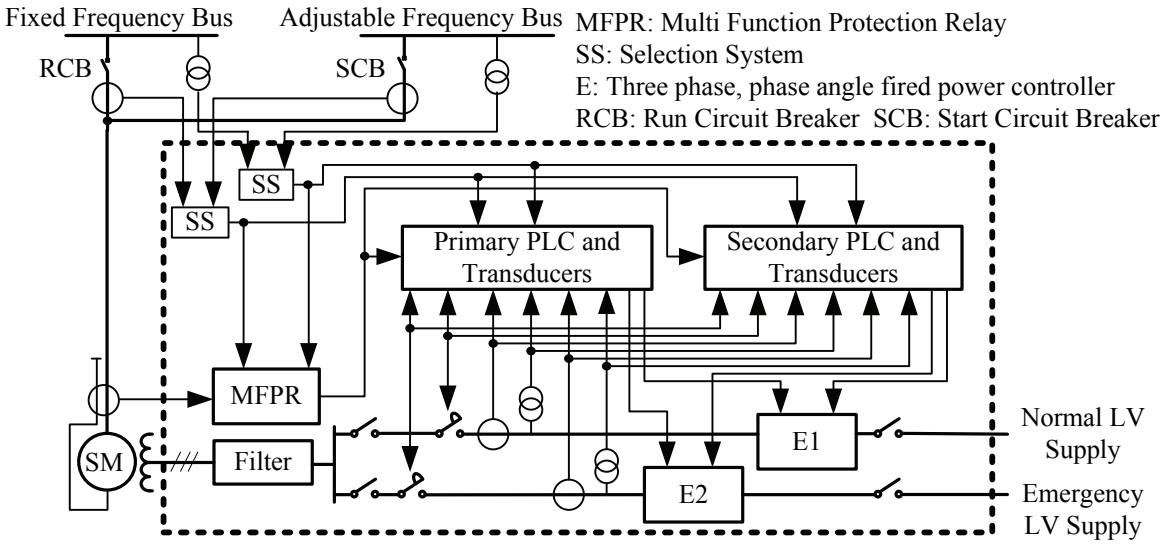

Fig. 2.6 Simplified motor excitation and protection panel block diagram [2.12]

Fig. 2.7 Adjustable speed drive (left), excitation and control panels (right)

3) Synchronous Motors: In general, for the selected converter topology, no special design criteria for motors are required in addition to the AC exciter and electrical requirements to suit the process [2.24]. This is due to near sinusoidal waveforms throughout the operating range. One of the motors is shown in Fig. 2.8. The motor (totally enclosed, self ventilated,

water to air cooled) is cooled with 2x70% tempered water coolers to allow for operation without a trip under most conditions when only one cooler is available.

Fig. 2.8 Synchronous motor during site testing

4) Control System and Safety Overview [2.12]: The overall system (Fig. 2.9) is designed with specific attention to safety, redundancy and process availability. The master control system has dual processors. All PLC systems are based on deterministic intercommunication busses within each cabinet with the standard manufacturer redundancy scheme. Communication busses are used as far as possible to minimize hardwiring. System interconnection external to cabinets is mainly via fibre optic Industrial Ethernet connections. The system is designed such that a failure in an Ethernet connection does not result in a trip during normal operation. A safety review has identified the required hardwired connections for example interlocking between breakers. Furthermore a hardwired and key interlocking scheme is in place between input and output breakers and the SFC cabinet. Selected control signals are 4-20 mA (redundant). Emergency trip signals from the process are fail safe hard wired. Information communication to the control room is also provided via fibre optic Ethernet communication for full system monitoring and alarming. Critical information and alarm signals are provided via a deterministic communication bus to the process control system for prompt action, for example to allow, where possible, synchronization prior to drive trips. Effective fault analysis can be performed by tracking PLC state machine operation history.

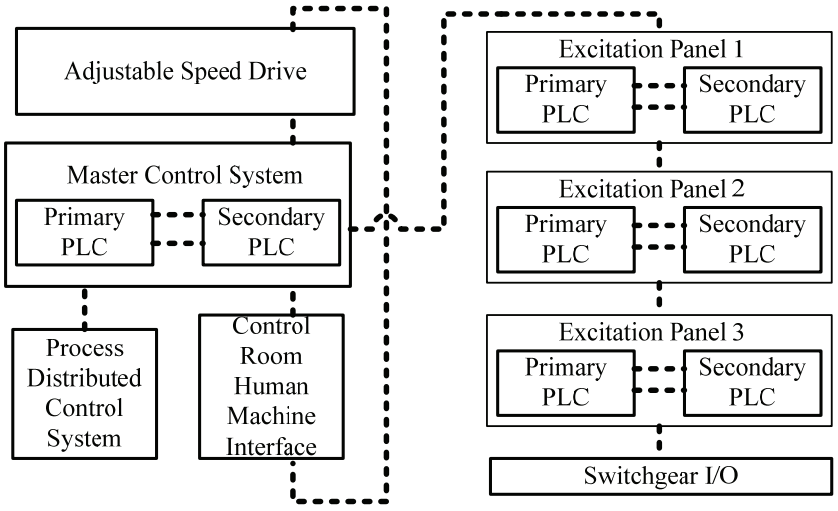

Fig. 2.9 Simplified system PLC block diagram [2.12]

2.5.3 Protection and Advanced Control

The topology has mainly been used in the past for induction motor applications and further protection and control functions for multiple bus synchronous motors were developed.

A. Overall Electrical Protection Functions

The protection functions as implemented from an overall protection and co-ordination study are shown in Table 2.II [2.12]. The philosophy is to obtain main and back-up protection for the drive input (transformer and power connections to the cells) and motor. Specially developed functions for this project included a modified process tolerant protection scheme [2.12], SFC synchronous motor out-of-step protection, exciter rotor diode fault protection (based on the detection of impedance changes outside acceptable ranges) and rotor thermal protection which is adjusted with the operating speed due to reduced cooling at lower speeds (no forced cooling) [2.12].

Table 2.II [2.12]

SYSTEM PROTECTION FUNCTIONS

Description	Input Protection	Motor Protection	
		Drive Operation	Line Operation
Switchgear	Overcurrent (definite time & IDMT curve), directional earth fault (definite time residual & core balance), under voltage	N/A	Non and directional overcurrent (definite time & curve), directional earth fault (definite time residual & core balance), under voltage, overvoltage, pole slip/under impedance
Excitation panel	N/A	Minimum field, field overload/overexcitation, motor diode fault (exciter circuit impedance variation detection)	
	N/A	Rotor I^2t (adjusted with speed)	Rotor I^2t
	N/A	Additional Stator I^2t (adjusted with speed)	Earth fault
	N/A	Additional stall protection (by means of lagging speed detection from reference)	Limitation in accordance with motor capability curve
Excitation panel relay	N/A	Motor differential, mechanical jam, restart block, reactive power, stator thermal model with RTD biasing, unbalance, phase reversal (selected for required variable frequency I & V accuracy sensing)	
SFC	Reactive power, differential real power, instantaneous overcurrent, undervoltage, overvoltage	Standard protection as per IEC & IEEE, modified process tolerant protection (allows synchronization prior to drive trip), transformer and reactor thermal protection	N/A

B. Multiple Bus Synchronization [2.12]

The feasibility of the SSASD concept is heavily dependant on the correct functioning of the new synchronization system. Synchronization principles and methods for up and down transfers of motors to and from a single bus are described in [2.25]. Previously the manufacturer internal synchronous transfer scheme only allowed transfers to the same bus from where the ASD is fed. Internal sensors to synchronize the drive output with the drive input are usually used. This application requires synchronization also to a different bus in

accordance with the single line diagram (Fig. 2.5) (due to different transformer incoming and possible loading conditions). Options for synchronisation are provided in chapter 1. It was decided to customize and further develop the manufacturers make before break scheme to cater for synchronous motors and multiple busses. The scheme uses a synchronization reactor and is generally associated with smoother transfers [2.12]. Multiple busses may also be required for other applications e.g. when two SFCs at different locations are used as back-up for each other (as discussed later in this chapter). An external synchronization relay is used to communicate the voltage phase and amplitude difference of the remote bus (e.g. the B bus) compared to the bus from where the ASD is fed (A bus). Logic is incorporated into the system to select the correct potential transformers for the required condition. The relay is also used as a synchronization check with a hardwired permissive contact to allow the closing command to be given to the breaker only when a real synchronism condition exists (avoiding the possibility for example of a communication link error).

The selected ASD is a 2 quadrant drive with no re-generation capability (unlike LCIs). The power during synchronization (up or down transfer) should therefore flow from the ASD to the bus being synchronized to with a positive angle ($\delta>0$) in accordance with the following approximation (neglecting resistance) [2.26]:

$$P = \frac{3 \cdot |V_C| \cdot |V_B|}{|X|} \cdot \sin(\delta) \tag{2-3}$$

where X is the reactance of the synchronizing reactor and V_C, V_B represent the bus voltages in Fig. 2.5. By default the ASD would synchronize its output voltage with its input voltage. Successful up-transfer of the motor to the remote bus requires the ASD to have its phase input reference equal to the remote bus. The ASD internal programming structure requires a positive reference angle (compared to the input of the ASD) that includes the difference between the A&B busses (leading or lagging) and an additional angle to promote power flow out of the ASD. The ASD phase reference convention in this case is opposite (phase V_B-Phase V_A) compared to the synchronizing relay (phase V_A-phase V_B due to project connections) and therefore needs to be negated. An overall negative signal is possible to occur, but with an addition of 360 degrees, a positive signal will always be

obtained reflecting the required angle. The phase reference signal can therefore be expressed as:

$$\delta_{ref} = \delta_{offset} - \delta_{sync} + 360^{o} \tag{2-4}$$

where δ_{ref} is the reference angle to the drive input, δ_{offset} the offset angle for positive power flow and δ_{sync} the angle difference between the drive input and output to obtain output synchronism with the remote bus. The maximum synchronization angle difference between the C and B bus is determined by considering the selected tolerance accuracy angle ($\delta_{tolerance}$) of the control system:

$$\delta_{m} = \delta_{offset} + \delta_{tolerance} \tag{2-5}$$

Finally a synchronization check angle (δ_{sync_check} monitored by the synchronization relay) is set slightly above δ_m. A graphical representation is shown below:

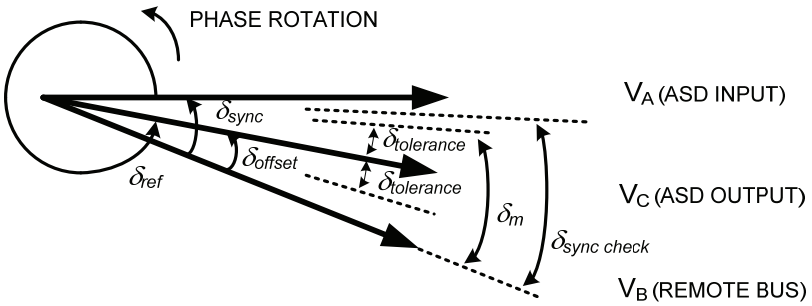

Fig. 2.10 Synchronization vector diagram example

An indication of the rms synchronizing current can be calculated from:

$$|I| = \frac{|V_C - V_B|}{|X|} = \frac{\sqrt{|V_B|^2 + |V_C|^2 - 2 \cdot |V_B| \cdot |V_C| \cdot \cos(\delta)}}{|X|} \tag{2-6}$$

IEEE Std 1566 [2.27] states that the utility current shall not rise above 120% of the motor rated current during up transfers and also that the drive current shall not rise to more than 120% of the motor rated current during down transfers on a transient basis (IEC standards do not provide specific requirements [2.28]).

Considering (2-6), δ=7.3^o for 120% current with X=0.106 p.u. (17 MVA base). The reactance value is taken is taken from the phase with the lowest reactance from the factory test certificate of the reactor (this results in the most conservative approach and associated allowable angle). In the case of this reactor, the reactance values of each phase were very close to each other and the maximum tolerance error was -0.75% (Phase A) compared to the design specification value of the reactor which had a tolerance specification of ±5%. In cases where only design values are known, the specified tolerance should be taken into account in the calculations. Furthermore, the reactor is a 3-phase structure, instead of three single-phase units, which means there may be a difference in inductance of the centre leg with respect to the outer legs which may need to be considered and some statistical mean should be applied to determine a realistic value of X. This was however not performed in this case since the reactance values of each phase were very close to each other and to the design specification (from the test certificate). It is assumed that ($\delta_{tolerance}$) is also large enough to compensate for reactor parameter variation with temperature.

Similarly the angle is approximately the same for the differential network current associated with the motor being connected to the line since the effective motor reactance is approximately the same as the reactor reactance. It is not fully clear what [2.27] defines as a transient basis. It has however been verified that the worst case estimated transient asymmetrical peak inrush current is within the drive system capabilities.

In [2.29] estimation is given based on ANSI standards for safe motor transfers (for break before make schemes associated with induction motors):

$$\delta_m = \arccos\left(\frac{|Ev_C|^2 + |Ev_B|^2 - 1.33^2}{2 \cdot |Ev_C| \cdot |Ev_B|}\right) \tag{2-7}$$

where Ev is the vectorial V/Hz. δ_m=72° for Ev_c and Ev_B= (1.1/0.98) p.u. representing a worst case condition with maximum expected network overvoltage and frequency variation. Even though the equation is for break before make abnormal conditions (fast transfer switching) it gives an indication that the 120% current is very conservative in terms of motor disturbance. (δ_{offset} was selected as 2° with $\delta_{tolerance}$ as 3° as a conservative starting point considering the ratings of the adjustable speed drive system). This results in a possible maximum δ=5° from (2-6) which is within the requirement of [2.27]. In cases where the synchronizing conditions can not be met for compressor C1 (the machine with adjustable speed capability), the synchronization process will time-out without causing a trip. Transfer conditions are studied in further detail in Chapter 5 & 6 with a focus on synchronous machines and transfers following faults.

C. Shaft Voltages, Bearing Insulation and Common Mode Voltages

The VSI-CHB topology is superior to most other VSI technologies regarding the generation shaft voltages [2.24]. The minimum configuration required to avoid detrimental effects of shaft voltages and bearing insulation for the selected converter topology is an insulated bearing [2.24] which is also implemented for this application. It has been shown in [2.35] that significant common mode voltages do exist with the selected topology especially between secondary windings of the transformer and ground but also at the motor. Furthermore for this case common mode voltages will also exist between the reactor and ground. The transformer and reactor have therefore been designed to cater for increased voltages [2.12].

D. Hazardous Area Considerations

The process plant hazardous area classification requirement for the motor in terms of IEC 60079 is defined as zone 2, temperature class T3 and gas group IIC (most sensitive gas group with lowest ignition energy). Exn(A) motors were accordingly selected.

1) Ignition Energy: The synchronization reactor and cable capacitance serve as a filter with anticipated near sinusoidal voltages at the output of the reactor and at the motor terminals (evaluated in detail in chapter 3 and 4). An output reactor, in the form of three

single phase inductors, acts as an effective common mode voltage filter [2.31] resulting in minimum shaft voltage with a stored energy below the ignition energy of the hazardous area in accordance with the principles outlined in [2.32]. The shift in the motor neutral voltage is then minimized and therefore the risk associated with possible inadequate creepage distances/ clearances (related to the neutral) is not significant and compliance with [2.33] and [2.34] is also achieved.

In systems without the common mode reduction effect of single phase reactors (e.g. when no reactor is used or when a 3 phase reactor is used), motor common mode voltages may be almost eliminated with a revised modulation strategy [2.35] and therefore the shaft stored energy will also be minimized for hazardous areas. A further benefit of this strategy is that other common mode voltages throughout the system are also minimized. This is not the case with LCI systems as shown in [2.36]. Additional precautions might therefore be required for LCI systems, e.g. an internal shaft brush of the electrostatic type [2.37] may be considered.

Requirements have been introduced in edition 3 of IEC-60079:15 [2.33] which required a risk assessment for potential stator winding discharge for all machines rated above 1 kV. The recently published edition 4 suppressed the requirements of a stator risk assessment but specifies that a steady state ignition test or "incendivity test" be performed to minimize the risk of occurrence of arcs or sparks capable of creating an ignition hazard during conditions of normal operation [2.34]. Possible air gap sparking risk assessment is still excluded due to the S1 continuous duty [2.34] (the motors are in any case always soft started – no DOL starts). The stator risk assessment was performed since the project was completed prior to the release [2.34] with results shown in Table 2.III. The sum of factors is greater than 6 and therefore additional measures were required for example pre-start ventilation/purging.

A purging system was however not regarded as essential by the manufacturer (at the manufacturing stage) due to soft starting and near sinusoidal waveforms. Ignition is most probable from short term discharges that occur as a result of switching transients, particularly those associated with motor starting conditions [2.33]. DOL starting is not applicable with converter operation reducing the likelihood of ignition significantly and it

is suggested that specific revised requirements for converter operation are added to the standard. A purging system was nevertheless installed during the installation period based on uncertainties of requirements that may have followed in edition 4 of IEC 60079-15. It is however shown in [2.38] that motors of up to 13.8 kV which are correctly designed for the hazardous area specification have successfully passed the steady state ignition tests. Future projects with VSI-CHB systems and similarly rated motor voltages, when correctly designed and tested, are therefore feasible and should therefore not require additional measures to comply with [2.34].

2) Thermal Considerations: The near sinusoidal output waveforms eliminates increased heating or hotspot concerns associated with harmonics produced by the converter. In LCI systems this additional heating due to harmonics is significant and extra caution with the motor design is necessary that normally results in a motor specially designed for the LCI application [2.39]. Also purging systems or Ex(p) motors may be required since rotor temperatures can reach very close (or exceed) to the T3 rating (200 ^{o}C) [2.39]. A purging system based on thermal considerations is therefore not required for this project. In the case of LCI systems, to obtain additional safety, a further challenge is that internal surfaces should cool down to less than 200 ^{o}C during the rundown period [2.39]. This is in case of a simultaneous gas leak and sudden loss of pressurizing air. The proposed system therefore provides improved protection for hazardous areas especially in the case of a failure of the purging system.

Table 2.III

STATOR WINDING DISCHARGE RISK ASSESMENT

Characteristic	Value	Factor
Rated voltage	11 kV	4
Average starting frequency	< 1 / week	0
Time between detailed inspections	4 years	1
Degree of protection (IP Code)	IP 55	1
Environmental conditions	Outdoor	1
Sum of factors		7

Other VSI topologies need further evaluation do determine the ignition and/or thermal risk associated with their output waveforms since the tests in [2.34] only covers sinusoidal waveforms. This is the topic of a future paper [2.40].

E. Reduced Flux Operation

The V/f (or flux) ratio and associated field current reference is automatically adjusted according to the load and speed (taking dynamic requirements into consideration) to minimize rotor thermal loading as described in [2.12] and also to ensure temperatures within the T3 rating.

2.5.4 Project Execution Experience and Considerations [2.12]

A. Design and Evaluation

Extensive front end (conceptual and basic engineering) work has been performed including network studies (load flow, short circuit, stability and harmonic analysis) and development of the system specifications to select the motor starting method and drive technology. The detail engineering phase included the development of a comprehensive system functional design specification with the associated complete system design. The design phase included the studies recommended in [2.27]. A project cost evaluation has indicated that the proposed VSI system cost is approximately the same as the alternative LCI system cost (considering a cable cost saving with the VSI system and the saving associated with a standard motor design instead of a motor design suitable for LCI operation).

B. Factory Acceptance Testing

In addition to the SFC heat-run test (with integrated transformer and external reactor) a comprehensive system functional test was performed including excitation panels, PLC panels and ASD operation with a small test synchronous motor to minimize possible rework on site. The ideal would have been to test the system with at least one of the actual motors since this combination has never previously been tested. The motor manufacturer and SFC manufacturer are located in different countries and the duration to ship the SFC

system to the motor manufacturer (or vice versa) posed a challenge on the project schedule and all parties were prepared to take the risk of addressing potential compatibility problems on site since possible site modifications should not require major hardware changes but probably significant control system optimization. One excitation panel (small item compared to the SFC) was however flown in to the motor factory and was functionally tested in combination with the motor following completion of the standard motor tests.

C. Installation

1) Cable Installation and Connections: Table 2.IV shows that the number of cables required for connection to the SFC cabinet is significantly smaller with the proposed system than with a conventional LCI system described in [2.9] of similar rating which requires step-up and step-down transformers for 11 kV application. This made the cable connections and external installation significantly easier than the LCI installation which was challenging even with the cables sized for an intermittent duty as calculated in [2.9]. This is mainly due to the increased current associated with the LCI operating at a lower input and output voltage. A continuously rated LCI system will have even more demanding cable installation work.

The ampacity calculations indicated that 4 x 11 kV single core 500mm^2 cables per phase are required between the substation and motor for the adjustable speed driven motor (C1) (550m distance between substation and motor). This is already demanding from an installation and termination point of view (see Fig. 2.8) for example at the motor terminals and the standard switchgear only allows for 4 terminations per phase). An alternative drive technology with an output voltage of 6.6kV (next standard lower voltage) would have resulted in the requirement of at least 1.67 times more copper (disregarding voltage drop considerations) and at least 3 additional single core cables per phase making the installation and termination of cabling extremely challenging. The additional cabling cost is significant and estimated as 21% of the cost of the SFC used for this project (considering 2008 USD/EUR/ZAR exchange rates). Furthermore pure soft started motors would have required a step-up transformer at the drive output to match the 11 kV switchgear voltage (lower switchgear voltage ratings results in unacceptably high busbar currents). Also, for

SSASD schemes, a step-up transformer would have been required to facilitate up and down transfers for the adjustable speed driven motor.

2) Substation and Transformer: The substation has a dedicated room for the drive system, excitation and control panels. Design considerations include the large transformer (housed in the highest cabinet section in Fig. 2.6) weight of 31.8 tons (74% of total ASD weight) with a specially designed removable roof section directly above the transformer to facilitate crane access. This was effective during installation and similarly it should be effective also for future removal of the transformer in the unlikely event of a serious failure (a spare transformer was procured as part of the project since it is a single point of failure).

Table 2.IV

COMPARISON OF SFC CABINET CABLE CONNECTIONS

Description	**LCI (12 pulse)**		**VSI CHB (30 pulse)**
Rating (MW)	15		15.5
Input/output voltage (kV)	3.03		11
Stepdown/isolation transformer (kV)	11/3.03 (external 3 windings)		11/1.38 (integrated 16 windings)
Step-up transformer (kV)	3.03/11 (external 3 windings)		N/A
Duty	Continuous	Intermittent (5 starts per hour)	Continuous
Number of single core 500mm^2 cabinet input cables	24	12	6
	(between step-down transformer and cabinet input)		(between 11 kV switchgear and cabinet input)
Number of single core 500mm^2 cabinet output cables	30	15	6
	(between step-up transformer and cabinet output, including transformer bypass cabling for pulse mode operation)		(between 11 kV switchgear and cabinet output)
Total number of cables connected to SFC cabinet	**54**	**27**	**12**

D. Site Testing and Commissioning (STC)

Important aspects and lessons learned regarding STC are highlighted (not all tests are described). This chapter only provides an overview of tests required as a prerequisite for

further tests. The detailed tests, associated with the research objectives are described in remaining chapters.

1) Pre-commissioning: Injection tests were done throughout the system to ensure correct phasing and polarities of all external SFC CTs and PTs. The ASD cooling water system posed some challenges during and following pressure testing with a pipe leak detected close to the mixing valve. This has occurred even though the system has passed pressure testing during the factory testing and therefore it was decided to do X-ray tests throughout the critical piping areas to minimize the risk of occurrence of future leaks. Minor additional welding was required.

2) Energisation and Open Loop Test: A failure has occurred a few days after the drive has been energized following the standard open loop tests. The root cause was a minute water leak in a cell cold plate (manufacturing defect), which caused a dc link flash-over that has progressed to the power connection area (between the transformer and the cells). The fault was cleared by switchgear back-up protection. The event justified further research to enhance ride-through also during normal operation associated fault conditions and is further discussed in chapter 6.

3) No-load Test (Compressor Uncoupled): This was the first time motors were connected to the ASD. The synchronous motors did not have any field protection circuitry since the drive loss of field, unbalance and overcurrent protection functions were regarded by the manufacturer as sufficient to protect against possible overvoltages from being generated in the field circuit during ASD operation. During line operation the out-of-step, undervoltage and minimum field protection was regarded as adequate to prevent overvoltages from being generated since a trip would occur prior to the out of step condition and the associated generation of overvoltages. It was not possible to have optimized control and protection settings for the very first start since fine tuning based on operating experience still had to be done.

Damage to machine exciter diodes have occurred directly after the first start. The diode fault monitoring function has correctly detected a faulty diode condition and the start was aborted on the second attempt. Subsequently the rotating exciter diodes were replaced and

the exciter was also fitted with overvoltage protection ("crow bar circuit"). All settings have also been reviewed and slightly been revised. No further failures have occurred following the modifications. It is however recommended to incorporate improved out-of-step protection functions in the ASD considering the frequency variation, since it is difficult to determine the optimal ASD settings to ensure a trip prior to the occurrence of dangerous overvoltages. Field winding overvoltage protection is recommended in all cases. A typical start-up recording is shown below in Fig. 2.11 illustrating the characteristics, considerations, and a smooth startup recording (low starting current).

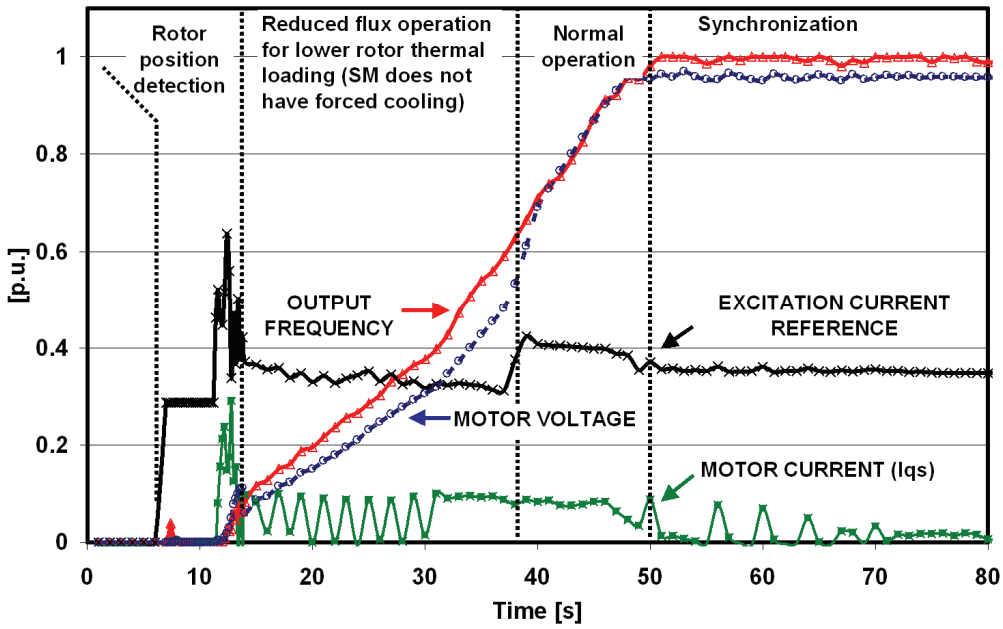

Fig. 2.11 NPP SSASD startup recording (no-load).

4) Load Test (Compressor Coupled): Load testing generally went well with typical fine tuning that was required on both the compressor and ASD control system. The thermal protection model has adequately detected process overloading (prior to process optimization) and has tripped the motor prior to any damage.

5) Redundancy Tests: Failures were practically simulated for all redundant components/systems including exciter supplies and ride-through was achieved (after fine tuning in some cases) for all cases with and without load.

2.5.5 Performance Evaluation and Optimisation

A. Efficiency and Power Factor

The efficiency and power factor determined during the factory acceptance test for the SFC (including the transformer and reactor, excluding the excitation panels) at 100% speed (and loads 25%-100%) were at least 97.1% and 0.97 p.u. respectively. The efficiency is slightly lower than typical LCI values (but approximately equivalent when a step-up transformer for the LCI is used) as previously discussed but the power factor is significantly higher as expected due to the features of the topology [2.41]. The power factor values slightly exceeds initial expected results and on site measurements resulted in an average power factor of 0.976. The small efficiency difference (between LCI and VSI) results in a minimal difference in total energy savings since the bulk of the energy savings are associated with adjustable speed control instead of dissipative flow methods (discussed in section 2.5.7). No additional power factor compensation is required to compensate for poor power factor – this may in some cases be required for LCI systems.

B. Waveforms and Harmonics

1) Output: Initial sites tests have indicated that under certain conditions the output waveforms are indeed unacceptable even with the features of the CHB topology due to long cable distances as introduced in chapter 1. This confirmed the need for dedicated research which is provided in chapter 3 and 4.

2) Input: Drive input waveforms (voltage and current) are near sinusoidal. The current Total Harmonic Distortion (THD) generally increases with a reduction in speed and/or reduction in current [2.12]. The THD is lower than 2.07% above 50% load and 80% speed (i.e. the operating range). The THD is significantly less than with a LCI (without filters) and complies with industrial standards e.g. IEEE Std 519. The input harmonics increase with the number of cells bypassed as shown in [2.23]. Only one cell should however be in the bypassed state and only for a short time due to the synchronization/SSASD scheme. The short duration under operation with one cell bypassed does not pose any expected problems since the harmonics are even then still below values permitted by IEEE Std 519 with a five cell configuration [2.23].

C. Synchronization Performance

The single line for the transfers is given in Fig. 5.4. The ASD current was measured at the output of the ASD from the ASD current transducer. The "Run Circuit Breaker" current was measured from the CT on the RCB (Fig. 5.4). The up and down transfers were successful for most conditions, but during initial process instabilities during full load it was necessary to increase δ_{offset} to 3^o and $\delta_{tolerance}$ to 4^o resulting in a maximum $\delta=7^o$ to ensure successful consistent transfers (within 60 s). Typical synchronization recordings are shown in Fig. 2.12 showing typical transient currents (within safe limits according to motor transient withstand capability and the drive ratings). Voltage waveforms were checked with a synchroscope and phasing stick probes (over the RCB) to be within limits (angle between the waveforms prior to transfer command). Furthermore a permanent synchronisation check relay is used during synchronisation to verify that the difference of voltage waveforms are within the angle limits as shown by $\delta_{sync\ check}$ in Fig. 2.10. The theoretical worst case current may be larger than the value stipulated in [2.27] but even under this worst case condition, the ASD and motor ratings capabilities are not exceeded in accordance with the theory in section 2.5.3. Transient currents during down transfers are not significant (and not shown), since the ASD accurately locks the frequency with the motor feedback voltage.

There is a significant period when the start circuit breaker and the run circuit breaker are both closed as shown in Fig. 2.12. During this time, power will flow from the drive into the AC mains. The ASD output current is near sinusoidal as previously explained and therefore other equipment on the bus should not be affected by unacceptable high frequency harmonics. The amplitude of this current is limited by ensuring the $\delta_{sync\ check}$ angle is not exceeded (in which case transfers will not be allowed). The ASD current is phased back to ensure that machine current is transferred and sourced from the mains supply before the ASD is stopped and the start circuit breaker opened (as shown in Fig. 2.12). Undesired arcing in the start circuit breaker and an unacceptable over voltage condition at the drive dc bus terminals are therefore avoided. Circuit breakers and the ASD are therefore not expected to age prematurely.

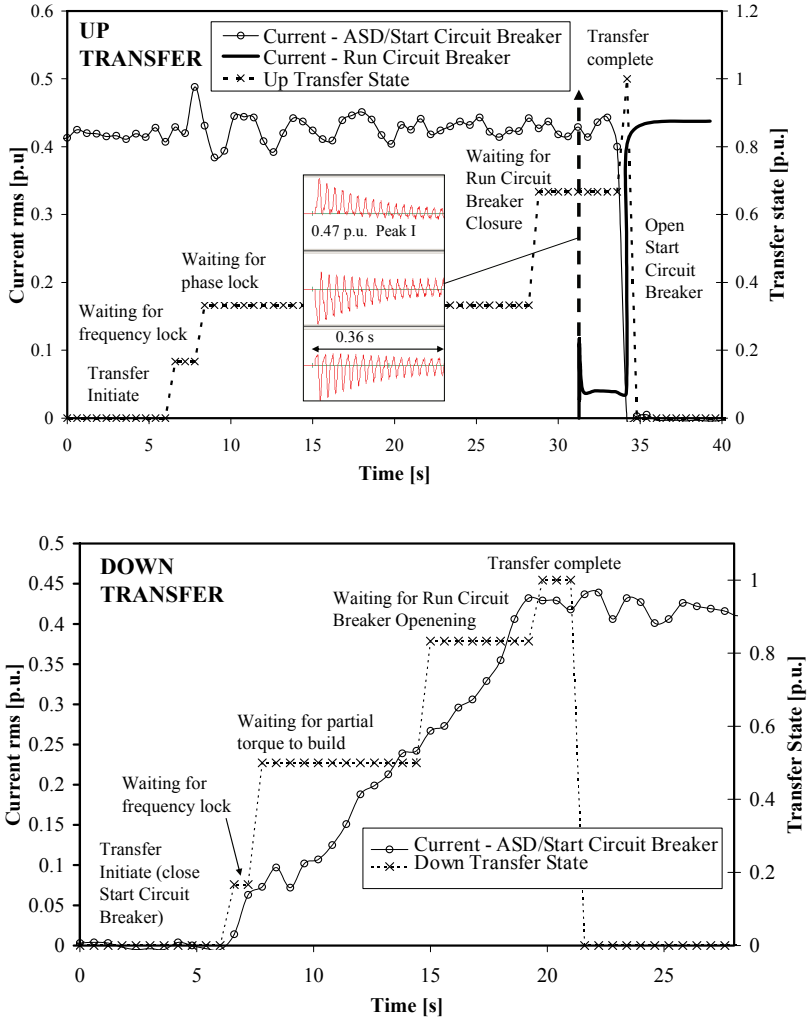

Fig. 2.12 Typical up and down transfer recordings

D. Ride-through Performance

Ride through is of critical importance since any incident where the ASD or SMs can not ride through an internal or external electrical disturbance results in major production losses. In selected cases ride-through was not possible. Chapters 5 and 6 are therefore devoted to ride-through research, theory, tests and experience.

2.5.6 Capital Cost Comparison

The capital expenses are significantly less with the SSASD (Table 2.V) compared to the conventional solution of a dedicated soft starter and dedicated ASD. The p.u. cost for all cost evaluations is defined as the cost of a 15.5 MW SSASD unit (i.e., 1 p.u.) [2.30].

Table 2.V

COST EVALUATION OF A STANDARD VERSUS SSASD SYSTEM

Description	Cost (p.u.)	
	SFC and ASD	SSASD
Soft Starter (SFC type)	0.72	
SSASD		1.00
Adjustable Speed Drive (VSI)	0.92	
Switchgear (variable frequency bus)	0.28	0.32
Control system	0.10	0.13
Additional civil/room costs	0.10	
Total	**2.11**	**1.45**

2.5.7 Energy Savings and Economics

The project in this case study has the requirement of optimal soft starting and ASD operation on one compressor as previously discussed and it is shown in the previous section that the SSASD option is the most cost effective. In addition there is the benefit of energy savings. In certain projects the only benefit may be energy savings and therefore this section evaluates the feasibility of a SSASD system purely for energy savings.

C. Energy Saving Determination

Centrifugal compressors are in many cases good candidates for energy saving with the use of ASDs where the flow required varies significantly from the rated value for significant periods. An explanation of the compressor operation and the physics behind the energy savings are given in [2.4], [2.5], [2.42]. The determination of energy savings requires input from all engineering disciplines. Operation principles for the specific compressor in this case study are discussed in in [2.43]. Furthermore the actual compressor curves and calculations are provided in [2.43] to justify an average effective mechanical energy saving of at least 2 MW (nominal load power is 14.1 MW) by using ASD control instead of

dissipative throttling and recycling flow control. This energy saving is associated with an average effective motor speed of 90.5% (normal situation).

D. Economic Evaluation

Load shifting is sometimes possible in industry and significant load variation with time can occur. In addition to energy savings, load shifting schemes should be considered with typical time of use tariffs. In petrochemical industries load shifting is not always possible and energy savings can continuously be achieved where applicable (e.g. instead of dissipative flow methods). In many cases it will be required to expand the study with time of use cost variation due to daily and yearly load variation. In this case an average effective power reduction of 2 MW (based on the previous section) is used for the purpose of a basic economic evaluation for illustrative purposes. The time of use tariff for industrial users in South Africa (with a notified maximum demand >1 MVA) is given in [2.44]. This results in an average rate of 20.86 c/kWh (2009/2010) (considering time of use rates per day which differ for weekdays, Saturdays, Sundays and also for high/low demand periods). South Africa is faced with electricity supply challenges requiring funding to ensure security of supply for an increasing demand. The electricity utility has therefore submitted a revised tariff application increase of 35 % per year to the National Energy Regulator of South Africa for the financial years 2010/11 – 2012/13 [2.45]. An increase of ≥ 25% per year has been approved for this period [2.46]. Thereafter an escalation of electricity 8% per year has been assumed. A summary of the economic evaluation is shown in the Table 2.VI [2.43]. The evaluation was done from 2009 for illustrative purposes. The justifiable capital is well above the cost of an ASD system (excluding the motor) including the additional capital required for a bypass scheme to enhance availability.

Industrial electricity prices in Europe, USA and other countries can easily be in excess of an equivalent 0.05 EUR/kWh or equivalent of 53 c/kWh (ZAR) probably with a lower inflation rate, but already applicable from the first year. This does make the case more favourable for many other countries especially where mechanical energy savings are larger than in this case study (which should in some cases easily be achieved).

LV ASD cost per kW rating generally reduces with an increase in power rating. A 15 MW MV ASD cost per kW rating is presently approximately equal to a medium sized LV ASD cost per kW rating. In general MV ASD costs per kW rating also decreases with an increase in power (with steps according to manufacturing sizes).

Table 2.VI

TYPICAL ECONOMIC EVALUATION[2.43]

Description	Data	Unit
Beneficial operation date	March 2010	
Capital investment	March 2009	
Evaluation until year	2023	
Present effective electricity tariff	20.86	c/kWh (ZAR)
Assumed increase in electricity tariff per year 2010-2012	25	%
Assumed increase in electricity tariff per year from 2013	8.00	%
Output power at reduced speed (P_{RS})	12.10	MW
ASD Efficiency (η_{ASD}) at reduced speed (assume no reduction in efficiency since nominal power and speed is not significantly reduced)	96.94	%
ASD losses at reduced speed (P_{RS}/η_{ASD})- P_{RS}	381.95	kW
Average effective mechanical energy saving	2.00	MW
Average effective input power saving	1.62	MW
Energy saving per year	14,174	MWh
Cost saving per year	2,956,725	R
Assumed minimum allowed hurdle rate / IRR	16.50	%
Justifiable capital	32,144,730	R (ZAR)

Note: 1 EUR = 11 ZAR (exchange rate Dec 2009) 100c = R1 (ZAR)

2.6 WIDER SYSTEMS PLANT OVERVIEW

2.6.1 Oxygen West

The plant consists of seven electrical trains, each with an 11 kV, 36 MW synchronous motor (SM) driving an air compressor and an 11 kV, 13.7 MW induction motor (IM) driving an oxygen compressor. Presently, the SMs are started with MG sets, whereas the IMs are started directly on line. Fig. 2.13 (b) indicates the single-line diagram of the system. Fig. 2.13 (c) provides a plot plan overview of the systems.

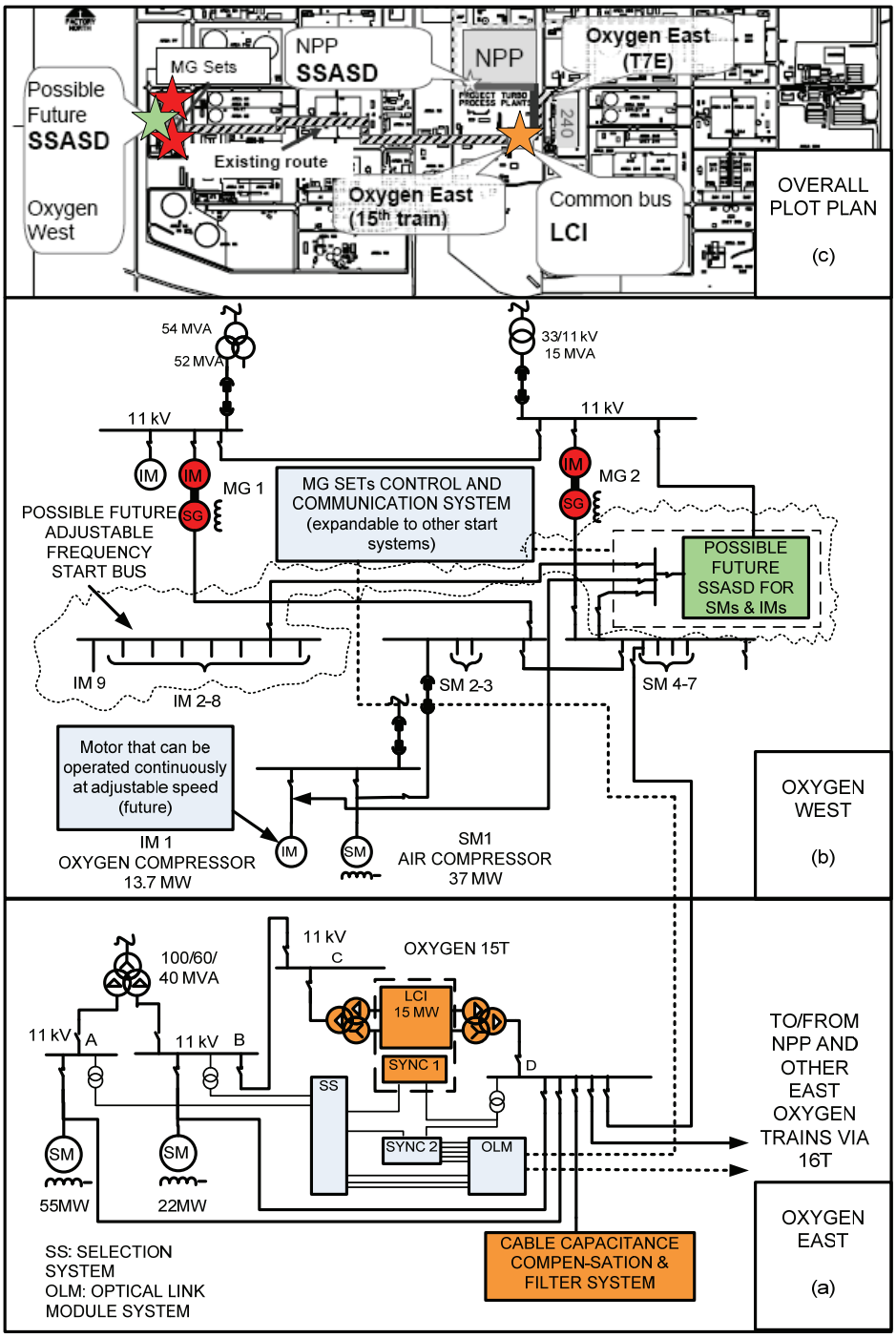

Fig. 2.13 Oxygen and NPP single-line and plot plan diagrams.

2.6.2 Oxygen East

Fig. 2.13 (a) illustrates the electrical infrastructure. The 15th train 55 MW and 22 MW synchronous motors are presently soft started with an LCI system, as described in [2.9].

The LCI is shown in Fig. 2.14 and the 55 MW motor in Fig. 2.15. The 55 MW motor is the first 4 pole motor installation in the world with a power rating ≥ 55 MW [2.47].

Fig. 2.14 12 pulse LCI (right), excitation and control panels (left)

Fig. 2.15 Main Air Compressor (MAC) 55 MW Motor

2.6.3 New Oxygen Trains and Integration with the NPP

The general philosophy at the entire plant is to have at least N-1 redundancy for start/drive systems. A new oxygen train 16 is in the execution phase and a similar LCI as for train 15 has been procured. The initial requirement is that the 15th and 16th train LCIs serve as back-up to each other, but in future the back-up of these LCIs to Oxygen East and Oxygen West may be required and the LCIs are planned to be used also for other existing and future Oxygen West Oxygen trains. It is also investigated whether the LCIs can serve as starting back-up to the NPP VSI-ML-H and vice versa (although this option is less likely to be implemented). The interconnections to the other Oxygen West trains and the NPP are discussed and shown in chapter 4. Guidelines (based on design, complexity, installation, shutdown, integration and commissioning considerations) on when to use a remote back-up system versus a local back-up system are provided in [2.30].

2.7 OXYGEN SOFT START AND DRIVE SYSTEM FEASIBILITY STUDY

This section provides in principle further benefits by means of case examples in an existing oxygen plant where challenges or opportunities may be addressed with an SSASD as described and quantified in [2.30].

2.7.1 Induction Motors IMs (13.7 MW)

The IMs are old, and some of the motors have been rewound. The motors may have become more sensitive for DOL starting because of rewinds or upgrades. These rewinds or upgrades were associated with some modifications that could affect the mechanical rigidity of the windings, which are especially stressed during starting. Failures due to DOL starting have been experienced as outlined in [2.30]. The additional thermal and mechanical stresses associated with starting are completely eliminated when using the soft-starting capabilities of the SSASD.

2.7.2 MG Set-Started SMs (36 MW)

The first portion of the startup is associated with IM action before the motor reaches synchronism with the output of the fluid coupling-based MG set from where the generator is ramped up to the supply frequency (before synchronization with the electrical network occurs). It appears that the starting rotor cage (damper bars) is not designed very conservatively, and significant heating occurs during startup, which is aggravated by poor cooling due to a slow rotational speed. Rotor damper bar failures have occurred, and this resulted in a decision to perform significant refurbishment work on the motors. Subsequently, maintenance and inspection intervals on the motors have been increased. An SSASD completely eliminates the use of the damper bars and IM action for starting purposes and associated failures will therefore be eliminated.

2.7.3 Energy Savings Study

The newer oxygen trains (15^{th} and 16^{th}) can be operated at full capacity and therefore benefit from the increased train efficiency. It is proposed not to share the loads between the other train compressors but to operate all oxygen compressors (13.7 MW motors) except one compressor at rated load (or the most efficient load point). The remaining compressor will then be used to regulate the flow efficiently by means of adjustable-speed operation. The advantage of this option is that energy is saved with SSASD adjustable-speed operation by avoiding the use of throttling on all motors during normal operation. Energy saving principles and saving estimation techniques are described in [2.4]. Energy can also be saved by switching the motors on and off more frequently and at optimal times with a soft start system and avoiding the risks associated with DOL starting. The plant maintenance department has conducted a study after the proposal has been made and estimated an energy saving at 3 MW (similar saving to the NPP energy saving).

2.7.4 MG Sets

Significant costs are required every five years to maintain fluid couplings. The oil coolers of the MG set (for the fluid coupling and the lube oil system) are reaching their end of life. It is estimated that the coolers will have to be replaced in the next 3 years. Spare parts are

expensive and some not available. MG set excitation systems needs replacement since no spare parts are available anymore. A soft starter or SSASD with the required redundancy built in with backup from another start system should eliminate the need of the MG sets.

2.7.4.1 LCI(s) used as Backup

LCI(s) may possibly be used in the future as a backup for other start or drive systems, but only in emergency situations and only as a soft starter. Additional filtering may be required to compensate for long cable distances. It has to be verified that no dangerous pulsating air-gap torques will be imposed to any of the SMs mentioned earlier. Furthermore, additional rotor position detectors may be required because of the long cable lengths. These aspects are investigated in chapter 3 and 4. The LCI also has the capability of performing a flying start [2.9], and it can be used in principle to catch a remote motor after an SSASD trip has occurred and to synchronize the unit with the fixed frequency supply before the process is disturbed.

2.7.5 Summary

It has been shown in [2.30] that an SSASD for the Oxygen Plant may be economically attractive with the most significant savings associated with the energy savings. The other savings strengthen the business case for a SSASD event further. Further consideration to the SSASD for Oxygen is suggested by thoroughly involving all engineering disciplines and incorporating the learning from the NPP SSASD. Research regarding long cable lengths and ride through capabilities are however needed to verify whether the proposed systems are feasible.

2.8 CONCLUSIONS

It has been shown that new technology VSI CHB ASDs can compete with conventional LCIs regarding efficiency with motors rated ≥ 11 kV. The CHB technology is also superior in terms of output waveforms, power factor and ease of installation regarding external

cabling. New technology can pose significant challenges during commissioning if the entire system (motor, ASD, excitation panels and control system) is not factory tested in combination.

Very large systems in excess of approximately 25 MW for new projects may be more efficient with LCI systems which have a proven reliability. LCIs may also be more beneficial for pure soft starting of very large motors (the negative aspects are not as applicable due to short duration operation, air cooled systems can be used and the benefit from proven reliability is obtained). LCIs may also still be recommended for very large applications especially where the risk of implementing new technology can not be mitigated (e.g. configurations where a bypass scheme is not feasible).

VSIs are more suitable for other applications especially with existing/standard motors rated ≥ 11 kV. No sound technical solution was previously available. System loss reduction opportunities have been investigated and it is shown that the selection of the motor (for new projects) has a significant impact on drive system efficiency. Case studies have shown that significant energy savings are possible for both existing and new project large compressor applications. The SSASD concept can be significantly more cost effective than the conventional solution of a dedicated soft starter and dedicated drive for certain next applications with multiple motors. The VSI-CHB technology, when correctly implemented does not pose any additional risk to existing or new motors, even when located in zone 2 hazardous areas.

The increased electricity tariffs and new technology that can address ≥ 11 kV applications make energy saving projects for large applications now more viable than ever before. SSASD systems may allow new technology to be applied economically with a lower risk level to address process and energy saving requirements for large drive systems.

Energy saving projects will however never be implemented if acceptable availability of the load is not achieved. Successful ride-through associated with internal fault conditions and external disturbances has been identified as an important topic requiring further research to enhance availability further. Furthermore a case study has shown that unacceptable output overvoltages can occur. This is especially important to address for applications with long

cable lengths associated with some projects and also where a SFC is used for availability improvement as back-up for another SFC where long cable lengths are normally encountered. Further research is therefore required to manage output overvoltages associated with long cable distances so that availability is not compromised. The remaining chapters address these concerns.

2.9 REFERENCES

[2.1] E. P. Wiechmann, P. Aqueveque, R. Burgos, J. Rodríguez, "On the efficiency of voltage source and current source inverters for high-power drives", *IEEE Trans. on Ind. Electron.*, vol. 55, no. 4, pp. 1771-1782, April 2008.

[2.2] Y. Suh, J. K. Steinke, and P. K. Steimer, "Efficiency comparison of voltage-source and current-source drive systems for medium-voltage applications," *IEEE Trans. Ind. Electron.*, vol. 54, no. 5, pp. 2521–2531, Oct. 2007.

[2.3] S. S. Fazel, "Investigation and comparison of multi-level converters for medium voltage applications," Dr. Ing. dissertation, Technische Universität Berlin, Berlin, Germany, 2007.

[2.4] H. N. Hickok, ''Adjustable speed—A tool for saving energy losses in pumps, fans, blowers and compressors,'' *IEEE Trans. Ind. Appl*., vol. IA-21, no. 1, pp. 124–136, Jan./Feb. 1985.

[2.5] R.A. Gutzwiller, R.J. Gerhart, H.N. Hickok, "A 10,000 HP AC adjustable-frequency compressor drive the economics of its application," *IEEE Trans. on Ind. Appl.*, Vol IA-20, no. 1, pp. 80-91, Jan./Feb. 1984.

[2.6] B.P Schmitt, R. Sommer, "Retrofit of fixed speed induction motors with medium voltage drive converters using NPC three-level inverter high-voltage IGBT based topology," in Proc. *IEEE Symp. on Industrial Electronics*, vol. 2, 2001, pp. 746-751

[2.7] N. Granö, "Electrical drive systems, drive systems with synchronous motors (LCI)," in *ABB Industrial Manual,* Lund, Sweden, Wallin & Dalholm Tryckeri, 1998, ch. 4, pp. 365-375.

[2.8] B. Wu, J. Pontt, J. Rodriguez, S. Bernet, S. Kouro, "Current-source converter and cycloconverter topologies for industrial medium-voltage drives," *IEEE Trans. Ind. Electron.*, vol. 55, no. 4, pp. 2786-2797, Jul. 2008.

[2.9] F. Endrejat and J. Piorkowski, ''Multiple large motor solid state soft start, control and communication system,'' in *Symp. on Power Electronics Electrical Drives Automation and Motion (SPEEDAM)*, Capri, 2004, pp. 561-566.

[2.10] M. Hiller, R. Sommer, M. Beuermann, "Medium voltage drives: An overview of the common converter topologies and power semiconductor devices," *IEEE Ind. Appl. Mag.*, vol. 16, no. 2, pp. 22-30, Mar./Apr. 2010.

[2.11] ABB (Brochure 2006), *MEGADRIVE LCI, Medium Voltage AC Drive for Control and Soft Starting of Large Synchronous Motors* [Online]. Available: http://www.abb.com/motors&drives

[2.12] F. Endrejat, B. van Blerk, and G. Vignolo, ''Experience with new large adjustable speed drive technology for multiple synchronous motors,'' in *Proc. Petroleum and Chemical Industry Committee (PCIC) Europe*, 2008, Weimar, Germany, pp. 196–205.

[2.13] Mitsubishi Electric Corporation, *Electric Drive Systems for LNG Compressor Drives,* document presented to Sasol Technology, November 2002

[2.14] *Adjustable Speed Electrical Power Drive Systems, Part 4: General Requirements—Rating Specifications for ac Power Drive Systems Above 1,000 V ac and Not Exceeding 35 kV*, IEC Standard 61800-4, 2002

[2.15] B. Wu, *High Power Converters and AC Drives*. Piscataway, NJ: IEEE Press, 2006.

[2.16] R. Schiferl, A. Flory, W. C. Livoti, "High temperature superconducting synchronous motors: Economic issues for industrial applications," in *Proc. IEEE Petroleum and Chemical Industry Committee (PCIC)*, Philadelphia, PA, 2006, pp. 259-267.

[2.17] C. Bailey, D. M. Saban, P. Guedes-Pinto, "Design of high-speed, direct-connected, permanent-magnet motors and generators for the petrochemical industry," *IEEE Trans. Ind. Appl.*, vol. 45, no. 3, pp. 1159 - 1165, May/Jun. 2009.

[2.18] Robert Meleia, "Efficiency, Design and Reliability – Interesting Issues and Observations", *LHM rotating machines conference*, South Africa, 2004

[2.19] F. Endrejat, "Induction motor modelling for efficient variable frequency operation and industrial application", M. Eng Research Dissertation, Dept. Elect. Eng., University of Pretoria, South Africa, 1998

[2.20] W de Lima Pires, HGG Mello, *Minimization of Losses In Converter-Fed Induction Motors–Optimal Flux Solution* [Online]. Available: http:// weg.com.br

[2.21] *IEEE Recommended Practice for Efficiency Determination of Alternating- Current Adjustable-Speed Drives, Part I Load Commutated Inverter Synchronous Motor Drives,* IEEE 995, 1987.

[2.22] F. Endrejat, P. Pillay, "The soft starters - adjustable speed systems for multiple MW Rated Motors," *IEEE Ind. Appl. Mag*, vol.14, no.6, pp. 27-37, Nov/Dec 2008.

[2.23] J. Rodríguez, P. W. Hammond, J. Pontt, R Musalem, P Lezana, M. J. Escobar, "Operation of a Medium-Voltage Drive Under Faulty Conditions," *IEEE Trans. on Ind. Electron.,* vol. 52, pp. 1080-1085, Aug. 2005

[2.24] O. Drubel, "Converter Dependent Design of Induction Machines in the Power range below 10MW", in *Proc. IEEE Int. Electrical Machines and Drives Conf. (IEMDC)*, 2007, Antalya, Turkey, pp. 1465-1470

[2.25] G. Saggewiss, R. Kotwitz, and D. J.McIntosh, "AFD synchronizing applications: Identifying potential methods and benefits," in *Proc. IEEE Petroleum and Chemical Industry Committee (PCIC)*, 2001, Toronto, Canada, pp. 83–89.

[2.26] W. D. Stevenson, "Load –flow solutions and control", in Elements of Power Systems Analysis, 4th ed., Singapore, McGraw Hill, 1982, ch. 8, pp. 206-208

[2.27] *Standard for Performance of Adjustable Speed AC Drives Rated 375 KW and Larger,* IEEE Standard 1566, 2006.

[2.28] B. Lockley, R. Paes, J. Flores, "A Comparison between the IEEE 1566 standard for large adjustable speed drives and comparable IEC Standards," in *Proc. Petroleum and Chemical Industry Committee (PCIC) Europe,* 2007, © IEEE. doi: 10.1109/PCICEUROPE.2007.4354012

[2.29] D. L. Hornak, D.W. Zipse, "Automated bus transfer control for critical industrial processes," *IEEE Trans. on Ind. Appl.*, vol. 27, no. 5, pp. 862-871, Sept./Oct. 1991.

[2.30] F. Endrejat and P. Pillay, "The soft starters-adjustable speed systems for multiple MW rated motors," *IEEE Ind. Appl. Mag.*, vol. 14, no. 6, pp. 27– 37, Nov./Dec. 2008.

[2.31] A. von Jouanne, H. Zhang, A. K. Wallace, "An Evaluation of Mitigation Techniques for Bearing Currents, EMI and Overvoltages in ASD Applications," *IEEE Trans. on Ind. Applicat.*, vol. 34, pp. 1113-1122, Sep/October 1998

[2.32] R. H. Paes, B. Lockley, T. Driscoll, M. J. Melfi, V. Rowe, and S. C. Rizzo, ''Application considerations for class-1 div-2 inverter-fed motors,'' *IEEE Trans. Ind. Applicat.,* vol. 42, pp. 164–170, Jan./Feb. 2006

[2.33] *Electrical apparatus for explosive gas atmospheres-Part 15: Construction, test and marking of type "n" electrical apparatus* ,IEC Standard 60079-15 (3rd edition), 2005

[2.34] *Electrical apparatus for explosive gas atmospheres-Part 15: Construction, test and marking of type "n" electrical apparatus* ,IEC Standard 60079-15 (4rd edition), 2010

[2.35] D. A. Rendusara, E. Cengelci, P. N. Enjeti, V. R. Stefanovic, J. W. Gray, "Analysis of common mode voltage—"neutral shift" in medium voltage PWM adjustable speed drive systems", *IEEE Trans. Power Electron.*, Vol. 15, no. 6, pp. 1124-1133, Nov., 2000

[2.36] R. E. Bushman *et al.*, "Calculation of neutral voltage shift in LCI driven induction motors," *IEEE Trans. Energy Conv.*, vol. 6, no. 3, pp. 507–513, Sept. 1991

[2.37] A. Muetze, H. William Oh, "Application of Static Charge Dissipation to Mitigate Electric Discharge Bearing Currents", *IEEE International Electric Machines and Drives Conference Record*, pp 1059-1066, May 2007

[2.38] S. Ul Haq, B. Mistry, R. Omranipour, "Behaviour of an insulation system in gas groups IIA, IIB & IIC," in *Proc. Petroleum and Chemical Industry Committee (PCIC) Europe*, 2010, Oslo, Norway, pp. 113-119.

[2.39] R. Emery, J. Eugene, "Harmonic Losses in LCI-Fed Synchronous Motors," *IEEE Trans. on Ind. Appl.*, Vol. IA-38 No.4, pp 948-954, Jul./Aug. 2002.

[2.40] S. Kanerva, S. Bono, B. Oberbauer, H. Persson, G. Scheuer, **"**Motor Design Considerations for Medium Voltage Adjustable Speed Drives in Hazardous Areas", in *Proc. IEEE Petroleum and Chemical Industry Committee (PCIC),* San Antonio, TX, 2010 paper no. PCIC-2010-11

[2.41] P. Hammond, "A New Approach to Enhance Power Quality for Medium Voltage AC Drives," *IEEE Trans. on Industry Applicat.*, vol. 33, pp. 202-208 No. 1, Jan./Feb. 1997.

[2.42] *Estimating Centrifugal Compressor Performance, Process Compressor Technology Volume 1,* 1st ed., Gulf Publishing Company (R.P. Lapina), ISBN 0-87201-101-1.

[2.43] F. Endrejat, B. van Blerk, ''Large medium voltage drives – efficiency, energy savings and availability,'' in *Proc. Petroleum and Chemical Industry Committee (PCIC) Europe*, Oslo, Norway, 2010, pp. 86-93.

[2.44] Eskom tariff book publication, *Tariffs and Charges – Effective from 1 July 2009* [Online]. Available: http://www.eskom.co.za/tariffs

[2.45] Eskom Press Release (1 December 2009), *Eskom Adjusts its Tariff Increase Application to NERSA* [Online]. Available: http://www.eskom.co.za.

[2.46] National Energy Regulator of South Africa (2010, February), *Media statement - NERSA's decision on Eskom's required revenue application - multi-year price determination 2010/11 to 2012/13* [Online]. Available: http://www.nersa.org.za

[2.47] Johannes Ahlinder, Thomas L. Johansson, "Synchronous Superlatives - Record-breaking electric motors give heavy industry more drive,", *ABB Review – special report*, June 2004, pp. 41-45.

3 RESONANCE OVERVOLTAGES AND LONG CABLE LENGTHS

This chapter describes overvoltage conditions in drive systems. The output resonance overvoltage phenomenon is illustrated and the general model for simulating resonance with VSI-CHB systems is developed. The parameters needed for analysis are defined and the resonance condition is expressed analytically for simplified analysis. Simulation results and associated test results are analysed in the time and frequency domain to prove the numerical model and also the simplified analytical equations. The test results are taken from the first 11 kV VSI-CHB drive for multiple standard insulation synchronous motors at a major chemical and process plant. Solutions to minimize overvoltage problems, previously not associated with VSI-CHB systems, are studied and recommendations are provided.

3.1 INTRODUCTION

The benefits outlined in the previous chapters with the VSI-CHB technology can only be achieved if long cable lengths can effectively be accommodated without unacceptable overvoltages. The VSI-CHB technology, suitable for induction and synchronous motor applications, now exists at high power ratings (e.g. > 13 MW) and voltage levels but supported with very limited actual site application and operational experience as outlined in Chapter 1. Higher voltage IGBTs are now used for high power applications to minimize overall component counts but are associated with fewer and/or larger voltage steps when compared to the application of low voltage IGBTs. It is however important to investigate the possibility of potential overvoltages associated with the larger/fewer voltage steps.

Specific attention is given to potential reflective wave and resonance induced overvoltage interactions between the inverter and motor which can be potentially dangerous or

damaging to the drive system. Motor insulation requirements associated with MV ASDs are well documented in literature and IEC 60034-18-42 standard [3.1]-[3.3]. The standard (and literature) focus however on the expected waveforms at the motor terminals considering cable effects, MV PWM waveforms and the reflective wave phenomenon. It has been stated that the switching surges associated with VSI-CHB systems are not likely to contribute to motor insulation problems due to the relatively small steps in voltage [3.4]. This was however based on low voltage IGBT cells. Resonance overvoltages (not specifically addressed in IEC 60034-18-42) have been reported in literature for certain applications associated with significant voltage steps/surges. References [3.5] and [3.6] show that unacceptable motor terminal resonance overvoltages can occur with a lower voltage two level inverter with a step-up transformer feeding a MV motor with a long cable distance. A filter [3.5] or alternative modulation strategy [3.6] were required to rectify the problem. Circuit breaker switching transients can excite resonance overvoltages at captive transformer fed motors [3.6]. In CSI PWM systems resonance can occur due to the inverter output capacitance and motor impedance, excited by drive harmonics. Typical solutions include correct sizing of the capacitor and/or selective harmonic elimination [3.8].

This chapter describes the output overvoltage resonance phenomena and provides the general model for simulating resonance. The parameters needed for analysis are defined. Simulation results are provided and associated test results to prove the model. The test results are taken from the first 11 kV VSI-CHB drive for multiple standard insulation synchronous motors at a major chemical and process plant.

The application configuration of the system is described in Chapter 2. A synchronisation, de-synchronisation and process control scheme is applied to improve process availability (to synchronise the adjustable speed driven motor before certain drive trip conditions) and also to facilitate soft starting of other motors. A synchronisation reactor is applied in applications with smooth make-before-brake transfers to limit the current during synchronization. This is also referred to as a bypass configuration. Further explanation for bypass configurations and current limitation during synchronisation is described in Chapter 2. It is important to evaluate the effect of the synchronisation reactor (normally not used with ASDs without a bypass configuration but used for SSASD systems).

3.2 MODELLING AND SIMULATION

This section provides the general model for simulating resonance. The parameters needed for analysis are defined. The VSI-CHB project described in Chapter 2 is used as a reference case to describe the application of the model. The applicable system single line diagram is shown in a simplified form in Fig. 3.1 The principles can be used for any VSI-CHB system.

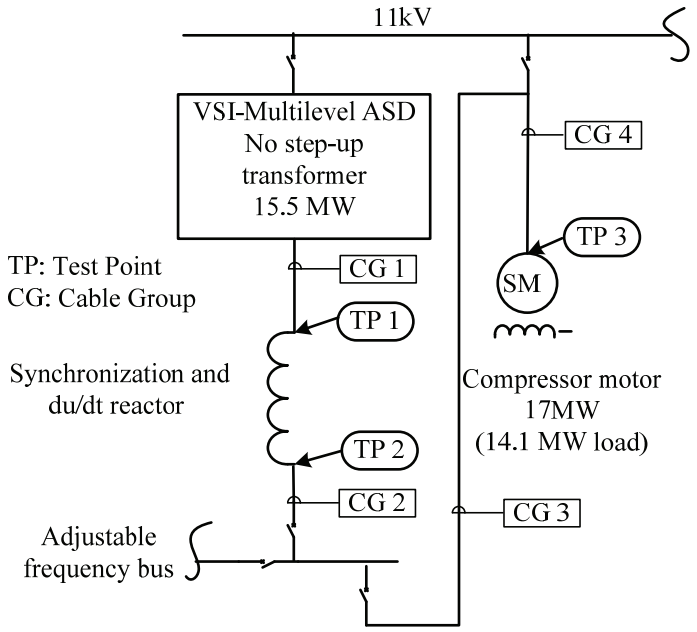

Fig. 3.1 Single line diagram and test point locations (cable lengths and parameters are given in Table C.2.I in Appendix C)

3.2.1 Inverter Modelling

The inverter topology and structure are shown in Fig. 2.2 (the rated voltage for each cell is 1375V with a cell DC bus voltage of 1856 V – this voltage is normally slightly higher due to a slightly higher than rated incoming bus voltage). Fig. 2.2 also shows the structure of each individual cell.

The selection of the number of cells is introduced in section 2.5.2 B1. The number of cells, K=5 per phase, were selected to obtain a minimum number of cells, while still obtaining sufficient voltage for synchronisation/bus transfer when 1 cell is out of service/bypassed as previously discussed. The standard high voltage cell of the manufacturer was chosen. The maximum rms output voltage (V_{out}) with all cells in service can be determined from equations presented in [3.9] as 12.85 kV with the following input parameters: rated cell voltage = 1375 V, transformer tap setting=1.05 for -5% tap and K=5. The maximum output voltage with one cell out of service is determined from further equations in [3.9] as 11.56 kV. This voltage is sufficient for synchronization and confirms that K=5 is the correct selection. Output voltages of only 10.3 kV and 9.0 kV can be reached with 2 cells and 3 cells respectively out of service [3.9], which means that synchronization (or an up transfer) will not be possible. This motivates the use the SSASD scheme to replace the first faulted cell before another cell fails as previously described. The principle behind the output voltages and associated cell bypass scheme is explained in section 5.2.5 A.

The number of cells selected also influences the harmonic levels. Traditionally more cells have been selected for high power drives since lower voltage cells were previously used. The reduced number of cells need to be evaluated in terms of the output voltage waveform quality, which is further investigated later in this chapter.

Modulation principles for VSI-CHBs are described in [3.8], [3.10]. Carrier based modulation schemes are mainly used for VSI-CHBs and classified in phase shifted and level shifted modulations. Other alternative modulation methods are described in [3.11]

Phase shifted modulation is chosen due to advantages of consistency in the switching frequency and device conduction period (same for all devices). Furthermore rotating switching patterns are not required. The phase shifted multi-carrier modulation is described and modelled as outlined in [3.8].

The effective inverter frequency, for VSI-CHB systems, is given by [3.8]:

$$f_{sw,inv}=2\cdot K\cdot f_c \tag{3-1}$$

The default switching /carrier frequency for each cell (f_c) is 404.5 Hz resulting in and effective inverter frequency ($f_{sw,inv}$) of 4.05 kHz. This effective inverter frequency is also reflected in the frequency spectrum (FFT) in Fig. 3.2. The complete inverter waveform has, at fundamental frequency, m=11 (2K+1) levels including the top half, midpoint and bottom half of the waveform [3.8]. However, the number of levels of an inverter is often referred to in industry as the amount of levels from phase to neutral, i.e. only the positive half of the output fundamental frequency is considered. The inverter can therefore then be classified as a 6 (K+1) level inverter.

All the triangular carriers have the same frequency and peak-to-peak amplitude but are phase shifted by any two adjacent carrier waves by $360^o/(m\text{-}1)$, i.e. by 36^o [3.8]. It is therefore possible to configure universal bridges as shown in the simulation model block diagram in Fig. B.1 (Appendix B) while ensuring that their carrier waves are shifted by 36^o. Further details are provided in Appendix B.

The synthesis of the phase voltages of VSI-CHB systems (with phase shifted modulation) and the associated illustration how the individual cell voltages amount to the terminal voltages are well documented and illustrated in [3.8], [3.9],[3.10], [3.11].

A simulation result example for the output voltage waveform (without any load connected) and associated Fast Fourier Transform (FFT) analysis are shown in Fig. 3.2.

3.2.2 Load Modelling

The load was initially comprehensively modelled including multiple π section transmission lines representing each cable (assuming 5 sections per cable). The three phase simulation diagram is shown in Fig. 3.3 with parameter values in given in Appendix C. This cable distributed parameter model approach is valuable to capture the high frequency travelling wave overvoltage effects (e.g. at the input of the reactor or at the motor for systems without a reactor). Furthermore this approach is also valuable for subsea applications where cable lengths are typically tens of kilometres (e.g 47 km in [3.14]).

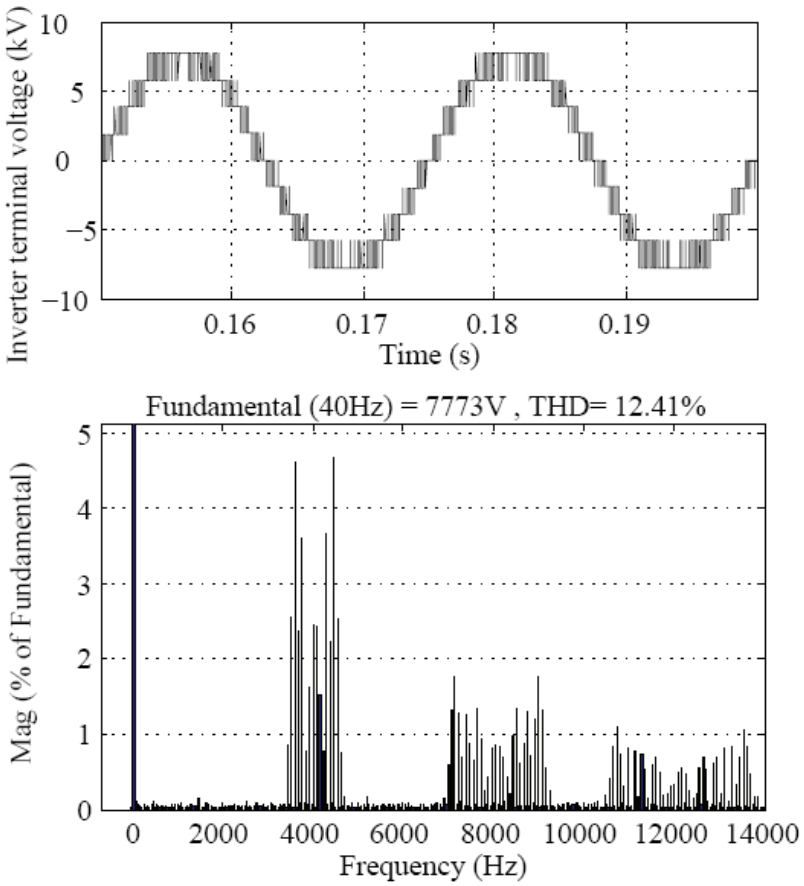

Fig. 3.2 Simulated inverter output phase to neutral voltage (modulating/fundamental frequency f_m=40 Hz, f_c= 404.5 Hz, modulation index m_a= 0.8)

The travelling wave theory, simulations and test results are well documented in literature (see, e.g., [3.5], [3.7], [3.15], and [3.16]). In accordance with the theory, high frequency travelling waves can be expected at the input of the reactor or at the motor terminals in the case of systems without reactors. The reactor and motor have highly inductive characteristics resulting in large load impedances and a reflection coefficient of approximately 1. Pulses in the multilevel steps can therefore be expected to double in initial amplitude, i.e. double the cell DC bus voltage.

The focus of this chapter is however on the overvoltages at the motor terminals with the presence of a reactor. Model simplification is investigated for more effective analysis. The reactor and cables between the converter and motor function as a low pass filter in accordance with the theory in [3.12].

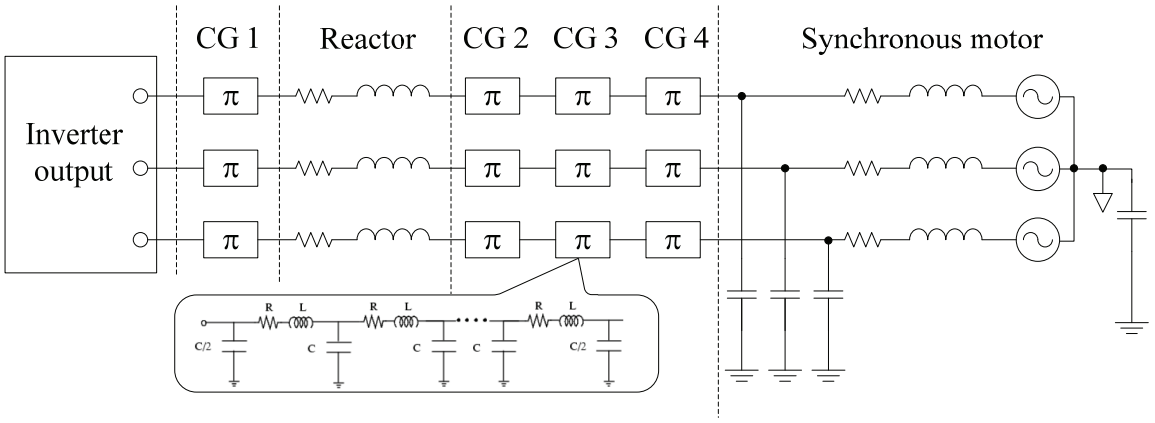

Fig. 3.3 Load simulation diagram

The resonant frequency of the reactor and total cable capacitance between the reactor and motor (C_{TC} as derived in Appendix C) can be is used as a first approximation to determine resonant frequency. This simplification represents a series RLC circuit. The well known equation for the resonant frequency of a RLC circuit is derived from first principles and differential equations/Laplace transforms as shown for example in [3.12] and [3.13]. The equation is shown below with parameters of the circuit.

$$f_o = \frac{1}{2 \cdot \pi \cdot \sqrt{L_{REACTOR} \cdot C_{TC}}} \tag{3-2}$$

The resonant frequency (f_o) is calculated as 3.12 kHz using the data in Appendix C. An approximation of the maximum frequency that can be represented by a single π model for the longest cable (a cable from CG 4) is given by [3.17]:

$$f_{m\pi} = \frac{1}{8 \cdot \sqrt{L_{uc} \cdot C_{uc}}} \tag{3-3}$$

where L_{uc} is the inductance per unit length (H/m) and C_{uc} is the capacitance per unit length (F/m) of one of the cables from CG4 (refer to Appendix C). This frequency ($f_{m\pi}$) is calculated as 19.5 kHz and is well above the effective pass band of the reactor filter since

$f_{m\pi} >> f_o$ and therefore there is no need to model the cables downstream of the reactor as transmission lines with multiple π-sections. Furthermore the reactor input frequency/ringing is typically in the order of several hundred kHz (this is verified by measurements in the next section and overvoltages due to the transmission line effect can be neglected downstream of the reactor due to the filter effect described above). An equivalent lumped load circuit model can therefore be used since the series inductance is large enough. The simulation model was therefore accordingly simplified and it was verified that identical output waveform results are obtained.

The model can further be simplified into a single phase equivalent circuit, assuming all phases are identical, as given in Fig. 3.4 for the purposes of determining the basic voltage transfer function. This assumption and simplification will be verified by confirming that the resonant frequency values from the comprehensive model, simplified model and test results are consistent (shown later in the chapter). The values of the circuit parameters are given in Appendix C.

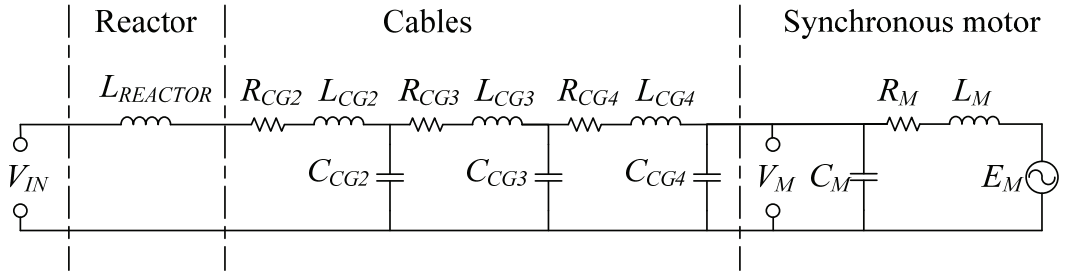

Fig. 3.4 Single phase equivalent circuit of the load components

The associated transfer function is given by (3-4) with V_M and V_{IN} shown in Fig. 3.4. The differential & Laplace equations can be derived for the circuit based on well known methodology as shown for example in [3.12] for frequency response analysis. The associated equations are therefore not repeated here.

$$H(j\omega) = \frac{V_M}{V_{IN}}(j\omega) \tag{3-4}$$

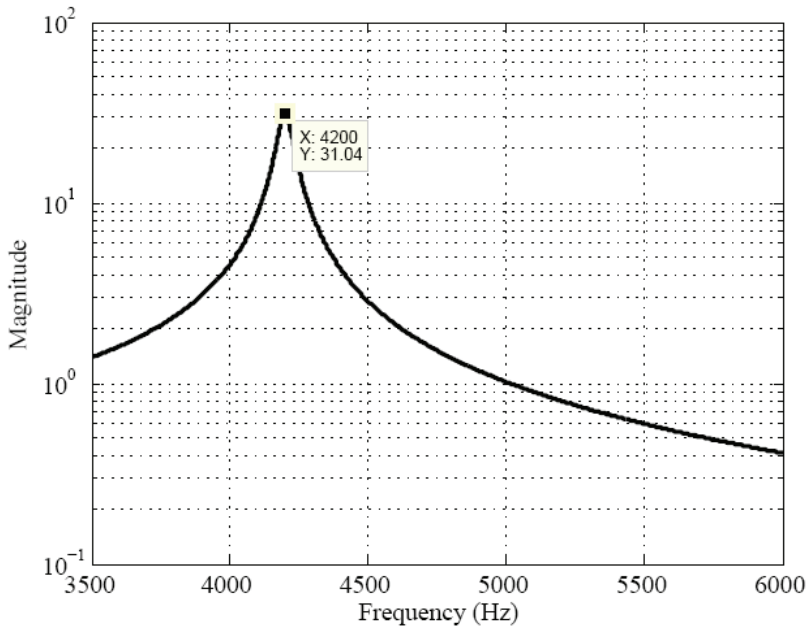

Fig. 3.5. Magnitude vs. frequency response example for $H(j\omega)$

Alternatively the circuit can be applied in frequency response analysis simulation packages and then solving for (3-4). The associated magnitude vs. frequency response can then readily be determined either from equations or simulation. Simulation results are shown in Fig. 3.5 (simulation package used is listed in Appendix B). The resonant frequency indicated in Fig. 3.5 will be checked for correctness by means of an alternative calculation described at the end of this section.

In [3.6] it is stated that the motor impedance does not have a significant influence for a VSI system in terms of the voltage transfer function (with a very long cable). In [3.5] a basic motor model (represented by a resistor, reactance and EMF) with a 2 level inverter and a step-up transformer was used and a resonance effect was however described. In [3.6] the effect of frequency variation has been incorporated in the cable parameters (L&R) using finite element analysis. The cable length was however very long (30 km). A shorter cable of 800m was purely represented by a capacitance in [3.5]. In this case the cable length is even shorter (550m for CG4 but with the same order of magnitude capacitance value) and the effect of frequency variation on cable parameter values was therefore not included for the initial evaluation. Furthermore cable capacitance has a more significant influence on the results than resistance. It has also been shown in [3.18], [3.19] that capacitance

typically does not have a significant variation with frequency around the resonant frequency range.

If cable parameter variation with frequency is not considered a pessimistic result in terms of the voltage transfer function magnitude occurs (i.e. larger values are obtained) [3.6]. Neglecting the variation does not have a major impact in the value of the resonant frequency. It has been shown in [3.7], that for frequencies in the kHz range it is important to include motor winding capacitance (phase to earth) and has therefore been included.

It will be beneficial to determine the resonance frequency for various case studies (e.g. cable lengths). The resonance frequency is the frequency where $|H(j\omega)|$ reaches a peak. The equation for $|H(j\omega)|$ is however not simple and a further simplification is more effective while achieving the same goal. Neglecting resistances, the equivalent circuit can be approximated as shown in Fig. 3.6 (the supply voltage and total inductance are represented as a Norton equivalent current source).

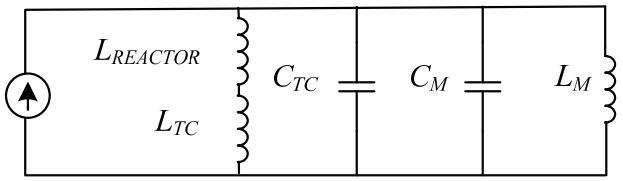

Fig. 3.6 Simplified single phase equivalent circuit to determine resonant frequency

The internal EMF of the motor can be neglected since the resonance voltage is far larger than the motor internal EMF. The parallel resonant frequency can now be expressed from the simplified circuit as:

$$f_r \approx \frac{1}{2\cdot\pi\cdot\sqrt{\left(\frac{(L_{REACTOR}+L_{TC})\cdot L_M}{L_M+(L_{REACTOR}+L_{TC})}\right)\cdot(C_{TC}+C_M)}} \tag{3-5}$$

The approximation results in a resonant frequency of f_r=4.19 kHz and agrees very well with the resonance frequency from the transfer function shown in Fig. 3.5. This is also consistent with results from the comprehensive 3 phase simulation model (Fig. 3.3).

3.2.3 System Modeling, Resonance Explanation and Simulation Results

Fig. 3.2 shows drive harmonics at and around the calculated system resonance frequency (4.2 kHz) which can excite overvoltages. Contributing factors to the resonance frequency are the drive output waveforms, reactor, cable and motor characteristics (inductances and capacitances). The reactor inductance and high capacitance of the long single core parallel cables have a major influence on the system resonance frequency. A simulation has been performed to illustrate the resonance phenomenon by using the inverter model output as input to the load model (simulation model is shown in Appendix B Fig. B.1). Fig. 3.7 shows the simulated results which illustrate significant amplification of harmonics in the resonant frequency area resulting in waveform distortion.

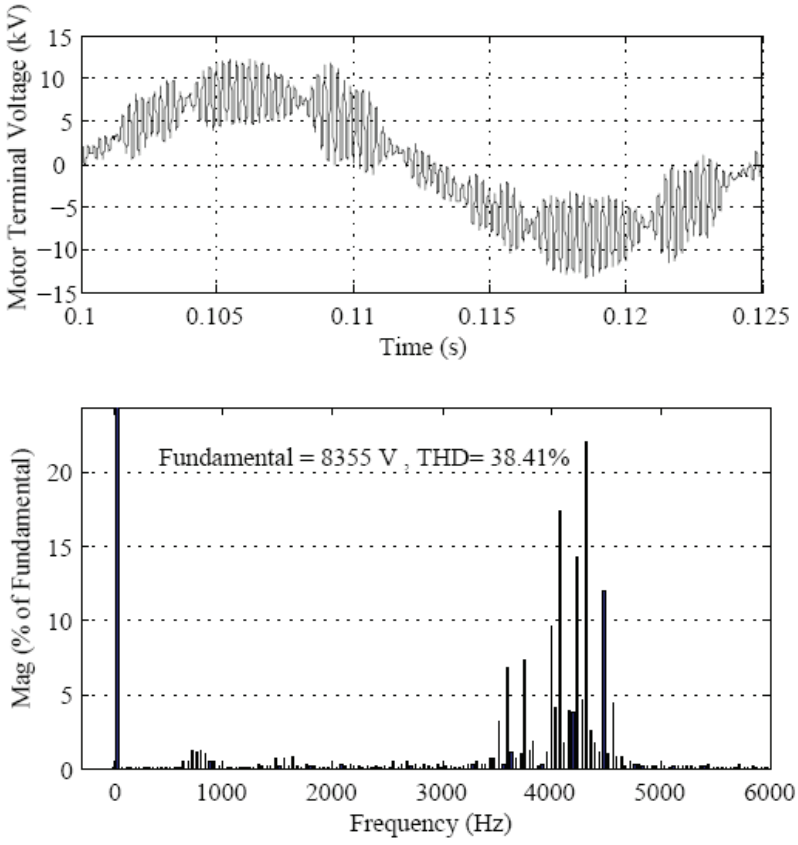

Fig. 3.7 Simulated motor phase to earth voltage (f_m=40 Hz, f_c= 404.5 Hz, m_a= 0.8)

3.3 INITIAL TESTS AND ASSESSMENT

Site measurements were used to verify the simulation results and correctness of the model. Tests were done to determine the maximum voltage, waveform shape and maximum du/dt values at the motor terminals. Similar tests were performed before and after the synchronization reactor to verify the effect of the reactor and cables. Fig. 3.1 shows the test point locations, Fig. 3.8 provides a picture of the test set-up and Fig. 3.9 shows the connection diagram of the test set-up.

Wideband voltage dividers with a high voltage withstand capability were used in conjunction with a wideband oscilloscope. A capacitive voltage divider was selected due to its compactness and availability. The specifications for the test equipment are given in Appendix C. Additional tests were conducted by an independent consultant with a resistive divider circuit, with similar results. Phase-phase test connections would have been preferred since TP1 waveforms should then have shown the PWM pattern more clearly and the phase to phase overvoltages and impact on phase to phase insulation could then directly be analysed. The rating of the test capacitor is however only 16 kV and phase-phase overvoltage measurements may substantially exceed this value. It was therefore decided to perform phase to earth measurements instead which is the normal application of the test capacitor. Analysis of phase waveforms is an acceptable method to analyse resonance overvoltage conditions since the phenomenon will be clearly visible on both phase and phase to phase waveforms as shown in [3.5]. Furthermore IEC 61800-4 [3.20] provides criteria to determine wether measured phase to earth values are within acceptable values. Successful elimination of the resonance condition will also be visible on phase-earth waveforms [3.5].

Measurements were taken at 400, 800, 1200 and 1500 rpm (4 pole motor). The worst voltage peak to peak values and peak to earth values were recorded at 1200 rpm at the motor terminals. Furthermore the system is designed for continuous operation between 1200 rpm and 1500 rpm. The results are therefore only shown for 1200 rpm in Fig. 3.10. The waveforms are displaced with respect to each other on the time axis for clarity. The test results (TP3) corresponds well with the simulation results in Fig. 3.7.

Fig. 3.8. Test set-up at the motor terminals

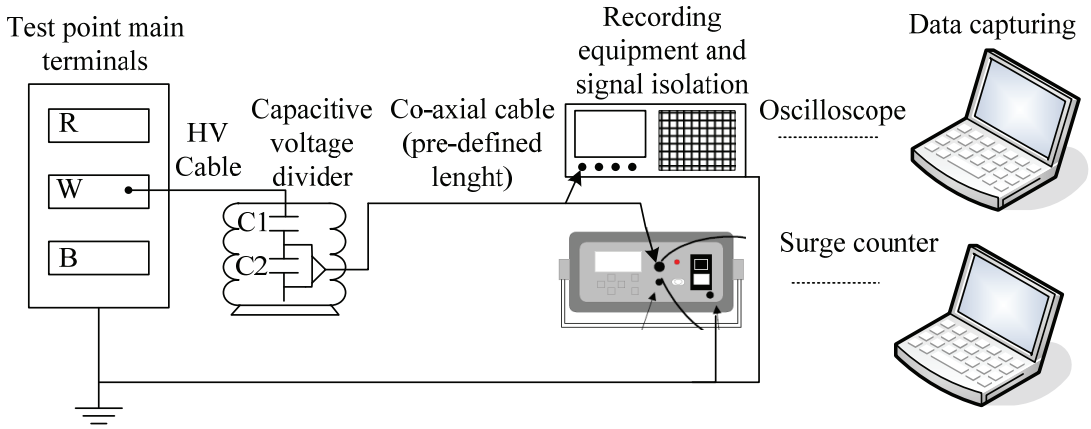

Fig. 3.9 Connection diagram of test set-up (capacitive divider)

The figure shows phase to earth voltage values for the reactor input, reactor output, motor terminals (from capacitor divider tests) and motor terminals (from resistive divider tests). The surge counter at the motor terminals did not record any pulses with rise times below 1.5 µs (maximum rise time detectable by the pulse counter), confirming the filtering effect of the reactor.

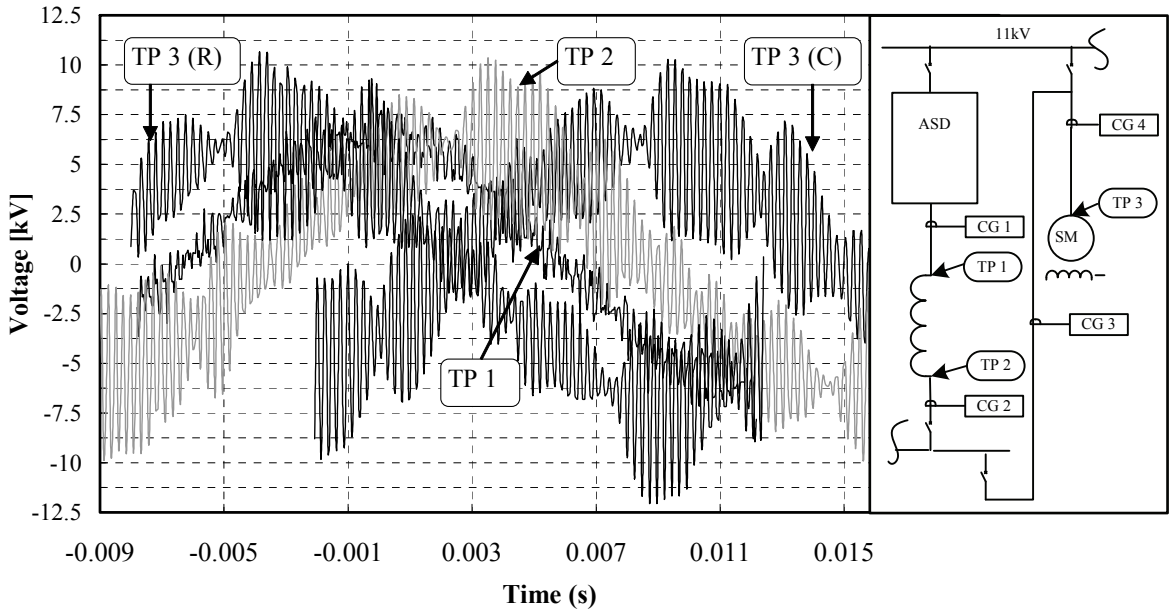

Fig. 3.10 Overview of voltage phase to earth waveforms at 40 Hz (1200 rpm; R: resistive divider; C: capacitive divider)

3.3.1 High Frequency Travelling Waves

The worst case du/dt values were recorded at TP1 (the input of the reactor) as shown in Fig. 3.10. Fig. 3.11 shows a higher resolution waveform and the characteristic traveling wave phenomenon as earlier described is clearly visible. A higher sampling rate is required to determine the du/dt rates as shown in Fig. 3.12. The recording is shown at nominal speed so that the maximum peak voltage at the input of the reactor is also shown.

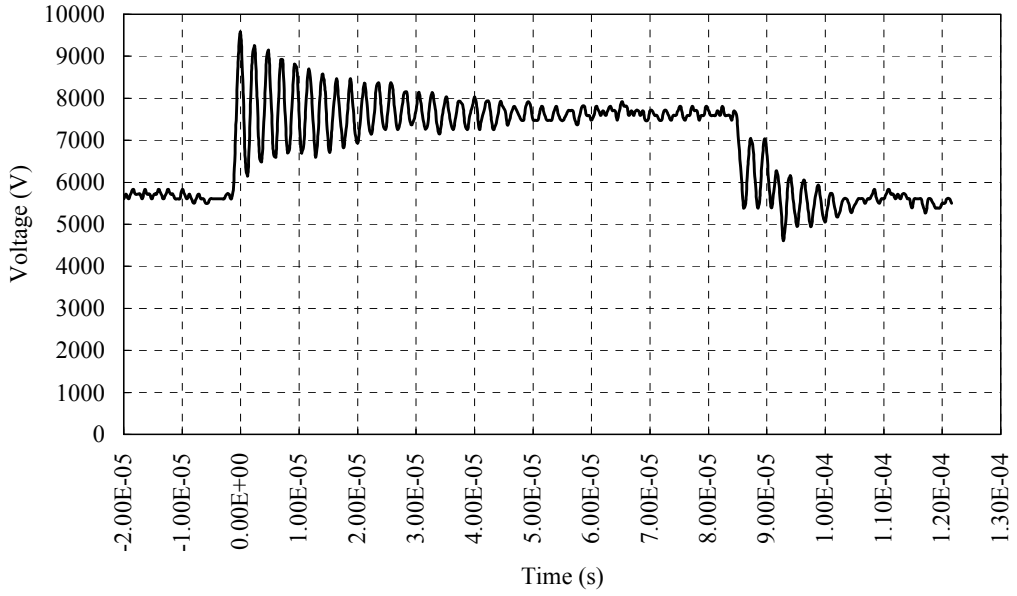

Fig. 3.11. Voltage phase to earth waveform at the input of the reactor (TP1, 1200 rpm, higher sampling rate)

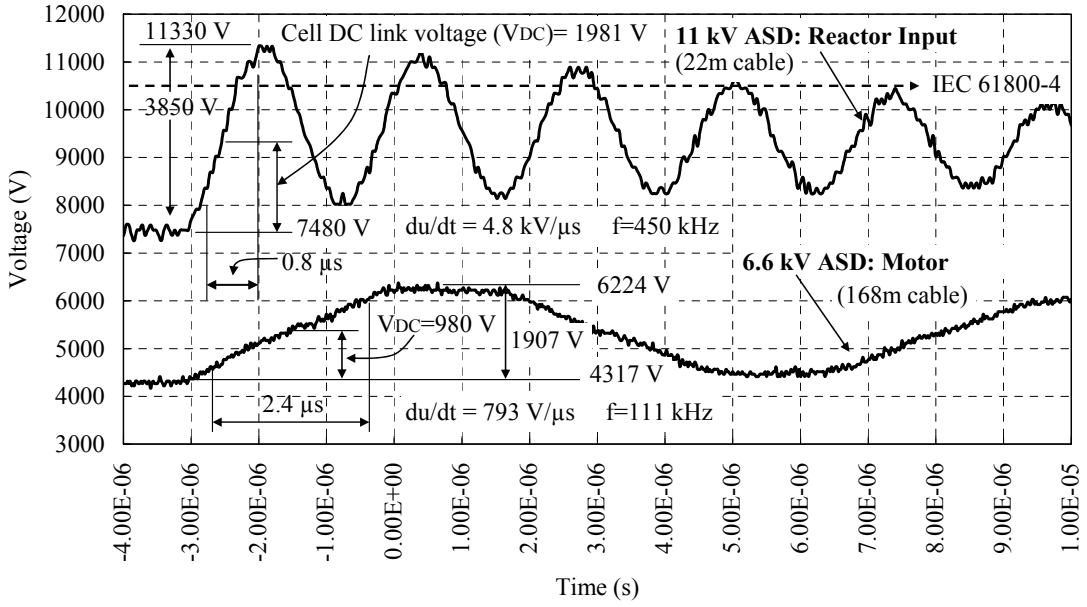

Fig. 3.12 Voltage phase to earth pulse waveforms (TP1, 1500 rpm, maximum sampling rate) at the input of the reactor (11 kV system) and at another motor terminals (6.6 kV system without reactor)

The maximum allowable step value as per IEC 61800-4 (for interturn insulation) with rise times below 1µs is 3 kV. The rise time, du/dt and amplitude definitions in IEC 68000-4

[3.20] are followed. The recordings at the reactor input show a maximum value of approximately 3.85 kV with rise times below 1 μs (Fig. 3.12). Furthermore according to IEC 61800-4 [3.20] a normal motor should be able to withstand a maximum voltage phase to earth (main insulation) of 0.9 x *Uins* (rated insulation voltage), i.e. 0.9x 11.55kV = 10.4 kV whereas a maximum value of 11.33 kV was recorded. Similar waveforms at the motor terminals for a system without a reactor may be expected; for a standard/old/existing motor insulation system. The interturn withstand capability in accordance with IEC 61800-4 may have been a concern. The IEC standard 60034-18-42 [3.21] provides qualification procedures for new motors and the recorded waveforms (without a reactor) can easily be managed. Motors fed from lower voltage VSI-CHB drives (e.g. 6.6 kV) present a smaller concern due to the smaller voltage steps as shown in Fig. 3.12. The figure also shows that the oscillation frequency for the 6.6 kV application with longer cable length is lower since the oscillation frequency reduces with an increase in cable length [3.15]. Longer cable lengths for higher voltage applications may therefore also present less severe cases due to a lower oscillation frequency and associated lower du/dt rates. The recorded values are however well within the capability of custom designed reactor with special insulation (withstand capability of du/dt=15 kV/μs and a winding breakdown voltage of 17 kV rms across the winding).

3.3.2 Maximum Peak Values at Motor

A far greater concern is the waveform shape and peak values recorded at the motor terminals as shown in Fig. 3.10 and with higher resolution in Fig. 3.13. The measurements show that phase to earth levels in terms of IEC 61800-4 are exceeded which can lead to premature motor failure since the motors do not have increased voltage withstand capability. The qualifying procedures in IEC 60034-18-42 do not specifically address resonance conditions for standard motors. The motor manufacturer has confirmed that the waveforms are unacceptable. Pulse evaluation curves shown in [3.22] confirm accelerated aging can be expected based on the measured waveforms. This thesis therefore focuses on this applicable resonance overvoltage phenomenon (which does not represent characteristic travelling waves).

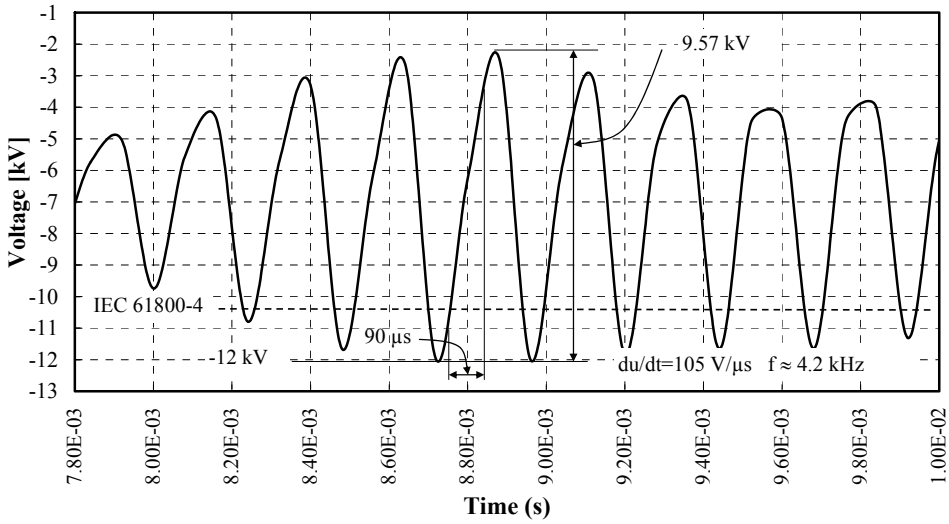

Fig. 3.13 Example of voltage phase to earth waveforms (TP3, 1200 rpm, zoomed in bottom section of Fig. 3.10) at the motor terminals

3.4 FURTHER COMPARISON OF SIMULATION AND TEST RESULTS AND RESONANCE EXPLANATION

The test and simulation results are best analyzed in the frequency domain. An FFT conversion has been performed on the measured data to obtain a frequency domain representation. The same FFT conversion process has been performed on the time domain simulation results (shown in Fig. 3.7) for additional verification. The results are shown in Fig. 3.14.

Good correlation between the simulated and test results are achieved since the amplitudes and frequencies are similar. The amplification of inverter harmonics around the calculated resonant frequency (from the transfer function/simplified equation) is clearly visible when compared to Fig. 3.2. (It is acknowledged that the inverter output phase to neutral waveform differs slightly in appearance from the inverter phase to earth waveform but the harmonics are still present at the same frequency bands and the cleaner phase to neutral waveform is still suitable for the comparison). Fig. 3.14 also shows that the resonance condition and approximate resonance frequency can easily be determined from test results and knowledge of the inverter output spectrum. The condition is applicable when the tests

results in the frequency spectrum are significantly larger than inverter output spectrum, The resonant frequency is where the effect of amplification is most severe.

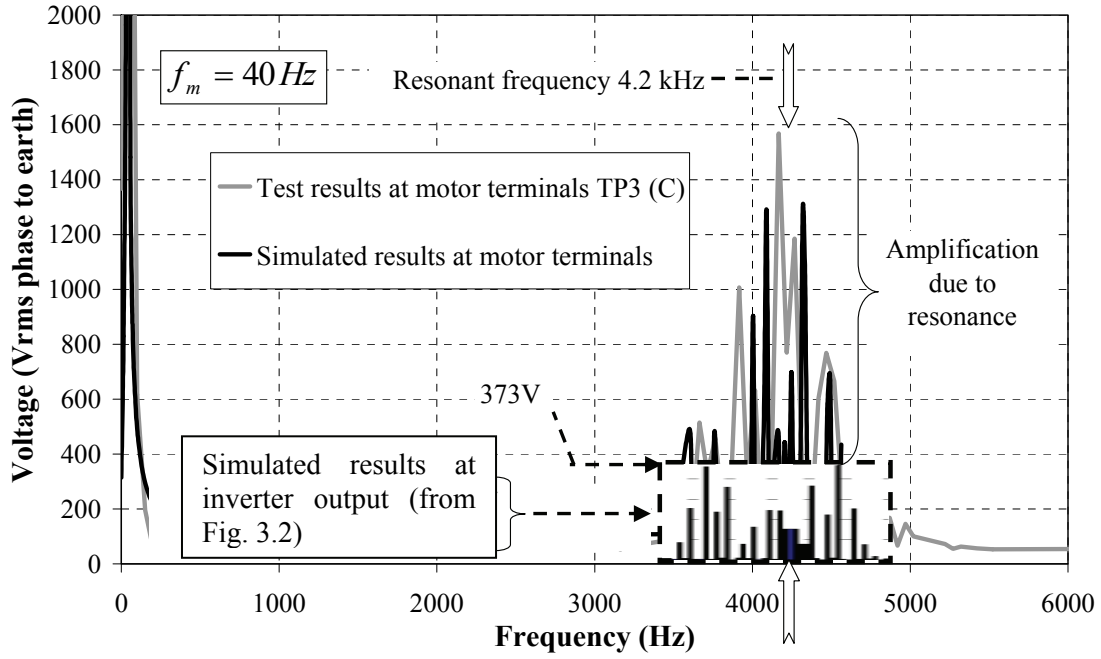

Fig. 3.14 FFT test and simulation results of motor phase to earth voltage (f_m=40 Hz, f_c= 404.5 Hz, m_a= 0.8)

3.5 SOLUTION AND SIMULATION RESULTS

More suitable carrier frequencies, modulation strategies and possibly a filter are solutions that can be considered. Alternative modulation strategies addressing selective harmonic elimination [3.23] can be investigated. A RC filter or sine filter can be used on the output of the reactor. Both type of filters may however be associated with concerns during synchronisation. The carrier frequency change is the most simplistic solution requiring minimum changes (hardware/software) and will therefore further be considered. The effective inverter switching frequency with a carrier frequency of 404.5 Hz (default) is 4.05 kHz as previously discussed, with sidebands on the harmonic spectrum around this frequency (other similar lower amplitude sidebands occur at higher multiples of this frequency). In order to avoid the excitation of resonances the effective inverter frequency should not be close to the system resonant frequency, i.e. it should be at around 2 kHz (or below) or preferably higher than 5 kHz where there is no amplitude amplification in

accordance with the transfer function (refer to Fig. 3.5). The higher frequency option is preferred since higher frequency multiple sidebands would then also be above the resonant frequency. A significantly higher carrier frequency is also preferred due to a reduction in the harmonic distortion in the inverter output waveform, which assists in improving the waveform at the motor terminals. An effective inverter frequency of 8 kHz (f_c=*800 Hz*) was therefore selected. Fig. 3.15 shows the simulation results with near sinusoidal waveforms. There is still some simulated resonance at the calculated system resonant frequency, but the magnitude is very small since the exciting harmonics are now extremely small.

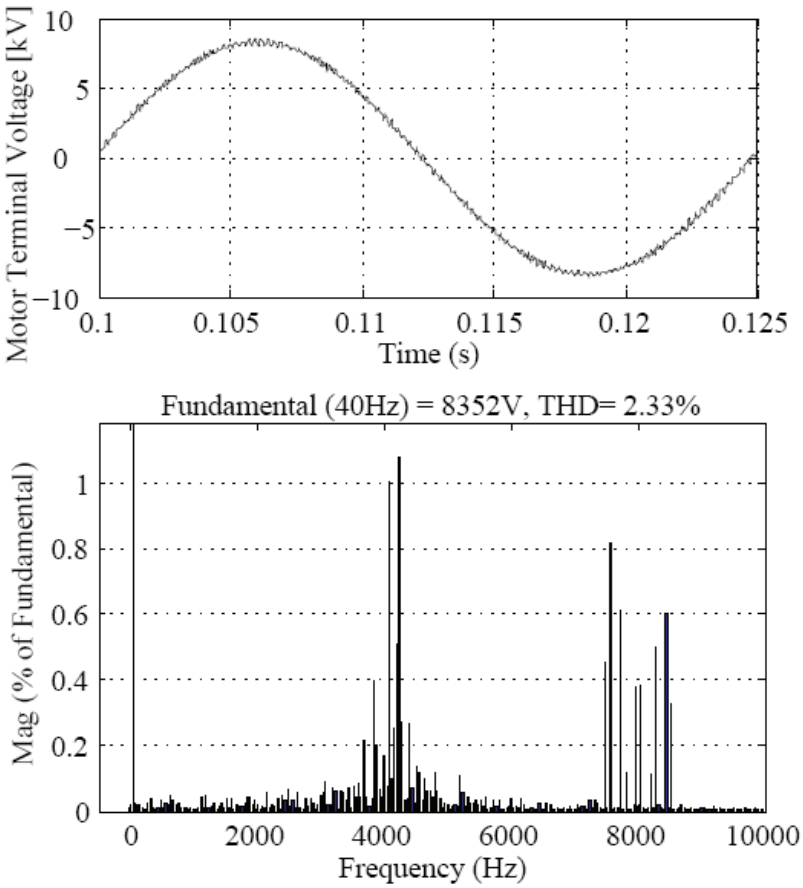

Fig. 3.15 Simulated motor voltage phase to earth (f_m=40 Hz, f_c= 800 Hz, m_a= 0.8)

The manufacturer has confirmed that no inverter derating is required at the higher frequency and that 800 Hz is also suitable in terms of the processor capability. This frequency is far away from the system resonance frequency influenced by the cable capacitance. The system designer should have accurate cable length information available

for typical MV projects. The total cable capacitance is therefore available (from data sheets and calculated as shown e.g. in Appendix C) but may not be exactly accurate due to possible changes in the cable route or due to capacitance variation with system conditions (e.g. temperature). These variations should however have a far smaller % change on the resonance frequency variation than the large % change in effective inverter frequency to move out of the resonance frequency band.

3.6 FURTHER TEST RESULTS AND EVALUATION

The process conditions did not allow shutdown of the motor for connection and removal of test equipment at the motor terminals after the carrier frequency change has been made. Tests were therefore only possible at the output of the reactor (with the synchronization concept as described in chapter 1 and 2, test equipment can be connected at the output of the reactor in the synchronized mode, the tests are performed in the de-synchronized mode and the equipment is again removed in the synchronized mode). The previous measurements (Fig. 3.10) indicate that the waveforms at the output of the reactor and at the motor terminals are very similar, as expected. The tests results therefore provide an acceptable indication of the effectiveness of the proposed modification and tests at the motor terminals were not deemed necessary. Fig. 3.16 shows the measured results which confirm the expected near sinusoidal waveforms predicted by the simulated results (Fig. 3.15). Further measured results are also shown in Fig. 3.17 at various frequencies, before the carrier frequency change has been made to show that the resonance phenomenon occurs similarly at different motor frequencies/speeds

Further simulations were performed by the drive manufacturer by including the effects of high frequency in the reactor and cables (considering the skin effect, by using finite element analysis software) with similar simulation results. The high frequency effects results in a 25% (3.9 kHz) higher frequency that was calculated initially with equation (3-2) mainly due to the reduction in the reactance and capacitance values. The inclusion of the motor parameters also has a significant and additional contribution in the increase in resonant frequency as per equation (3-5).

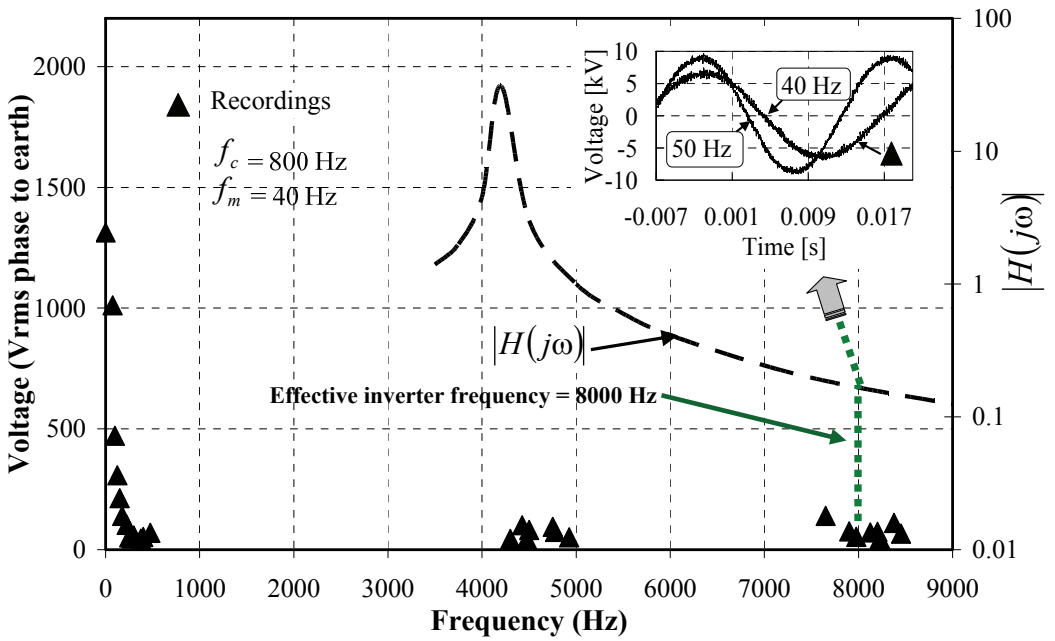

Fig. 3.16. Voltage recordings from field tests after the carrier frequency (f_c) change

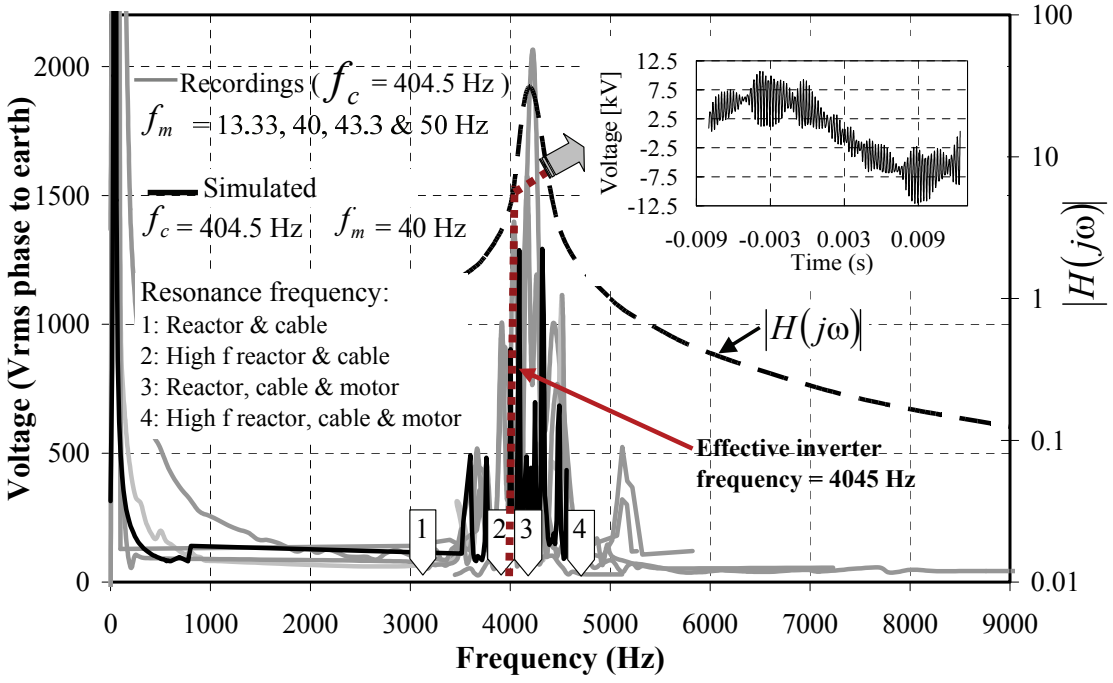

Fig. 3.17 FFT Voltage recordings from field tests at the default carrier frequency (f_c) and associated recorded phase to earth waveforms at 40 Hz (1200rpm)

The high frequency cable and reactor parameters result in an approximate 14% overall increase in the resonance frequency (including the motor) for this case study (i.e. 4.77 kHz). Fig. 3.17 shows that the simulation resulted in adequate accuracy confirming the theory presented earlier.

The effect on the calculated resonance frequency by not including high frequency effects or all parameters is shown in the Fig. 3.17. Even with all parameters and effects included, the approximate resonance frequency remains far off the effective inverter frequency with the new proposed carrier frequency.

It can be concluded that the exact high frequency parameter values are not that important (consistent with the theory in the previous section) especially if the effective inverter frequency is selected far away resonance and well above the frequency where no amplitude amplification occurs in accordance with the transfer function.

The simulation model and resonance calculation can therefore be used to analyse the resonance effect with further case studies for illustrative purposes and to determine optimal strategies to manage resonance.

3.7 MAXIMUM OVERVOLTAGES

The worst case condition is estimated by the simulation in Fig. 3.18 where the cell carrier frequency has been increased to 420 Hz to obtain an effective inverter frequency of 4.2 kHz at the system resonance frequency.

Fig. 3.18 shows severe peak phase to earth voltages of approximately 20 kV which could have been expected, i.e. almost 2 times the maximum voltage stipulated by IEC 61800-4 for normal motors. The next chapter researches worst case conditions for other cable lengths.

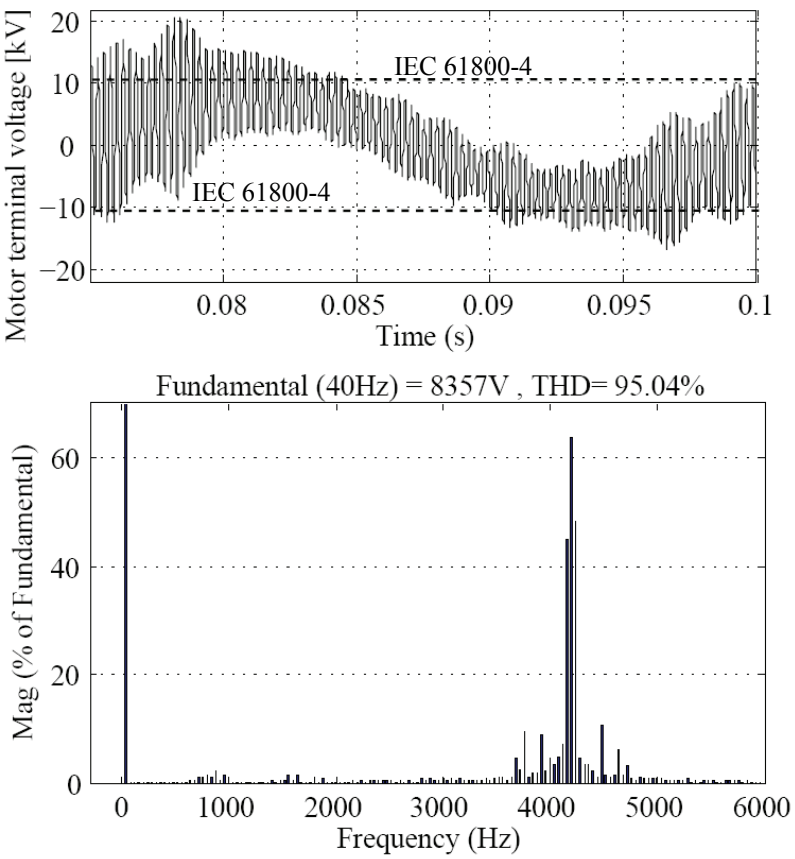

Fig. 3.18 Simulated motor voltage phase to earth (f_m=40 Hz, f_c= 420 Hz, m_a= 0.8)

3.8 CONCLUSIONS AND RECOMMENDATIONS

Field test results show that unacceptable overvoltage effects can occur in medium voltage multilevel drive systems, ultimately leading to premature motor failure and associated production losses. Motor voltages associated with high frequency travelling waves may be a concern in some cases with larger voltage steps associated with higher voltage output drives (in systems without a synchronization reactor). Resonance overvoltages can be far more severe than travelling wave overvoltages. Surge counter test equipment used to detect overvoltage problems is not effective to detect resonance overvoltage conditions. It is therefore recommended to perform oscilloscope tests as well. Simulation and subsequent test results show that the resonance effects can be minimized with the implementation of an optimal carrier frequency. The effect of model complexity and parameter variation with frequency has been investigated showing simplification opportunities. A simplified model was therefore developed to show potential worst case resonance scenarios. A simplified

calculation method was developed which can be used to conveniently determine suitable carrier frequencies to avoid resonance. Overvoltages associated with smaller motor lower voltage VSI-CHB drive applications (e.g. 6.6 kV) are unlikely to be associated with unacceptable travelling wave or resonance overvolatges. It has been shown that potential resonance becomes more likely with larger drive systems with reactors.

High power applications are becoming more in demand, are mostly process critical and a bypass configuration is often advised. Multiple motor applications are also encountered in the petrochemical industry. A synchronisation reactor is typically used in these systems and the overvoltage problem can effectively be addressed by the selection of the correct carrier frequency to avoid resonances. The reactor also eliminates the possibility of travelling wave overvoltages at the motor terminals. Existing and new motors with a high rated voltage and with standard insulation can therefore now benefit from large adjustable speed drive technology. The simulation model and simplified equations were proven with a site case study. These models are used in the next chapter to develop a generalized design approach for drive systems with various cable lengths and motors sizes. Further research is required to study the effect of various motor sizes and cable lengths which is addressed in the next chapter.

3.9 REFERENCES

[3.1] W. Chen, G. Gao, and C. A. Mouton, “Stator insulation system evaluation and improvement for medium voltage adjustable speed drive applications,” in *Proc. IEEE Petroleum and Chemical Industry Committee (PCIC)*, 2008, Cincinnati, OH, pp. 1–7.

[3.2] M. K.W. Stranges, G. C. Stone, and D. L. Bogh, “Progress on IEC 60034-18-42 for qualification of stator insulation for medium-voltage inverter duty applications”, in *Proc. IEEE Petroleum and Chemical Industry Committee (PCIC)*, 2007, Calgary, pp. 1–7.

[3.3] S. U. Haq, “A study on insulation problems in drive fed medium voltage induction motors,” Ph.D thesis, Dept. Elec. Comp. Eng., University of Waterloo, Ontario, Canada, 2007

[3.4] J. A. Oliver and G. C. Stone, "Implications for the application of adjustable speed drive electronics to motor stator winding insulation," *IEEE Electr. Insul. Mag.*, vol. 11, no. 4, pp. 26–32, Jul./Aug. 1995.

[3.5] J. Rodríguez, J. Pontt, C. Silva, R. Musalem, P. Newman, R. Vargas, and S. Fuentes, "Resonances and overvoltages in a medium-voltage fan motor drive with long cables in an underground mine," *IEEE Trans. Ind. Appl.*, vol. 42, no. 3, pp. 856–863, May/Jun. 2006.

[3.6] R. O. Raad, T. Henriksen, H. Raphael, and A. Hadler-Jacobsen, "Converter-fed subsea motor drives," *IEEE Trans. Ind. Appl.*, vol. 32, no. 5, pp. 1069–1079, Sep./Oct. 1996.

[3.7] M. Berth, L. Küng, and E. F. D. E. Limbeck, "Switching overvoltages in motor circuits," *IEEE Trans. Ind. Appl.*, vol. 37, no. 6, pp. 1582–1589, Nov./Dec. 2001

[3.8] B. Wu, *High Power Converters and AC Drives*. Piscataway, NJ: IEEE Press, 2006.

[3.9] ASIRobicon, *HV Water Cooled Harmony User Manual*, Appendix A, Performance Capabilities, Manual number 19001105, May 2005

[3.10] J. Rodríguez, P.W. Hammond, J. Pontt, R. Musalem, P. Lezana, M. J. Escobar, "Operation of a Medium-Voltage Drive Under Faulty Conditions", *IEEE Trans. Ind. Electron.*, vol. 52, no. 4, pp. 1080-1085, Aug. 2005.

[3.11] J. Rodriguez, L.G. Franquelo, S. Kouro, J.I. Leon, R.C. Portillo, M.A.A Prats, M.A. Perez, "Multilevel Converters: An Enabling Technology for High-Power Applications," *Proc. IEEE,* vol. 97, no. 11, pp. 1786-1817, Nov. 2009.

[3.12] A. Papoulis, *Circuits and Systems – A Modern Approach*, Holt, Rinehart and Winston Inc., 1980

[3.13] A. Greenwood, *Electrical Transients in Power Systems*, 2nd ed., John Wiley & Sons Inc., 1990

[3.14] G. Scheuer, B. Monsen, K. Rongve, T. Moen, E. Vitanen, "Subsea compact gas compression with high speed VSDs and very long step-out cables," in *Proc. Petroleum and Chemical Industry Committee (PCIC) Europe,* Barcelona, Spain, 2009, pp.163-173.

[3.15] R. J. Kerkman, D. Leggate, and G. L. Skibinski, "Interaction of drive modulation and cable parameters on AC motor transients," *IEEE Trans. Ind. Appl.*, vol. 33, no. 3, pp. 722–731, May/Jun. 1997.

[3.16] A. F Moreira, T. A. Lipo, G. Venkataramanan, and S. Bernet, "Highfrequency modeling for cable and induction motor overvoltage studies in long cable drives," *IEEE Trans. Ind. Appl.*, vol. 38, no. 5, pp. 1297–1306, Sep./Oct. 2002.

[3.17] Matlab Simulink, Version 7 Release 14, Transmission Line Model Notes

[3.18] R. Wetter, B. Kawabani, J. Simond, "Voltage stresses on PWM inverter fed induction motors: Cable modeling and measurement," in *Proc. International Conference on Electrical machines (ICEM)*, 2004, CD-ROM, Paper 273.

[3.19] P. Mäki-Ontto, H. Kinnunen, J. Luomi, "AC motor cable model for bearing current and over-voltage analysis," in *Proc. International Conference on Electrical machines (ICEM)*, 2004, CD-ROM, Paper 367.

[3.20] *Adjustable Speed Electrical Power Drive Systems—Part 4: General Requirements—Rating Specifications for a.c. Power Drive Systems Above 1000 V a.c. and not Exceeding 35 kV*, IEC 61800-4, 2002.

[3.21] *Rotating electrical machines - Part 18-42: Qualification and acceptance tests for partial discharge resistant electrical insulation systems (Type II) used in rotating electrical machines fed from voltage converters*, IEC 60034-18-42, 2008.

[3.22] M. Kaufhold, K. Schäfer, K. Bauer, and M. Rossmann, "Medium and high power drive systems; Requirements and suitability proof for winding insulation systems," in *Proc. International Electrical Insulation Conference (INSUCON)*, 2006, pp. 86–92.

[3.23] L. Li, D. Czarkowski, Y. Liu, and P. Pillay, "Multilevel selective harmonic elimination PWM technique in series-connected voltage inverters," *IEEE Trans. Ind. Appl.*, vol. 36, no. 1, pp. 160–170, Jan./Feb. 2000.

4 GENERALIZED DESIGN APPROACH FOR VSI AND LCI SYSTEMS WITH LONG CABLE

There is a need to research the occurrence of potential overvoltage problems on VSI-CHB systems for a wider range of conditions and applications. The resonance overvoltage possibility with the conventional LCI technology, previously not applied for long cable lengths, is also evaluated. Requirements for the two technologies are compared throughput the chapter. A comprehensive case study is presented involving both technologies with several large synchronous motors (combined rating of approximately 500 MW) and cable lengths up to 3 km. As it is not always practical to perform advanced simulations to determine the suitability of a project proposal, a generalized design approach for both technologies and various cable lengths and motor sizes is developed. The design approach also provides a convenient guide to determine solutions for both technologies to solve the resonance problem with long cable lengths.

4.1 INTRODUCTION

A case study in Chapter 2 has shown that MV VSI-CHB system technology can compete in some areas of conventional LCIs for large synchronous motor systems. Reliability has not yet been proven as for LCI systems but schemes have been proposed to enhance the availability as discussed in Chapter 1 and 2. LCIs may still be more beneficial for pure soft starting of very large motors (the negative aspects are not as applicable due to short duration operation), air-cooled systems may be used in stead of water cooled systems (larger air cooled systems are generally available for LCIs with less maintenance) and the benefit from proven reliability is obtained. LCIs may also still be recommended for very large applications especially where the risk of implementing new technology (unproven for the size range) can not be mitigated. There is therefore a need to investigate the influence of long cables in LCI systems as well.

Motor insulation requirements associated with MV ASDs are well documented in literature and the recently published IEC standards as discussed in the previous chapter. The standard (and literature) focus however on MV PWM VSIs and is based on the expected waveforms (reflective wave phenomenon) at the motor terminals considering cable effects.

It has however been shown in the previous chapter that waveforms at motor terminals when fed by VSIs can be significantly different to the expected waveforms when long cable distances are involved due to resonance effects. The standard also does not cover topologies i.e. current source inverter / LCI topologies (and is not applicable for soft start requirements). Manufacturers of LCI systems normally specify that an output cable length of only a few hundred meters is allowed (e.g. 200 m [4.1]), however application requirements can call for far longer cable lengths.

This chapter focuses on the VSI-CHB and LCI technologies with synchronous motors. The models developed in the previous chapter are used to develop a generalized design approach for VSI-CHB systems with various cable lengths and motors sizes. The relevant background theory provided in the previous chapter is extended for analysis of LCI systems as well.

4.2 THEORY

4.2.1 Load Modelling and Resonance Principles

Both LCIs and VSIs can contain current and voltage harmonics, respectively, in their output spectrum that excite resonances at or around the load system resonance frequency (f_r). The load system is regarded as all system components downstream of the output of the inverter terminals. These may include a step-up transformer / reactor /filter, cabling and the motor. Load modelling principles are similar for LCIs and VSIs and described in the previous chapter. It is shown in the previous chapter that the load model can be simplified with a lumped parameter approach (instead of distributed parameters) since the resonance frequency is typically in the order of several kHz (with an output reactor/transformer present). Simplified equations are also presented in the previous chapter that can be used to

estimate the system resonance frequency. It is necessary to model the output of the inverters as an input to the load model to determine the motor terminal voltage and current waveforms.

4.2.2 VSI Theory

The output waveforms of most commercial voltage source inverters can be modelled in accordance with [4.2]. It has been shown in previous chapters that presently the VSI-CHB bridge topology is one of most likely topologies to compete with LCI systems for high power applications with a high output voltage (≥ 11 kV). The theory, topology drawings and modelling principles for VSI-CHB systems are described in the previous chapter. Typical simulated output voltage waveforms and the associated frequency spectrum are also shown in the previous chapter. The current is near sinusoidal and not shown (without output cable effects). The relationship between the number of levels, fundamental frequency, carrier frequency, effective inverter frequency and harmonic spectrum is described in the previous chapter.

4.2.3 LCI theory

The LCI hardware block diagram is given in Chapter 2 and LCI current source inverter theory is covered in [4.3]. This section describes LCI theory as background for the case study section. Integer harmonics currents seen at the LCI system output (machine side) are given by [4.1], [4.4]:

$$i_n = \frac{1}{n} \cdot \frac{\sqrt{a^2 + b^2 - 2 \cdot a \cdot b \cdot \cos(2 \cdot \alpha \cdot \mu)}}{2 \cdot d_x} \tag{4-1}$$

$$I_{ni} = i_n \cdot I_1 \tag{4-2}$$

with

$$a = \frac{1}{n-1} \cdot \sin\left(\frac{(n-1) \cdot \mu}{2}\right) \tag{4-3}$$

$$b = \frac{1}{n+1} \cdot \sin\left(\frac{(n+1).\mu}{2}\right) \tag{4-4}$$

I_{ni} = Amplitude of the inverter harmonic current of the order n

n = $6 \cdot k \pm 1$ and $k = 1, 2, 3, 4, 5 \ldots$

μ = overlap angle [rad]

α = firing angle [rad]

d_x = relative direct voltage drop

The above equations refer to a smooth d.c. current. The actual ripple of the d.c. current effects mainly the harmonic order 5. Therefore the order 5 harmonic is corrected with the following equation [4.1], [4.5]:

$$corr5 = 5 \cdot \left(\frac{1}{5} \cdot \frac{6.46 \cdot 2 \cdot w}{5-1} - \frac{7.13 \cdot 2 \cdot w}{5}\right) \tag{4-5}$$

$$\text{with} \quad w = \frac{\Delta I_d}{2 \cdot I_d} \tag{4-6}$$

Typical simulated output waveforms (provided by the manufacturer of the LCI) and the current frequency spectrum are shown in Fig. 4.1 and Fig. 4.2. A typical compressor start-up curve (as shown in [4.1]) is used for the load vs. speed/frequency characteristic.

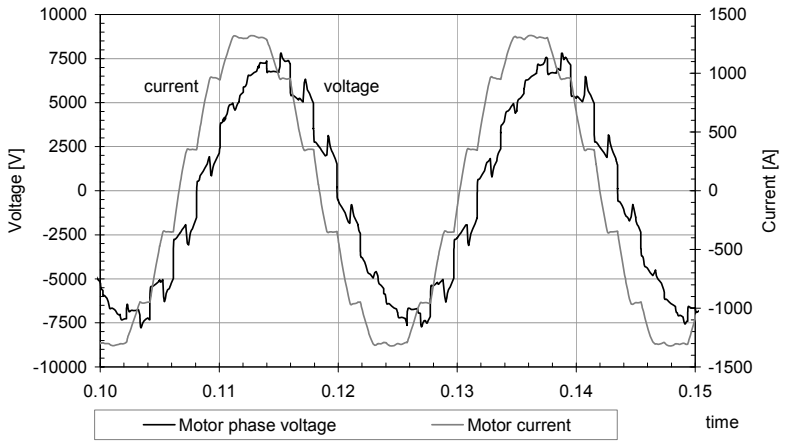

Fig. 4.1 Example of LCI output waveforms – 42.4 Hz operation (no cable effects) [4.1]

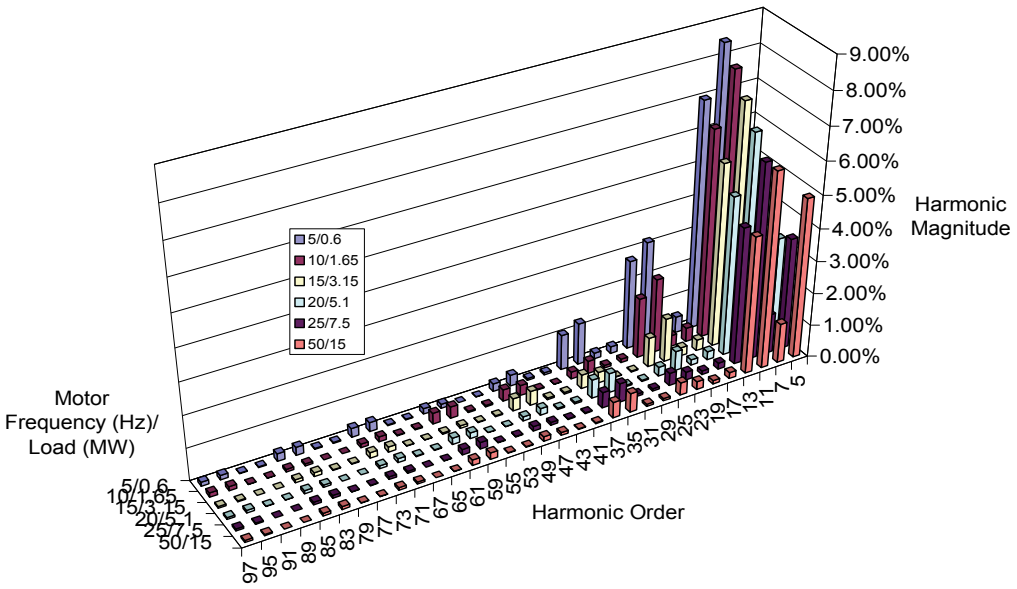

Fig. 4.2 Example of LCI output current harmonic spectrum [4.1]

4.2.4 System Modelling

The system modelling uses the inverter model output as input to the load model to determine the waveforms at the machine terminals. The detailed description of the VSI-CHB system model with an output reactor is given in the previous Chapter. The LCI system model is shown Fig. 4.3 [4.1]. The output transformer is required for the 12 pulse configuration since the machine has a single stator winding. Furthermore the output voltage of the LCI is stepped-up with the transformer to match the machine voltage rating.

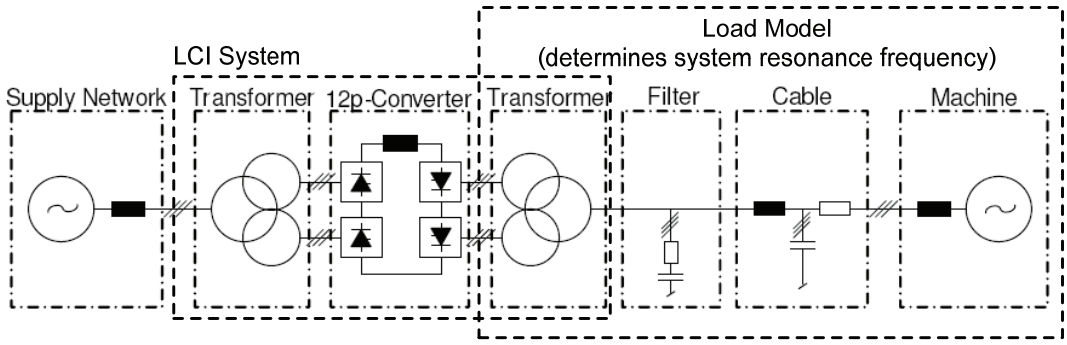

Fig. 4.3 System Model with LCI [4.1]

4.2.5 Pulsating Torques

In LCI driven motors, pulsating torques of various frequencies are superimposed on the air-gap torque. Although the amplitudes of such pulsating torques may be small compared to the driving torque, they can excite resonances/torsional excitations, when their frequency coincides with a natural frequency of the rotating mechanical system.

Pulsating torques are described in further detail in [4.1] with associated curves. In VSI systems pulsating torques are generally significantly less than in LCI systems and with VSI-CHB systems pulsating torques decrease to typically 1 % of motor base rating [4.6] (near sinusoidal currents).

4.3 ROTOR POSITION DETECTION

Rotor position detection principles for LCIs are described in [4.7]. The rotor position needs to be known to determine accurate firing of the thyristors in the LCI. Flux calculation is used for motor cable lengths shorter than the maximum allowed length (l_{max}). Flux calculation is accomplished by a pulse from the excitation into the field winding of the synchronous motor.

By measuring the stator voltage at the LCI terminals, the controller can determine the position of the rotor. Rotor position detection during initial “DC link pulsing” [4.3] at low speeds may be challenging where sufficient voltage feedback might also not be available for the flux calculation due to the voltage drop across the long cables.

Experience from previous projects has shown that motor cable lengths longer than 500 meters [4.1] will create problems for the controller to determine the position using the method mentioned above.

VSI systems typically follow the same principle to detect the initial position, but does not require “DC link pulsing” and is therefore less dependent on rotor position detection.

Synchronous motors with cable lengths longer than 500m have successfully been started in with a VSI (e.g. the system described in the previous chapters).

It is however recommended to confirm with the specific manufacturer of the drive system whether there is a need for position detection when long cable distances are involved since it depends on vendor specific internal control strategies (typically open loop vector control is used with a flux regulator determining the excitation current and magnetising component of the stator current). Furthermore it is also recommended to include rotor overvoltage protection in the case of a possible out of step-condition during initial start-up.

4.4 CASE STUDIES

4.4.1 Introduction

The effect of cable length, output reactance and motor size on resonance frequency is studied first by means of case studies using parameters of actual motors. The parameters are provided in Appendix C.

Secondly an actual configuration on a large petrochemical plant is studied. Fig. 4.4 shows the overall single line diagram for the start/drive systems in the case studies. The system background is described in Chapter 2.

The Oxygen West and East plants air compressor synchronous motors are presently started by MG-sets (traditional approach). The MG-sets are however outdated (limited spares available) and back-up from an alternative modern static frequency converter starting source is desired as described in chapter 2.

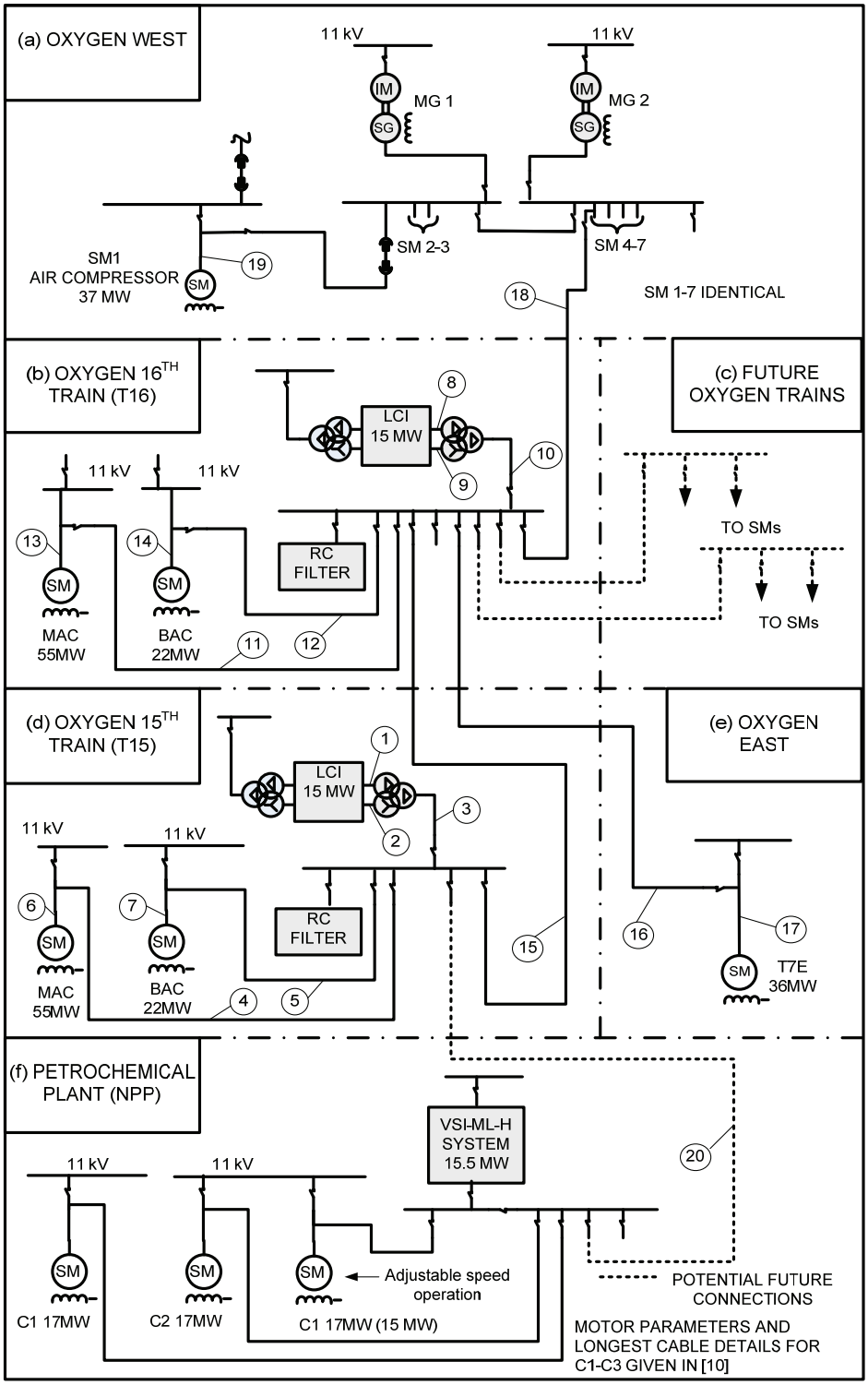

Fig. 4.4 Overall single line diagram (cable details in Appendix C)

The general philosophy of the entire plant is to have at least N-1 redundancy for start/drive systems. A new petrochemical plant (NPP) was commissioned with a VSI-CHB system as described in Chapter 2 for both soft start and ASD operation. A potential back-up from another starting system (either local or remote) should be investigated to fulfil the N-1 requirement. Oxygen train 15 has a LCI start-up system as described in Chapter 2.

A new oxygen train 16 is in the execution phase and a similar LCI as for train 15 has been procured. The initial requirement is that the 15th and 16th train LCIs serve as back-up to each other, but in future the back-up of these LCI to Oxygen West/other systems may be required. It is also investigated whether the LCIs can serve as starting back-up to the NPP VSI–CHB and vice versa (although this option is less likely to be implemented). Synchronization schemes, interlocking and control considerations are not in the scope of this chapter but overviewed in Chapter 2. System parameters are provided in Appendix C.

4.4.2 Resonance Simulation VSI-CHB

Simulation and test results are comprehensively described in Chapter 3. The ASD, reactor, motor and cable parameters are given in Appendix C. Chapter 3 provides the test results at the default carrier frequency which corresponds closely with the simulation results. The system resonance frequency occurs at the peak of the voltage transfer function $|H(j\omega)|$ which can be close to significant harmonics at and around the effective inverter frequency (as discussed in Chapter 3). Significant harmonic resonance distortion excited by the inverter harmonics can therefore occur. The voltage amplification associated with each inverter voltage harmonic (V_{ni}) is given by

$$V_n = V_{ni} \cdot |H(j\omega)| \tag{4-7}$$

The combined effect of all the applicable harmonics is illustrated in Chapter 3 (e.g. Fig. 3.17). Selected results for the NPP are shown in Chapter 3 but in this chapter further case studies are evaluated for a wide range of applications.

4.4.3 Effect of Cable Length, Output Reactance and Motor Size on Resonance Frequency

The analysis from the previous chapter is now expanded for various motor sizes and cable lengths. Equation (3-5) can effectively be used to estimate the effect of cable length with and without the reactor. The parameters for the cables, motor and reactor are given in Table C.2.II of Appendix C. Total cable capacitance, inductance and resistance are calculated on the same basis as was done in Table C.2.I of Appendix C. It is assumed that the cable size/quantity does not increase with length to compensate for increased voltage drop. This may only be applicable for extremely long cables since a large derating factor for the cables have been applied associated with the ampacity calculations for typical petrochemical projects. The results are shown in Fig. 4.5. The figure shows that with the default carrier frequency resonance would have occurred with the case study motor in the previous chapter (17 MW) at the effective inverter frequency (4 kHz) when the cable length is 600 m. An associated simulation has been performed with results shown in Fig. 4.6.

Similarly to the results in Fig. 3.18, overvoltages reaches approximately 2 times the maximum allowed by IEC 61800-4. Fig. 4.5 also illustrates resonance that can occur with short cable lengths, e.g. with the parameters and simulation results shown in Fig. 4.7. It can be observed that the resonance condition is more severe since less damping is applicable due to the lower resistance with the shorter cable.

Fig. 4.5 indicates that resonance without a reactor is only likely at significantly longer cable distances e.g. several kilometers (approximately 3 km in the case study with the default carrier frequency). Resonance with smaller motors (without a reactor) is even less likely (Fig. 4.5). Very long cable distances are required to create a potential resonance condition in this case. Furthermore potential resonance also decreases with smaller motors with reactors since it is more likely for the system resonance frequency to be below the effective inverter frequency, especially for longer cable lengths. VSI-CHB systems have traditionally been used more commonly for lower power motors, shorter cable lengths and smaller excitation voltages (due to the smaller voltage steps with lower voltage systems) making the possibility of resonance extremely rare and this is possibly why the phenomenon has not been widely published.

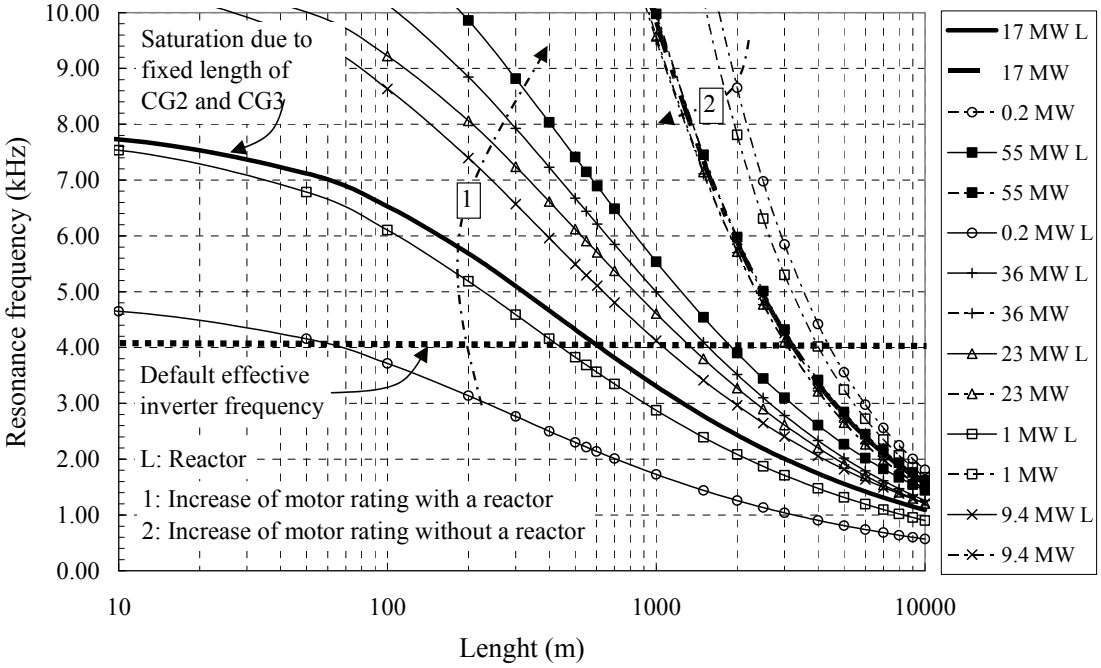

Fig. 4.5 Effect of cable length, motor rating and reactor on the resonance frequency

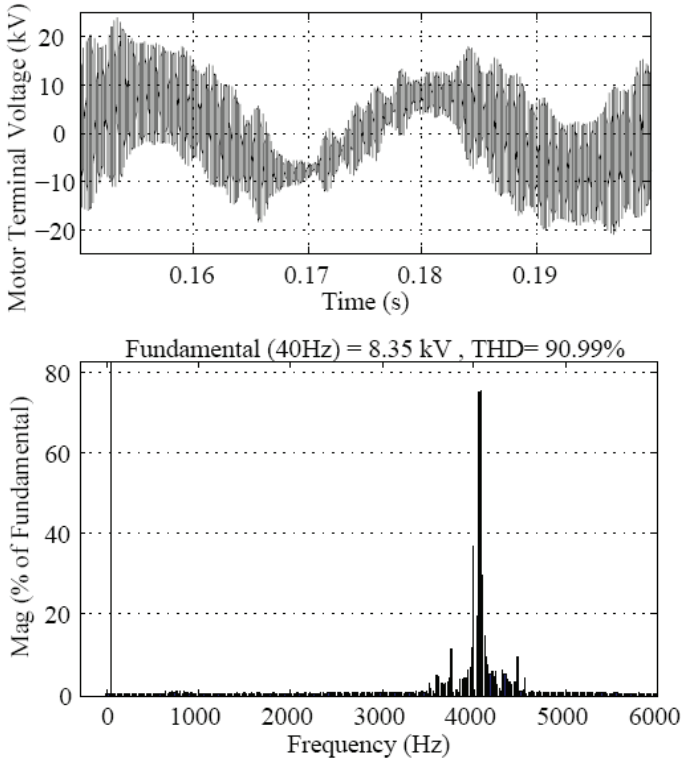

Fig. 4.6 Simulated motor phase to earth voltage (f_m=40 Hz, f_c= 404.5 Hz, m_a= 0.8, l=600m)

Large motor systems with reactors and typical cable lengths are far more likely to suffer from resonance conditions since the system resonance frequency is likely to be close to or in the region of the effective inverter frequency.

In summary, the resonance frequency reduces with an increase in cable length. Reactance at the output of the inverter (e.g. due an output reactor) reduces the resonance frequency. A similar relationship can be expected for LCI systems (a step-up transformer also adds reactance to the output circuit). The resonance frequency generally increases with an increase in motor size when reactance is present in the output circuit (e.g arrow 1 in Fig. 4.5). The resonance frequency is significantly larger without output reactance and there is less dependence on motor size (e.g. arrow 2 in Fig. 4.5). Longer cable lengths are therefore more likely in general to create resonance problems since harmonics are more significant at lower frequencies for both VSI and LCI systems.

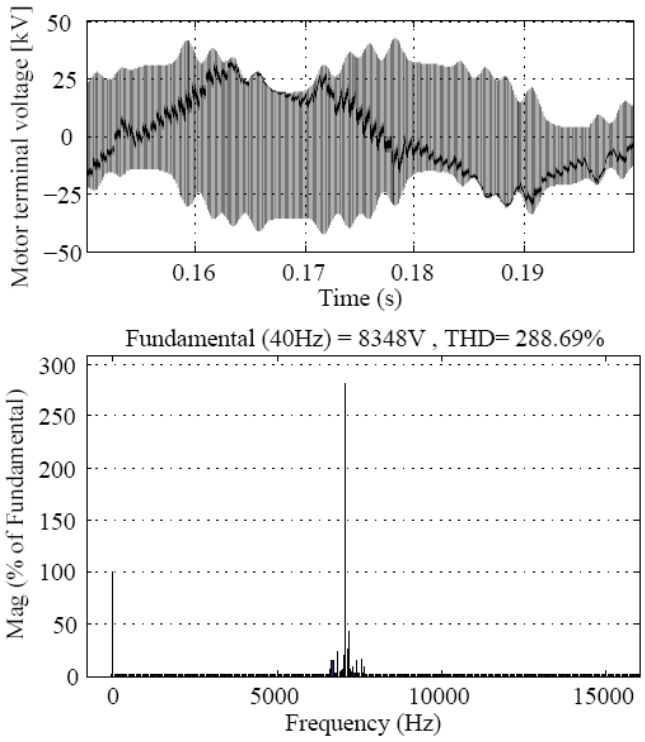

Fig. 4.7 Simulated motor phase to earth voltage (f_m=40 Hz, f_c= 712 Hz, m_a= 0.8, l=50m)

4.4.4 Carrier Frequency Considerations

Several options can be considered to eliminate resonance conditions with the carrier frequency change options as preferred solution as discussed in chapter 2. Further carrier frequency change methods are evaluated. In Method 1 the effective inverter frequency and its harmonic band (e.g. Fig. 4.8 provides a zoomed in example of the harmonic band) is selected below the resonant frequency while ensuring that the higher order harmonic bands are above the resonant frequency.

This is shown in Fig. 4.9 and the bold arrows represent the harmonic bands (based on the inverter modelling – Fig. 3.2). The benefit of this method is that the effective inverter frequency is low and therefore benefits from overall lower inverter losses. This method is more applicable for short cable lengths due to higher resonance frequencies. Fig. 4.10 shows a simulation example with acceptable results by using Method 1 (note the improvement compared to Fig. 4.7).

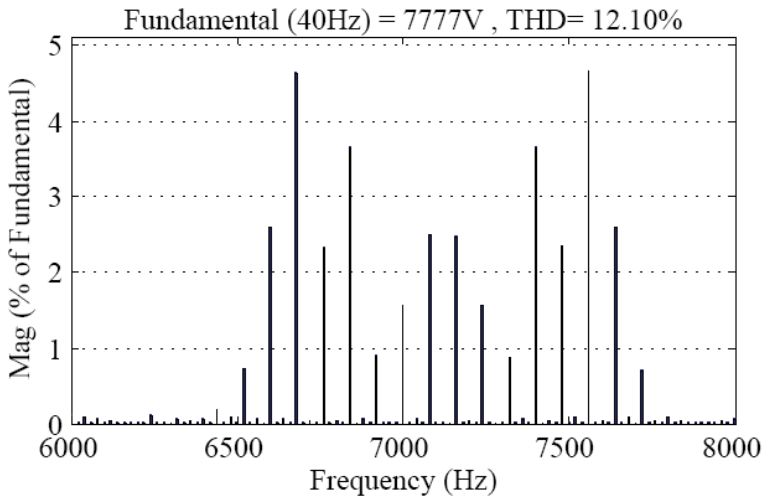

Fig. 4.8 Simulated inverter phase to neutral voltage spectrum band around the effective inverter frequency of 7.12 kHz (f_m=40 Hz, f_c= 712 Hz, m_a= 0.8)

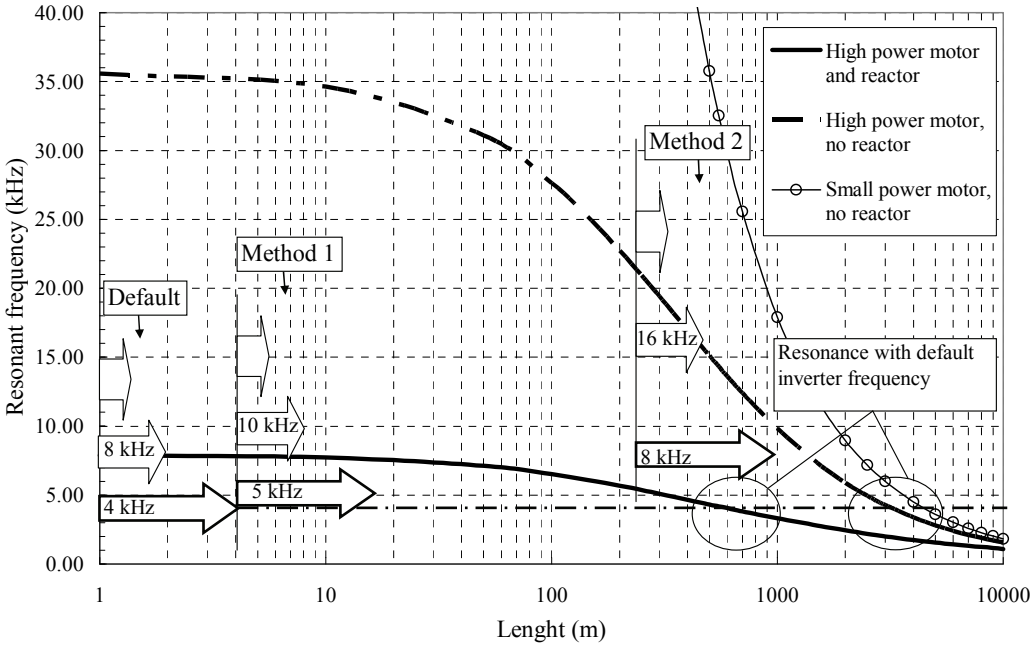

Fig. 4.9 Carrier frequency selection

In the case of longer cable lengths (large motors), the default effective inverter frequency band is typically in the range of the resonance frequency and it is necessary to increase the inverter frequency to ensure that the band is above the resonance frequency (Method 2 shown in Fig. 4.9). The higher order harmonic bands are then also above the resonant frequency. This method can also be used for very long cable distances (e.g. 3000m) without a reactor. Method 2 can be used in most cases if the higher carrier frequency is acceptable (considering that for short cable distances it implies a high carrier frequency). It has been shown in [3.8] that the multilevel VSI CHB topology is superior to other VSI topologies regarding the maximum carrier frequency and associated losses. Significantly higher carrier frequencies can be realized than shown in the actual case study but with an associated increase in converter losses with typical losses shown in [3.8]. In most cases with a reactor and long cable distances, Method 2 should be considered since a very high carrier frequency should not be required. In most cases without a reactor with typical cable lengths (e.g. below 1000 m) it should not be necessary to increase the carrier frequency (see Fig. 4.5).

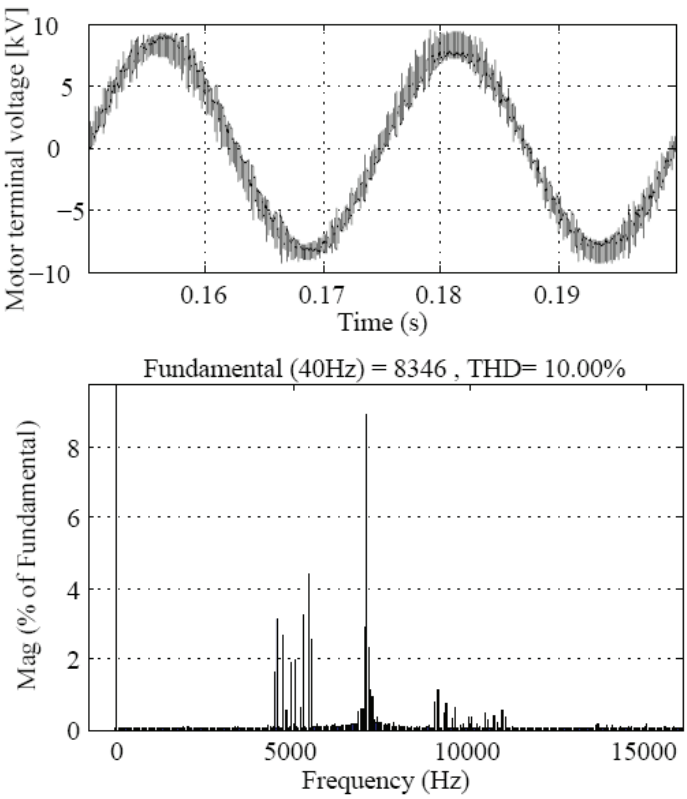

Fig. 4.10 Simulated motor phase to earth voltage (f_m=40 Hz, f_c= 500 Hz, m_a= 0.8, l=50m)

Fig. 4.9 was used as an example showing the general proposed approach. The actual selection of the inverter frequency should however be done on a case by case evaluation for the specific application. The approach of Fig. 4.9 can also be used when other methods are available e.g. to determine the harmonics in the resonance area to be eliminated or to be reduced with selective harmonic elimination [3.10]. In the case of some current source converter topologies, e.g. the load commutated inverter topology a carrier frequency change is not applicable and a suitable filter (e.g. RC filter) will have to be added to reduce the excitation of resonances. The removal of the reactor is another alternative if break-before-make transfers can be accommodated.

This increased carrier frequency method is also suitable for longer cable distances e.g. the VSI-CHB at NPP can theoretically also be used to start a motor as far as Oxygen West (Fig. 4.4 – length of cable groups 20 + 15 + 18, i.e. approximately 3.85 km).

4.4.5 Resonance Simulation – LCI [4.1]

The parameters used for the simulations are given in Appendix C.3. The resonance frequencies from the simulation for the case study are given in Table 4.I (similar relationship to the curves in Fig. 4.5 when comparing the cable lengths in the Appendix). The typical harmonic orders of 12-pulse operation are shown in bold, which will be generated by the LCI and excite the resonance frequency at the corresponding motor frequencies. The harmonic orders marked with "*" are not typical for 12-pulse operation. They are either eliminated completely or appear with very small amplitudes (see Fig. 4.1). These latter harmonic orders can be neglected.

The table also shows which harmonic order will excite the cable resonance during start-up and at what motor frequency. Example: with the T16 LCI starting Oxygen T7E, the order 85 harmonic current will have the same frequency as the cable resonance at a motor frequency of 50 Hz (85 * 50 Hz = 4250 Hz).

Equation (4-7) was used to determine the distortion by each voltage harmonic with voltage source systems. However with current source (LCI) systems the voltage distortion associated with current source harmonics can more conveniently be determined by

$$V_n = I_{ni} \cdot |Z(j\omega)| \tag{4-8}$$

During a start-up the motor frequency is increasing continuously and all harmonic orders n·fM are exciting the resonance – first the high orders then the lower orders (like a train rolling over a bump in a railway rail until it stands).

As expected the lowest resonance frequency occurs with the longest cable length. The lower order current harmonics also normally have higher amplitudes (Fig. 4.1) and therefore a worst case example of the impedance $|Z(j\omega)|$ curve is given for the lowest resonance frequency in the case study in Fig. 4.11. The associated voltage distortion is given in Fig. 4.12.

Table 4.I

RESONANCE FREQUENCIES OF VARIOUS START-UP CONDITIONS [4.1]

		T16 starts MAC16	T15 starts MAC16	T16 starts BAC16	T16 starts T7E	T15 starts BAC16	T15 starts T7E	T15 starts NPP C1	T16 starts OxWest	T15 starts OxWest
Resonance frequency [Hz]		6859	5366	6232	4250	3963	3474	2640	2078	1961
harmonic order		**Motor harmonics frequencies coinciding with resonance frequencies [Hz]**								
37										**53.00**
41	*								50.68	47.83
43	*								48.33	45.60
47									**44.21**	**41.72**
49								**53.88**	**42.41**	**40.02**
53	*							49.81	39.21	37.00
55	*							48.00	37.78	35.65
59								**44.75**	**35.22**	33.24
61								**43.28**	**34.07**	32.15
65	*							40.62	31.97	30.17
67	*							39.40	31.01	29.27
71							**48.93**	**37.18**	**29.27**	**27.62**
73							**47.59**	**36.16**	**28.47**	**26.86**
77	*						45.12	34.29	26.99	25.47
79	*					50.16	43.97	33.42	26.3	24.82
83						**47.75**	**41.86**	**31.81**	**25.04**	**23.63**
85					**50**	**46.62**	**40.87**	**31.06**	**24.45**	**23.07**
89	*				47.75	44.53	39.03	29.66	23.35	22.03
91	*				46.7	43.55	38.18	29.01	22.84	21.55
95					**44.74**	**41.72**	**36.57**	**27.79**	**21.87**	**20.64**
97					**43.81**	**40.86**	**35.81**	**27.22**	**21.42**	**20.22**

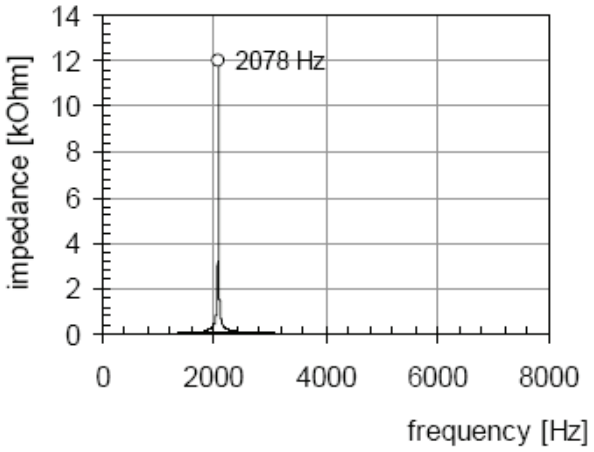

Fig. 4.11 LCI output impedance characteristic (start-up of Oxygen West with T16) [4.1]

Other applications might even have longer cable lengths and therefore even more unfavourable resonance conditions can exist. Fig. 4.1 shows that harmonic lower orders (e.g. 11) have a far higher magnitude and can excite a system resonance frequency of 550Hz. This is associated with a very long cable distance but with a lower $|Z(j\omega)|$.

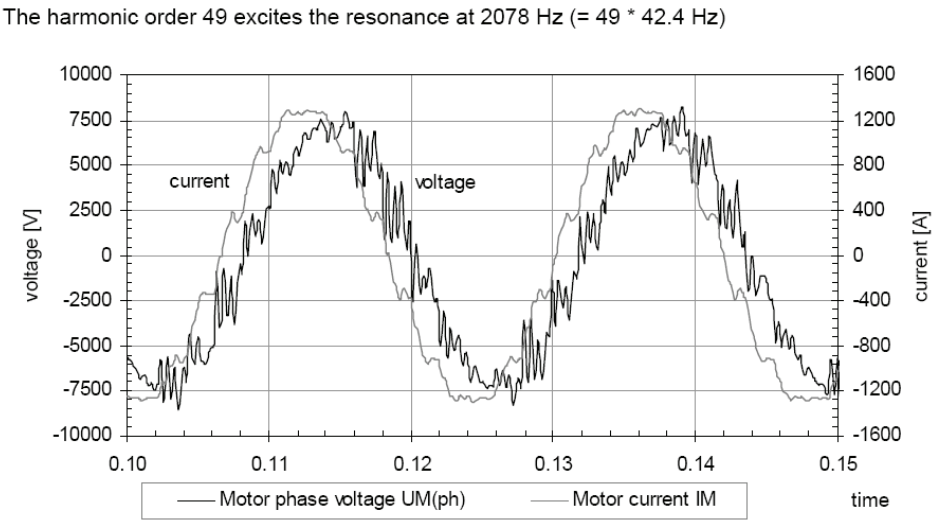

Fig. 4.12 Start-up of Oxygen West with T16 LCI at 42.4 Hz [4.1]

The fundamental current (I_1) is the highest at line frequency (50 Hz) due to the compressor start-up characteristic (assuming maximum acceleration torque is not applied throughout the speed range). Even though the harmonic currents may not be exactly at the resonance frequency, the excitation with the higher LCI harmonic amplitudes (I_{ni}) can be severe based on equation (4-2) and (4-8). This is also the frequency where the LCI operates a longer time (due to synchronization). Fig. 4.13 shows an example for this condition with significant harmonic distortion. Similar waveforms are applicable at 52 Hz (i.e. the maximum frequency with +4 % tolerance).

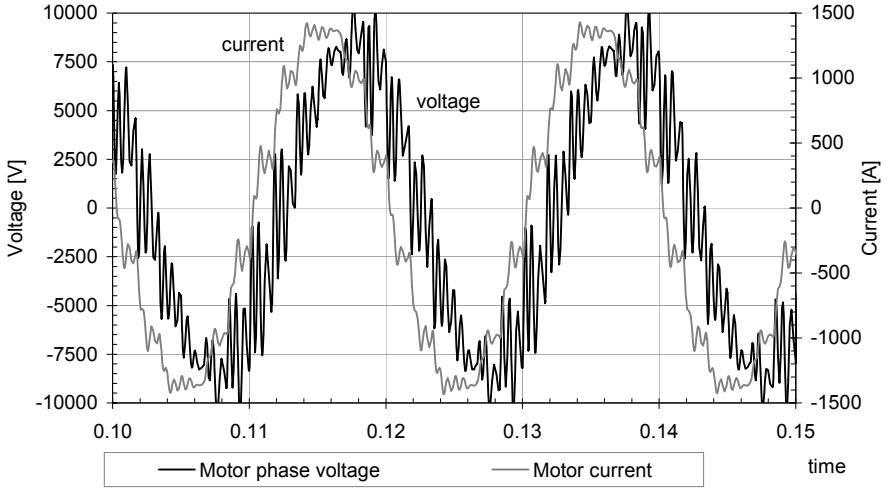

Fig. 4.13 Start-up of Oxygen West with T15 LCI at 50 Hz (no filter installed)

4.4.6 Output Filter [4.1]

Since the LCI is load commutated (with no option of a carrier frequency change), the options proposed for the VSI system to eliminate excitation of resonances are not feasible and the only alternative is to vary the LCI system output characteristic by selecting an appropriate filter to reduce the impedance ($|Z(j\omega)|$) value. The installation of an R-C filter onto the start-up tie (Fig. 4.4) can reduce the impedance of any resonance frequency, which in turn will reduce the excited voltage distortion, depending on the filter resistance. A reduction in the resistance improves the damping but increases the filter loss. The resistance has been selected by making a compromise between damping capability and filter loss. The proposed filter and parameters are shown in Fig. 4.14, the effect on the impedance in Fig. 4.15 and on the voltage waveform in Fig. 4.16.

Only one filter is required for all start-up conditions and can be installed at the start-up bus of train 16 (Fig. 4.4). The filter is only rated for intermittent start-up conditions and is therefore a compact low cost solution.

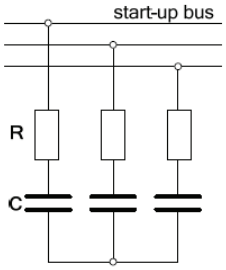

System Data	
Nominal voltage of start-up network	11 kV
Voltage variation	± 5 %
Fundamental frequency	0 .. 50 Hz
Filter Data	
Capacitance C per phase	5 µF
Resistance R per phase (of low inductance)	100 ohm

Fig. 4.14 Proposed filter and characteristics [4.1]

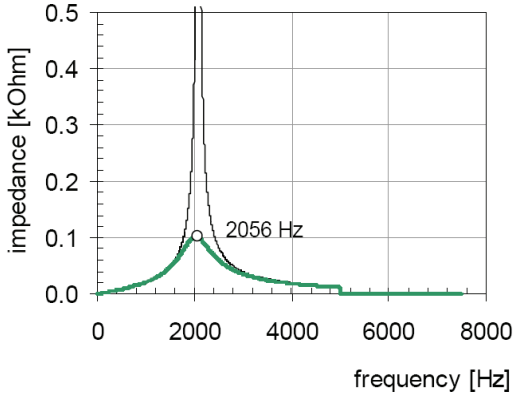

Fig. 4.15 LCI output impedance characteristic with RC filter (start-up of Oxygen West with T16) [4.1]

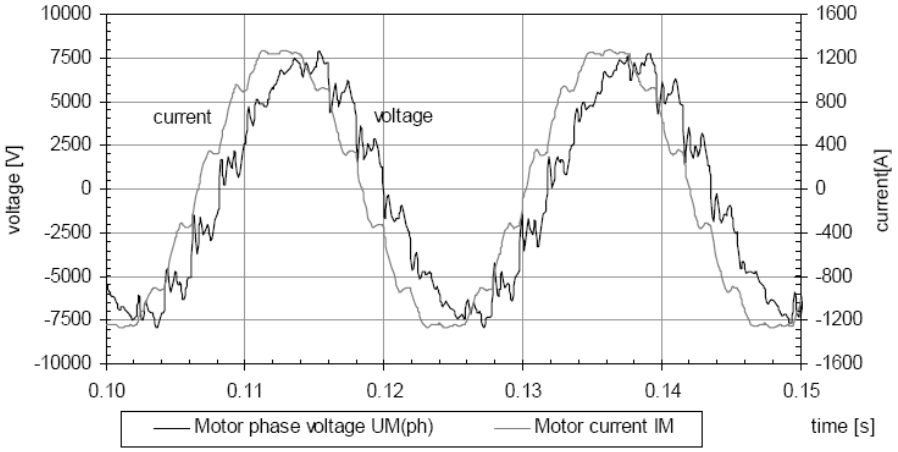

Fig. 4.16 Start-up of Oxygen West with T16 LCI at 42.4 Hz (with RC filter) [4.1]

4.4.7 Waveform Acceptance Criteria

A. Effect on Insulation

Continuous operation - The maximum allowable step value as per IEC 61800-4 [3.20] (for interturn insulation) with rise times below 1μs is 3 kV. Recently IEC 60034-18-42 has however been published which describe possible insulation aging associated with an inverter duty motor and also provides qualifying procedures for ensuring stator winding suitability. IEC 60034-18-42 recommends that qualifying of inverter duty turn insulation is only required where the in-service impulse rise time is less than 500 ns [4.18]. Inter turn insulation problems are therefore not foreseen for the systems in the case study due to the lower frequency oscillations (relatively low resonance frequency). This may however be required for VSI systems without an output filter or reactor as discussed in Chapter 3. The qualification procedures/tests for groundwall insulation and slot corona & end winding stress for new motors (especially with VSI systems) should be followed in accordance with [4.18] based on the expected waveforms at the motor terminals. These tests were however not conducted for old or existing plant motors.

IEC 61800-4 indicates that a normal motor should be able to handle a maximum voltage phase to earth (main insulation) of 0.9 x Uins (rated insulation voltage) i.e. 0.9x 11 kV = 9.9 kV whereas a maximum value of 11.33 kV phase to earth was recorded for the VSI case study as shown in Chapter 3. Similarly worst case distortion with LCI systems can also reach / exceed this value (e.g. 10 kV shown in Fig. 4.13).

Premature motor failure may therefore be expected under these conditions. Furthermore associated oscillation currents occur which can lead to excessive heating. Fig. 4.7 indicate that far worse waveforms than those measured for conditions where the effective inverter frequency is centred at the system resonance frequency.

IEC 61800-4 does not give an indication regarding the effect of the repetition rate of the pulses/oscillations. An indication can be obtained from [4.15]. The ratio of the pulse/resonance frequency to the fundamental frequency (f_p/f_f) can typically be 100 (e.g. 5 kHz vs. 50 Hz) and for severe resonance cases the ratio of the fundamental vs. pulse peak-

to-peak voltage of 1 is possible (Fig. 4.16). Rapid lifetime reduction (100x) under severe conditions can therefore be expected (from curves in [4.15]).

The standards are not applicable for pure soft starting applications and failures are far less likely due to short operation during starting and the number of starts per year is also normally low.

B. Converter Performance[4.1]

Multiple zero crossings can occur due to the various excitations during start-up for the cases where shown in Table 4.I. The multiple zero crossings of the resonance can impede the controller function. Also, there can be excitation close to the synchronization frequency of 50 Hz e.g. for T15 LCI starting the T16 BAC (Table 4.I), which may impede the synchronization.

This may also be applicable for the other cases where frequencies close to 50 Hz are shown considering that the network frequency variation in industrial facilities may be specified to vary as much as ± 2% to ± 5% ([4.19]). An example is the voltage waveform with zero crossings given in Fig. 4.13. An RC filter is recommended for these scenarios. E.g. for a plant frequency variation specification of ± 4%, an RC filter would have been recommended for T7E, the West trains and the NPP (Table 4.I).

Such large frequency variations are unlikely in a large industrial plant (continuously large fluctuating loads and separate supply networks that may be associated with significant frequency variations are uncommon). It is however still important to asses the risk of zero crossings for the maximum expected frequency variation during synchronisation associated with the specific plant.

4.4.8 Other Characteristics

Successful start-up of all motors has been verified by simulation. Furthermore it has been verified that the pulsating torques are within acceptable limits. It is important to verify that the drive string can accommodate the value of the applicable pulsating torques. No

disturbing pulsating torques are developed on the base of the cable resonances. The simulation results and evaluation are shown in [4.1].

4.5 SUMMARIZED DESIGN APPROACH AND EXAMPLES

The theory and case studies provided the details of how to conduct ASD system design with long cable lengths. The design approach is summarized in a flow chart in Fig. 4.17 that can be used as basis for a wide range of applications.

Conceptual designs can be conducted by following the solid line and thereby avoiding comprehensive simulations. Examples on how to apply the flow chart to determine whether rotor position detection equipment or a filter is required is shown in Table 4.II for LCI based systems.

The flow chart also shows a summarized approach for VSI systems. The execution of the VSI flow chart blocks can be performed in accordance with the theory of Chapter 3. The dashed line approach is more advanced and can be followed in later project stages for verification.

The dashed line approach may also add refinement to the design and in some cases eliminate the requirement of an additional filter (LCI) or a selective harmonic elimination or revised carrier frequency (VSI).

.

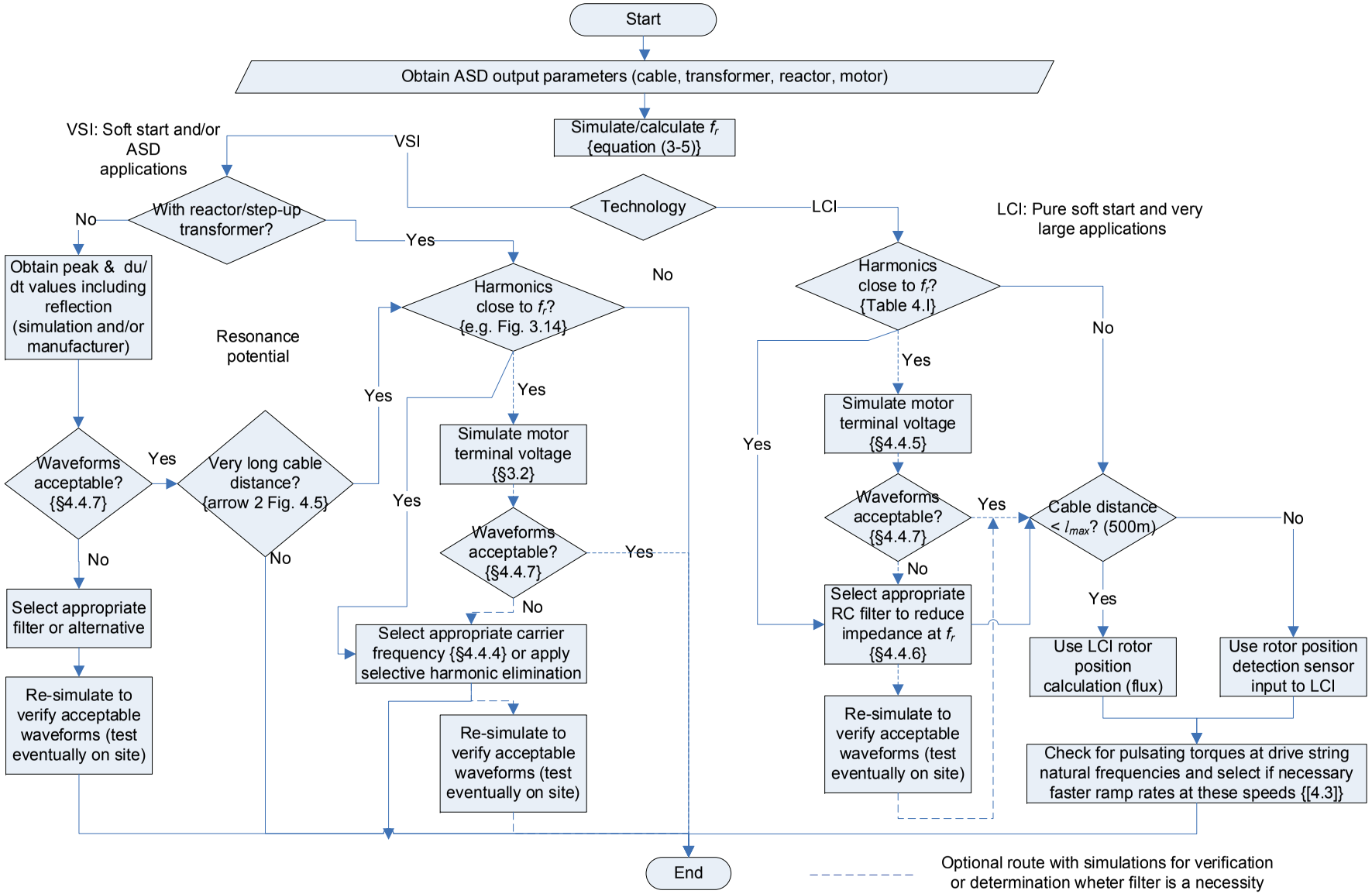

Fig. 4.17 Design approach flow chart for ASDs with long cable lengths

4.6 CONCLUSIONS AND RECOMMENDATIONS

There is a need for both VSI-CHB and LCI technologies for large drive systems with long cable lengths (e.g. several hundred meters) in the petrochemical industry. Resonance overvoltage conditions can occur in both systems with long cables distances. This chapter has shown how to determine when inverter harmonics will excite resonance overvoltages. Strategies to determine the optimal carrier frequency are proposed and acceptance criteria to ensure that the machine and converter will function safely and effectively are provided. Overvoltages associated with smaller motor lower voltage VSI-CHB drive applications (e.g. 6.6 kV) are unlikely to be associated with unacceptable travelling wave or resonance overvoltages. It has been shown that potential resonance becomes more likely with larger drive systems with reactors.

A design approach is described to determine when revised modulation strategies (optimal carrier frequency/selective harmonic elimination) or a filter is required for VSI and LCI systems respectively. It is recommended to include well described requirements in international standards to address resonance conditions. Ultimately it is shown that effective, safe, reliable and low cost solutions exist to extend the capabilities and application of VSI and LCI systems.

Break-before-make transfers (with no reactor required) or selective harmonic elimination can be considered for future applications as an alternative to the carrier frequency change method in unusual applications which would have required unacceptably high carrier frequency to avoid resonances (e.g. where increased converter losses due to a high carrier frequency can not be accommodated). In the case of the absence of a reactor, it is important to verify that the motor can withstand travelling wave effects.

Table 4.II

FLOW CHART APPLICATION EXAMPLES

Description	Train 16 LCI starts the 16 T MAC motor	Train 15 LCI starts T7E
Obtain parameters (See Fig. 4.4 & Appendix for LCI output transformer, motor and cables)	Cables 8/9, 10, 11, 13 and MAC parameters)	Cables 1/2, 15, 16, 17 and 36 MW motor parameters)
Calculate/simulate resonance frequency	f_r=6859 Hz (Table 4.I)	f_r=3474 Hz (Table 4.I)
Harmonics close to f_r?:	No - Table I shows that no harmonic orders coincide with any motor frequency in the operating range (blank column) **No RC filter required**	Yes - Table I shows that harmonic order 85 coincide with motor frequency 50 Hz (not desired for synchronization) **RC filter (Fig. 4.14) required**
Cable distance (combined length of all applicable output cables) < l_{max} (500m)?	Yes, cables 10,11,13 = 20+25+105=150m <500m **No rotor position sensor required**	No, cables 15, 16, 17 =500+700+70=1270 > 500m **Rotor position sensor required**

4.7 REFERENCES

[4.1] F. Endrejat, P. Burmeister, P. Pillay "Large adjustable speed and soft-started drives with long cable lengths", in *Proc. Petroleum and Chemical Industry Committee (PCIC) Europe,* Barcelona, Spain, 2009, pp.153-162

[4.2] B. Wu, "High Power Converters and AC Drives", IEEE Press, Willey Interscience, 2006

[4.3] N. Granö, "Electrical drive systems, drive systems with synchronous motors (LCI)," in *ABB Industrial Manual,* Lund, Sweden, Wallin & Dalholm Tryckeri, 1998, ch. 4, pp. 365-375.

[4.4] *Semiconductor converters - General requirements and line commutated converters - Part 1-2*, IEC 60146-1-2, application guide, 1993 ed. 3.

[4.5] D. E. Rice, "A detailed analysis of six-pulse converter harmonic currents", *IEEE Trans. Ind. Appl.*, vol. 30, No. 2, pp. 294-304, Mar./Apr. 1994.

[4.6] T. F. Kaiser, R. H. Osman, R. O. Dickau, "Analysis guide for variable frequency drive operated centrifugal pumps," in *Proc. of the Twenty-Fourth International Pump Users Symposium*, pp. 81-106, 2008.

[4.7] J. Davoine, R. Perret, H. Le-Huy, "Operation of a self-controlled synchronous motor without a shaft position sensor", *IEEE Trans. on Ind. Appl.*, vol. IA-19, no. 2, pp. 217-222, Mar./Apr. 1983

[4.8] S. S. Fazel, "Investigation and Comparison of Multi-Level Converters for Medium Voltage Applications", Dr.Ing dissertation, Technische Universität Berlin, 2007

[4.9] L. Li, D. Czarkowski, Y. Liu, P. Pillay, "Multilevel Selective Harmonic Elimination PWM Technique in Series-Connected Voltage Inverters", *IEEE Trans. Ind. Appl*, Vol. IA-26, No. 1, pp 160-170, Jan/ Feb 2000

[4.10] Matlab Simulink, Version 7 Release 14, Transmission Line Model Notes

[4.11] R. Wetter, B. Kawabani, and J. Simond, "Voltage stresses on PWM inverter fed induction motors: Cable modeling and measurement," in *Proc. ICEM*, 2004, CD-ROM, Paper 273.

[4.12] P. Mäki-Ontto, H. Kinnunen, and J. Luomi, "AC motor cable model for bearing current and over-voltage analysis," in *Proc. ICEM*, 2004, CD-ROM, Paper 367.

[4.13] Adjustable Speed Electrical Power Drive Systems—Part 4: General Requirements—Rating Specifications for a.c. Power Drive Systems Above 1000 V a.c. and not Exceeding 35 kV, IEC 61800-4, 2002.

[4.14] R. J. Kerkman, D. Leggate, and G. L. Skibinski, "Interaction of drive modulation and cable parameters on AC motor transients," *IEEE Trans. Ind. Appl.*, vol. 33, no. 3, pp. 722–731, May/Jun. 1997.

[4.15] M. Kaufhold, K. Schäfer, K. Bauer, and M. Rossmann, "Medium and high power drive systems; Requirements and suitability proof for winding insulation systems," in *Proc. INSUCON*, 2006, pp. 86–92.

[4.16] A. F Moreira, T. A. Lipo, G. Venkataramanan, and S. Bernet, "High frequency modeling for cable and induction motor overvoltage studies in long cable drives," *IEEE Trans. Ind. Appl.*, vol. 38, no. 5, pp. 1297–1306, Sep./Oct. 2002.

[4.17] L. Li, D. Czarkowski, Y. Liu, and P. Pillay, "Multilevel selective harmonic elimination PWM technique in series-connected voltage inverters," *IEEE Trans. Ind. Appl.*, vol. 36, no. 1, pp. 160–170, Jan./Feb. 2000.

[4.18] M.K.W. Stranges, G.C. Stone, D.L. Bogh, "Progress on IEC 60034-18-42 for Qualification of Stator Insulation for Medium-voltage Inverter Duty Applications" *IEEE Petroleum and Chemical Industry Committee Technical Conference Record*, Paper PCIC-2007-6, September 2007

[4.19] B. Lockley, R. Paes, J. Flores, "A Comparison between the IEEE 1566 Standard for Large Adjustable Speed Drives and Comparable IEC Standards", *PCIC Europe* 2007

5 RIDE-THROUGH

This chapter provides an overview of ride-through theory with a focus on MV ASDs and soft started synchronous machines. The importance to ensure ride-through for both on-line and ASD operation is described. A general machine model is presented to model these conditions dynamically. The overall ride-through modelling and a simplified general strategy which addresses constraints on the re-closing angle are presented. This chapter forms the theoretical basis for further research and practical case studies in the next chapter.

5.1 INTRODUCTION

Medium Voltage (MV) Synchronous Machines (SMs) are used for large industrial compressor motor drives (>13 MW) as outlined in Chapter 1. These machines are usually fed from strong supplies with low source impedances. Process availability is of primary concern since production losses can potentially negate the benefits of ASDs. Critical applications may be equipped with an ASD bypass scheme to enable change over to direct-on-line operation without a process interruption (e.g. for maintenance or repair work on the ASD). The reverse process is also possible to resume ASD operation (e,g, SSASD scheme). The drive system availability is enhanced with the motor's ability to ride through the ASD faults and external disturbances which cannot be addressed with the SSASD scheme.

The size of large compressor motors normally do not allow for DOL starting. This is mainly due to significant starting current which may result in unacceptable voltage drops or even equipment damage as discussed in Chapter 1. The problem is normally solved by

soft starting and for very large machines typically with SFC soft starting. Machines associated with SFC soft starting or in a SSSASD scheme must be capable to also operate directly one line. Significant currents which are not normally evaluated may however still occur due to synchronous machine transfer switching currents. Transfer currents are defined for the purpose of this chapter where the main supply to the motor is removed and whereafter the machine is connected to another supply by means of a break before make transfer. An example is a fast bus transfer [5.1] which is often encountered in the petrochemical industry to enhance the ride-through capability of machines. The associated transfer currents are normally not considered in the system design. Compressors must be able to ride through most external voltage dips. This applies to the direct-on-line mode of operation and to ASD mode of operation. Bus transfer ride-through with soft started SMs (e.g. in a SSASD scheme) is essential to evaluate since this has not been sufficiently documented in literature but forms an important and integral part of SSASD applications.

Dynamic voltage restoration or additional energy storage elements were suggested to achieve ASD ride-through for the power rating and topology addressed in this thesis [5.2]. Power system stabilizers are sometimes suggested for on-line SM ride-through [5.3]. There is a need to investigate whether these additional measures are required. Furthermore suitable schemes should be developed to ensure safe and effective ride-through performance.

SFC started synchronous machine excitation and excitation controller sensitivity for voltage dips for both line and ASD operation has not been well documented in the literature and needs further investigation. This chapter provides the background theory and models which will be used in the following chapter for the case studies and ride-through/availability research.

5.2 RIDE THROUGH PRINCIPLES

5.2.1 Voltage Dip Characterisation

The definition of a voltage dip (also known as a “voltage sag”) as per NRS 048-2 [5.4] is used for the purposes of this thesis: “A sudden reduction in the r.m.s. voltage, for a period

of between 20 ms and 3 s, of any or all of the phase voltages of a single-phase or a polyphase supply". Industries normally have internal and/or external standards for maximum allowable voltage drop limits at various voltage levels. Proposed allowable limits are often given in tables or curves for various industries and requirements, e.g. CBEMA, ITIC, SEMI 47, IEC [5.5], [5.7]. At medium voltage levels, typical industrial plant voltage tolerance levels are specified as shown in Table 5.I. The highest frequency of voltage dips for industrial facilities typically occur in the shaded area Y and industrial end users are normally expected to protect their systems for these voltage dips. The limits are based on the consensus of the NRS 48 working group [5.6] and shown in the table extract from NRS 048-2 [5.4] (Table 5.I). This is also in line with equipment dip immunity class C1 which provides "a reasonable level of equipment immunity to many dips" [5.7].

External dips can however be significantly deeper and a relatively large number of dips also occur in the X1 category [5.4]. Even deeper dips may occur based on the specific site conditions and it is recommended to record these dips over a time period of several months or even years before a site specific specification can be finalized (next chapter provides a case study). Further dip classifications (e.g. Type I-III) including unsymmetrical conditions are provided in [5.8].

Table 5.I

CHARACTERIZATION OF VOLTAGE DIPS ACCORDING TO DEPTH AND DURATION (50 Hz) [3.8]

Residual Voltage (Ur) [%]	Duration (t) [ms]		
	20 < t ≤ 150	150 < t ≤ 600	600 < t ≤ 3000
90 > Ur ≥ 85	Y		
85 > Ur ≥ 80			Z1
80 > Ur ≥ 70		S	
70 > Ur ≥ 60	X1		Z2
60 > Ur ≥ 40	X2		
40 > Ur ≥ 0	T		

Class C1 for type III dips (Ur ≥ 80 between 110 ms and 3000s)

5.2.2 Process Immunity Time

Voltage dip ride-through principles are extensively covered in [5.7] with the proposed approached to determine the Process Immunity Time (PIT) and to design the electrical systems to ride though this duration. The PIT for chemical processes are typically significantly longer [5.7] than the X and Y categories in Table 5.I. This is especially advantageous e.g. for the re-acceleration of induction motors in groups following voltage dip recovery. Normal synchronous motors are however not suitable for conventional re-acceleration several hundred milliseconds after the voltage dip due to the loss of machine stability/pole slipping during attempted re-acceleration. This situation should therefore be avoided and it is expected that standard synchronous machines ride through most voltage dips associated with a plant. This automatically ensures ride-through compliance with the typical chemical plant process immunity times.

5.2.3 Line Operated Synchronous Machine Voltage Dip Ride-through

A. Ride-through for Stable Machine Operation

The worst case of synchronous machine ride-through evaluation in terms of stability is symmetrical three phase dips. It should therefore be investigated whether ride-through can be achieved for three phase voltage dips as a starting point. If symmetrical voltage dip ride-through cannot be achieved, ride-through can be optimised by optimising protection settings and schemes for unsymmetrical voltage dips [5.9], [5.10]. This is especially applicable on systems with weak networks or with high source impedances.

B. Voltage Dip Torques

Transient torques are dependent on the magnitude and duration of the voltage dips. The deepest dip (100%, also classified as an interruption) results in the worst case torques. Duration of half a cycle will result in the worst case torques for 2 and 3 phase dips which results in similar magnitudes [5.9], [5.11]. This is however not a realistic dip/protection clearing time. Thereafter there is a sinusoidal-like torque speed dependence whereof the oscillation gradually reduces and then the torque offset increases as shown in [5.9]. For longer durations (e.g. above 100 ms), the torque generally increases with the dip duration

for 3 phase dips [5.11]. The worst case is therefore practically regarded as a 3 phase 100 % dip and at the point just before the machine would have become instable after voltage recovery. Only three phase voltage dips were therefore modeled (other dip types result in lower torques [5.11]. Torques in the unstable region are not analyzed since the protection schemes (out-of-step and/or under voltage) will trip the machine prior to voltage recovery that would have resulted in instability. The undervoltage protection curve, out-of-step and under excitation protection is set based on the results of the stability study.

5.2.4 ASD Voltage Dip Ride-Through

The normal voltage dip withstand capability associated with a typical VSI-CHB is given in Fig. 5.1 [5.12].

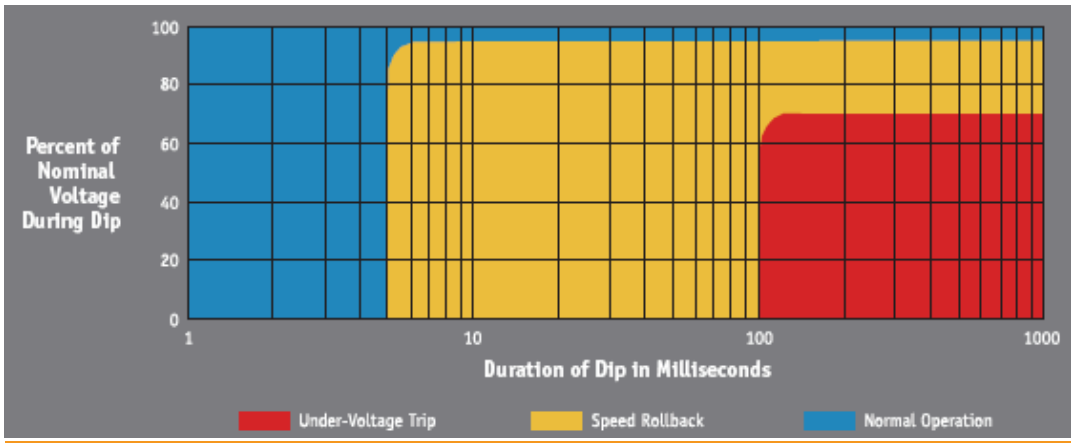

Fig. 5.1 Typical VSI-CHB voltage dip withstand capability [5.12]

Even dips in the Y category (Table 5.I) approaches the under-voltage trip level (e.g. 70% remaining voltage for 150 ms) in Fig. 5.1. Dips in the X1 category will result in an undervoltage trip. Further measures are therefore required to enhance ride-through. Large compressor applications have a significant inertia and therefore the load inertia ride-through method based on the principle described in [5.13] is ideal to enhance ride through since no additional hardware is required. During significant dips and cell faults (i.e. when the red area is approached in Fig. 5.1.) no torque producing current is provided and the cell DC bus voltages are kept to the minimum required level by operating the machine as a generator to enhance ride-through (referred to as inertia ride-through). The motor is

therefore allowed to coast and act as a generator due to the existing rotor excitation. In cases where the voltage dip effects the power source of the excitation system, an evaluation is required to verify whether the excitation system has sufficient magnetic inertia to ride to ride through the dip. This should however in many cases not be a concern since the AC excitation system normally has a long time constant. Chapter 6 investigates this further with case examples. The ASD output is synchronized with the motor voltage when the voltage dips recovers. Stability concerns as with the DOL case are therefore not applicable.

5.2.5 Fault Tolerant Operation and Redundancy

A. ASD Redundancy

The faulty cell bypass principle for redundant cells is described in [5.14], [5.15]. It has already been shown in section 3.2.1 that rated voltage can be achieved with one cell bypassed. The voltages that can be achieved with 2 and 3 cells bypassed were also given. These voltages are achieved with a concept referred to as "neutral shift" as described in [5.14]. The process is briefly explained here. After a cell failure has occurred, the bypass contactor (Fig. 2.2) operates and shorts out the faulty cell. During this process the output current is stopped completely while the ASD reconfigures the cell control to maximize the possible output voltage: The star-point of the modules is floating and not connected to the neutral of the motor. Therefore, the star-point can be shifted away from the motor neutral, and the phase angles of the cell voltages can be adjusted, so that a balanced set of motor voltages is obtained even though the cell group voltages are not balanced. After the bypass contact operation has been completed, the ASD is restarted to continue with operation with the "neutral shifted". Diagram examples based on those shown in [5.15], are given in Fig. 5.2 and Fig. 5.3 (for the VSI-CHB in Fig. 2.2), to assist with the explanation. The necessary angles α, β, and γ can be calculated in accordance with the equations provided in [5.15].

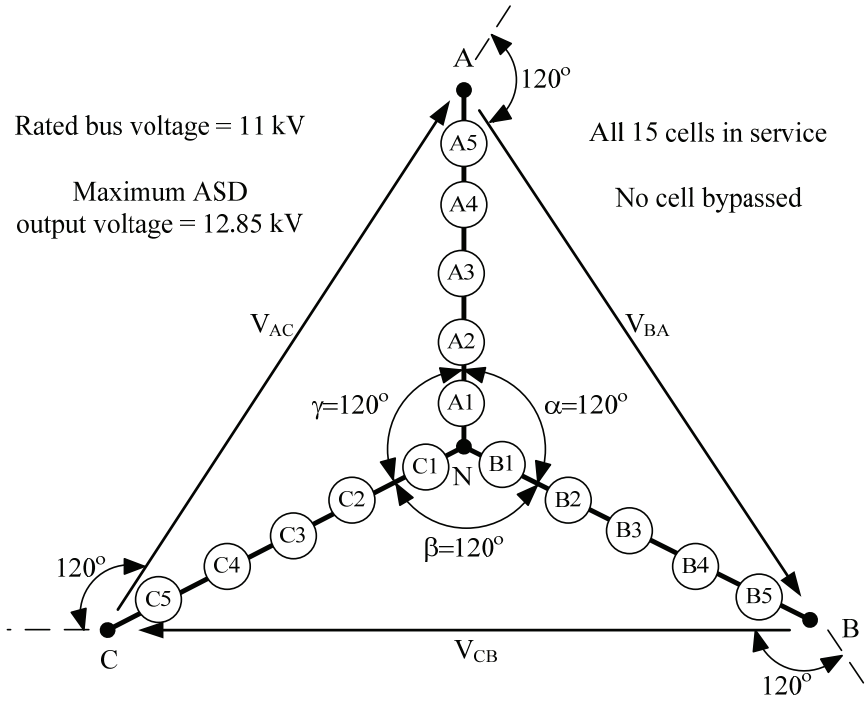

Fig. 5.2 VSI-CHB cell configuration with all cells in operation

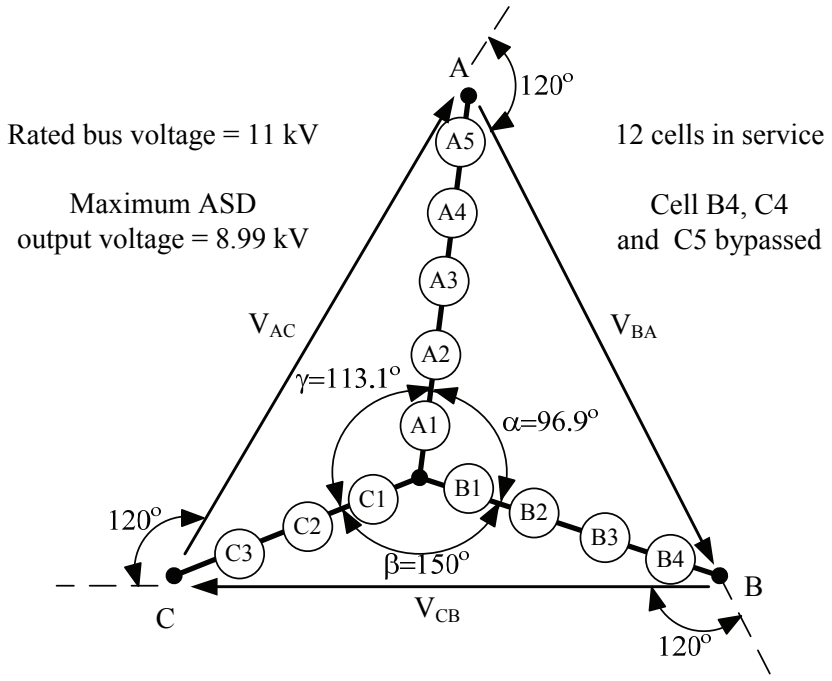

Fig. 5.3 VSI-CHB cell configuration with selected faulty cells bypassed

The process during which a cell is bypassed resembles a T category dip in Table 5.I (temporary interruption) as far as the machine stator supply is concerned. The same principle of load inertia ride-through also occurs as described in the previous paragraph

during a cell bypass action. It has been shown that for MV Multilevel VSI drives that the bypass time of a faulty cell was recorded as 250ms [5.14]. The next chapter will present actual site case study recordings for the VSI CHB with a higher voltage rating. Furthermore the impact on typical compressor applications will be investigated.

The failure of redundant components (e.g. cooling pumps, fans) do not result in any interruption of output to the motor. Certain faulty components can be replaced on-line, but selected components, e.g. power cells must be replaced off line but with the SSASD concept this does not result in production loss as described in Chapter 1.

B. Excitation Redundancy

Excitation panel redundancy is described in Chapter 2. On-line replacement of channel components is possible when configured as shown in Fig. 2.6.

5.3 EQUIPMENT AND SYSTEM LIMITS

5.3.1 Fast Bus Transfer Angle

The background theory of the fast bus transfer principle is provided in [5.1], [5.16]. “Fast”, “Delayed-in-phase”/ “First phase coincidence”, “Residual voltage”, and “Time delayed” transfer methods are applied in industry. In the case of synchronous machines only the “fast” method is normally used since the other methods are associated with the risk of losing machine stability (resulting in an out-of-step condition). This thesis focuses therefore on the “fast method” but it will be verified by means of a case study in the next chapter whether the “fast” method is in fact the correct method compared to the other methods. A typical petrochemical transfer equivalent circuit is shown in Fig. 5.4.

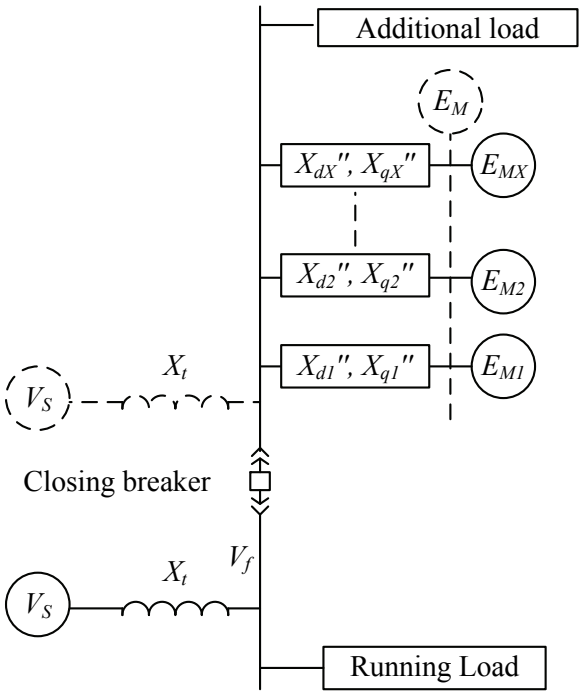

Fig. 5.4 Typical petrochemical power transfer equivalent circuit with synchronous machines

The maximum allowable angle limit for a safe transfer (or reclose) has traditionally been calculated from ANSI C50.41-2000 requirements and equation 5.1 as also discussed in Chapter 2 [1.61]:

$$\delta_m = a\cos\left(\frac{\left|Ev_m\right|^2 + \left|Ev_s\right|^2 - 1.33^2}{2\cdot\left|Ev_m\right|\cdot\left|Ev_s\right|}\right) \tag{5.1}$$

where Ev_m and Ev_s are the vectorial V/Hz values in p.u. for the machine and the source (to which the machine will be transferred to) respectively.

This equation has however been based on induction motors started directly on line and may not adequately represent large soft started synchronous machines. It is therefore important to investigate all equipment and system limitations to determine the maximum angle allowed when large synchronous machines are encountered.

Equipment withstand limits are first investigated from a maximum symmetrical current withstand capability point of view. Equipment design takes into consideration the forces associated with the maximum asymmetrical current that can occur based on the relevant X/R ratio.

5.3.2 Synchronous Machine Current Limits

Synchronous machine windings are normally braced to withstand the short circuit current at rated voltage (V_{rm}) which can be described as [5.17]:

$$I_{mm} = \frac{V_{rm}}{X_d''} \tag{5.2}$$

where X_d'' is the direct axis sub-transient reactance.

5.3.3 Transformer Current Limits

An estimate of the maximum current to which a transformer is braced can be obtained from [5.17]:

$$I_t = \frac{V_t}{X_t} \tag{5.3}$$

Where V_t is the rated transformer primary voltage and X_t is the transformer reactance. Transformer withstand capability in terms of time current curves are provided in standards/guides e.g. in [5.18], [5.19].

5.3.4 Busbar Voltage Drop Limits

Internally end users should not be the originators of voltage dips exceeding the agreed limits for a specific plant – typically similar to the limits discussed in section 5.2.1. Often

petrochemical plants have their own specifications based on the plant design. Voltage dips associated with internal events e.g. motor re-acceleration following bus transfers should therefore not cause busbar voltage drops in excess of specified limits. These specified limits are often more conservative than the values in the shaded area in Table 5.I, e.g. as given in [5.20].

5.3.5 Mechanical Load/ Drive String – Transient Torques

Mechanical systems are normally designed to withstand the machine short circuit currents, but it should be verified that all dynamic transient conditions can be handled by the mechanical system. This is normally performed with a torsional analysis study based on the torque generated for the worst case electrical conditions.

5.4 SYNCHRONOUS MACHINE AND SYSTEM MODELING

5.4.1 Electromagnetic Synchronous Machine Modeling

Electromagnetic SM modelling is normally applied for transient ride-through analysis. Several models are suitable for electromagnetic transient simulations including the model used in this thesis and shown in Fig. 5.5 [5.21], [5.22]. The modelling is based the equivalent circuit in Fig. 5.5 and given by equations (5.4)-(5.15) derived from the theory in [5.22]. The descriptions of the symbols are provided in the list of symbols. These models or similar models are usually applied in simulation packages (e.g. in [5.24], [5.25]) for verification of system stability and ride-through studies. Machine saturation is modelled as outlined e.g. in [5.22]. The next chapter illustrates the use of the model in the simulation package [5.24] with a sixth order state space model.

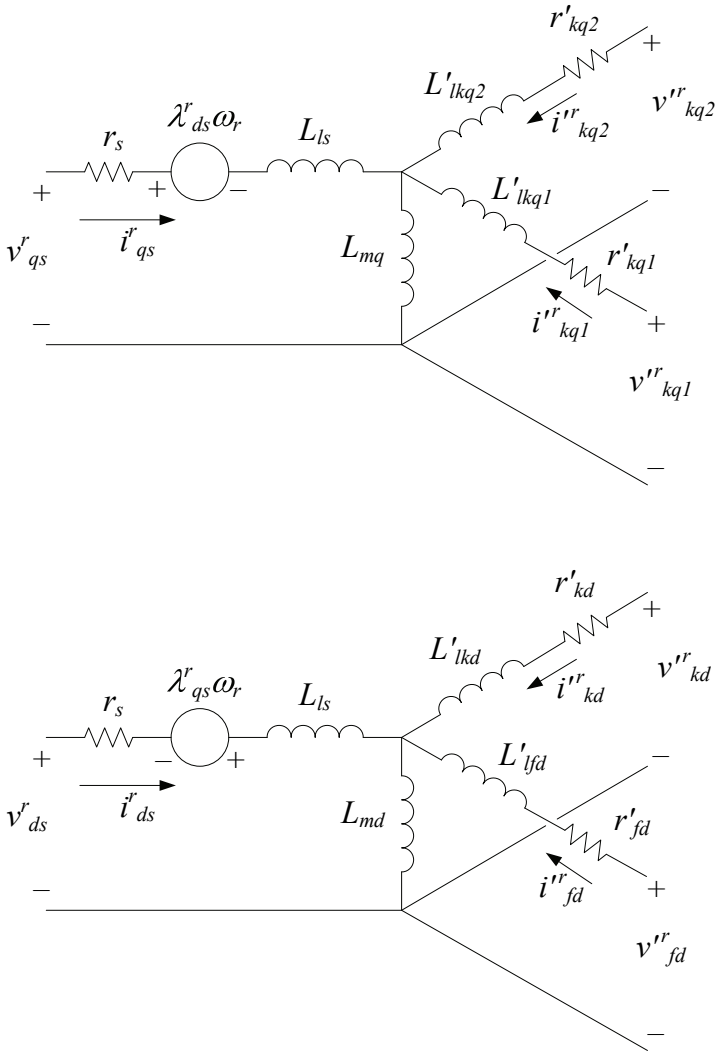

Fig. 5.5 Synchronous machine equivalent circuit (reference frame fixed in rotor -Park transformed)

$$v^r_{ds} = r_s i^r_{ds} - \omega_r \psi^r_{qs} + \frac{d}{dt}\psi^r_{ds} \tag{5.4}$$

$$v^r_{qs} = r_s i^r_{qs} + \omega_r \psi^r_{ds} + \frac{d}{dt}\psi^r_{qs} \tag{5.5}$$

$$v''^r_{fd} = r'_{fd}\, i''^r_{fd} + \frac{d}{dt}\psi''^r_{fd} \tag{5.6}$$

$$v'^{r}_{kd} = r'_{kd}\, i'^{r}_{kd} + \frac{d}{dt}\psi'^{r}_{kd} \tag{5.7}$$

$$v'^{r}_{kq1} = r'_{kq1}\, i'^{r}_{kq1} + \frac{d}{dt}\psi'^{r}_{kq1} \tag{5.8}$$

$$v'^{r}_{kq2} = r'_{kq2}\, i'^{r}_{kq1} + \frac{d}{dt}\psi'^{r}_{kq2} \tag{5.9}$$

$$\psi^{r}_{ds} = L_{ls} i^{r}_{ds} + L_{md}\left(i'^{r}_{kd} + i'^{r}_{fd}\right) \tag{5.10}$$

$$\psi^{r}_{qs} = -L_{ls} i^{r}_{qs} + L_{mq} i'^{r}_{kq2} \tag{5.11}$$

$$\psi'^{r}_{fd} = L'_{fd}\, i'^{r}_{fd} + L_{md}\left(i^{r}_{ds} + i'^{r}_{kd}\right) \tag{5.12}$$

$$\psi'^{r}_{kd} = L'_{lkd}\, i'^{r}_{kd} + L_{md}\left(i^{r}_{ds} + i'^{r}_{fd}\right) \tag{5.13}$$

$$\psi'^{r}_{kq1} = L'_{lkq1}\, i'^{r}_{kq1} - L_{mq} i^{r}_{qs} \tag{5.14}$$

$$\psi'^{r}_{kq2} = L'_{lkq2}\, i'^{r}_{kq2} + L_{mq} i^{r}_{qs} \tag{5.15}$$

SFC started or driven SMs have rotating brushless exciters (with a generator/rotating transformer feeding the rotating rectifier circuit to ensure flux production at zero speed) and AC phase controlled excitation controllers (often redundant). A typical brushless exciter is shown in Fig. 5.6. The associated excitation/protection panel is shown in Fig. 2.6. This configuration results in a fairly long time constant for the exciter circuit. The excitation controller and exciter are modelled as shown in Fig. 5.7 to reflect performance during longer system disturbances correctly (e.g. power factor control during load variations). This exciter model was provided by the manufacturer of the motor & excitation system. The parameters/symbols are aligned with IEEE Standard 421-5 definitions [5.23]. Similar models are also provided in [5.23]. Compressors have typical load characteristics

as shown in Fig. 5.8.

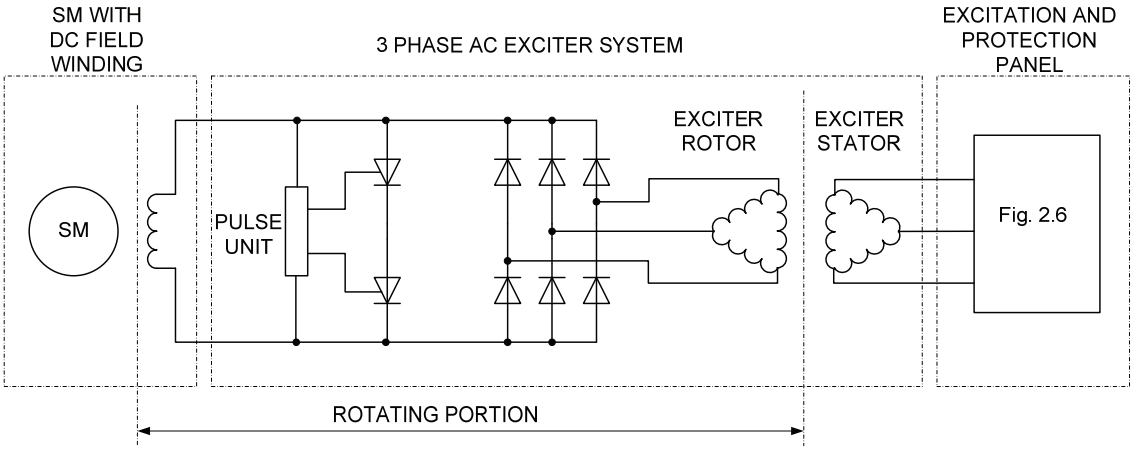

Fig. 5.6 Brushless excitation system for SFC started SM

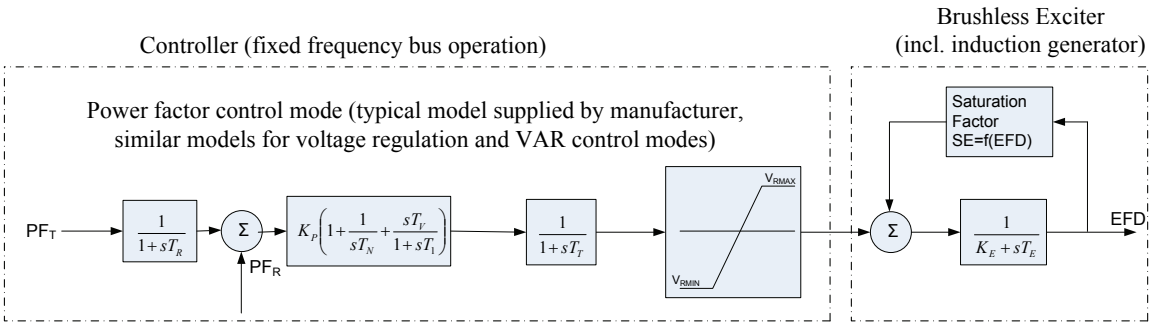

Fig. 5.7 Excitation controller and brushless exciter

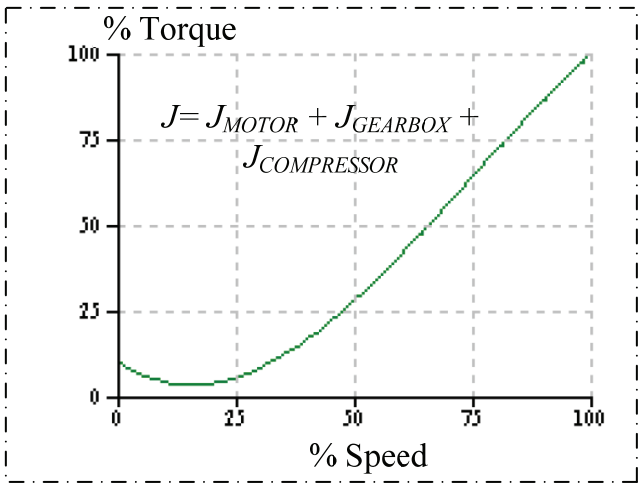

Fig. 5.8 Load model

The development and population of these models are however time consuming and normally performed later in a project stage. Furthermore numerous time consuming simulations are normally required. Simulation result examples of these models are provided in the next chapter. A more effective initial approach is suggested to determine whether the system design is within limitations and to determine the associated maximum transfer angle (next section).

5.4.2 Sub-transient Synchronous Machine Modelling – Generalized Analytical Model

A single or equivalent motor scenario is investigated as a starting point for analysing the maximum transfer angle. Furthermore the effect of the running load on the healthy bus (Fig. 5.4) is neglected since it is assumed the incoming transformer impedance is far lower than the equivalent impedance of the synchronous motors on the running bus. This results in a worst case scenario in terms of bus voltage drop. All the following equations are presented in p.u.

The worst case conditions which affect the limits described in section 5.3 occur in the machine sub-transient state (before the current reduces). The current is assumed as steady state, for the purpose of analysis, only in the short period of the sub-transient state. Kirchoff's laws in the phasor domain [5.30] can therefore be applied, by considering Fig. 5.4 to determine the rms current in the sub-transient state when using sub-transient motor reactances. An estimate of the transfer current is therefore given by:

$$\left|\overline{I_f}\right| = \left| \frac{\left|\overline{V_s}\right| \cdot \left(\cos(\delta_s) - j \cdot \sin(\delta_s)\right) - \left|\overline{E^o}\right| \cdot \left(\cos(\delta_s) - j \cdot \sin(\delta_s)\right)}{jX_t + jX_m''} \right| \tag{5.16}$$

Where $\left|\overline{V_s}\right|$ is the transformer source supply voltage, $\left|\overline{E^o}\right|$ is the motor internal e.m.f. just before the transfer, X_m'' is the effective sub-transient motor reactance and δ_s is the angle between the source supply voltage and the motor internal EMF just before the transfer

breaker closing (i.e. the transfer angle). The maximum allowable angles for the machine and transformer limits can be estimated by solving equation (5.16) to avoid exceeding the current values in equation (5.2) and (5.3) respectively. The value of X_t represents the saturated value under worst case conditions, i.e. it comprises of only the leakage inductance of the transformer.

The current for multiple machines can be determined by using the equivalent subtransient impedance of all the machines in parallel as X_m".

A more accurate approach is to apply two axis machine theory. Furthermore, it is necessary to determine the voltage drop of the bus due to the transfer which is not represented by equation 5.16. Fig. 5.9 provides the sub-transient phasor diagram reflecting the transfer. This diagram is developed for transfer purposes based on principle of pre- and post fault phasor diagrams as described in [5.26] but customized for sub-transient transfer conditions.

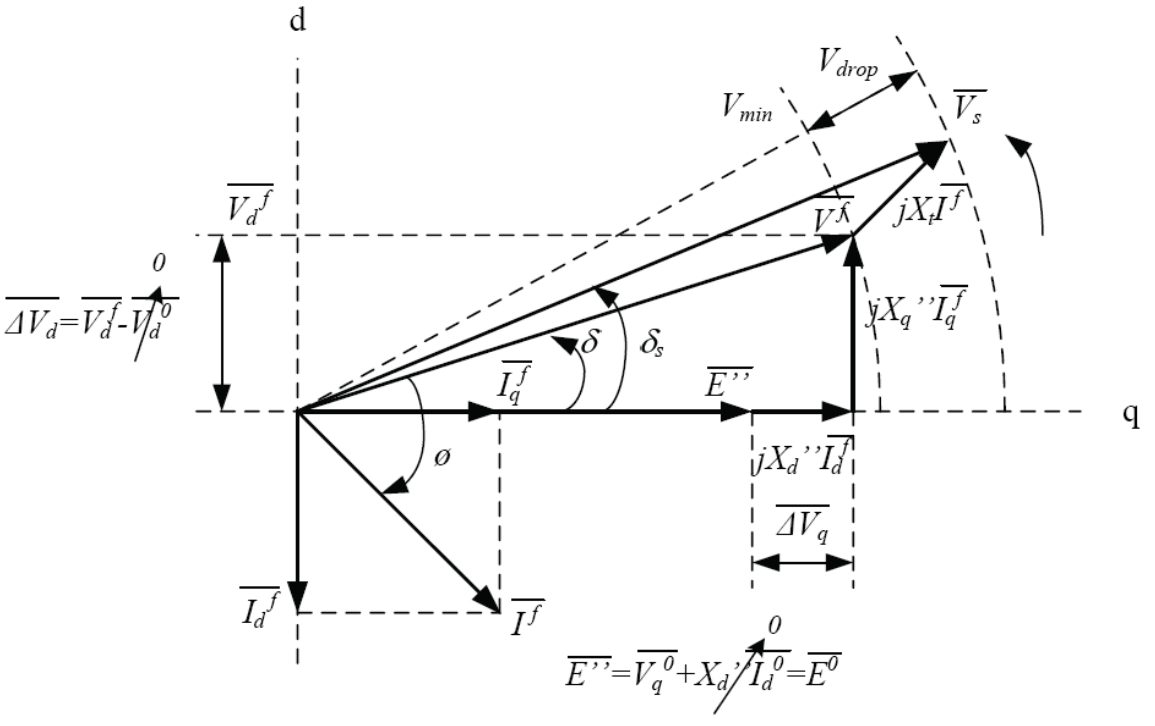

Fig. 5.9 Sub-transient two axis phasor diagram for synchronous motor transfers

The pre-fault^0 condition represents the moment just before the transfer breaker is closed and the fault^f condition represents the condition directly after the transfer.

The machine can be represented as an under-excited motor due to the drop in internal EMF which is represented by $\overline{E^o}$ as the pre-closing phasor. $\overline{V^f}$ is the motor terminal voltage phasor directly after transfer closure (i.e. reflecting the busbar voltage). $\overline{V_s}$ represents the source voltage phasor.

The equations for the subtransient state can now be developed from Fig. 5.9 in accordance with the transient phasor diagram principles described in [5.26]. The current following at closure is estimated as:

$$\overline{I_f} = k \cdot \left(\frac{\left|\overline{V^f}\right| \cdot \sin(\delta)}{X_q''} + \frac{j \cdot \left(\left|\overline{V^f}\right| \cdot \cos(\delta) - \left|\overline{E^o}\right| \right)}{X_d''} \right) \tag{5.17}$$

$$\text{Where} \qquad k = e^{\frac{-t}{\tau''}} \tag{5.18}$$

and τ'' is the effective transfer current time constant. This constant τ'' is approximately the same as τ_d'', the subtransient direct access short circuit time constant and δ is the machine power angle directly after the transfer. Even though (5.17) represents a steady state equation, the factor k can be used to describe the transient nature of the current in accordance with the principles in [5.26] (in the sub transient region and assuming the sub-transient current >> the eventual steady state current). The time t is of interest in the subtransient state (a worst case is after the first half cycle when the first peak occur, i.e. 10 ms). The source voltage can be expressed as:

$$\left|\overline{V_s}\right| = \left\| \left|\overline{V^f}\right| \cdot \cos(\delta) + j \cdot \left|\overline{V^f}\right| \cdot \sin(\delta) + j \cdot X_t \cdot \overline{I_f} \right| \tag{5.19}$$

The source voltage $\left|\overline{V_s}\right|$ is typically represented by 1 p.u. and the machine voltage prior to reclosing $\left|\overline{E^o}\right|$ can be estimated from the decay associated with the open circuit machine time constant and the reduced speed of the machine. The transformer reactance X_t can be used as an approximation of the total source reactance X_s since $X_t >> X_s$ (on the same base

units). An initial approach is to assume $\left|\overline{E^o}\right|$ also as 1 p.u., which is a worst case approach if typical bus transfer angles are applicable between $\left|\overline{E^o}\right|$ and $\left|\overline{V_s}\right|$. The effect of this assumption is illustrated in Chapter 6. The minimum allowable bus voltage (not to violate the plant power quality specification) is represented by $\left|V_f\right|$. The angle δ can be obtained from equations (5.17) to (5.19). The source voltage vector is known from:

$$\overline{V_s} = \left|\overline{V^f}\right| \cdot \cos(\delta) + j \cdot \left|\overline{V^f}\right| \cdot \sin(\delta) + j \cdot X_t \cdot \overline{I_f} \tag{5.20}$$

The maximum allowable transfer angle can now be determined from:

$$\delta_s = \arctan\left(\frac{\mathrm{Im}\left(\overline{V_s}\right)}{\mathrm{Re}\left(\overline{V_s}\right)}\right) \tag{5.21}$$

The same approach can be followed for multiple synchronous machines by determining the equivalent synchronous motor impedances and representing the motors as a single motor. In cases where there is a significant difference between the source and motor speed (i.e. significant slip), the associated current contribution also needs to be taken into account as described in [5.27]. Transfer durations are however not associated with a significant speed drop as will be shown in a case study in the next section. The electromagnetic torque as a function of reclosing angle is derived and given in [5.28].

These analytical equations will be used in the next chapter and compared with the numerical approach.

5.5 PROTECTION TO ENHANCE RIDE THROUGH

General protection principles, issues and schemes associated with medium voltage drives are outlined in [5.29]. Specific attention is however not given to the VSI-CHB fault

tolerant schemes and internal ASD protection co-ordination. These aspects will be investigated by means of a case study in the next chapter.

5.6 CONCLUSIONS

This chapter has provided the background theory for ride-through addressing internal and external disturbances. Furthermore models have been provided that can be used to determine the theoretical ride-through capability. Inertia-ride through appears to be a suitable approach for MV ASD petrochemical drives although other more cost intensive methods have been proposed in literature. It is also important to achieve DOL ride-through in SSASD schemes without exceeding system design conditions during transients. The importance of correct protection co-ordination and principles is highlighted. The models will be utilised in the next chapter for ride-through research by means of case studies.

5.7 REFERENCES

[5.1] D. L. Hornak, D.W. Zipse, "Automated Bus Transfer Control for Critical Industrial Processes," *IEEE Trans. on Ind. Appl.*, vol. 27, no. 5, pp. 862-871, Sept./Oct. 1991.

[5.2] A. von Jouanne, P. N. Enjeti and B. Banerjee, "Assessment of ride-through alternatives for adjustable speed drives," *IEEE Trans. on Ind. Appl.*, vol. 35, no. 4, pp. 908-916, Jul./Aug. 1999.

[5.3] O. T. Tan and R. Thottappillil, "Static VAR compensators for critical synchronous motor loads during voltage dips," *IEEE Trans. on Power Syst.*, vol. 9, no. 3, pp. 1517-1523, Aug. 1994.

[5.4] *Electricity supply — Quality of Supply Part 2: Voltage Characteristics, Compatibility Levels, Limits and Assessment Methods*, NRS 048-2, 2007

[5.5] E. F. Fuchs, M.A.S. Masoum, "Power Quality in Power Systems and Electrical Machines", USA, Elsevier, 2008

[5.6] Ulrich Minnaar, "NRS 048 part 7: Application Practices for End Customers – First Draft", presented at the stakeholder workshop NRS 048 Quality of supply, SABS Pretoria, 7 July 2009

[5.7] M. H. J. Bollen *et al.*, "Voltage dip immunity of equipment and installations," CIGRE/CIRED/UIE Joint Working Group C4.110 report, Apr. 2010

[5.8] M. H. J. Bollen, *Understanding Power Quality Problems: Voltage Sags and Interruptions*, New Jersey, IEEE Press, 2000.

[5.9] F. Carlsson, "On impacts and ride-through of voltage sags exposing line-operated AC-machines and metal processes," Doctoral Dissertation, Royal Institute of Technology, Stockholm, Sweden 2003

[5.10] G. de Beer, "Analysis and effect of large synchronous motors on power systems", M. Ing thesis, Dept. Electrical Engineering, North-West University, Potchefstroom, South Africa, 2005

[5.11] F. Carlsson, C. Sadarangani, "Behavior of Synchronous Machines Subjected to Voltage Sags of Type A, B and E," *EPE Journal*, Vol. 15, no. 4, pp. 1-8, Dec 2005

[5.12] F. Endrejat, B. van Blerk, and G. Vignolo, ''Experience with new large adjustable speed drive technology for multiple synchronous motors,'' in *Proc. PCIC-Europe*, 2008, pp. 196–205.

[5.13] J. Holtz, W. Lotzkat, S. Stadtfeld, "Controlled AC drives with ride-through capability at power interruption," *IEEE Trans. on Ind. Appl.*, vol. 30, no. 5, pp. 1275-1283, Sep./Oct. 1994.

[5.14] D. Eaton, J. Rama, P. Hammond, "Neutral shift - five years of continuous operation with adjustable frequency drives**,** *IEEE Ind. Appl. Mag.*, vol. 9, no. 6, pp. 40-49, Nov./Dec. 2003

[5.15] J. Rodríguez*,* P.W. Hammond*,* J. Pontt*,* R. Musalem, P. Lezana, M. J. Escobar, "Operation of a Medium-Voltage Drive Under Faulty Conditions", *IEEE Trans. Ind. Electron.*, vol. 52, no. 4, pp. 1080-1085, Aug. 2005.

[5.16] J. Piorkowski, B. Rademeyer, "The application of modern power transfer equipment on critical motor buses at the Sasol plants in Secunda," Power Summit, South Africa, 2002.

[5.17] G. F. Walsh, "The effects of reclosing on industrial plants", Proceedings of the American Power Conference, Volume XXIII, pp. 768-778, 1961

[5.18] *IEEE Guide for Protecting Power Transformers*, IEEE Standard C37.91, 2008

[5.19] *IEEE Guide for Liquid-Immersed Transformer Through-Fault-Current Duration*, IEEE Standard C57.109, 1993 (R2008)

[5.20] General electrical Sasol specification, SP-60-1, Rev. 4

[5.21] L. Wand, J. Jatskevic and H. W. Dommel, "Re-examination of synchronous machine modeling techniques for electromagnetic transient simulations," *IEEE Trans. on Power Syst.*, vol. 22, pp. 1221-1230, August 2007

[5.22] P. C. Krause, O. Wasynczuk, S. D. Sudhoff, *Analysis of Electric Machinery*, IEEE Press, 1995

[5.23] *IEEE Recommended Practice for Excitation System Models for Power System Stability Studies*, IEEE Standard 421-5, 2005

[5.24] MATLAB Simulink, SymPowerSystems, Release R2008a

[5.25] Electrical Transients Analysis Program (ETAP), Version 7.1.0

[5.26] O. I. Elgerd, *Electric Energy Systems Theory*, McGraw-Hill, 1982, ch. 4, sec. 4.13, pp. 100-114.

[5.27] M. G. Say, *Alternating Current Machines,* Longman Scientific & Technical, 5th ed., 1992

[5.28] M.S. Sarma, *Synchronous machines – their theory, stability and excitation* systems, Gordon and Breach Science Publishers, 1979

[5.29] J. Gardell, P. Kumar, "Adjustable Speed Drive Motor Protection Applications and Issues", Rotating Machinery Protection Subcommittee of the IEEE Power System Relaying Committee Working Group J1 report, 2008, www.pes-psrc.org

[5.30] J. W. Nilson, *Electric Circuits*, Addison-Wesley Publishing Company, 3rd ed., 1990

6 RIDE-THROUGH AND AVAILABILITY CASE STUDIES

The theory in the previous chapter is applied in this chapter to study ride-through performance with first-of-its kind case studies. The application of the numerical and analytical models is illustrated. The studies are supported by selected tests and performance recordings. MV drive design and availability improvements are described based on actual testing and experience on site.

6.1 INTRODUCTION

Chapter 5 provides the necessary background theory and models for the case studies. All case studies are based on multiple motor schemes with the capability to transfer the motors from ASD supply to the fixed frequency bus supply. The overall description of the systems is given in Chapter 2. The case studies are based on two compressor applications.

6.1.1 Process Gas Compressor (PGC)

The case studies include the first installed VSI-CHB ASD with a high output voltage of 11kV for SMs. The ASD is applied for soft starting three synchronous motors and to control the speed of only one of them, the Process Gas Compressor (PGC) or compressor C1 in Fig. 2.5. The ASD is capable of soft starting synchronous motors, synchronization and bumpless transfer to the utility supply as described in Chapter 2. Each of the three motors is rated 11 kV 17 MW for standardization. System design, testing, commissioning and operation experience are described in Chapter 2. The system single line diagram and pictures are shown in Chapter 2.

6.1.2 Main Air Compressor (MAC)

A second machine studied is an 11 kV 55 MW SM (so far the largest 4 pole synchronous motor installed in the world, Fig. 2.14) used for a Main Air Compressor (MAC). This machine forms part of a different multiple motor soft start scheme utilizing LCI technology as described in Chapter 2.

6.2 MAXIMUM TRANSFER ANGLES

6.2.1 Comparison of Calculated and Simulated Values

The estimated maximum transfer angles and currents calculated from the theory in section 5.4.2 are given in Table 6.I for the system with the PGC. The system parameters are provided in Appendix C.

The results can be compared with results from the dynamic simulation model described in section 5.4.1.The model is shown in Appendix B Fig. B.2. Examples of simulation results are given in Fig. 6.1 - Fig. 6.5 for the PGC. The instantaneous currents shown in Fig. 6.2, show transient characteristics similar to short circuit currents, but with additional transients with temporary DC averages due to the machine speed variation and oscillation, which eventually die out before symmetrical stabilization occurs.

Calculated examples of rms currents for selected transfer angles shown in Table 6.I are indicated in Fig. 6.3 and Fig. 6.5. The differences between the calculated results and dynamic simulation results (Fig. 6.3) occur because the calculated results represent only a single point effective subtransient value whereas the simulation results represent the variation of the current for the shown duration. The calculated results do however provide a good indication of the average initial rms current (after the transfer) obtained from the dynamic simulation. The calculations are therefore effective to provide an initial estimation of what the effect of the transfer conditions (angle and voltages) on the average transfer current will be.

Table 6.I

MAXIMUM TRANSFER ANGLES AND ASSOCIATED CURRENT(R.M.S)

Description	Single Machine		Two Identical Machines	
	Current (kA)	Angle (δ_s) (° deg)	Current (kA)	Angle (δ_s) (° deg)
Traditional approach (Ev_m=1 p.u., Ev_s=1 p.u.)	4.9 (eq. 5.16)	83 (eq. 5.1)	8.3 (eq. 5.16)	83 (eq. 5.1)
Maximum current estimate (E^0=1 p.u.)	11.2 (eq. 5.16)	180	16.5 (eq. 5.16)	180
Machine limit (V_{rm}=1, V_s=1, E^0=1)	8.7 (eq. 5.2)	102 (eq. 5.16)	8.7 (eq. 5.2)	102 (eq. 5.16)
Transformer limit (Vt=1, V_s=1, E^0=1)	15.7 (eq. 5.3)	N/A	15.7 (eq. 5.3)	143.8 (eq. 5.16)
Busbar voltage drop limit (solution of equations 5.17-5.21)				
V^f = 0.9 p.u. E^0 = 1 p.u.	2.9	35		
V^f = 0.9 p.u. E^0 = 0.85 p.u. (Simulations in Fig. 6.1 -Fig. 6.3)	2.93	46		
V^f = 0.85 p.u. E^0 = 1 p.u.	3.9	44	3.9	19.7
V^f = 0.85 p.u. E^0= 0.8 p.u. (Simulations in Fig. 6.4-Fig. 6.5 for single machine)	4	58	4.2	36.2
V^f=0.7 p.u. E^0=0.8 p.u.			6.9	48.9
V^f=0.7 p.u. E^0=1 p.u.			6.8	27.9

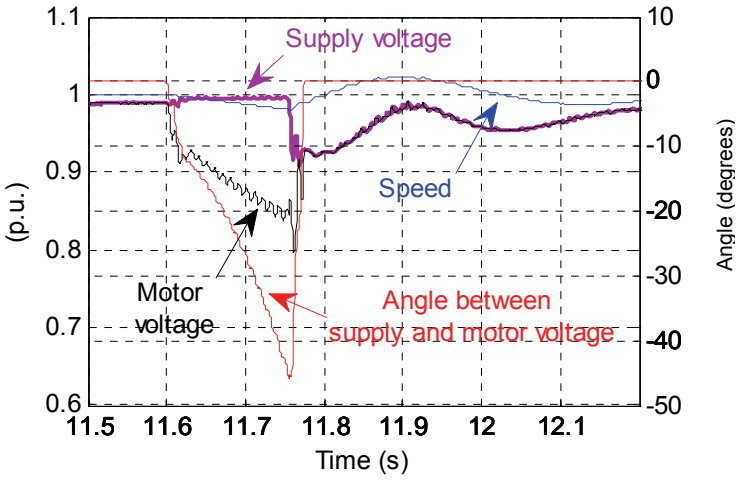

Fig. 6.1 Bus and motor voltage and angle (between motor and supply voltage) during a bus transfer (δ_s=46 ° deg)

Furthermore the simulated bus voltage is also aligned with the calculated bus voltage and therefore this confirms that the simplified method is effective/conservative from a busbar voltage drop point of view. The simulated bus voltage drops are similar on all three phases and not shown. The assumption has previously been made that the speed variation of the

motor voltage is not significant and for the purposes of the calculation method nominal speed was used. The actual simulation with the dynamic model has shown that the speed drop is only 2% prior to the transfer and justifies this assumption. The calculation methods can therefore be used as an initial tool for system sensitivity analysis in terms of voltage drops and equipment limits.

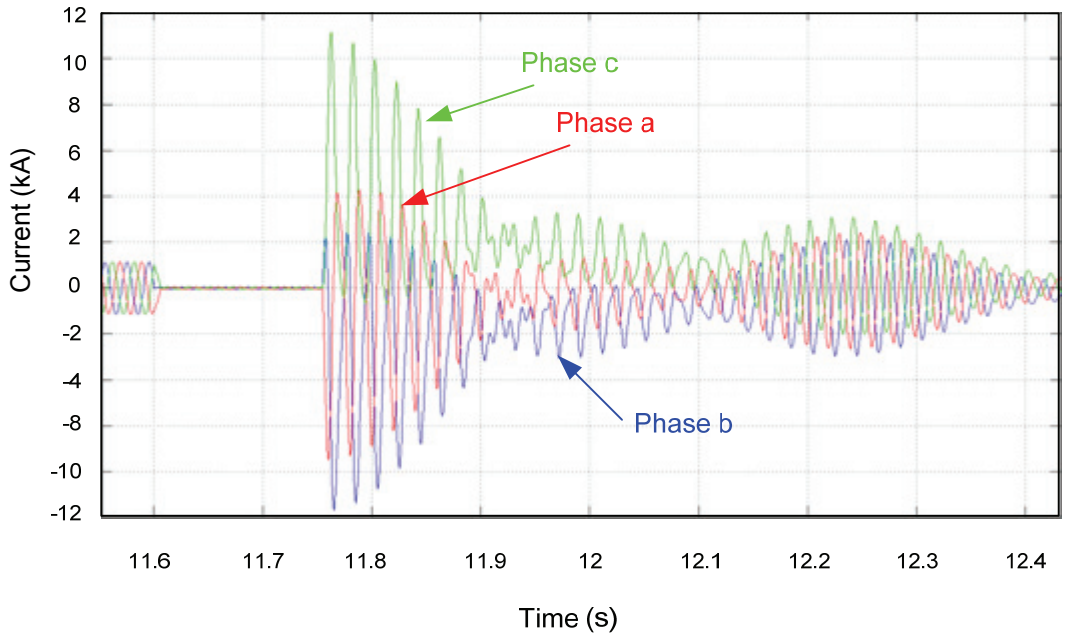

Fig. 6.2 Current during a bus transfer (instantaneous) (δ_s=46 º deg)

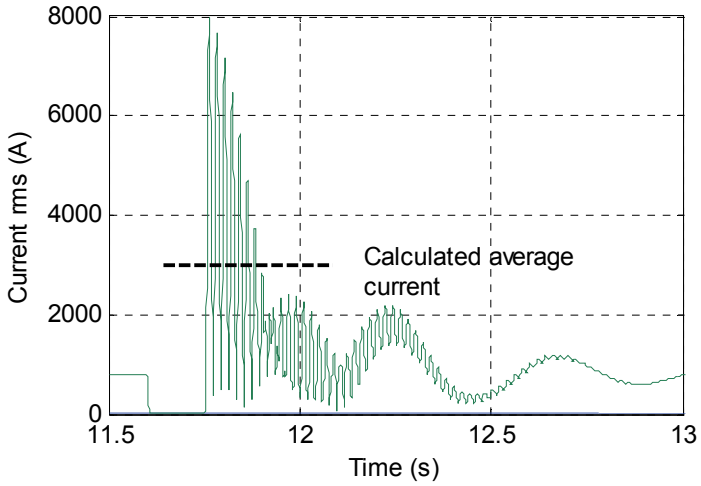

Fig. 6.3 Current during a bus transfer (rms, derived from *Iq* & *Id*) (δ_s=46 º deg)

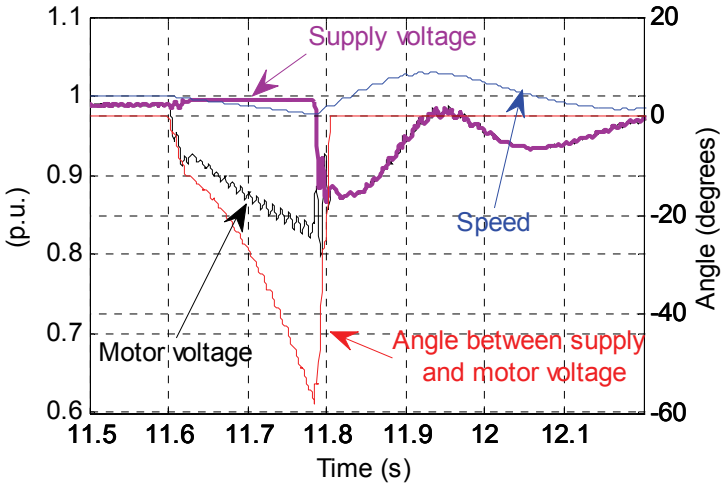

Fig. 6.4 Bus and motor voltage and angle (between motor and supply voltage) during a bus transfer (δ_s=58 º deg)

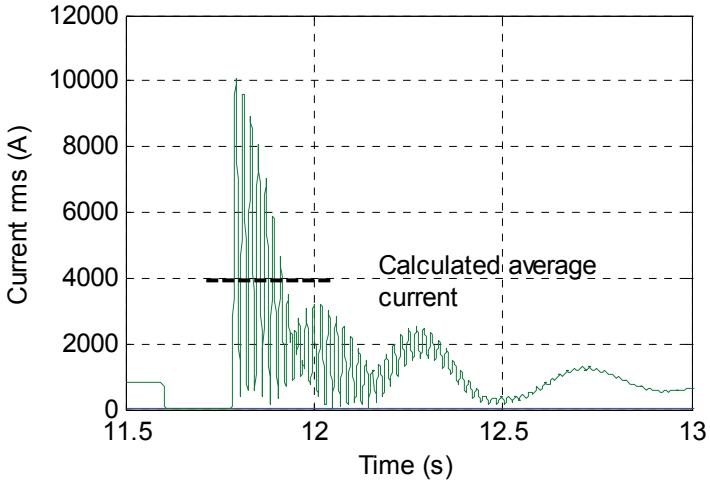

Fig. 6.5 Current during a bus transfer (rms, derived from *Iq* & *Id*) (δ_s=58 º deg)

6.2.2 Sensitivity Analysis

Table 6.I shows the maximum allowed transfer angles associated with busbar voltage limitations are far smaller than maximum angles associated with the machine, transformer and traditional approach limitations. The busbar voltage drop limit is therefore most

sensitive to the transfer angle for large SFC started machines. An initial worst case approach is to assume E^0=1 and V^f equal to the maximum bus drop allowed.

6.2.3 Compliance with Limitations

Strict limitations for petrochemical plants are sometimes set, even stricter than the limitations in Table 5.I. The specification of the petrochemical plant where the case studies are located calls for a maximum voltage drop of 10% at 11 kV [6.1]. This requirement has however been based on DOL motor starting current. It can be shown that a fast transfer can occur in 100 ms [6.2] based on the operating times of breakers, fast transfer device and protection relay processor times (from the point where the initial source breaker is open until the point where the tie breaker/new source breaker is closed). The de-acceleration rate will be the largest at full load and the associated angle after 100 ms can be simulated from the model in section 5.4.1 to be 27º as shown in Fig. 6.6. Table 6.I shows that there is no concern for single machine transfers since the angles are larger in all cases, however for two machines, the bus voltage may drop to below 85% which is in certain environments unacceptable. A bus voltage of 70% can however still be met (which is still acceptable in terms of the shaded area in area Table 5.I), This is shown in Table 6.I in the scenario with 2 machines, E^0=1 and V^f=0.7 and a transfer angle of 27.9º (larger than the fast transfer angle of 27º) . In the case study one machine is however fed from an ASD and therefore the single machine case study is applicable under normal conditions and no voltage limit problems are foreseen. Inrush currents associated with the ASD transformer must still be accounted for (discussed later).

After it has been estimated that the system design is within acceptable limits from the simplified model from section 5.4.2, it is proposed to perform electromagnetic and mechanical dynamic modeling as described in section 5.4.1 (typically later in the project stage). This serves as a final measure to ensure that the machines can ride-through all required conditions as described in the following sections by means of case studies.

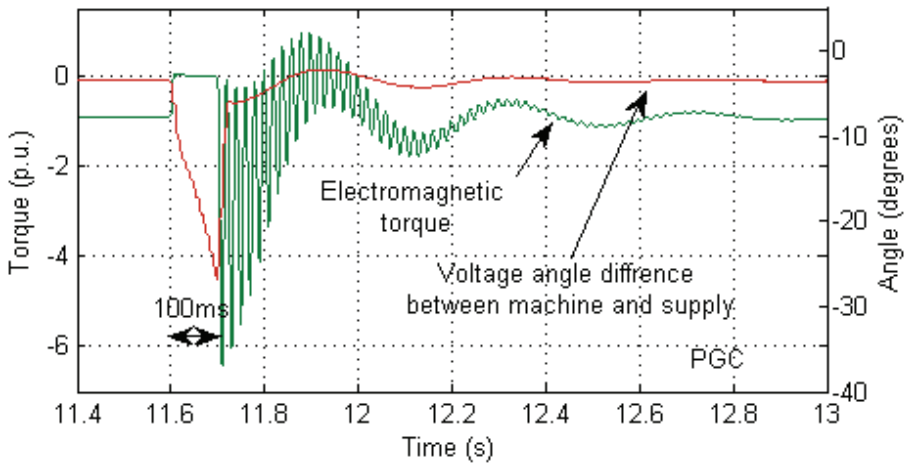

Fig. 6.6 Machine re-acceleration following a tranfer

6.3 ON-LINE VOLTAGE SAG RIDE THROUGH

Fig. 6.7 illustrates from simulations that on-line (50 Hz) MAC motor operation is stable for the recorded voltage dips (all types shown for a 18 month period) . The three phase dip curve is conservative compared to those of smaller synchronous motors on site. The figure shows both fixed excitation and results where the excitation supply dips with the same p.u. value as the main supply. No significant benefit can be therefore be obtained by feeding the excitation from an Uninterruptible Power Supply (UPS) (i.e. fixed excitation vs. obtaining excitation supply from a conventional supply which drops in voltage in a similar way as the main supply). This is due to the long time constant (Appendix C) of the exciter (Fig. 5.4). Similarly improved excitation control will not have a significant effect in the region where voltage dips were recorded. It is only necessary to include the controller model for longer disturbances (e.g. power factor control for load disturbances). It is also shown that the single machine model (with the plant source impedance parameters) results (Fig. 6.7) and the entire network model results do not differ significantly and a single machine model is therefore sufficient for further investigation.

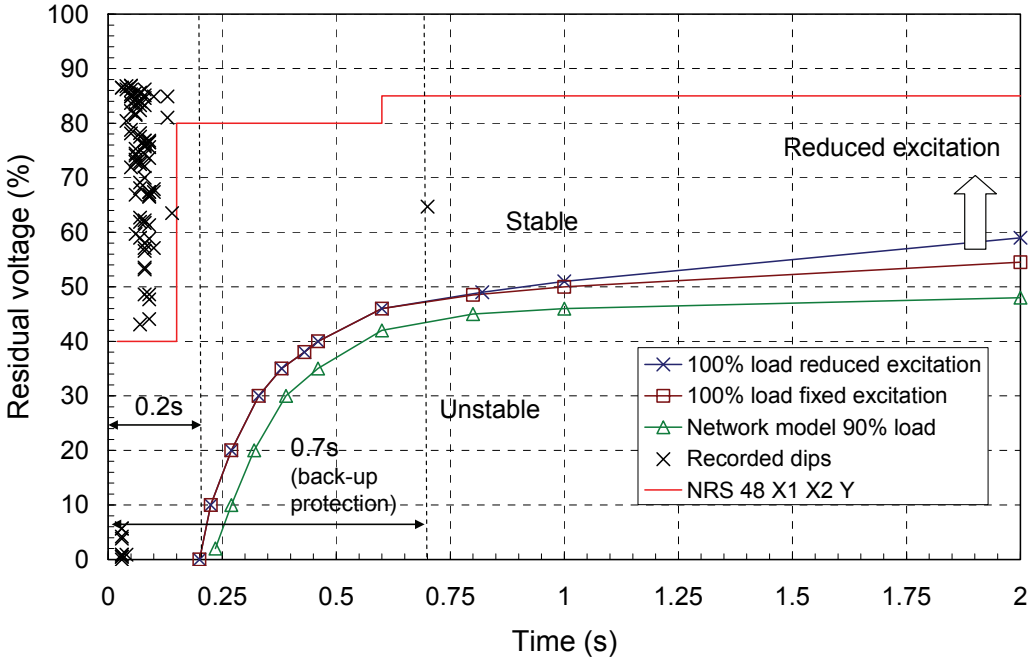

Fig. 6.7 Line Operated Voltage Tolerance Curves and Recorded Voltage Dips (MAC 55MW)

6.4 ASD VOLTAGE DIP/ INTERRUPTION RIDE-THROUGH

6.4.1 Overall Voltage Dip/ Interruption Ride-through Capability

ASD operation for the PGC process requirements is limited between 80% and 100% speed. The drive system ride-through capability was verified by removing input voltage and then recording the operating parameters until the drive has tripped. The coast down simulations from the theory in section 5.4.1 and site tests results in Fig. 6.8 show a gradual speed drop due to the large compressor & motor inertia and associated drop in voltage (function of excitation and speed). The voltage drops as a function of both speed and magnetic inertia after the excitation has been removed due to the undervoltage trip (taking into account the exciter time constant shown in Appendix C). This means that even if the excitation had been supplied from a source which also dips significantly (which resembles the same situation as removed excitation), the inertia ride-through method will still be suitable since voltage is available due to the magnetic inertia. Good correlation between simulations and site tests is achieved and therefore the model can also be used to simulate other scenarios.

The site tests were only allowed during lightly loaded conditions due to process restrictions. Simulated results for speed (which is the most important parameter for the process) are therefore presented for the full load condition.

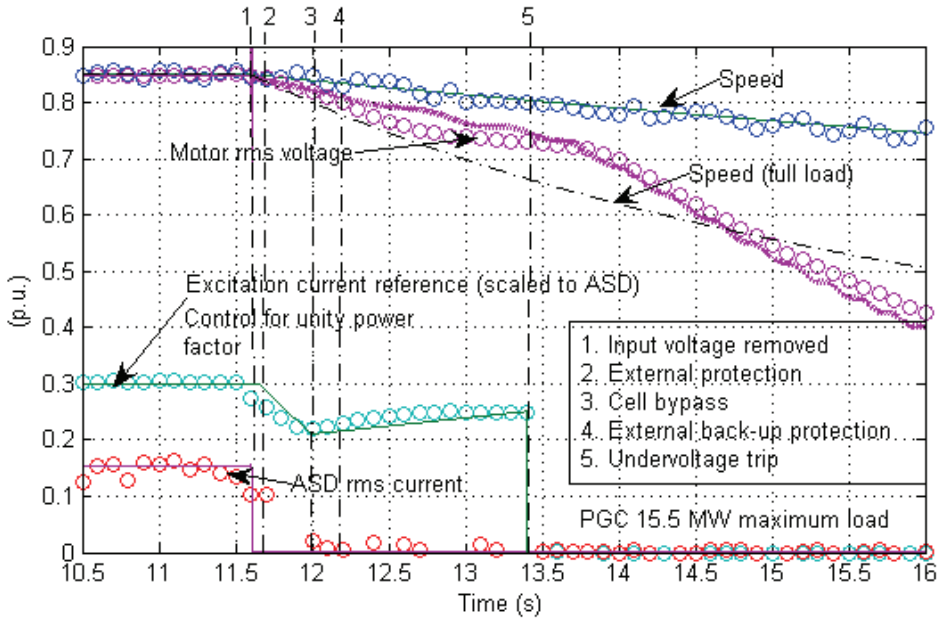

Fig. 6.8 SM coast down test recording points and simulations after ASD input voltage has been removed

ASD internal cell faults are bypassed in accordance with principles described in the previous chapter. A cell bypass time of 450 ms (significantly longer than recorded voltage dips) is shown on Fig. 6.8 (line 3). This cell bypass time is based on recordings of the bypass operation time which is discussed later in more detail.

The speed reductions associated with the disturbance or fault durations shown in Fig. 6.7 have no impact on the continuation of the specific plant process. External protection (line 2) shown in the figure is regarded as protection outside the ASD, e.g. an upstream fault cleared by transformer differential or cable differential protection (typical 120 ms clearance duration). Fig. 6.8 shows that ASD ride-through can even be achieved for faults cleared by external system back-up protection (line 5). This is not possible with DOL operation (Fig. 6.7). In weak supply systems with frequent longer duration dips the ride-

through features of the ASD may therefore strengthen the business case when deciding on purchasing an ASD.

Actual on site ride-through recordings scenarios are shown in Fig. 6.9, Fig. 6.10 and Fig. 6.11. The recordings confirm successful ride-through as predicted by the simulations and coast down tests.

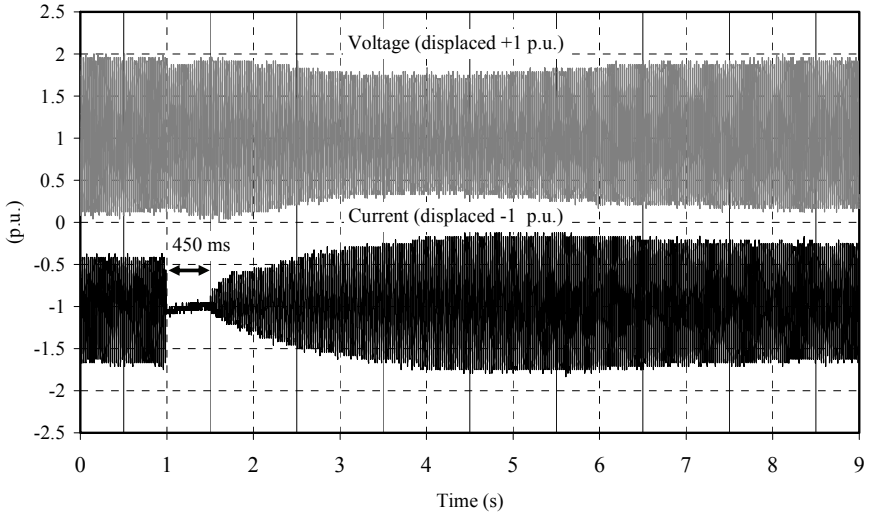

Fig. 6.9 Oscilloscope cell bypass recording

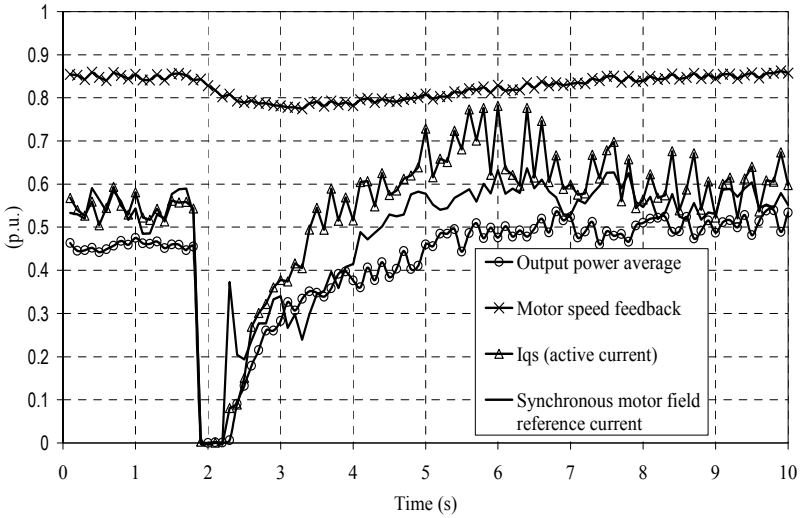

Fig. 6.10 ASD Ride-through Recordings (PGC) – Faulty Cell Bypass

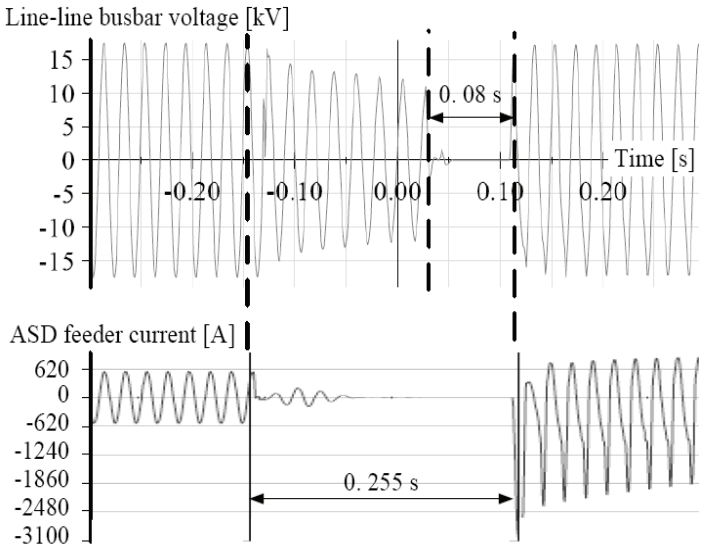

Fig. 6.11 ASD Ride-through Recordings (PGC) –Voltage Dip & Interruption

6.4.2 Cell Fault Ride-through Examples

Fig. 6.9 and Fig. 6.10 show successful bypass operation but that the time of 450ms is significantly longer with this higher voltage level drive than the 250 ms in [6.4]. This is mainly due to differences in the construction and size of the bypass contactors. The implication is a more significant disturbance to the process (Fig. 6.10) in terms of load speed. Compressor applications can normally accommodate this performance without a detrimental effect to the process, but lower inertia and/or low speed applications (e.g. extruders) may need further evaluation. It is proposed to optimise the fault detection, and drive reconfiguration time for these applications. This may be achieved by optimizing the existing method or for future development by considering an alternative method, for example in [6.6] an artificial intelligent based fault diagnosis and reconfiguration scheme is proposed. Experimental results show that fault clearance time within 100 ms [6.5] is possible which will improve ride-through performance for demanding processes significantly. A further benefit of the scheme in [6.5] is that bypass contactors are not required for cell inverter side faults. An alternative fault detection scheme with fast fault detection is based on output voltage frequency analysis and proposed in [6.6]. Some of these schemes do however not address a solution to ride through / bypass front end faults

of the cell (e.g. DC link or diode bridge faults investigated later in this chapter). It is recommended to investigate semiconductor switch methods as a replacement for the bypass contactors, especially for other applications requiring faster bypass operation.

Power electronic N-1 redundancy in LCI systems is achieved by an additional thyristor in series per leg which does not require any re-configuration scheme and ride-through challenges associated with thyristor failures with LCIs are normally not a concern.

6.4.3 Transformer Inrush Currents

Transformer inrush currents can be estimated from the theory in [6.3] taking conscience of a pre-charge/ magnetizing circuit fitted in the drive system. Fig. 6.11 provides an example which shows the inrush current. In the case of an ASD and on-line synchronous machine that needs to be transferred, the busbar voltage drop can be minimized by reaccelerating the normal synchronous motor first by conventional fast transfer and to delay the reacceleration of the ASD driven motor until after the synchronous motor transfer current has significantly decayed. This means that the ASD feeding breaker will have to be tripped at transfer initiation and then reclosed at a suitable time. A suitable reclose time can be determined, for example from for example Fig. 6.3 i.e. 1 s after the transfer initiation (after the current has significantly reduced). Fig. 6.8 illustrates that 1s can easily be accommodated and the ASD can successfully reaccelerate without tripping the process (since the speed reduction is only approximately 15% for 1s). This optimization is not required for this case study project since transfer currents associated with up to two synchronous motors directly connected can be accommodated for NRS 48 recommended values (Table 6.I). The machine transfer currents are also significantly higher than transformer inrush currents (for this project) and one ASD/transformer connected machine and one directly connected machine presents a less severe situation than two directly connected machines. The scheme should however be considered in cases with weaker source impedances.

6.5 TRANSIENT TORQUES

It is suggested to evaluate the transient torques during and following different ride-through conditions and to perform the drive string torsional analysis to verify that all components can accommodate the torques. Significant torque values can be reached under several conditions. The electromechanical model described in the previous chapter is useful for this analysis. Transient torques are most significant when the ASD is not connected and therefore the largest SFC started motor which is operated on-line as the normal operating mode will be used for the case studies, i.e. the MAC motor.

6.5.1 Short Circuit Torques

For reference, the maximum 3 phase and 2 phase short circuit torques provided by the manufacturer of the MAC motor are respectively 8.09 p.u. and 8.43 p.u. Machines are typically designed to withstand 10 p.u. torques [6.7].

6.5.2 Voltage Dip Torques

The modeling approach followed is conservative in order to estimate worst case transient torques based on the theory in section 5.2.2.

The worst case is therefore practically regarded as a 3 phase dip and at the point just before the machine would have become instable after voltage recovery i.e. approximately 200ms from Fig. 6.7 for a 100 % dip).

Fig. 6.12 shows electromagnetic torque (air-gap) simulation results for the worst case voltage dip (100% depth, 200 ms based on Fig. 6.7) and also for a less severe case (100% depth, 100 ms). The simulation correlates closely with simulated values provided by the motor manufacturer also shown on the figure. The MAC application drive string components (coupling, gearbox, compressor) are designed to accommodate a maximum mechanical torque of 5.75 p.u (similar values apply for connected loads with other applications, i.e. 3-5 times rated torque) [6.7]). The simulated torques from torsional analysis seen by the drive string components are significantly less than the air-gap torque and the entire drive string can accommodate the worst case torques (confirmed by the compressor manufacturer) which are also lower than the short circuit torques.

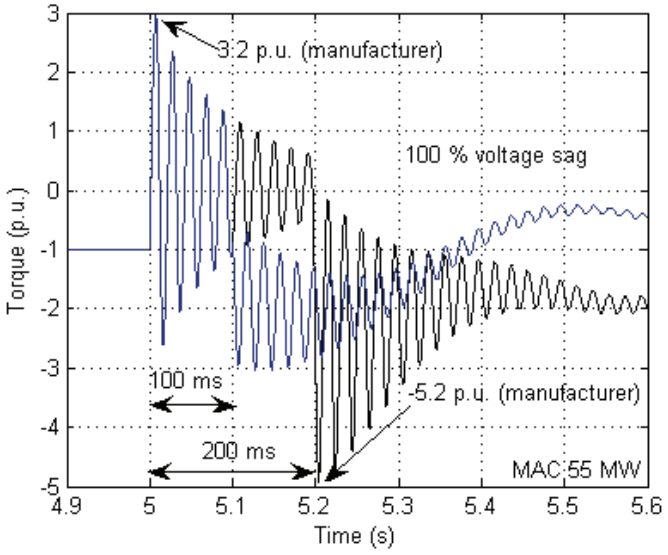

Fig. 6.12 Transient Air-gap Torques associated with Voltage Dips

6.5.3 Transfer Torques

A transfer is applied for the MAC motor where the LCI starting current is stopped prior to the transfer. The maximum allowable angle for safe fast bus motor transfers can be estimated from equation (5.1). The LCI transfer is not identical to a fast bus transfer but the angle estimation is used as an initial indication. The angle is δ_m=72^o for Ev_m=(1.1/0.98) and Ev_s= (1.1/0.98) representing a worst case condition with worst case network overvoltage and under frequency values.

This is for a resultant maximum vectorial V/Hz of 1.33 between the motor residual V/Hz vector (e.g. C bus in Fig. 2.5) and supply V/Hz vector (e.g. A bus in Fig. 2.5). Even though this standard is intended for induction motors, the angle value is used as a starting point for illustration of associated synchronous motor torques.

The simulated air-gap torque results are shown in Fig. 6.13. The air-gap torque (6 p.u.) is only slightly more than the maximum allowed mechanical torque and the lower torsional mechanical torque will therefore be within the design margin.

The ANSI maximum angle or a resultant vectorial V/Hz of 1.33 therefore also seems reasonable for this application. The torque is also below the short circuit torques. A maximum angle of 10 degrees (this is a typical boundary setting) can however easily be achieved with controlled LCI synchronized transfers with very low torques as shown in Fig. 6.13.

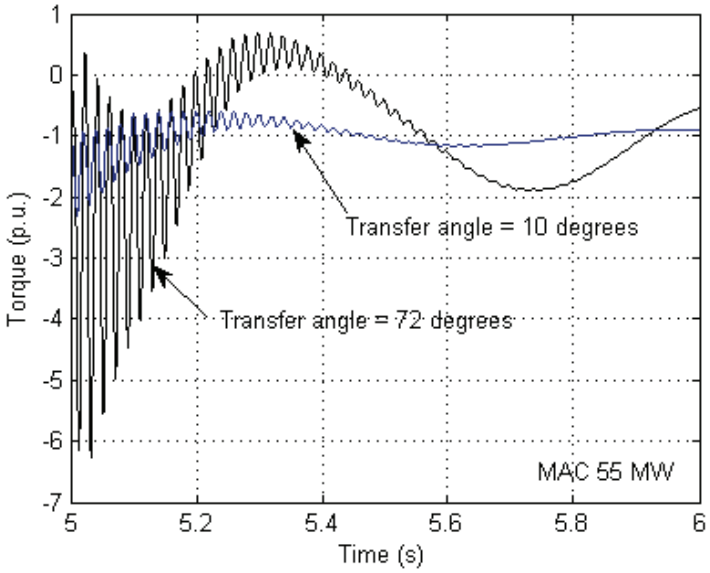

Fig. 6.13 Transient Air-gap Torques: Motor Transfer from ASD to Line (Break-before-make)

Calculations given in Chapter 2 provide the maximum synchronization angle for a make-before-break transfer (PGC) with an ASD output/synchronization reactor as 7.2 degrees. This is to limit the synchronization current within acceptable limits (to protect the ASD and avoid nuisance trips). This small angle is associated with very smooth transfers from a torque perspective. Site experience has however shown that reliable transfers with slightly smaller boundary angles cannot always be guaranteed since the controller has difficulty meeting the synchronization window constraints (e.g. during process upsets).

An ASD with an output reactor may also have to be operated at a higher switching frequency to avoid resonance overvoltages as shown in Chapter 4.

A transfer where the machine current is phased back and then synchronized on a break-before make principle (in terms of the inverter firing and closing of the run breaker) should

however easily be achieved based on a wider allowed transfer angle. This is subject to a compatible ASD system design with overvoltage protection (in cases where the RCB is closed after the SCB has opened) and suitable excitation control. This is possible without endangering any equipment mechanically as previously shown and an output reactor is then not required. The removal of the output reactor has therefore the advantage that the ASD can be operated at the optimal carrier frequency (lowest losses) with the added benefit of increased reliability (one less single point of failure). Furthermore the controller will not have difficulty in meeting the synchronization window constraints.

6.6 SINGLE POINT OF FAILURES

The ASD has the capability to ride through internal faults where redundancy is built in. ASD single point of failures (e.g. an ASD input transformer failure) will however result in a process trip.

6.6.1 ASD Back-up

Critical applications may therefore require a back-up or remote ASD for a "flying start" to eliminate a process trip. Possible ASD back-up alternatives are described in Chapter 1, 3 and 4.

6.6.2 Machine Re-acceleration

The ASD back-up option for critical applications might be avoided in some cases, by re-accelerating the machine to line frequency in induction motor (IM) mode after the ASD has tripped. This is done with a synchronized closure of the Run Circuit Breaker (RCB – see Fig. 2.5) at the first phase coincidence. The field winding is shorted after the ASD failure, and synchronization after RCB closure is similar to DOL started SMs. The SM design (damper windings /pole shoes) must be suitably rated for the induction motor acceleration mode. Furthermore a synchronizing function similar to that of a DOL started machine must be installed. This option does need further evaluation since there is a risk that the inrush currents are too large and voltage collapse may be possible. Large IMs can normally only be started-up at no or light load conditions. There is a further risk that that

the machine will not be able to re-accelerate since the torque is not large enough compared to the load torque requirement. This may only be possible above a certain speed depending on the machine torque, load torque and inertia.

Synchronized closure of the RCB and re-acceleration of a normal synchronous motor with the field supply active may only be possible for a small frequency difference or rate of change between the supply frequency and the machine voltage frequency (mainly determined by the ASD speed prior to the fault). The ASD speed will therefore have to be close to the nominal speed to avoid losing synchronism (out-of–step condition) following the transfer. If the ASD speed is significantly below nominal speed a successful transfer in synchronous motor mode is unlikely.

Fig. 6.14 illustrates examples of the decaying machine voltage, angle and first phase coincidence (between the motor voltage and supply voltage) when the ASD trip has occurred at nominal speed. This is a worst case assumption in terms of time since the first phase co-incidence would occur faster when the ASD has been operated at lower speeds prior to the trip. Furthermore it is assumed that the ASD output is in phase with the supply voltage just before the trip (this is the worst case since it will take the longest for the first phase co-incidence to occur).

6.6.3 Synchronous Machine Transfer and Re-acceleration

Fig. 6.6 shows that a fast transfer (principle described in [6.9]) to the fixed bus supply in synchronous motor mode is possible. The fast transfer time is typically 100ms (control and breaker operation time). The transfer angle is 27º which approaches the limits of typical fast transfer boundary settings. This is however only possible following a transfer from nominal speed. Similarly, a transfer at the first phase co-incidence (also referred to as delayed in phase transfer [6.9]) in synchronous motor mode is also possible as shown in Fig. 6.14. The bus voltage drop is within the NRS 48 Y category limits since the value below 80% voltage has duration of approximately 100 ms (less than 150 ms of the Y category and the voltage is above 70 %).

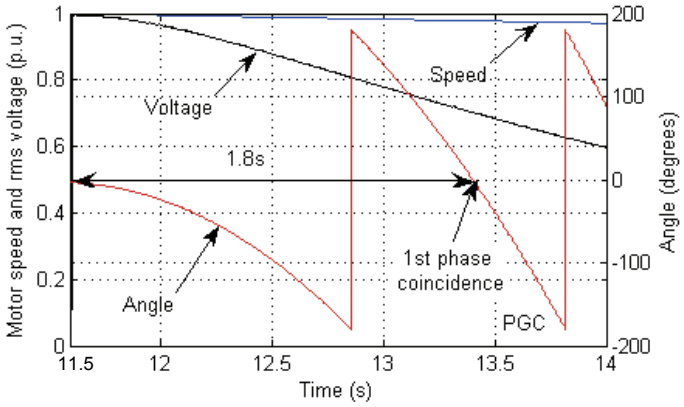

(a) 10% load

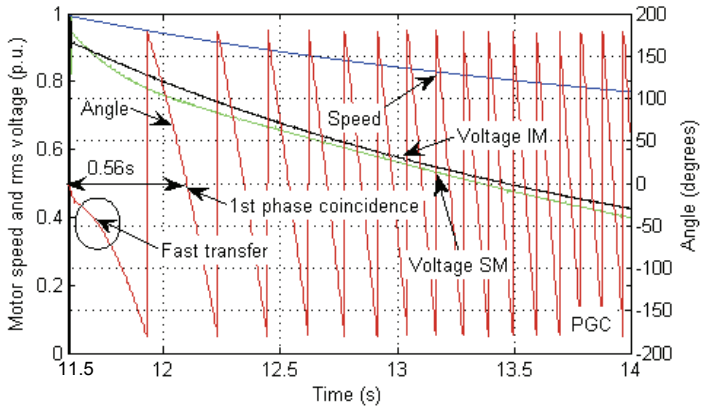

(b) 100% load

Fig. 6.14 First phase coincidence between supply voltage and motor voltage

A delayed in phase transfer at other lower operating speeds for example as shown in Fig. 6.16 at the minimum ASD operation speed is associated with severe current/torque transients and voltage drops. This is due to pole slipping (or machine instability) as can be seen by the load angle which does not recover.

Pole slipping occurs even from the second phase coincidence (from nominal speed) at a speed of approximately 90% as shown in Fig. 6.17. If this scheme is used in future, it is essential to block the delayed in phase transfer below speeds where there is a risk that the machine might not recover.

It can therefore be concluded that a successful transfer may occur above 95 % speed (Fig. 6.15 b) but is not possible below 90% speed. Depending on the moment of ASD failure a transfer between 90 % and 95% speed might be possible. In some cases the process might be saved by implementing a transfer since the average effective motor speed is 90.1 % (as mentioned in Chapter 2). The possibility of a successful transfer will increase during lighter loaded conditions (e.g. Fig. 6.14 (a)).

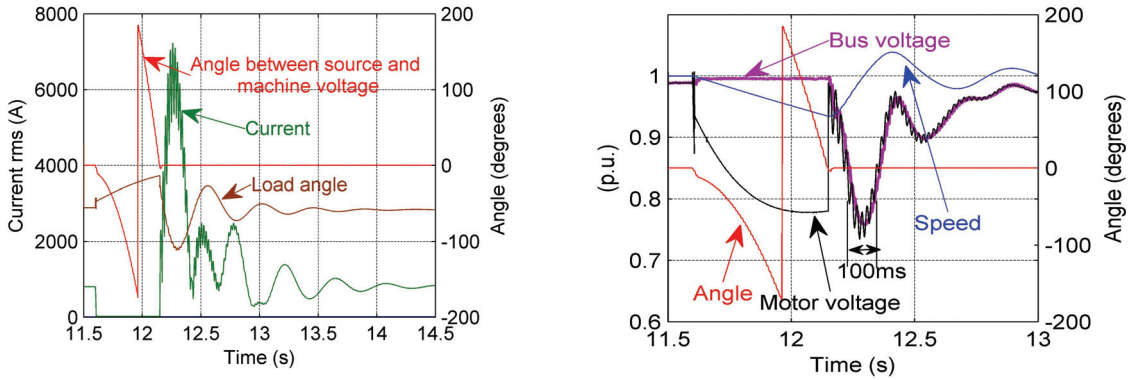

(a) (b)

Fig. 6.15 Re-acceleration at first phase coincidence (approximately 95% speed)

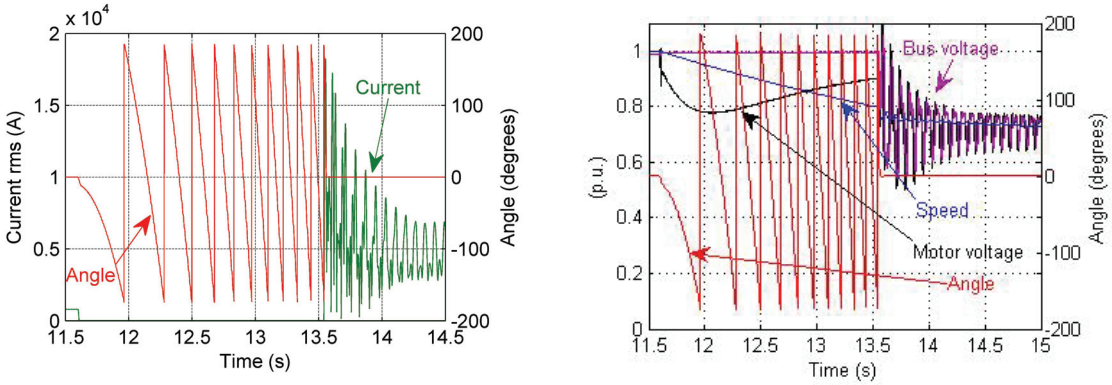

(a) (b)

Fig. 6.16 Attempted re-acceleration simulation at minimum ASD operating speed of 80% (in phase transfer)

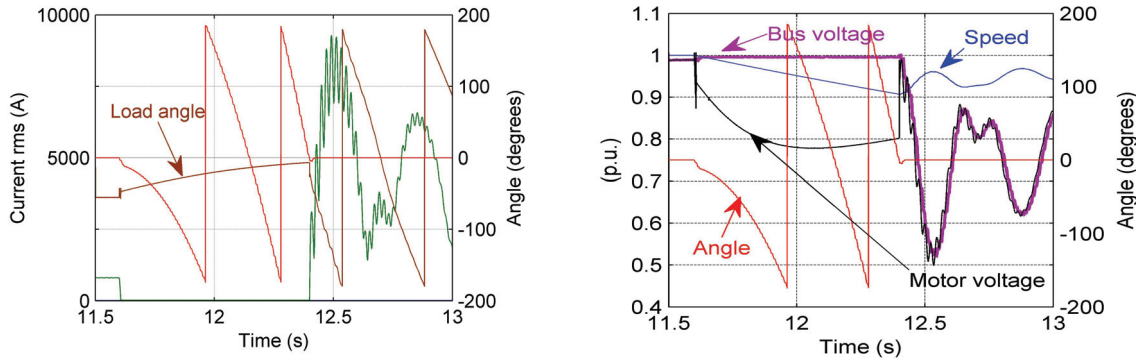

(a) (b)

Fig. 6.17 Attempted re-acceleration simulation from approximately 90% speed.

6.6.4 In Phase Induction Machine Re-acceleration

An induction motor (or synchronous motor designed for induction motor mode re-acceleration) may be transferred at the first phase co-incidence (principle described in [1.61] with potential successful re-acceleration). Fig. 6.18 illustrates a simulated example with typical induction motor parameters as given in Appendix C. The machine voltage decay characteristic is similar to that of the synchronous machine (Fig. 6.14) since the synchronous machine excitation has been removed after the trip has occurred (for the purposes of that simulation). (Usually when excitation is removed, a trip to the motor is issued). Re-closure may also be timed for safe re-acceleration based on the decayed back emf value in accordance with principles in [6.9] if there is sufficient motor torque to re-accelerate the load. It can also be illustrated that even induction motors may not be able to re-accelerate from the minimum rated adjustable speed which is the case for this application if an induction motor had been used. Large induction motors are normally designed to start from light load conditions and re-acceleration during full load is difficult to achieve. There is however merit to investigate whether and from what speed an induction machine can be re-accelerated for each specific application.

Furthermore it is important to verify that the inrush currents (for all ride-through conditions) are within limits of the upstream protection settings when determining the boundary conditions. These protection curves should be well above the inrush currents considering time and current pick-up values (e.g. the curve for the ASD feeder in the protection co-ordination study discusses later).

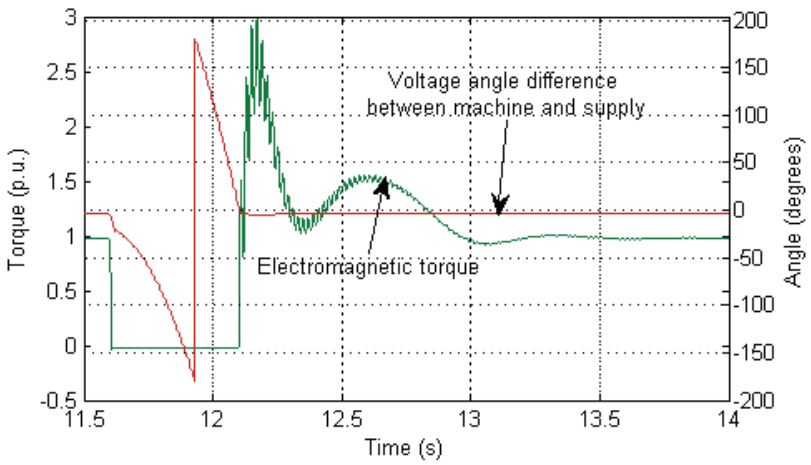

Fig. 6.18 First phase coincidence transfer, re-acceleration of induction motor (induction motor motoring torque positive convention)

6.7 ASD PROTECTION AND DESIGN TO ENHANCE RIDE-THROUGH AND AVAILABILITY

6.7.1 Introduction

The fault tolerant operation of the ASD in terms of the cell bypass has the objective to bypass all cell faults and to continue with operation. Recordings in Fig. 6.10 proves the principle and successful cell bypasses have also occurred for IGBT faults. Faults on the DC link and rectifier front end are however not detected by the schemes in [6.5] and [6.6]. The present scheme of the manufacturer also bypasses front end faults, e.g. based on a blown cell front end fuse. It is however unclear whether all cell faults will be contained within the cell under all conditions. A detailed site ASD failure case study [6.10] for the SSASD system for the NPP driving described in Chapter 2 is used to investigate fault propagation and to review the related ASD design and protection principles.

6.7.2 Case Study Event Description

In October 2005, the entire ASD system was energized to conduct functional testing and to check the water cooling system. Start-up plans were in progress to bump start one of the synchronous motors but due to excitation problems this was not possible and the ASD was left energized in an idle mode, namely, the input transformer was energized without the power cells gating. The ASD was in this mode for several hours when it suffered a failure causing the 11 kV feeder breaker 52-2 to trip. Fig. 6.19 shows the recorded fault current measured on 11 kV primary side during the ASD failure that caused the feeder breaker to trip. The ASD was taken out of service and thoroughly inspected. The visual inspection revealed considerable damage to the power Cell A2 (Fig. 2.2) rectifier and capacitors and signs of arcing on most cell input busbars.

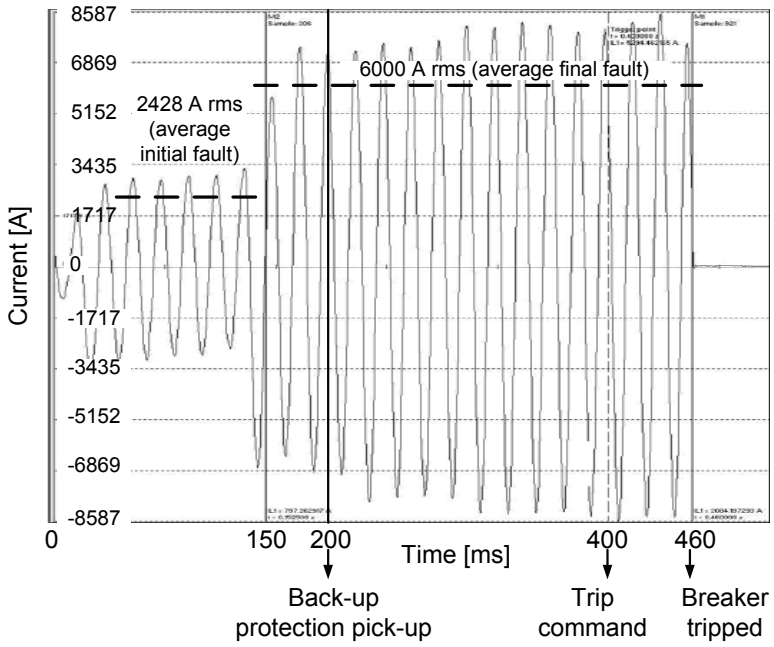

Fig. 6.19 ASD Feeder (52-2) fault recording at 11kV side

Maximum transformer secondary short circuit current is calculated at 6438 A rms at 1375V based on the lowest winding impedance at 1.47 MVA. This short circuit current with reference to 11 kV is equal to 805 A rms. An initial analysis of the captured current waveform indicated that the fault first occurred in one power cell (i.e. cell A2) which is

represented by the first half cycle shown in Fig. 6.19. This is taking into consideration that the arc current is less than the bolted short circuit current in accordance with [6.11].The fault then progressed due to arcing to two other power cells via the common busbars resulting in an average initial fault current as shown in Fig. 6.19. Further arcing to additional cells resulted in escalation to an average final fault current as illustrated in Fig. 6.19.

6.7.3 ASD Failure Analysis

This incident called for a full investigation to determine the root cause of ASD failure, to review the ASD internal protection which did not operate properly and the ASD's incapability to isolate the faulted power cell.

The initial findings were that the ASD has suffered severe damage to power cell A2 and associated busbar, Fig. 6.20. The incoming 11 kV feeder breaker (52-2) tripped and isolated the ASD. It was decided to ship all 15 power cells to the original manufacturer for detailed inspection and testing by the manufacturer.

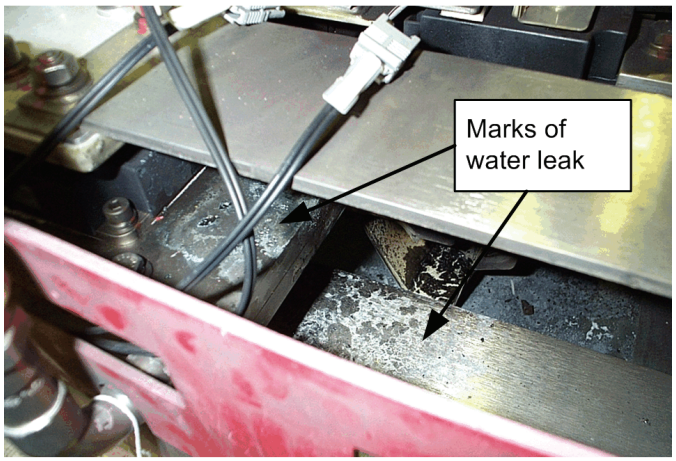

Fig. 6.20 Power Cell A2 showing water marks

The faulty power cell A2 was dismantled by the manufacturer and fully examined. It revealed signs of cooling water leak that possibly existed for some time and eventually compromised the DC link insulation causing it to flash over. The arcing phenomena and

arc propagation are based on the theory provided in [6.13]. It was not possible to determine how long this leak had persisted because the location is not easily visible as it is covered by cell power components. In fact, when the faulty cell was subjected to standard water pressure test at the factory, no sign of water leak was noticed. However, when test was repeated at 150 % standard test pressure and the cell was left under this pressure for several hours, a minute leak from one location in the cold plate was observed. Based on these results, it was decided to subject the cold plate for faulty cell A2 to further testing at a specialized material testing laboratory. The follow-up laboratory testing verified that there was a leak in the cold plate. It also showed a very small crack. The cold plate manufacturer was consulted and it became apparent that a new cold plate design had been used for this ASD that is more compact and effective for thermal conduction. For comparison purposes, a healthy cold plate was subjected to a similar high-pressure water test and no water leak was detected.

It was impractical to change the cold plates for the fifteen power cells or even institute a method to detect such a minute water leak with the ASD in service. Instead, it was decided to implement the following measures to contain any future power cell failure damage.

1. Fully tested the remaining 14 power cells and the two spare cells at the factory under water pressure and established no cooling water leak.
2. Replaced the uninsulated busbar work of the ASD with cable bus (the manufacturer has agreed to this recommendation). Also, installed additional barriers and spacing to avoid arcing between cells and the bus. The damage to this ASD could have been minimized had it not arced to the common bus work. Although a power cell failure is a rare occurrence, the ASD should be designed to limit damage to the faulted cell.
3. Conducted comprehensive review of the ASD internal protection to ensure coordinated fast tripping in the event of a cell failure. A review of the field protection data (Fig. 6.19) showed that the 11 kV feeder breaker (52-2) tripped on a back up protection within 460 ms due to power cell failure rather than initiated by a trip signal from the ASD. This ASD design has two internal protection schemes that are intended to adequately detect a power cell or a secondary winding transformer failure and initiate a main breaker trip in a shorter time than 460 ms to limit potential fault damage. The ASD protection scheme is discussed in the next section.

It should be noted that since January 2006 when the ASD was placed in operation no further cold plate cooling water leaks has been experienced.

6.7.4 ASD Protection Co-Ordination and Settings

Fig. 6.21 shows a simplified single line diagram with the main protective functions. Fig. 6 illustrates the associated protection co-ordination curves based on the ASD internal protection, feeder protection settings and cell fuse selection.

A. ASD Over-current Protection

Due to the multiple transformer secondary windings, conventional protection schemes are not adequate to protect against transformer windings and cabling faults. Conventional differential protection is impractical due to the amount of current transformers (CTs) required. The fault current on transformer secondary windings (high impedance and small MVA rating compared to the primary) is low and conventional protection schemes will be sluggish to clear a secondary fault. The ASD manufacturer has developed a novel Input Protection scheme to detect secondary fault current. The input protection scheme consists of a reactive power function and a differential real power function suitable for the detection of short-circuit and arcing faults respectively.

Reactive power protection continuously measures the drive input reactive power with respect to transformer primary side to determine whether a fault has occurred on the secondary side of the transformer. For example, a short-circuit in one of the secondary windings will result in poor power factor on the high-voltage side of the transformer. This technique is far more effective than conventional apparent current based schemes since the ASD normally operates close to unity power factor.

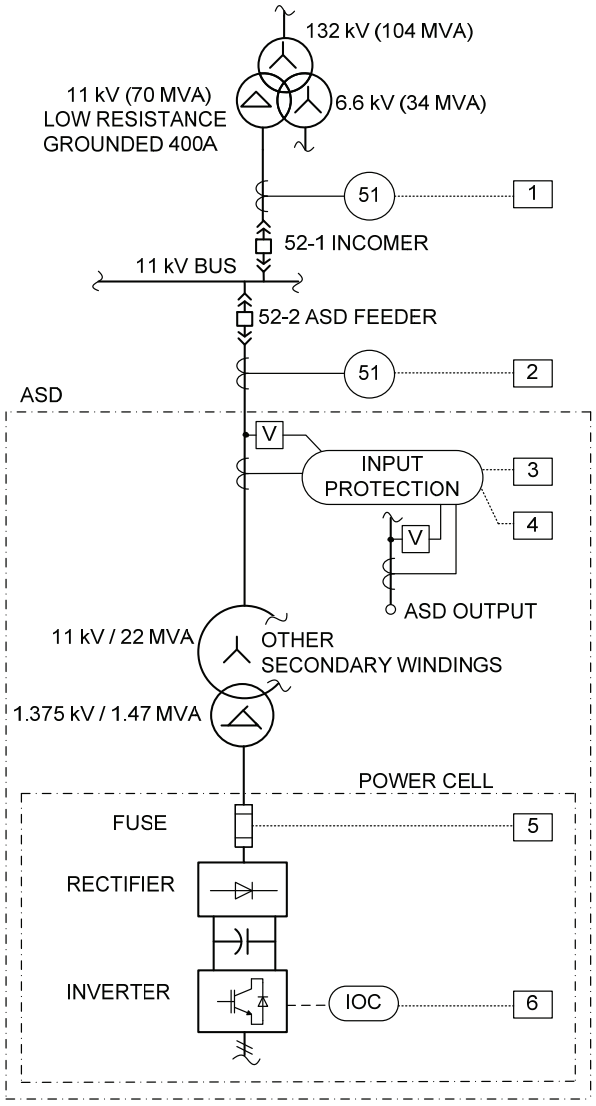

Fig. 6.21 Protection co-ordination single line diagram

Differential real power protection measures the differential real power between the ASD input and output and is therefore suitable to effectively detect high impedance/arcing faults (associated with additional losses). The overall sensing and tripping time depends on the fault severity, factory default settings and any additional time delay settings. The input protection was however set to alarm mode during the initial idle mode of operation (at the time of the ASD failure in October 2005).

These input protection functions are plotted in terms of current (referred to 11 kV) in Fig. 6.22 for analysis associated with the incident. The reactive power protection curve shows that the ASD Input protection would have taken 300 ms to send a trip signal, had the input protection been activated. On this basis, the overall trip time would have been 360 ms which includes 60 ms for the breaker and associated control. This is less than the 460 ms that it actually took the backup breaker to operate during the incident in October 2005. The ASD damage could have been reduced had the breaker operated in 360 ms instead of 460 ms.

B. ASD Over-current Protection

It is often overlooked but is critical to ensure ride through and availability of the ASD and to minimize process upsets. A summary of main points of the coordination curves of Fig. 6.22 is as follows:

- The new power cables installed between transformer secondary windings and the cells are adequately protected by the ASD internal protection.
- Adequate margins are shown between the ASD Input Protection (curves 3&4), feeder back-up protection (curve 2, 52-2) and the main switchgear incomer (curve 1, 52-1).
- The feeder back-up protection is set to ensure operation before the transformer thermal damage curve limits are reached. This back-up protection adequately functioned to protect the transformer during the event that took place during commissioning in October 2005.
- A short circuit fault (e.g. “maximum fault level transformer secondary” as shown in Fig. 6) in a power cell is sensed by both the Input Protection reactive power scheme (curve 3) and the cell fuse protection (curve 5). Proper coordination between them is vital. When a power cell fuse operates, the intent is that a faulty power cell is automatically bypassed without causing process interruption. In the event that the reactive power scheme is activated before the cell fuse it would initiate an ASD trip. Likewise, the Input Protection differential real power (curve 4) scheme must co-ordinate with the fuse curve to avoid an unwarranted ASD trip. Fig. 6 shows mis co-ordination (as found) in certain zones between the Input Protection and the fuse protection. In addition, it can be seen that the ASD Input Protection may create nuisance tripping when energizing the ASD transformer due to inrush current. The

inrush problem was addressed by disabling the Input Protection for 0.5s when energizing the ASD transformer. In addition to correct fuse co-ordination with upstream devices, it is important to design the system such that nuisance fuse trips will not occur based on external disturbances as outlined in [6.18].

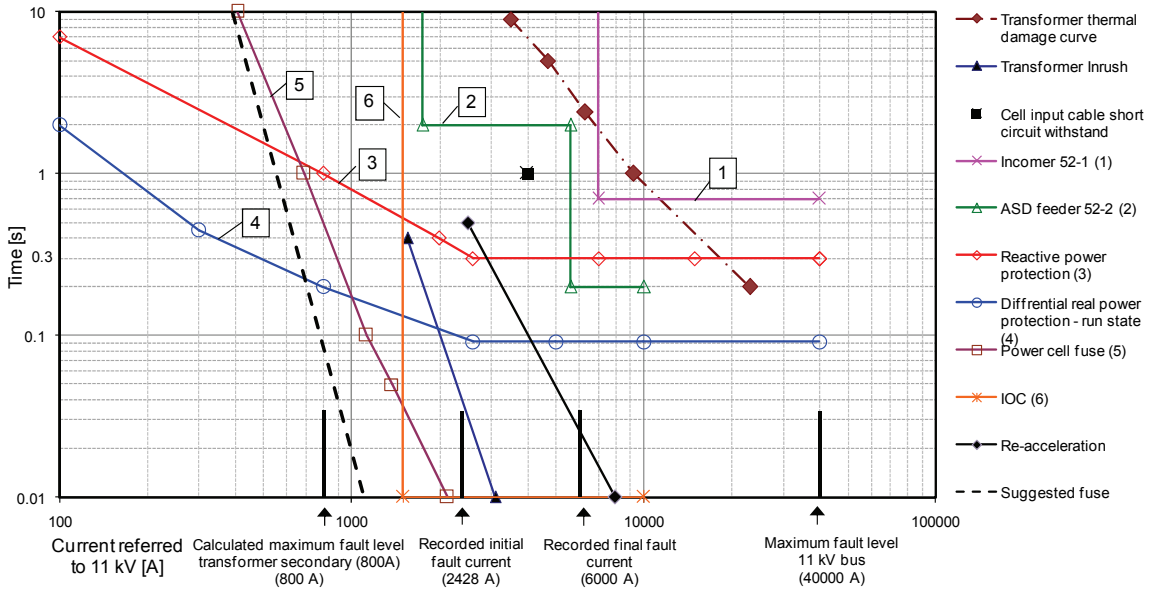

Fig. 6.22 Protection co-ordination curves for ASD - all currents shown are referred to 11 kV

C. Ground Fault Protection

The 11 kV supply system is a low resistance grounding system having a neutral grounding compensator & resistor to limit the ground fault current to 400A. The stator winding insulation of the synchronous motors has been designed for this grounding system with conventional trip schemes when directly operated on the 50 Hz bus supply. The ASD transformer delta based secondary windings and the ASD output are both ungrounded. A ground fault on the ASD output is normally detected by a voltage displacement and is only alarmed. For this ASD application, a trip command was selected because the motor phase to ground insulation is not rated for continuous operation at line-line voltages which will be experienced during a ground fault.

Due to the critical nature of this application, the motor insulation system should have been designed to continuously withstand line to line voltage till the ground fault is addressed. Pure soft started motors do not need an increased insulation specification since the operation with the ASD is of short duration.

The low voltage 525 V MCC supply to the ASD is of high resistance grounding (HRG) system at 5A. The ASD distributes the power to auxiliary loads including the motors for the cooling water pumps and air-cooled heat exchanger fans.

The HRG system is normally selected to limit damage associated with ground faults as well as to maintain process continuity. For this specific application it was decided to trip on a HRG fault because of the redundancy in the system (normal and emergency 525 V supply feeders). However, for this application, low voltage ground faults in the ASD has resulted in the 525 V feeder circuit to trip, initiating transfer to the emergency power which also tripped on ground fault resulting in an ASD trip. A review of the ground protection showed that the ASD low voltage supply scheme is incompatible with the HRG system (no dedicated HRG fault detection on individual internal ASD auxiliary feeders). To address this problem, isolation transformers (delta-star, with star winding solidly grounded) in the normal and emergency feeders were installed to ensure that internal ASD feeders to auxiliary circuits clear ground faults effectively (i.e. avoiding the 525 V normal feeder, emergency feeder and ASD trip).

This is similar to a retrofit application for a UPS system that was not designed for HRG as discussed in detail in [6.14]. For future ASD applications, it is recommended that the internal ASD low voltage circuits be designed to be compatible with HRG system for increased reliability and to avoid adding an isolating transformer.

D. Excitation System Considerations for Ride-Through

Excitation systems (diagram shown in Fig. 5.4) for adjustable speed driven SMs are not necessarily designed optimally for on-line operation. Furthermore unacceptable sensitivity to voltage dips may be applicable. A detailed analysis is beyond the scope of this section

but the intention is to create awareness of the importance of the excitation system which can compromise ride-through performance. This section therefore provides a high level description of how the excitation system can affect ride-through and availability by means of selected case examples.

1)Exciter rotor diode fault supervision: One method of detecting a diode fault is based on the detection of impedance rate of change outside acceptable limits [6.12]. This impedance is measured in the excitation panel with the potential transformers and current transformers and associated transducers shown in Fig. 2.6. The impedance change does not only occur due to a diode fault but also during a voltage dip condition since the flux in the machine does not change instantaneously while the voltage does. It is therefore essential to include the correct ranges or time delays based on the stability study results. A nuisance trip has once occurred with the NPP SSASD PGC system directly after a voltage dip. Thereafter the necessary modifications have been made to stabilise the protection. A better alternative is to implement a scheme based on the detection of the ripple current which occurs with the failure of a diode.

2)Excitation Controller: It is possible that the power factor controller may act incorrectly during voltage dip conditions due to the temporary power factor change during and following the dip. This has in one case resulted in a trip of the MAC due to over current combined with under excitation. It is important to either override/stabilise the power factor with voltage control during the dip condition (implemented in case of the MAC) or to verify that the power factor control loop is slow enough.

3)Channel Redundancy: Excitation panels for critical applications may have redundant channels as shown in Fig. 2.6. This has proven to be very beneficial and the failure of channel component(s) have in a few cases avoided the trip of the process since on-line replacement of the faulty component was possible. Two modes of operation are offered by some manufacturers, parallel operation or standby operation. Normally one channel is fed from the emergency/critical supply. Under deep and prolonged voltage dip conditions, the critical factory generation may be islanded resulting in a frequency drift between the two supplies. If the operation mode is selected to run in parallel circulating currents due to the frequency difference will occur, resulting in reduced excitation current to the machine and

eventually a trip (e.g. reactive power trip). Applications in this configuration should therefore only be used in the standby configuration.

4)Rotor pulse unit: Fig. 5.4. illustrates a rotor pulse unit (alternatively a crow bar circuit is used) used to short out the rotor during out-of-step conditions for overvoltage protection of the rotor and its components. During voltage dip conditions, this unit may fire unnecessarily if the setting is too low. This may in turn result in temporary induction motor operation and intermittent firing of the pulse unit which was associated in two cases with excessive vibration levels of the MAC (and eventual shutdown of the machines and failure of the pulse unit). The pulse unit was replaced and the setting has been increased and stable operation was achieved even for deeper voltage dips than in the previous two events.

5)Other aspects and protection: Some of the protection functions normally encountered in the ASD or DOL protection relays may be duplicated in the excitation panel. It is essential to review all settings as part of the dip proofing and stability studies.

6.8 SUCCESS OF MODIFICATION AND FURTHER OPERATING EXPERIENCE

Since January 2006 when the ASD system was fully placed in service, the overall performance has been very good in spite of some problems. The drive is designed as described in chapter 2 in more detail so that upon loss of one power cell, the ASD will successfully bypass the faulty cell without causing it to shutdown. If the ASD suffers a second power cell failure, the ASD, under this condition, would not be capable of producing the required output voltage to achieve motor synchronization. Therefore, the operation procedure for this ASD is such that following the loss of first power cell the operator immediately initiates a motor transfer to 50 Hz bypass mode and the ASD is shutdown to replace the faulty power cell.

The ASD has experienced two failures since it has been placed in service. In the first instance, the ASD suffered a cell malfunction (IGBT fault). The ASD performed as

designed and the cell was successfully bypassed. The cell bypass condition was alarmed. The operator then manually issued a command for the ASD to accelerate the motor, synchronize it with the supply bus frequency and to transfer it to the 50 Hz supply. The ASD was then de-energized (52-2 opened) and the faulty power cell was replaced with a spare. The ASD was re-energized and placed in service. The ASD re-synchronized its output with the running synchronous motor and re-transferred it to ASD mode. This event did not cause any process interruption.

In the second event, a cell was damaged but the fault/arcing was contained within the cell due to ASD design modification improvement introduced in October 2005. However, the differential real power protection did trip the drive since the power cell fuse was not co-ordinated with the input protection as explained in the previous section. The subsequent investigation revealed that all remaining 14 power cells were intact.

6.9 FURTHER ENHANCEMENT

An ASD must not pose danger (outside the limits specified in standards) to personnel when an arc fault occurs, i.e. the energy must be limited. This can be done by ensuring fast enough fault clearance in accordance with [6.11] or by providing a design that is internally arc resistant. In the event of the case study the energy was within acceptable limits, however the damage to the ASD was significant. If this event had occurred during plant operation the downtime also would have been unacceptable due to the amount of repair work required. Light sensors are gaining popularity to detect arcing faults and to reduce fault clearance time and to limit the associated energy and damage [6.15]. These sensors should be considered throughout the ASD, e.g. the transformer section, busbar/cable sections and in the cells. In the case of a faulty cell, fast fault detection is possible which can initiate the drive reconfiguration process and associated bypass of the faulty cell.

6.10 CONCLUSIONS AND RECOMMENDATIONS

Line fed and ASD fed SMs driving large compressor loads can survive system faults and voltage dips without additional compensation or energy storage as proven by case studies. It is recommended to verify the ride-through capability first by simulation before

considering additional equipment to enhance ride through. It is essential to optimise protection settings so that ride through is not compromised while still protecting the equipment. ASD fed SMs have far better survivability characteristics than line fed SMs and can even survive faults cleared by back-up protection. In weak supply systems with frequent longer duration dips the ride-through features of the ASD may strengthen the business case when deciding on purchasing an ASD.

The maximum transfer angle (e.g. with fast bus transfers) may be limited by the allowable busbar voltage drop as the governing criterion. A simplified method has been developed to determine the maximum angle allowed and to verify whether a system design is within acceptable limits. The busbar voltage drop can be improved when the direct-on-line machines are re-accelerated first followed by the ASD machine re-acceleration. SMs can ride-through certain ASD faults that do not result in an overall trip (e.g. the cell bypass fault tolerant scheme).

Correct system design, protection settings and transfer angle settings are important to limit current and torques within system and drive string (load) capabilities while ensuring successful ride-through. In critical applications a “flying start” ASD back-up or re-acceleration should be investigated for possible process ride through after an ASD single point of failure has occurred. It has been shown that the process may be saved by re-acceleration following a transfer in some cases by means of delayed in phase transfers. In many cases below speeds of 95 % a transfer will however not be successful. A suggestion for future research is to investigate machine re-acceleration in further detail by addressing various loading conditions, machine design parameters (and sized) and a comparison of induction motor versus synchronous motor reacceleration.

A new ASD system case study suffered a failure during commissioning in October 2005. The investigation revealed that the problem was caused by a minute cooling water leak that caused a power cell failure and escalated to bus fault and ASD shutdown. Several improvements were implemented to the ASD design to avoid recurrence. The bare bus connection between the fifteen power cells was replaced with cables and additional barriers added to avoid arcing between cells or between a power cell and the associated busbar. A

propagating arcing fault is therefore unlikely. No other water leak incident has taken place since the ASD was placed in service in January 2006.

The ASD Input Protection scheme underwent a thorough review to ensure proper coordination between various devices and increase drive availability. It should be noted that information related to ASD internal protection co-ordination is typically not readily available unless specifically asked for from the manufacturer. The findings of the project resulted in increased collaboration between the end user and the ASD manufacturer in enhancing the ASD protection.

Following the improvements that were introduced in late 2005, the ASD has suffered two failures that were associated with power cells. In the first case, the ASD functioned as designed and bypassed the faulty cell and the ASD remained in service with no process interruption. In the second case, a cell failure occurred causing the ASD to trip but the damage was contained within the cell. It is believed that the design modification and protection enhancements carried out following the incident of October 2005 have considerably helped to mitigate the impact of subsequent two events. An ASD trip in the second event could have been avoided if proper coordination between the cell fuse and ASD input protection was possible.

It is important to ensure that the plant high voltage and low voltage grounding system is compatible with the ASD grounding. In this case, the plant has high resistance grounding and was incompatible with low voltage ASD supply that resulted in tripping on ground fault. A delta/star with solidly grounded neutral was installed to address this problem.

The IEC 61800-4, IEEE 1566 -2006 [6.16] and ANSI/IEEE Std C37.96-1988 [6.17] standards when revised should include a section covering ASD internal protection coordination with upstream devices and ASD grounding system compatibility with existing plant high and low voltage grounding. Furthermore a section on ride-through methods and principles should be included.

6.11 REFERENCES

[6.1] *General Electrical Specification*, Sasol Specification, SP-60-1, Rev. 4, 2004

[6.2] A. P. Gabba, J. D. Hill, "Make automatic power source transfers a success for your plant," *IEEE Trans. on Ind. Appl*., vol. 37. no. 2, pp. 423-433, Mar/Apr. 2001.

[6.3] *Principles of Electrical Machines and Power Electronics*, John Wiley & Sons, NY, 1989

[6.4] J. Rama, D. Eaton, P. Hammond, "Targeting Five years of AFD Operation Without Interruption", in *Proc. IEEE Petroleum and Chemical Industry Committee (PCIC)*, 2001, pp. 91-99.

[6.5] S. Khomfoi, L. M. Tolbert, "Fault Diagnosis and Reconfiguration for Multilevel, Inverter Drive Using AI-Based Techniques", *IEEE Trans. Ind. Electron.*, vol. 54, no. 6, pp. 2954-2967, Dec 2007

[6.6] P. Lezana, R. Aguilera, J. Rodríguez, "Fault Detection on Multicell Converter Based on Output Voltage Frequency Analysis," *IEEE Trans. Ind. Electron.*, vol. 56, no. 6, pp. 2275-2283, June 2009

[6.7] F. Carlsson, C. Sadarangani, "Behavior of Synchronous Machines Subjected to Voltage Sags of Type A, B and E," *EPE Journal*, Vol. 15, no. 4, pp. 1-8, Dec 2005

[6.8] F. Carlsson, "On Impacts and Ride-through of Voltage Sags Exposing Line-operated AC-Machines and Metal Processes," Doctoral Dissertation, Royal Institute of Technology, 2003

[6.9] D. L. Hornak, D.W. Zipse, "Automated Bus Transfer Control for Critical Industrial Processes," *IEEE Trans. on Ind. Appl.*, vol. 27, no. 5, pp. 862-871, Sept./Oct. 1991

[6.10] F. Endrejat, R.A. Hanna, J. Shultz, "Ensuring availability of a large adjustable speed drive for process gas compressor application rated 11 kV, 15.5 MW (20778 hp)," *IEEE Trans. on Ind. Applicat.*, vol. 46, no.5, Sep./Oct. 2010, doi: 10.1109/TIA.2010.2058082

[6.11] *IEEE Guide for Performing Arc-flash Hazard Calculation*, IEEE Standard 1584, 2002.

[6.12] F. Endrejat, B. van Blerk, and G. Vignolo, ‘‘Experience with new large adjustable speed drive technology for multiple synchronous motors,’’ in *Proc. Petroleum and Chemical Industry Committee (PCIC) Europe*, 2008, Weimar, Germany, pp. 196–205.

[6.13] D. Sweeting, “Arcing faults in electrical equipment ,“ in *Proc. IEEE Petroleum and Chemical Industry Committee (PCIC),* 2009,Anaheim, CA, pp. 1-11.

[6.14] D. Murray, J. Dickin, R. A. Hanna, T. Morin, "High Resistance Grounding - Avoiding Unnecessary Pitfalls," *IEEE Trans. on Ind. Appl*., vol. 45. no. 3, pp. 1146-1154, May/Jun. 2009.

[6.15] J.A. Kay, J. Arvola, L. Kumpulainen, “Protection at the speed of light: Arc-flash protection combining arc flash sensing and arc-resistant technologies “,in *Proc. IEEE PCIC, 2009, pp.* 367-373.

[6.16] *Standard for Performance of Adjustable Speed AC Drives Rated 375 KW and Larger,* IEEE Standard 1566, 2006.

[6.17] *IEEE Guide for AC Motor Protection* , ANSI/IEEE Std C37.96, 1988

[6.18] JM Van Coller, AA Beutel, N Maphalala, F Endrejat, J Msimango, “Failure of LV ASD Supply-side Fuses due to MV Motor Fuse Operation”, *IEEE International Conference on Industrial Technology*, India, December 2006

7 CONCLUSIONS AND RECOMMENDATIONS

This chapter provides conclusions and recommendations regarding the research objectives. This thesis aims to answer questions related to the application of large medium voltage drives in the petrochemical industry. The findings and suggestions for further research are summarized in this chapter.

7.1 CONCLUSIONS ON OBJECTIVES

7.1.1 Main Objective

The main objective to contribute to knowledge towards successful application of large MV ASDs in petrochemical industry has been met by meeting the specific objectives as described below supported by first of its kind case studies. The results of the research allow new MV ASD technology to be applied economically with a lower risk level to address process requirements and energy saving opportunities for large drive systems.

7.1.2 Specific Objectives

A. Introduction and Literature Study

A comprehensive literature study was conducted which illustrates limitations of the present MV drive technologies for the petrochemical industry. It is shown that the VSI-CHB technology may potentially be utilised for higher application voltages and power ratings with adjustable speed benefits that were previously not available for large compressor applications. Several benefits of applying the SSASD concept for high power synchronous motors with the VSI-CHB technology are described and motivated. Potential benefits in

terms of availability, energy savings, hazardous areas, capital cost of equipment and switching surge overvoltages were outlined. Several problem areas have however been identified which need to be addressed before the technology can effectively be applied. Challenges for successful application and key research questions supported by the literature study were outlined with associated conclusions provided below.

B. Technology Feasibility

It was shown that new technology VSI CHB ASDs can compete with conventional LCIs regarding efficiency with motors rated ≥ 11 kV. The CHB technology is also superior in terms of output waveforms, power factor and ease of installation regarding external cabling.

Very large systems in excess of approximately 25 MW for new projects may be more efficient with LCI systems which also have a proven reliability. LCIs may also be more beneficial for pure soft starting of very large motors (the negative aspects are not as applicable due to short duration operation, air cooled systems can be used and the benefit from proven reliability is obtained). LCIs may also still be recommended for very large applications especially where the risk of implementing new technology can not be mitigated.

VSIs are more suitable for other applications especially with existing/standard motors rated ≥ 11 kV. System loss reduction opportunities have been investigated and it is shown that the selection of the motor (for new projects) has the most significant impact on drive system efficiency. Case studies have shown that significant energy savings are possible for both existing and new projects with large compressor applications. The SSASD concept and associated synchronisation schemes were proven to be successful with synchronous machines. It was shown that the SSASD scheme can be significantly more cost effective than conventional schemes with the added benefit of increased availability.

The increased electricity tariffs and new technology that can address ≥ 11 kV applications make energy saving projects for large applications now more viable than ever before.

Additional outlined technical benefits associated with medium voltage adjustable speed operation increases the feasibility of energy savings projects even further. Overvoltage concerns, ride-through performance and availability are fields identified which require dedicated research (focus area of this thesis) to verify the technical feasibility of the technology.

C. Resonance Overvoltages and Long Cable Lengths with VSI-CHB Systems

Numerical simulation results confirmed by field test results show that unacceptable overvoltage effects can in fact occur in medium voltage (11-16 kV) multilevel drive systems which can ultimately lead to premature motor failure and associated production losses. Motor voltages associated with high frequency travelling waves may be a concern in some cases with larger voltage steps associated with higher voltage output drives (in systems without a synchronization reactor). Resonance overvoltages can be far more severe than travelling wave overvoltages. Simulation and subsequent test results show that the resonance effects can be minimized with the implementation of an optimal carrier frequency. The effect of model complexity and parameter variation with frequency has been investigated showing simplification opportunities. A simplified analytical model was therefore developed to show potential worst case resonance scenarios. A simplified calculation method was developed which can be used to conveniently determine suitable carrier frequencies to avoid resonance.

High power applications are becoming more in demand, are mostly process critical and a bypass configuration is often advised. Multiple motor applications are often encountered. A synchronisation reactor is typically used in these systems and the overvoltage problem can effectively be addressed by the selection of the correct carrier frequency to avoid resonances. The reactor also eliminates the possibility of travelling wave overvoltages at the motor terminals. Existing and new motors with a high rated voltage and with normal insulation can therefore now benefit from large adjustable speed drive technology.

D. Generalized Design Approach for VSI and LCI Systems with Long Cable Lengths

There is a need for both VSI-CHB and LCI technologies for large drive systems with long cable distances (e.g. several hundred meters) in the petrochemical industry. Resonance overvoltage conditions can occur in both systems with long cables distances. It has been shown how to determine when inverter harmonics will excite resonance overvoltages for a wide range of cable lengths and power ratings. Strategies to determine the optimal carrier frequency for VSI-CHB systems are proposed and acceptance criteria to ensure that the machine and converter will function safely and effectively are provided. Overvoltages associated with smaller motor lower voltage VSI-CHB drive applications (e.g. 6.6 kV) are unlikely to be associated with unacceptable travelling wave or resonance overvolatges. It has been shown that potential resonance becomes more likely with larger drive systems with output reactors/transformers.

A design approach flow chart was developed to determine when revised modulation strategies (optimal carrier frequency/selective harmonic elimination) or a filter is required for VSI and LCI systems respectively. Ultimately it is shown that effective, safe, reliable and low cost solutions exist to extend the capabilities and application of VSI and LCI systems.

E. Ride-through

The theory for successful ride-through addressing internal and external disturbances was provided for both ASD and on-line operation. Furthermore general machine models were provided that can be used to determine the theoretical ride-through capability. It is also important to achieve DOL ride-through in SSASD schemes without exceeding system design conditions during transients. The overall ride-through modelling, a simplified general strategy and associated analytical equations which addresses constraints on the re-closing angle are presented. The importance of correct protection co-ordination and principles is highlighted.

F. Ride-through and Availability Case Studies

Line fed and ASD fed SMs driving large compressor loads can survive system faults and voltage dips without additional compensation or energy storage as proven by case studies. It is recommended to verify the ride-through capability first by simulation before considering additional equipment to enhance ride through. ASD fed SMs have far better survivability characteristics than line fed SMs and can even survive faults cleared by back-up protection. Inertia-ride through is a suitable approach for MV ASD petrochemical drives although other more cost intensive methods have been proposed in literature. In weak supply systems with frequent longer duration dips, the ride-through features of the ASD may strengthen the business case when deciding on purchasing an ASD.

The maximum transfer angle (e.g. with fast bus transfers) may be limited by the allowable busbar voltage drop as the governing criterion. The simplified method was successfully (verified by simulation) used as an initial tool to determine the maximum angle allowed and to verify whether a system design is within acceptable limits. The busbar voltage drop can be improved when the direct on line machines are re-accelerated first followed by the ASD machine re-acceleration.

Correct system design, protection settings and transfer angle settings are important to limit current and torques within system and drive string (load) capabilities while ensuring successful ride-through. In critical applications a “flying start” ASD back-up or re-acceleration should was investigated for possible process ride through after an ASD single point of failure has occurred. It has been shown that the process may be saved by re-acceleration following a transfer in some cases by means of delayed-in-phase transfers. In many cases below speeds of 95 % a transfer will however not be successful.

The SSASD and machine may be perfectly capable to ride-through voltage dips and disturbances but it has been shown that traditional excitation system designs may be too sensitive for voltage dip conditions resulting in unnecessary trips. Stable rotor diode protection, redundancy operation in excitation channels, rotor pulse unit/crow bar protection all require careful attention in dip proofing studies to ensure ride-through.

SMs can successfully ride through certain ASD faults that do not result in an overall trip (e.g. the cell bypass fault tolerant scheme). A new ASD system case study was however presented where a cell failure occurred during commissioning and ride-through could not be achieved. The investigation revealed that the problem was caused by a minute cooling water leak that caused the power cell failure and escalated to bus fault and ASD shutdown. Several improvements were implemented to the ASD design to avoid recurrence. The bare bus connection between the fifteen power cells was replaced with cables and additional barriers added to avoid arcing between cells or between a power cell and the associated busbar.

The ASD Input Protection scheme underwent a thorough review to ensure proper coordination between various devices and increase drive availability.

Following the improvements that were introduced, the ASD has suffered two failures that were associated with power cells. In the first case, the ASD functioned as designed and bypassed the faulty cell and the ASD remained in service with no process interruption. In the second case, a cell failure occurred causing the ASD to trip but the damage was contained within the cell. The design modification and protection enhancements carried out have considerably helped to mitigate the impact of subsequent two events. An ASD trip in the second event could have been avoided if proper coordination between the cell fuse and ASD input protection was possible.

Important improvements were described for high impedance earthing systems to ensure that the plant high voltage and low voltage grounding system is compatible with the ASD grounding to ensure ride through during ground faults.

7.2 RECOMMENDATIONS

International standards (e.g. IEC 61800-4, IEC 60034-18-42 , IEEE 1566 and ANSI/IEEE Std C37.96) when revised should include sections covering resonance overvoltages, ride-through requirements for SSASD systems with synchronous machines (including fast

transfer and synchronisation requirements), revised hazardous area requirements, ASD internal protection coordination with upstream devices and ASD grounding system compatibility with existing plant high and low voltage grounding.

Break-before-make transfers (no reactor required) or selective harmonic elimination should be investigated as alternatives to the carrier frequency change methods in applications requiring an unacceptably high carrier frequency (e.g. where increased converter losses or control processor performance can not be accommodated).

Break-before-make transfers can safely be achieved from a machine perspective, eliminating the need for a synchronization reactor used in make-before-break transfers.
The benefits are increased efficiency, reliability, availability and easier control to meet the more relaxed synchronization window (wider angle). It is therefore recommended to investigate the application of break-before-make transfers and associated ASD design, especially for new projects where motors can be specified to accommodate the VSI output waveform characteristics considering travelling wave effects (resonance is only likely for very long cable lengths).

Surge counter test equipment used to detect overvoltage problems in drives is not effective to detect resonance overvoltage conditions. It is recommended to develop test equipment to conveniently detect resonance overvoltages. In the mean time, it is recommended to perform oscilloscope tests in addition to surge counter tests.

The VSI-CHB topology allows potential further development for future higher output voltages that can be ideally matched with new technology higher voltage machines (already available) for very large applications. The use of even higher voltage IGBTs in the multilevel structure should be investigated for the applications to reduce component counts to acceptable levels.

In weak supply systems with frequent longer duration dips the ride-through features of the ASD should be incorporated in the business case when deciding on purchasing an ASD.

Arc detection principles should be considered in power cell and ASD designs especially where bare copper busbars cannot be replaced with insulated/segregated busbars or cable word. Spreading arcing faults can then be minimised and cell bypass initiations can be triggered for cell faults (especially the front end section).

A suggestion for future research is to investigate machine re-acceleration following ASD single point of failures in further detail. Aspects that should be addressed include various loading conditions, minimum speeds for successful re-acceleration, machine design and control parameters, machine sizes and a comparison of induction motor versus synchronous motor reacceleration.

The VSI-CHB technology is also being considered for wider application in the renewable energy and distributed generation field and the findings of this research could be expanded accordingly.

The sensitivity of excitation panels (in SSASD systems) to voltage dips justifies further research in this field to provide detailed design and protection recommendations.

It is recommended to perform further research to further develop alternative VSI and CSI PWM technologies for application at higher rated voltages to compete with the VSI-CHB technology. Similar research than performed in this thesis should also be conducted for these technologies regarding ride-through, availability, hazardous areas and overvoltages for eventual comparison and potential high power, high voltage application in the petrochemical industry.

The importance of performing comprehensive research on the application of new large MV ASDs for synchronous machines in actual petrochemical site environments has been shown. Many of the findings listed above are essential for successful operation but these are difficult to address with conventional research and development before ASDs enter the market. It is therefore suggested to incorporate the lessons learned early in the research and development stages of new MV drive systems.

Ultimately it has been shown that new VSI-CHB technology should be considered in certain conventional LCI adjustable speed applications areas for new projects. Furthermore energy saving opportunities associated with existing higher output voltage motor applications can now be explored with VSI-CHB technology and the SSASD scheme (previously not possible with LCI technology).

Appendix A

AUTHOR'S PUBLICATIONS

Note: All publications except for those in (brackets) are directly related to this thesis.

A.1 JOURNALS

[1] F. Endrejat, R.A. Hanna, J. Shultz, "Ensuring availability of a large adjustable speed drive for process gas compressor application rated 11 kV, 15.5 MW (20778 hp)," *IEEE Trans. on Ind. Applicat.*, vol. 46, no.5, pp. 1843 - 1849 Sep./Oct. 2010

[2] F. Endrejat, P. Pillay, "Overvoltages in Medium Voltage Multilevel Drive Systems," *IEEE Trans. on Ind. Applicat.,* vol. 45, no. 4, pp. 1199-1209, Jul./Aug. 2009

[3] F. Endrejat, P. Pillay, "The soft starters - adjustable speed systems for multiple MW Rated Motors," *IEEE Ind. Appl. Mag.,* vol.14*,* no.6, pp. 27-37*,* Nov./Dec. 2008.

[4] J. Auret, F. Endrejat, B.A.R. Machado, "Certification of Explosion Protected Motors fed by Variable Speed Drives – Proposed Requirements," *Energize -The Independent Power and Energy Journal of Southern Africa*, Jul. 2005, pp. 60-66

[5] (F. Endrejat, G.J. Delport, "Modeling of a Fin-fan Cooler System with Variable Speed Drives", *The Transactions of the South African Institute of Electrical Engineers*, Vol. 89 No 2, pp. 56-63, June 1998)

[6] Planned for submission: F. Endrejat, P. Pillay, "Ride-through of medium voltage synchronous machine compressor drives," *IEEE Trans. on Ind. Applicat.*, largely based on [] and further related work in Chapters 5 and 6.

A.2 SPECIFICATIONS/STANDARDS

[7] F. Endrejat, *Medium Voltage AC Adjustable Speed Drive Systems*, Sasol Specification, SP-60-55, Rev. 2, 2009.

[8] (F. Endrejat, *Low Voltage AC Adjustable Speed Drive Systems*, Sasol Specification, SP-60-34, Rev. 3, 2010.)

A.3 HANDBOOKS

[9] F. Endrejat, B. van Blerk, and G. Vignolo, ''Industrial experience: a case study,'' in *A Current Perspective on Motors and Drives*, Chapter 9, Crown Publications, South Africa, 2010.

A.4 CONFERENCES AND OTHER PUBLICATIONS

Papers in IEEE Sponsored Peer Reviewed Conference Proceedings

[10] F. Endrejat, B. van Blerk, ''Large medium voltage drives – efficiency, energy savings and availability,'' in *Proc. Petroleum and Chemical Industry Committee (PCIC) Europe*, Oslo, Norway, 2010, pp. 86-93.

[11] F. Endrejat, P. Pillay, "Ride-through of Medium Voltage Synchronous Machine Compressor Drives," in *IEEE International Electrical Machines and Drives Conference (IEMDC),* Miami, FL, 2009, pp. 909-915.

[12] F. Endrejat, P. Burmeister, P. Pillay "Large adjustable speed and soft-started drives with long cable lengths", in *Proc. Petroleum and Chemical Industry Committee (PCIC) Europe,* Barcelona, Spain, 2009, pp.153-162

[13] F. Endrejat, R. Hanna, J. Shultz, "Ensuring availability of a large adjustable speed drive for process gas compressor application rated 11 kV, 15.5 MW (20778 hp)," in *Proc. IEEE Petroleum and Chemical Industry Committee (PCIC),* Anaheim, CA, 2009, pp. 133-139.

[14] F. Endrejat, B. van Blerk, and G. Vignolo, ''Experience with new large adjustable speed drive technology for multiple synchronous motors,'' in *Proc. Petroleum and Chemical Industry Committee (PCIC) Europe*, 2008, Weimar, Germany, pp. 196–205.

[15] F. Endrejat, P. Pillay, "Resonance Overvoltages in Medium Voltage Multilevel Drive System," in *IEEE International Electrical Machines and Drives Conf.*, Antalya, Turkey, 2007, pp 736-741.

[16] (JM Van Coller, AA Beutel, N Maphalala, F Endrejat, J Msimango, "Failure of LV ASD Supply-side Fuses due to MV Motor Fuse Operation", *IEEE International Conf. on Industrial Technology*, India, December 2006)

[17] F. Endrejat, P. Pillay, "Soft start/adjustable speed systems for multiple MW rated motors," in *Proc. IEEE Petroleum and Chemical Industry Committee (PCIC)*, Philadelphia, PA, 2006, pp. 349-358.

[18] (F. Endrejat, H.R. van Niekerk, G.J. Delport, "Energy Efficiency and Performance Considerations of Variable Frequency Drives for Air-cooled Heat Exchangers*", IEEE International Symposium on Industrial Electronics*, 1998, pp. 312-316)

Papers in Peer Reviewed Conference Proceedings (previously not IEEE sponsored but now also IEEE sponsored)

[19] (F. Endrejat, J. Piorkowski, "Multiple Large Motor Solid State Soft Start, Control and Communication System", *Symposium on Power Electronics, Electrical Drives, Automation and Motion,* Italy, Capri, 2004, paper no. D134)

[20] (F. Endrejat, G.H. Müller, "Effects of Modern High Efficiency Motors on Low Voltage Networks", *International Conference on Electrical Machines*, Brugge, Belgium, 2002, paper no. 312)

Other Publications

[21] F. Endrejat, B. van Blerk, "Large Adjustable Speed Drives – Efficiency, Energy Savings and Availability" *LHM Rotating Machines Conference*, Sun City, July 2008

[22] F. Endrejat, "Power Drive Systems used in Potentially Explosive Atmospheres – Factors to consider", *South African Flame Proof Association Symposium*, 19 July 2007

[23] (F. Endrejat, H.R. van Niekerk, G.J. Delport, "The Feasibility of Variable Speed Drives for Air-cooled Heat Exchangers with Respect to Energy Consumption and Performance", *Proceedings of the Seventh Southern African Universities Power Engineering Conference*, 1998, pp. 187- 190.)

Masters degree

[24] (F. Endrejat, *"Induction Motor Modelling for Efficient Variable Frequency Operation and Industrial Application"*. Masters Degree Dissertation, University of Pretoria, 1999)

Appendix B

SIMULATION MODELS

B.1 INTRODUCTION

The simulation models shown are built in MATLAB Simulink with SymPowerSystems models (R2008a)

B.2 OVERVOLTAGE MODEL WITH VSI-CHB SYSTEM

The simulation model is shown in Fig. B.1 and used for selected simulation studies in Chapter 3 and 4.

B.3 RIDE-THROUGH MODEL

The simulation model is shown in Fig. B.2 and used for selected simulation studies in Chapter 6.

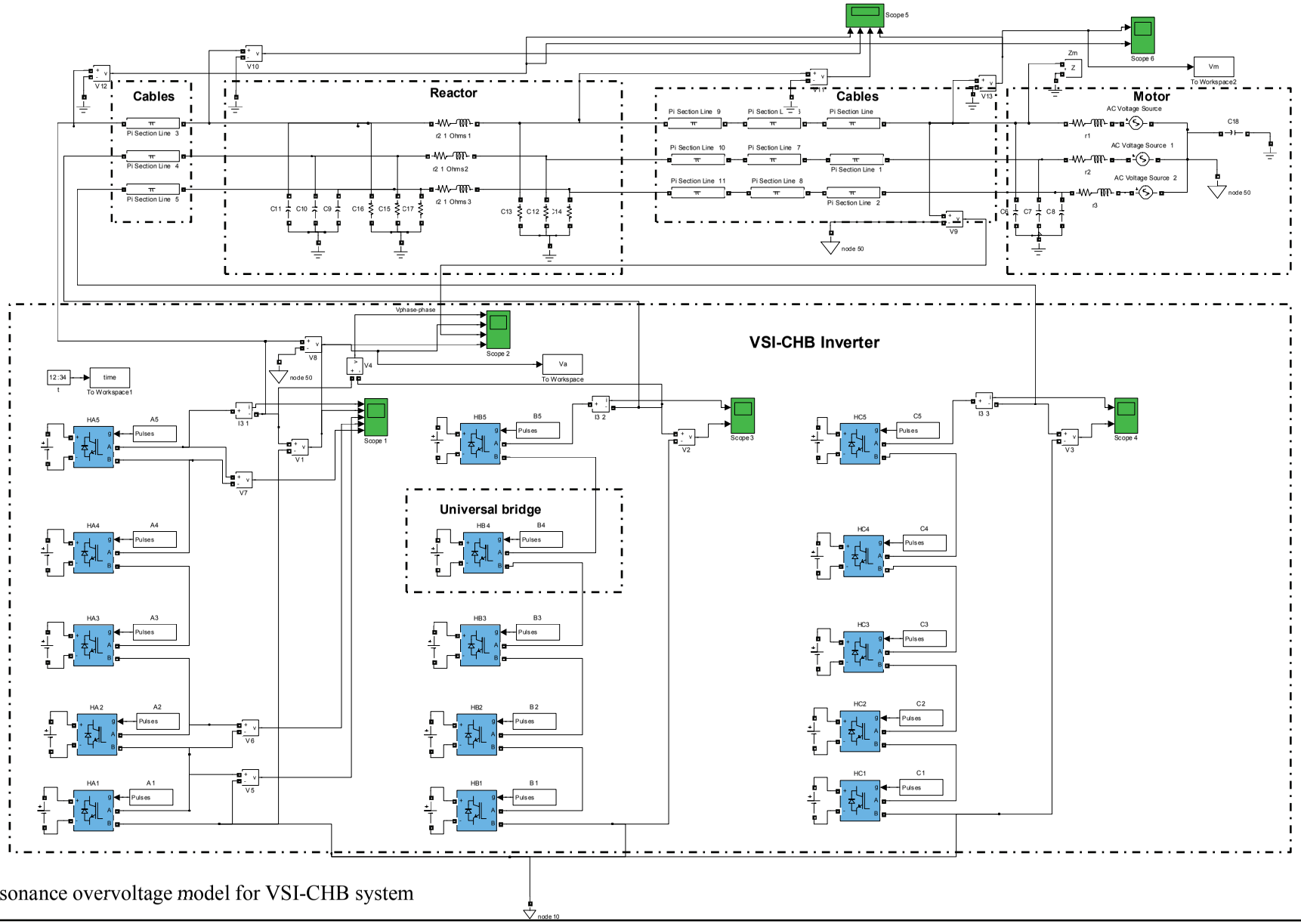

Fig B.1 Resonance overvoltage model for VSI-CHB system

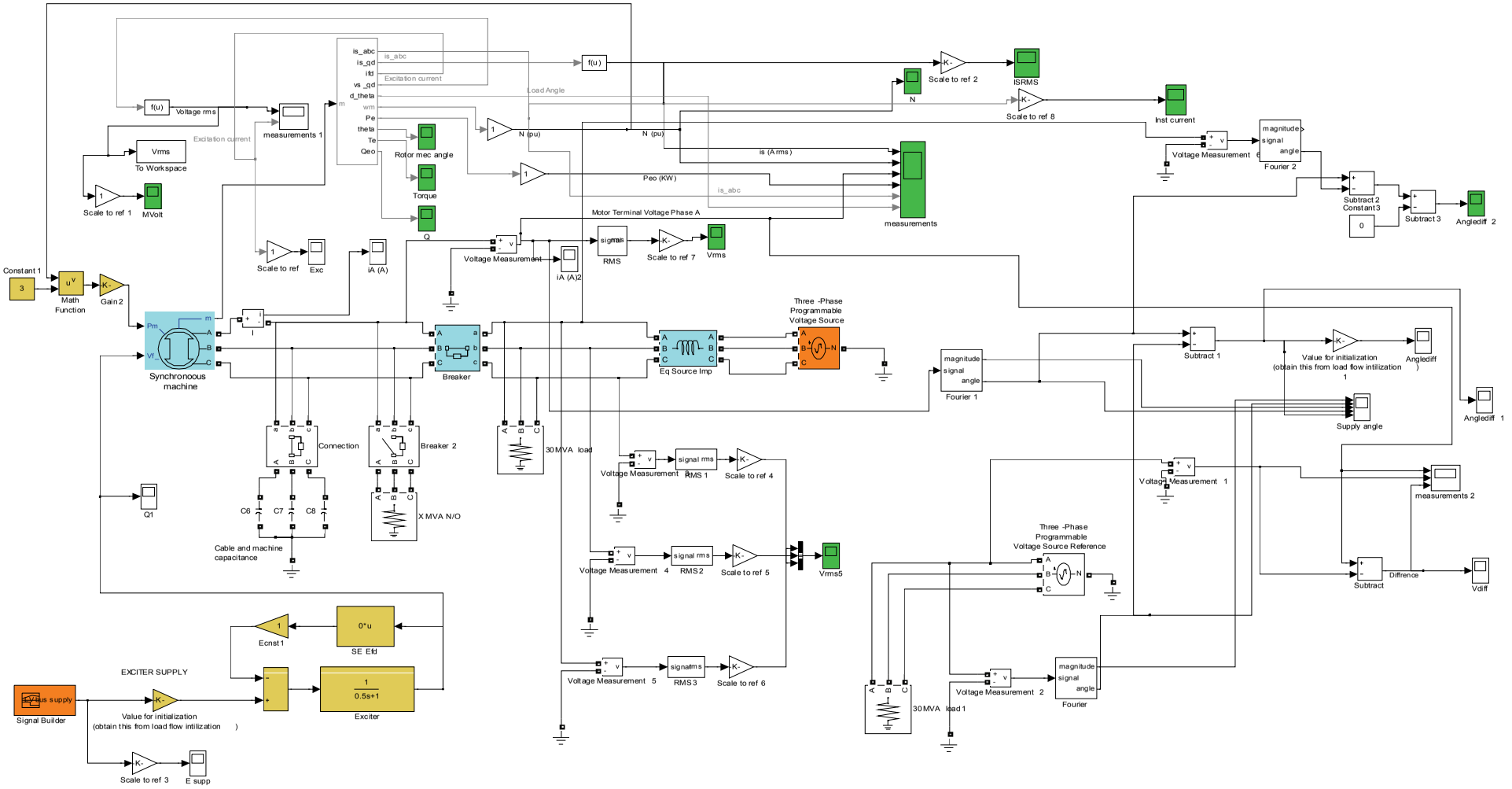

Fig B.2 Simplified SM ride through model (transfer/reclose/stability characteristics)

Appendix C

DATA

C.1 TEST EQUIPMENT SPECIFICATIONS

The test equipment used for the recordings in chapter 3 are given below.

The manufacturer specifications for the capacitor divider sensor are:

Bandwidth:	6 Hz to 8 MHz
Rated voltage:	16 kV
Hi-pot voltage ratings:	33 kV ACrms, 150kV DC, 150 kV impulse
Capacitance values:	80 pF (C1) & 20 nF (C2)
Divider ratio:	251 (C1+C2)/C1

(A correction factor of 1.1 was applied to match the results from the pre-tested resistive divider circuit, representing a conservative approach.) The manufacturer specifications for the recording equipment are:

Oscilloscope:	500 MHz
Surge counter:	Pulses with rise times ≤ 1.5μs

C.2 SIMULATION DATA AND CALCULATIONS FOR VSI-CHB CASE STUDIES

The simulation parameters used in Chapter 3 are as follows:

The XLPE cable data and calculations for the total equivalent parameters are given in Table C.2.I.

Table C.2.I

CABLE DATA AND CALCULATIONS

Cable Group (CG)	Number of single core cables per phase (n_c)	Cross Sectional Copper Area (mm^2)	Length of each single core cable (l) (m)	Resistance (R_{uc}) per single core cable unit length (Ω/km)	Inductance ($L_{uc} \cdot 10^3$) per single core cable unit length (mH/km)	Capacitance ($C_{uc} \cdot 10^9$) per single core cable (nF/km)	Total resistance for cable group ($R_{CG} = l \cdot R_{uc} \cdot 10^{-3}/n_c$) ($\Omega$)	Total inductance for cable group ($L_{CG} \cdot 10^{-3} = l \cdot L_{uc} \cdot 10^{-3}/n_c$) (mH)	Total capacitance for cable group ($C_{CG} \cdot 10^{-9} = l \cdot C_{uc} \cdot n_c \cdot 10^{-3}$) (nF)
1	2	500	22	0.051	0.299	454	0.00056	0.003291	19.976
2	3	240	70	0.098	0.325	345	0.00229	0.007576	72.45
3	2	240	23	0.098	0.325	345	0.00113	0.003734	15.87
4	4	500	550	0.051	0.299	454	0.00701	0.041142	998.8

Total values between reactor and motor terminals		
Resistance $R_{TC} = R_{CG2}+R_{CG3}+R_{CG4}$ (Ω)	Capacitance $C_{TC}=C_{CG2}+C_{CG3}+C_{CG4}$ (F)	Inductance $L_{TC}=L_{CG2}+L_{CG3}+L_{CG4}$ (H)
0.0104	$1.09 \cdot 10^{-6}$	$5.25 \cdot 10^{-5}$

The reactor value used is $L_{REACTOR}$=0.0024 H (reactor resistance is neglected).

17 MW motor parameters used are: L_M=0.0018 H, R_M=0.02 Ω and C_M=3.02*10^{-7} F (phase to earth). (The C_M value is from a manufacturer for the approximate machine size, this value is not as important since the total cable capacitance is significantly larger. The neutral to earth capacitance value has been assumed to be the same, which has a negligible effect on the simulation results).

The parameters used in Chapter 4 to evaluate the effect of cable length, output reactance and motor size on resonance frequency are given in Table C.2.II.

Table C.2.II

CABLE, MOTOR AND REACTOR PARAMETERS

Motor				Cable		
Rating MW	Type	Inductance mH	Capacitance nF	Description	Capacitance nF/km	Inductance mH/km
0.2	Induction	100.00	30	1x3c 25 mm^2	201	0.395
1	Induction	30.81	50	1x3c 95 mm^2	308	0.318
9.4	Induction	2.76	159	3x2x1cx 500 mm^2	454	0.299
17	Synchronous	1.80	302	3x4x1c 500 mm^2	454	0.299
23	Synchronous	3.30	350	3x4x1c 500 mm^2	454	0.299
36	Synchronous	2.42	450	3x5x1c 500 mm^2	454	0.299
55	Synchronous	0.86	500	3x7x1c 500 mm^2	454	0.299

Notes

3% reactor (with motor rating as base) used for all motors

Typical motor capacitances used (the cable capacitance, reactor impedance and motor impedance have a more significant influence on the resonance frequency)

All cables are XLPE Cu and values are given per individual cable

The parameters applied for the site case studies in Chapter 4 associated with the single line diagram shown in Fig. 4.4 are given below

C.3 SIMULATION DATA AND CALCULATIONS FOR LCI CASE STUDIES [4.3]

Table C.3.I

CABLE DETAILS (REFERENCE FROM FIG. 4.4)

Reference	Voltage [kV]	Type / Cross section [mm²]	Length[m]	No. of cores
1	3.03	AWA 500	40	2x(3x1C)
2	3.03	AWA 500	40	2x(3x1C)
3	11	AWA 500	30	2x(3x1C)
4	11	SWA 300	20	2x(3C)
5	11	SWA 300	30	1x(3C)
6	11	AWA 500	105	7x(3x1C)
7	11	AWA 500	95	3x(3x1C)
8	11	AWA 500	45	2x(3x1C)
9	3.03	AWA 500	45	2x(3x1C)
10	11	AWA 500	20	1x(3x1C)
11	11	AWA 500	35	1x(3x1C)

12	11	AWA 500	25	1x(3x1C)
13	11	AWA 500	105	7x(3x1C)
14	11	AWA 500	95	3x(3x1C)
15	11	AWA 500	500	1x(3x1C)
16	11	AWA 500	700	1x(3x1C)
17	11	AWA 500	70	5x(3x1C)
18	11	SWA 300	2400	2x(3C)
19	11	AWA 500	70	5x(3x1C)
20	11	AWA 500	950	1x (3x1C)

Table C.3.II

CABLE ELECTRICAL PROPERTIES

Voltage grade and construction	No. of cores	Size	R	X_L	C
		[mm²]	[Ω/km] (90°)	[Ω/km] (50 Hz)	[μF/km]
6.35/11 kV Cu/XLPE/PVC/ AWA/PVC	1C	500	0.051	0.090	0.585
6.35/11 kV Cu/XLPE/PVC/ SWA/PVC	3C	300	0.079	0.085	0.491

Table C.3.III

MOTOR PARAMETERS (ALL MOTORS RATED 11 kV)

Ref	Rated Power [MW]	Rated Speed [rpm]	Rated Current [A]	$\sqrt{x_d'' * x_q''}$ [%]
MAC (T15/T16)	55	1500	2919	20.21
BAC (T15/T16)	23	1500	1224	24.01
Oxygen West/East (SM1-7, T7E)	36	3000	2100	27.68

Table C.3.IV

LCI OUTPUT TRANSFORMER PARAMETERS

Voltage rating	11/3.03/3.03 kV (no load)
Apparent power rating	18250 / 2 x 9125 kVA
Vector Group	Dd0y1
Short circuit impedance (one secondary shorted)	9%
Short circuit impedance (both secondaries shorted)	10%

C.4 RIDE THROUGH DATA

The parameters used in Chapter 6 are given below:

Table C.4. I
SYSTEM PARAMETERS (50 HZ)

Description	MAC	PGC
Nominal Rating (MW)	55	17
Rated line-line voltage (kV)	11	11
Source Impedance, 100 MVA base (p.u)	0.261	0.319
Total Inertia J (kgm^2)	4709	3472
Exciter constant K_E (p.u.)	1	1
Exciter time constant T_E (s)	0.6	0.5
Saturation function S_{Emax} (p.u.)	0	0
Nominal speed (rpm)	1500	1500
Exciter rated 3 phase voltage (V AC)	325	280
Exciter rated 3 phase rated current (A AC)	120	85
Field winding nominal current (A DC)	330	236
Load torque-speed curve	Fig. 5.6	Fig. 5.6

Table C.4.II
EQUIVALENT CIRCUIT SYNCHRONOUS MACHINE PARAMETERS (MACHINE BASE)

Description of per unit parameters	Unit	MAC	PGC
Z_B (base impedance)	Ω	2.20	7.11
X_d (d-axis synchronous reactance) (saturated test)	p.u.	1.157	1.68
X'_d (d-axis transient reactance) (saturated test)	p.u.	0.215	0.13
X''_d(d-axis sub-transient reactance) (saturated test)	p.u.	0.142	0.10
X_q (q-axis synchronous reactance)	p.u.	0.649	1.53
X'_q (q-axis transient reactance, not provided by manufacturer for MAC, assumed to be the same as X_q which can be assumed in accordance with [C.1])	p.u.	0.649	1.57
X''_q(q-axis sub-transient reactance) (saturated)	p.u.	0.212	0.22
X_{ls} (leakage reactance)	p.u.	0.123	0.08
T'_d (d-axis transient short circuit time constant) (saturated test)	s	0.593	0.28
T''_d (d-axis sub-transient short circuit time constant) (saturated/unsaturated test)	s	0.021	0.039
T''_q(q-axis sub-transient short circuit time constant)	s	0.04	0.068
Rs (Stator resistance)	p.u.	0.0023	0.003

Conversion of the machine parameters in Table C.4.II to the presentation in Fig. 5.3 is done in accordance with [5.21]. The parameters are converted, based on the relationship described in the equations shown below [5.21], in the simulation package (Simulink SymPowerSystems Matlab R2008), to the required dq model parameter values (Fig. 5.3). The parameters X_{mq} and X_{md} are determined from (C.1) and (C.2) (the associated inductance L values are obtained from X=2πfL throughout).

$$X_q = X_{ls} + X_{mq} \tag{C.1}$$

$$X_d = X_{ls} + X_{md} \tag{C.2}$$

X'_{lkq1} and X'_{lfd} are determined from:

$$X'_q = X_{ls} + \frac{X_{mq} X'_{lkq1}}{X'_{lkq1} + X_{mq}} \tag{C.3}$$

$$X'_d = X_{ls} + \frac{X_{md} X'_{lfd}}{X'_{lfd} + X_{md}} \tag{C.4}$$

X'_{lkq2} and X'_{lkd} are determined from:

$$X''_q = X_{ls} + \frac{X_{mq} X'_{lkq1} X'_{lkq2}}{X_{mq} X'_{lkq1} + X_{mq} X'_{lkq2} + X'_{lkq1} X'_{lkq2}} \tag{C.5}$$

$$X''_d = X_{ls} + \frac{X_{md} X'_{lfd} X'_{lkd}}{X_{md} X'_{lfd} + X_{md} X'_{lkd} + X'_{lfd} X'_{lkd}} \tag{C.6}$$

Similarly, the resistances can be obtained from simultaneous solution of derived synchronous machine time constant equations as shown in [5.21].

The assumption was made that only one damper winding is necessary (e.g. the kq2 winding in Fig. 5.3) for the simulations to represent the sub-transient state adequately while still obtaining suitable performance for stability analysis (typical assumption as per

[5.21]). The parameters in Table C.4.II are therefore suitable for entering into the "Synchronous Machine pu Standard" salient pole model in the simulation package Matlab Simulink SympowerSystems (R2008). The parameters X'_q and T''_q are then not required for input into the model [C.2]. The simulation method and assumptions are accurate enough for the required analysis since good correlation has been achieved, as shown in Chapter 6 (the PGC test results from run down recordings and MAC manufacturer results compare well with the simulation results).

Table C.4. III
EQUIVALENT CIRCUIT INDUCTION MACHINE PARAMETERS (MACHINE BASE)

Nominal rating:	11kV ;14.5MW; 50 Hz
Parameters:	R_1= 0.004417 p.u.; X_1= 0.16298 p.u.; R_2'= 0.00602 p.u.; X_2'= 0.09048 p.u; X_m= 8.5585 p.u.; same load torque speed curve and total inertia as SM PGC assumed; Z_B=8.35 Ω

REFERENCES

[C.1] R. K. Begamudre, *Electro-Mechanical Energy Conversion with Dynamics of Machines*, John Wiley & Sons, India, 1988

[C.2] Mathworks, "Synchronous machine", Simulation model description/users guide, Matlab Simulink SympowerSystems (R2008)